Application of the peat archive as tool in environmental chemistry

Dissertation zur Erlangung des Grades

Doktor der Naturwissenschaften

(Dr. rer. nat.)

An der Fakultät Biologie/Chemie/Geowissenschaften

Vorgelegt von

Sabine Thüns

geb. am 12.07.1979 in Starnberg

Die vorliegende Arbeit wurde in der Zeit von 05/2007 bis 01/2015 in Bayreuth am Lehrstuhl für Hydrologie unter Betreuung von Herrn Dr. Michael Radke und Herrn Professor Dr. Christian Blodau angefertigt.

Vollständiger Abdruck der von der Fakultät für Biologie, Chemie und Geowissenschaften der Universität Bayreuth genehmigten Dissertation zur Erlangung des akademischen Grades eines Doktors der Naturwissenschaften (Dr. rer. Nat.).

Dissertation eingereicht am 18.06.2014

Zulassung durch die Promotionskommission: 02.07.2014

Wissenschaftliches Kolloquium: 19.01.2015

Amtierender Dekan: Prof. Dr. Rhett Kempe

Prüfungsausschuss:

Prof. Dr. Andreas Held (Erstgutachter)

Dr. Michael Radke (Zweitgutachter)

Prof. Dr. Anke Jentsch (Vorsitz)

Prof. Dr. Cornelius Zetsch

Ich widme diese Arbeit meinen wunderbaren Eltern, meiner tollen Schwester und all meinen herzensguten Freunden.

TABLE OF CONTENTS

Application of XAD-resin based passive air samplers to assess local (roadside) and regional patterns of persistent organic pollutants

How suitable are peat cores to study historical deposition of PAHs?

Evaluation of peat cores as archives of polychlorinated biphenyl deposition rates

Ombrotrophic peat bogs are not suited as natural archives to investigate the historical atmospheric deposition of perfluoroalkyl substances

Comparison of atmospheric travel distances of several PAHs and metals calculated by two fate and transport models (The Tool and ELPOS) with experimental values derived from a peat bog transect

LIST OF FIGURES

ABBREVIATIONS

ACN	acetonitrile
B[a]A	benzo[*a*]anthracene
B[a]P	benzo[*a*]pyrene
B[b]F	benzo[*b*]fluoranthene
B[e]P	benzo[*e*]pyrene
B[ghi]P	benzo[*ghi*]perylene
B[j]F	benzo[*j*]fluoranthene
B[k]F	benzo[*k*]fluoranthene
B[b+k+j]F	sum of B[b]F, B[k]F and B[j]F
Chry	chrysene
c-PAH	PAH found in gas phase and on particles (c for changing)
CTD	characteristic travel distance
DCM	dichloromethane
ELB	Eagle Lake Bog
ELPOS	Environmental Long-range Transport and Persistence of Organic Substances Model
ETD	experimentally derived travel distances
Flt	fluoranthene
GB	Giant Bog
GC-MS	gas chromatography-mass spectrometry
GLB	Great Lake Bog
g-PAH	PAH mainly present in the gas phase
HPLC-ESI-MS/MS	high performance liquid chromatography electrospray ionization tandem mass spectrometry

IAEA	International Atomic Energy Agency
ICP-MS	Inductively coupled plasma mass spectrometry
Ind	indeno[1,2,3-cd]pyrene
K_{AW}	air water partition coefficient
K_{OA}	octanol air partition coefficient
K_{OC}	organic carbon partition coefficient
K_{OW}	octanol water partition coefficient
LOD	limit of detection
LOQ	limit of quantification
m	slope of the regression
MB	Mer Bleue Bog
m/z	mass to charge ratio
n.a.	not analyzed
n.c.	not calculated
n.d.	not detected
n.q.	not quantified
NCI	negative chemical ionization
OPL	Opeongo Lake
PAH	polycyclic aromatic hydrocarbon
PAS	passive sampler
Phen	phenanthrene
PCB	polychlorinated biphenyl
PFAS	polyfluorinated alkylated substances
PFOA	perfluorooctanoic acid
PFOS	perfluorooctane sulfonic acid

PP	polypropylene
p-PAH	PAH mainly found bound to particles
Pyr	pyrene
QuEChERS method	formed from "Quick, Easy, Cheap, Effective, Rugged, and Safe"
r-CTD	relative characteristic travel distance
r-ETD	relative experimentally derived travel distance
SB	Spruce Bog
s.d.	standard deviation
SIM	single ion monitoring
US-EPA	United States Environmental Protection Agency
XAD	highly absorbent resins

SUMMARY

Ombrotrophic peat bogs are natural archives of atmospheric deposition of pollutants. Therefore, peat profiles can be used to study the chronology of environmental contamination with harmful pollutants such as polycyclic aromatic hydrocarbons (PAHs), polychlorinated biphenyls (PCBs), and per- and polyfluorinated alkylated substances (PFAS). These mostly carcinogenic organic compounds are ubiquitously present in the environment. To derive historical deposition rates from the peat archive the pollutants have to be persistent and immobile, and an accurate dating technique is needed to calculate the age of the analyzed peat. To test these requirements and the accuracy of peat archives twelve peat profiles were sampled in four bogs in Ontario, Canada, as well as surface peat in one bog. To make sure sampling sites were not influenced by local roads, we analyzed the concentration decrease in the air from the roads into the bogs. Aerobic or anaerobic degradation of PCBs and PAHs did not occur over a 3-year period in incubation experiments. The heterogeneity of concentrations within a bog was determined in surface samples and by sampling three peat cores per bog. Concentrations varied up to 70 % indicating a high heterogeneity. A vertical sampling resolution of 5 cm lead to imprecision in the dating of sampled peat segments. Temporal deposition trends inferred from peat cores are generally in agreement with trends derived from a sediment core sampled close by, but rates are higher to the sediment for PAHs but similar for PCBs. Indication for mobility of PAHs was minor but has been observed in peat for PCBs and PFAS.

To predict the environmental behavior of pollutants, e.g. the atmospheric travel distance of pollutants, computer models can be used. To evaluate the results of these models experimentally derived travel distances of PAHs were determined using the peat bog archives along a transect originating at a large mining area. The comparison of the modeled and experimentally derived travel distances indicate that the computer models give realistic results for most PAHs.

We conclude that peat cores are suitable archives for inferring atmospheric deposition trends for PAHs, but not for PCBs and PFAS. Due to the relatively low temporal resolution short-term events might not be discovered. The analysis of more than one core per site is suggested to provide realistic reconstructed deposition trends and inventories.

ZUSAMMENFASSUNG

Hochmoore sind natürliche Archive der atmosphärischen Schadstoffdeposition. Deshalb können diese Moorarchive genutzt werden um die Chronologie der Umweltverschmutzung durch Schadstoffe wie polyaromatische Kohlenwasserstoffe (PAHs), polychlorinierte Biphenyle (PCBs), und polyfluorierte Kohlenwasserstoffe (PFAS) zu untersuchen. Diese, meist krebserregenden Stoffe, sind in der Umwelt weit verbreitet. Um historischen Depositionsraten im Moorarchiv bestimmen zu können, dürfen die Schadstoffe in diesem nicht abgebaut werden oder mobil sein. Zudem ist eine zuverlässige Altersbestimmung des zu untersuchenden Torfs von Nöten. Um diese Bedingungen und die Zuverlässigkeit des Moorarchives zu untersuchen wurden zwölf Torfkerne aus vier Hochmooren in Ontario, Kanada, sowie Oberflächenproben aus einem Hochmoor beprobt. Um zu garantieren, dass die Probenahmestellen nicht von lokalen Straßen beeinflusst wurden, untersuchten wir die Abnahme der Konzentrationen von der aus Straße in die Moore. Weder für PCBs noch für PAHs wurde über 3 Jahre ein Abbau in Laborexperimenten beobachtet. Die Heterogenität der Konzentrationen in den Oberflächenproben und in den Torfkernen lag bei bis zu 70 % innerhalb eines Moores. Die Beprobung von 5 cm Schichten führte zu einer hohen Unsicherheit in der Datierung der Depositionsraten. Die durch die Torfkerne bestimmten Depositionsraten passen zeitlich sehr gut zu denen mit einem Sedimentkern aus einem nahen See bestimmten. Allerdings sind die Raten für PAHs aus dem Sediment um Faktor vier höher. Im Moorprofil wurde keine Mobilität von PAHs beobachtet, allerdings von PCBs und PFAS.

Um das Umweltverhalten von Schadstoffen, wie z.B. die atmosphärischen Transportweiten vorherzusagen, werden häufig Computermodelle genutzt. Um deren Ergebnisse zu überprüfen wurden experimentell bestimmte Transportweiten von PAHs bestimmt. Hierzu wurden Hochmoore entlang eines Transektes im Abwind eines großen Abbaugebietes beprobt. Der Vergleich der modellierten und experimentell bestimmten Transportweiten belegen, dass die Computermodelle für die meisten PAHs realistische Ergebnisse liefern.

Hochmoore sind somit geeignete Archive für die atmosphärischen Depositionsraten für PAHs aber nicht für PCBs und PFAS. Durch die relativ geringe zeitliche Auflösung können kurzfristige Ereignisse maskiert werden. Um realistische Depositionsraten und Inventare zu rekonstruieren, ist es ratsam mehr als einen Torfkern pro Moor zu beproben.

x

EXTENDED SUMMARY

1. Introduction

1.1 Rationale

Pollution is not a new phenomenon. In fact, pollution caused by heavy metals can be traced back to the Roman Empire and still causing concerns today. During the last century the rapid growth in chemical and agrochemical industries has resulted in the environmental releases of a large number of new chemical compounds into the environment. Over the last decades, there has been an increasing focus on a subset of harmful organic chemicals, mostly of anthropogenic origin, that are commonly classified as Persistent Organic Pollutants (POPs) (Shatalov et al., 2004). Because of their harmful effects many environmental pollutants have been banned or their emissions have been restricted. To demonstrate that these regulations are effective, recent concentrations of the pollution in the environment have to be compared to historical ones. These are not always available but can be obtained of natural archives of pollution as sediment or peat cores. Ombrotrophic peat profiles have been used to improve our knowledge about historical contamination pattern, especially of heavy metals. They are promising natural passive samplers for atmospheric pollutants as they only receive wet and dry deposition but no terrestrial inputs. In combination with continuous growth, limited degradation, and the possibility of dating by ^{210}Pb, they can be used as archives of atmospheric deposition of multiple classes of organic contaminants and are a nearly ideal medium for recording temporal changes (Rapaport and Eisenreich, 1988). Peat cores have been used to study historical deposition rates of POPs before (Berset et al., 2001; Dreyer et al., 2005; Malawska et al., 2002; Rapaport and Eisenreich, 1988; Sanders et al., 1995b). Nevertheless, they have only been studied at single locations, using single cores and few groups of chemicals. Aim of this work was to analyze if peat cores are suitable to study historical deposition rates of POPs and how reliable these archives are as diagnostic tool in environmental chemistry.

1.2 Peat archives

Dated lake sediments cores have been used to determine the historical input of contaminants. Nevertheless, dynamic lake processes (bioturbation, sediment focusing, resuspension) and the delivery of substances from non atmospheric sources might mislead the interpretation (Rapaport and Eisenreich, 1988). In contrast, chemical input occurs only by atmospheric deposition to ombrotrophic peatlands and they are isolated from surface

and groundwater flow (Sanders et al., 1995a). Due to their high content of organic material (up to 90 %) they form an ideal medium to accumulate organic contaminants (Berset et al., 2001). Due to the prevailing anaerobic and acidic conditions in ombrotrophic bogs microbiological degradation and transformation of hydrophobic organic compounds are limited (Rapaport and Eisenreich, 1988). Therefore, hydrophobic contaminants are almost conserved in the peat matrix over decades. This is why peat bogs form an excellent archive for the determination of depositional changes of environmental contaminants.

1.3 Pollutants

1.3.1 POPs

In this study we analyzed polycyclic aromatic hydrocarbons (PAHs), polychlorinated biphenyls (PCBs), and polyfluorinated alkylated substances (PFAS). These are classes of organic pollutants. All of them are widely distributed in the environment and resist to a high degree biotic and abiotic degradation. They accumulate along the food chain and have harmful effects. They are transported over long distances and reach remote areas. Therefore, several of them are banned worldwide. To predict their potential for long range transport computer models are used.

1.3.2 PAHs

Polycyclic aromatic hydrocarbons (PAHs) are a group of over 100 different chemicals composed of fused benzene rings. They are formed during incomplete combustion or high temperature pyrolytic processes of fossil fuels and other organic materials. Therefore, they are ubiquitously present in the environment (Wild and Jones, 1995). The predominant source of PAHs are anthropogenic emissions, while some arise from natural combustion like forest fires (Baek et al., 1991; Wilcke, 2000). They were one of the first groups of atmospheric pollutants to be identified as carcinogenic and mutagenic (Baek et al., 1991). Due to their structure their carcinogenic potential differs. The most potent carcinogens are the benzo[b]fluoranthene, benzo[k]fluoranthene, benzo[j]fluoranthene, benzo[a]pyrene, benzo[a]anthracene, dibenzo[a,h]-anthracene, dibenzo[a,l]-anthracene, and indeno[1,2,3-*cd*]pyrene (IARC, 1998). The United States Environmental Protection Agency (USEPA) and the European Community have listed PAHs as priority pollutants (Wild and Jones, 1995). Several studies have monitored their concentrations in the environment (Hung et al., 2005; Jacob et al., 1993; Niederer et al., 1995).

Most of the PAHs are neither very volatile nor very soluble and will adsorb on almost any solid surface. They have a strong affinity for organic matter (Berset et al., 2001). Still they have the potential to travel long distances e.g. bound to particles in the atmosphere (Björseth et al., 1979).

Besides photolysis and chemical degradation, microbial degradation is the major degradation process of PAHs resulting in the decontamination of sediment and surface soil (Cerniglia, 1992; Haritash and Kaushik, 2009). Nevertheless, the extent of biodegradation in sediments has been discussed in several publications. While Lei et al. (2005) observed a 50-80 % removal of 2- to 5-ring PAHs in field-contaminated sediment during 24 weeks of incubation under aerobic conditions, Schneider et al. (2001) reported no degradation of PAHs in sediment cores sampled in the Great Lakes. The degradation of PAHs in peat has never been studied before. Because of the high organic matter content of peat a very high fraction of PAH is adsorbed. This limits the bioaccessibility (Johnsen and Karlson, 2007) and therefore degradation should be very slow or does not occur (Eriksson et al., 2000; Johnsen et al., 2005). In the experiments by Lei et al. (2005) no degradation of PAHs was observed under anaerobic conditions. They also saw that degradation was inhibited at a pH below 4.5. These two conditions apply to the anaerobic parts of ombrotrophic bogs and limit the PAH degradation there.

In several studies sediments and peat cores have been used to analyze historical deposition rates of PAHs (Berset et al., 2001; Dreyer et al., 2005; Lima et al., 2003; Malawska et al., 2006; Mastran et al., 1994; Sanders et al., 1995b; Usenko et al., 2007; Yunker and Macdonald, 2003). The suitability of these archives to represent truthful rates for PAHs has been discussed but to our knowledge never systematically studied.

1.3.3 PCBs

Polychlorinated biphenyls (PCBs) are produced by chlorination of biphenyls and comprise a class of 209 congeners. The general structure of the chemically very stable compounds is shown in Fig. 1.

After their production started in 1929, they were widely used as dielectric fluid in the electrical industry, and as an additive in a range of products such as copying paper, sealants and plastics (Badsha and Eduljee, 1986). After production peaked in the 1960s and their large production volume and worldwide use, PCBs became distributed in the environment globally (Tanabe, 1988).
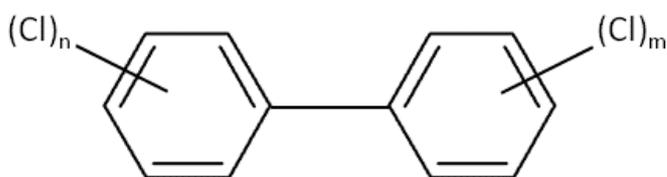
Fig. 1: Structure of PCBs; n and m give the number of chlorines

Some of these congeners are highly toxic and have both carcinogenic and teratogenic properties (Safe, 1989). Due to their persistence, toxicity and potential for bioaccumulation, PCBs have caused considerable public, governmental and scientific interest and concerns since the mid-1960s (Harrad et al., 1994). Production of PCBs was banned by the United States Congress in 1979 and by the Stockholm Convention on Persistent Organic Pollutants in 2001 (Himberg and Pakarinen, 1994; UNEP, 2001). Depending on their chlorine substitution PCBs are hydrophobic, lipophilic, and poorly degradable. Due to their low degradation rates, they are still present in several environmental compartments (Berset et al., 2001). For the lighter and intermediate PCB congeners atmospheric reaction with the OH radical is the major loss process. The higher chlorinated congeners are mainly deposited bound to particles (Wania and Daly, 2002). After deposition, for example to sediments, anaerobic reductive dechlorination might occur (Li et al., 2009a). As lower chlorinated biphenyls can be co-metabolized aerobically, higher chlorinated biphenyls are potentially fully biodegradable in a sequence of reductive dechlorination followed by aerobic mineralization of the lower chlorinated products (Abramowicz, 1990; Field and Sierra-Alvarez, 2008). Nevertheless, PCBs are slower to biodegrade in the environment than are many other organic chemicals (Beyer et al., 2009). They can undergo volatilization from secondary sources such as soil, vegetation, water, atmospheric particles, and products containing PCBs (Jartun et al., 2009). Therefore, detectable concentrations of PCBs can still be found in several environmental compartments like sediments, soil, plants and along the food chain (Dawn Pier et al., 2002; Li et al., 2009b; Michelutti et al., 2009; Moser and McLachlan, 2002)

1.3.4 PFAS

Polyfluorinated alkylated substances (PFAS) consist of a hydrophobic alkyl chain with a hydrophilic functional group. The alkyl chain is partly or fully fluorinated and typically contains between 4 and 18 carbon atoms. They are surface active substances which repel water, grease and dirt and are therefore used as detergents or impregnating agents in car-

pets, textiles, leather and paper, in polymer production, in fire-fighting foams, in cosmetics and cleaning agents as well as in numerous other industrial and consumer applications (Sturm and Ahrens, 2010). The global production was up to several thousands of tons in the 1990s (Paul et al., 2008). Nowadays PFAS are detected worldwide in the environment even in remote regions like the Arctic and the Antarctic. Since the 1990s, they are regarded as a new and emerging class of environmental contaminants because of their persistence, their toxic properties, their bioaccumulative potential and their worldwide detection in humans, wildlife and abiotic environment. Today, manufacturing and use of several PFAS has been legislatively restricted or voluntarily phased out by their producers (Dreyer et al., 2012). Perfluorooctane sulfonic acid (PFOS) and perfluorooctanoic acid (PFOA) are the most widely studied PFAS (Calafat et al., 2006).

1.4 Study objectives

1.4.1 Suitability of peat archives

Peat cores have been used previously as archives of atmospheric pollutant deposition. But to our knowledge the suitability of bogs as archives for organic pollutants and the uncertainties inherent to this archive have not been analyzed. Such a critical evaluation is the objective of the present study and we therefore analyzed the following aspects:

- We analyzed the influence of local roads to the sampling locations using passive samplers (study 1) to make sure these sites represent regional deposition patterns.

- To study the degradation within peat, aerobic and anaerobic degradation long-term incubations were carried out for 3 years (study 2 and 3).

- To determine the accuracy of peat archives the heterogeneity of concentrations and deposition rates of PAH and PCB records within one bog was studied by analyzing surface samples with reference to the microtopography within a bog (study 2 and 3).

- Finally, we compared the deposition rates of PCBs and PAHs derived from the peat archives to those derived from the sediment core (study 2 and 3).

- The mobility of PFAS, PAHs and PCBs within peat was discussed by analyzing historical deposition rates (study 2, 3, and 4).

1.4.2 Comparison of experimentally determined travel distance with model results

We studied the historical deposition rates of PAHs to 4 peat bogs along a transect in the downwind area of a big industrial zone. The decline of the deposition rates of PAHs along this transect gives information about the atmospheric travel behavior of these compounds. We calculated the characteristic travel distance of several PAHs and compared these results with the distances obtained by two computer models used to predict travel distances (study 5).

2. Experimental

2.1 Sampling

From 2007 to 2009 five peat bogs in Eastern Ontario, Canada were sampled: Giant Bog (GB), Eagle Lake Bog (ELB), Spruce Bog (SB), Green Lake Bog (GLB), and Mer Bleue Bog (MB). Except for MB the bogs are located along a transect in the downwind of Greater Sudbury (Fig. 2).
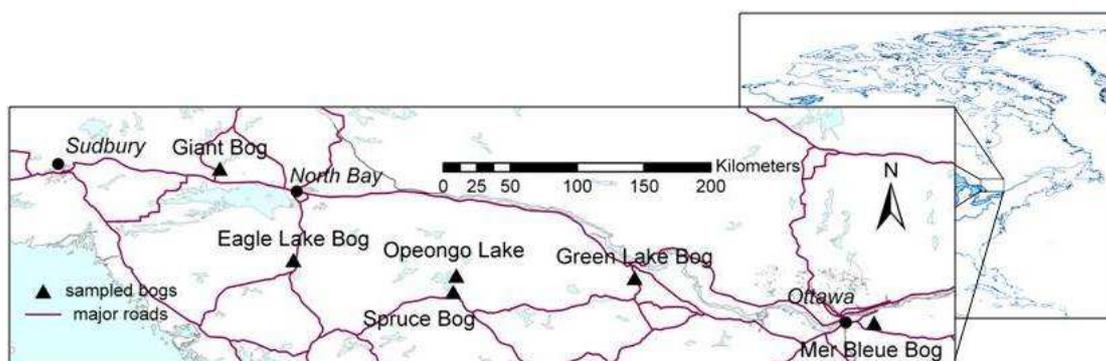
Fig. 2: Locations of sampled peat bogs and Opeongo Lake in Ontario, Canada, in relation to North America

Samples were taken at the domed ombrotrophic section of the bogs at the largest possible distance to nearby roads. Triplicate peat cores were sampled with a box corer from undisturbed hollows and were cut into 5 cm segments with a knife in the field; each segment was wrapped in aluminum foil, transferred to a plastic bag and stored in a cooler. At the MB site, we sampled 2 extra cores as well as peat water. Only in these two cores we analyzed PFAS. Surface peat was sampled at MB by cutting it with a knife just below the living vegetation at 5 hollows and hummocks, respectively. One sediment core was sampled with a gravity corer at the deepest point of Opeongo Lake. It was sectioned in 1-cm intervals. All samples were frozen directly after arrival in the laboratory. Peat and sediment samples were freeze dried, milled to a fine powder in a pebble mill and kept frozen until extraction.

To verify that the sampling locations in the peat bogs were not influenced by local sources like roads we analyzed the decline of air concentrations along a transect from the roads into the bogs. Therefore, we deployed passive samplers (PAS) from the end of May until early September 2009 to determine the concentration of PAHs and PCBs in air.

These PAS consist of a stainless steel mesh cylinder filled with XAD-2 resin and were mounted approx. 50 cm above ground on steel poles. At each bog except MB, duplicate PAS were deployed along a transect from the road into the bog.

2.2 Degradation experiments

A sufficiently large amount of peat was sampled at Mer Bleue from the layer directly below the active vegetation (aerobic) and from the catotelm (anaerobic peat sampled from approx. 10 cm below the water table), respectively. These samples were homogenized and split into aliquots which were used for the incubation experiments. Peat samples were incubated under controlled aerobic and anaerobic conditions in the laboratory at optimal degradation conditions to simulate a longer degradation time. Both aerobic and anaerobic incubations were carried out at 15° C in the dark. Three replicates were sacrificed after 2, 5, 9, 13, 20, 26, and 33 months and analyzed for their PAH and PCB content.

2.3 Extraction and analysis

2.3.1 PCBs and PAHs

After addition of a solution containing isotope-substituted PAHs and PCBs, 5 g of milled peat or sediment were extracted with pressurized liquid extraction with hexane. The extract was reduced to about 1 mL with a rotary evaporator. For clean-up, the extracts were then quantitatively transferred to columns containing aluminium oxide and silica gel. These columns were eluted with hexane and hexane/dichloromethane 3/1 (v/v) as described by Dreyer et al. (2005). The combined extracts were evaporated to approx. 1 mL by use of a rotary evaporator and then subjected to size exclusion chromatography using Bio-Beads for further clean-up. The extracts were evaporated to 1 mL by a rotary evaporator and finally evaporated to dryness under a gentle stream of nitrogen. Prior to injection, samples were redissolved in a solution containing two deuterated PAHs and one isotope-substituted PCB in nonane and transferred to glass vials.

We quantified 12 PAHs and 15 PCB congeners and analyzed them by ion trap GC-MS and quadrupole GC-MS.

Deposition rates of the individual compounds were calculated by dividing the measured mass of PAHs per peat segment by the number of years covered by this segment and the

surface area sampled. Deposition rates determined for Opeongo Lake were corrected by division with a sediment particle focusing factor of 1.16 taken from Muir et al. (2009).

2.3.2 PFAS

For extraction, 2 g of ground samples were weighed into polypropylene tubes. Each segment was extracted and analyzed in duplicate so that the intra-core and inter-core concentration variations could be determined. Prior to the extraction, a standard solution containing mass-labelled PFAS was spiked directly to each peat sample. Samples were ultrasonicated and after extraction, samples were centrifuged. For clean-up a modified QuEChERS (formed from "Quick, Easy, Cheap, Effective, Rugged, and Safe") method was used.

The peat water sample was spiked with mass-labelled PFAS and extracted by solid phase extraction using Oasis WAX cartridges. After the extraction, cartridges were washed with Millipore water and 0.1 % formic acid, dried for 30 minutes, and eluted with acetonitrile for neutral PFAS and methanol and 0.1% ammonium hydroxide for ionic PFAS. 25 were determined by high performance liquid chromatography electrospray ionization tandem mass spectrometry (HPLC-ESI-MS/MS).

2.3.3 Metals

For determination of Cu and Zn, 200 mg of the milled peat samples were digested by a microwave assisted acid dissolution technique (Bauer et al., 2008) and analyzed by ICP-MS (Inductively coupled plasma mass spectrometry) at the environmental geochemistry group of the University of Bayreuth.

2.3.4 PAHs and PCBs in PAS

The XAD-2 resins were Soxhlet extracted, the extracts were then concentrated by a rotary evaporator and under a stream of nitrogen, and finally analyzed with GC-MS (PAHs) and High-Resolution GC-MS (PCBs). Internal standards were used to correct for recovery, and Mirex was used as injection standard for both PAHs and PCBs. Results are reported as sequestered amount of each compound per PAS (ng PAS^{-1}). For PAHs, these amounts were also converted into air concentrations (ng m^{-3}) using the length of the deployment period and compound specific sampling rates.

2.4 Dating

Dry-milled subsamples were submitted to Flett Research Ltd (Winnipeg, Canada) or to the Institute of Environmental Geochemistry (University of Heidelberg, Germany) for ^{210}Pb analysis. In 4 cores the activity of ^{241}Am was measured as additional chronostratigraphic marker. The peat cores were dated using ^{210}Pb ($t_{1/2}$ = 22.26 years) and the constant rate of supply (CRS) model (Appleby and Oldfield, 1978).

2.5 Quality assurance and quality control

Perfluorinated materials or fluorinated polymers were avoided during sampling and sample preparation. The analytical procedure was evaluated for PAHs and PCBs by analyzing commercially available certified reference material (IAEA-159, Sediment; n = 5). Laboratory blank samples were analyzed with every set of samples.

2.6 Calculation of travel distances

2.6.1 Calculation of ETDs

Individual segments of 5 cm span periods of 20 to 30 years. Therefore, we based our analyses on the segments showing the maximum PAH deposition rate. For each compound, the maximum deposition rates from each of the three replicate cores per bog were log-transformed and linearly regressed against the distance of the sampling site from the Inco Superstack in Sudbury area. In cases where the decline of the deposition rates was significant (p < 0.1) the negative reciprocal of the slope m (km^{-1}) of the regression line was used to derive the ETD for the respective compound. The error of the slope of the regression was used to estimate the uncertainty of the ETDs.

To facilitate the comparison of measured and calculated transport distances, we eliminated this source of uncertainty by normalizing the PAH transport distances to those of aerosol particles. As a proxy for the transport distance of particles under the prevailing environmental conditions in the study area, we used the average transport distance of two metals (Cu and Zn) and of Ind. Subsequently, we refer to the normalized distance as r_{metal}-ETD and r_{Ind}-ETD.

2.6.2 Calculation of CTDs

Both models used here have been designed to distinguish between chemicals with low and high LRTP (Beyer et al., 2003). They are fugacity models that can be used for level III calculations (no equilibrium, inter-compartment transport). The Tool is a generic 3-compartment (air, soil and water) steady-state fugacity model and ELPOS (version 2.2) is a steady-state box model which takes into account eight compartments: air, water, sediment, four soil compartments (natural, agricultural, industrial, urban), and plants (Beyer and Matthies, 2001). Both models require several input parameters for each compound: the air-water (K_{AW}) and octanol-water (K_{OW}) partition coefficients as well as degradation half-lives ($t_{1/2}$) in air, water, soil and sediment. Optionally the organic carbon partition coefficient (K_{OC}) can be entered.

Based on their gas/particle partitioning behavior in the rural atmosphere of Eastern Canada, PAHs can be divided in 3 groups (Su et al., 2006): g-PAHs that are almost exclusively present in the gas phase (e.g., phenanthrene (Phen) and fluoranthene (Flt)), c-PAHs (c for changing partitioning behavior) that are present in the gas phase in summer and particle bound in winter (e.g., benzo[a]anthracene (B[a]A) and chrysene (Chry), and p-PAHs that are almost exclusively particle bound all year long (e.g., benzo[b+k]fluoranthene (B[b+k]F), benzo[a]pyrene (B[a]P) and indeno[1,2,3-cd]pyrene(Ind)).

Some of the default environmental input parameters of both models were adjusted to reflect the characteristics of Southern Ontario. The input values were adjusted for three temperature scenarios reflecting annual average (4°C), summer (13 °C), and winter (0°C) conditions in Southern Ontario (Environment Canada, 2011) for the Tool, while ELPOS has a built-in routine to adjust input values to the given temperature. The response of the CTD calculated by both models to changes in input values was tested by a sensitivity analysis as described in Wania and Dugani (2003). As for ETDs, relative CTDs were calculated by normalizing the CTDs of PAHs to the CTD of the metals and Ind.

3. Results

3.1 Suitability of peat cores

3.1.1 Influence of roads (study 1)

The peat cores sampled in the peat bogs were sampled at maximum distance possible to the roads. To verify that the samples are not mainly influenced by emissions originating from traffic we installed PAS between the roads and the sampling locations. We then analyzed the concentrations in the PAS as a function of distance to the road. At GB concentrations increased substantially within the first 20 meters and then decreased significantly ($p < 0.05$) from 100 m onwards. The unexpected concentration increase within the first 100 m of the transect is most probably due to the road being elevated approx. 3 m above the bog. At ELB, no significant spatial trend was observed, while at GLB the concentrations of two PAHs increased significantly along the transect into the bog. This increase cannot be caused by road traffic. The two samplers close to the road were covered by vegetation and this might have caused lower uptake of these PAHs. Or the samplers located in the bog were influenced by residential activities of the houses close by. These activities are supposed to have been minor by the time of the studied historical deposition rates.

In contrast, at SB concentrations were highest directly next to the road and then decreased along the transect. This observation is similar to findings by Tuhácková et al. (2001) and Pathirana et al. (1994) who reported an exponential decrease of PAH concentrations in roadside soils and leaf litter between 1 and 30 m distance from the road. Generally, the ratio between highest and lowest concentrations within one bog was ≤ 2 indicating the similarity of concentrations along the transect. Thus, we conclude that the influence of roadside emissions on PAH levels was rather low.

For PCBs, no dependence of concentration on distance from the road was observed. This was to be expected since vehicular emissions are no source of atmospheric PCBs.

The results of this study also demonstrated that a deployment period of approx. 3 months during summer is sufficient to determine reliable and robust estimates of the atmospheric levels of the studied PAHs. Thus, we conclude that the PAS used in this study – which are usually deployed for longer periods – can also be used to determine seasonal trends The PAS used in this study are only suitable to analyze trends of gas phase PAHs. Parti-

cle bond PAHs deposit faster and therefore after even shorter distances than gas phase PAHs (Lee, 1991). With respect to the primary aim of this study, we conclude that the sampling sites in the bogs were receiving regionally rather than locally (i.e., traffic related) emitted PAHs.

3.1.2 Degradation of pollutants in peat (study 2 and 3)

Both PCBs and PAHs were not degraded in the anaerobic and aerobic incubation experiments. Although there is some scatter in the data, we consider these interpretations valid based on the large number of samples and replicates they are based on. The regularly analyzed production rates of CO_2 and CH_4 indicated an active peat degrading microbial community in the anaerobic setup. The incubation experiments were carried out at relatively high temperature while turnover in the field is limited by colder temperatures. The anaerobic incubations were not limited by an accumulation of the decomposition products CO_2 and CH_4, which in undisturbed bogs limits the overall microbial turnover in deeper peat layers (Moore et al., 2006). We therefore assume that our results can be extrapolated to longer time scales, although the incubation period was much shorter than the period covered by the peat cores.

3.1.3 Intra peat heterogeneity (study 2 and 3)

Except for Flt, the PAH concentrations in surface samples taken at Mer Bleue were significantly ($p < 0.05$; n=5) higher in hollows than in hummocks. The $\sum_{12}$ PAH concentration was 225 ± 34 ng g^{-1} in hollows and 142 ± 31 ng g^{-1} in hummocks. This finding illustrates the influence of microtopography on PAH concentrations in surface peat. To obtain comparable samples it is therefore important to only sample hollows or hummocks. We only sampled hollows.

A measure for the total historical deposition per surface area is the inventory of contaminants. Such inventories were calculated for the period from around 1880 to present for each individual core. The average $\sum_{12}$ PAH inventories of the four bogs ranged from 4.6 mg m^{-2} to 7.5 mg m^{-2}. The relative standard deviations of the $\sum_{12}$ PAH inventories at the four bogs with replicate cores were between 15 and 32 % which is similar to the deviation of the surface samples. This reflects the heterogeneity of PAH concentrations between different hollows of an individual bog and the combined uncertainty of the sampling and analytical methods. The standard deviation of the inventories of $\sum_{11}$PCBs ranged from 15 % to 59 %. The 15 % are comparable with the deviation found for PAHs, but the deviation found for inventories of PCBs in GB is almost twice as high as the one

for PAHs. In one core of GB we determined high rates of Tetra-PCBs, which cause this high deviation. As the PCB concentrations are close to the detection limit in most samples they inherit a high uncertainty. Therefore, this data should be taken with precaution.

3.1.4 Dating of peat cores (study 2)

The mean total residual unsupported ^{210}Pb activity in the dated peat cores was 0.64 ± 0.17 Bq cm^{-2}, which is higher than the average activity of 0.35 ± 0.11 Bq cm^{-2} measured by Turunen et al. (2004) in Canadian bogs but in the range of soil inventories reported for North America (0.31 - 0.84) by Urban et al. (1990).

The dating method used is based on the assumption of post-depositional immobility of atmospherically derived constituents. Nevertheless, the mobility of ^{210}Pb in peat has been variably discussed (Shotyk et al., 1997; Vile et al., 1999) but dating with ^{210}Pb is still a popular dating method. The ^{210}Pb activity in the peat cores as well as in the sediment core decreased exponentially as a function of cumulative dry weight ($R^2 > 0.8$), indicating a low mobility of lead in the sampled cores. Therefore, the dating of the peat sampled here is not assumed to be biased by the mobility of lead.

The 5 cm segments of the peat cores represented very different time spans (Fig. 3).
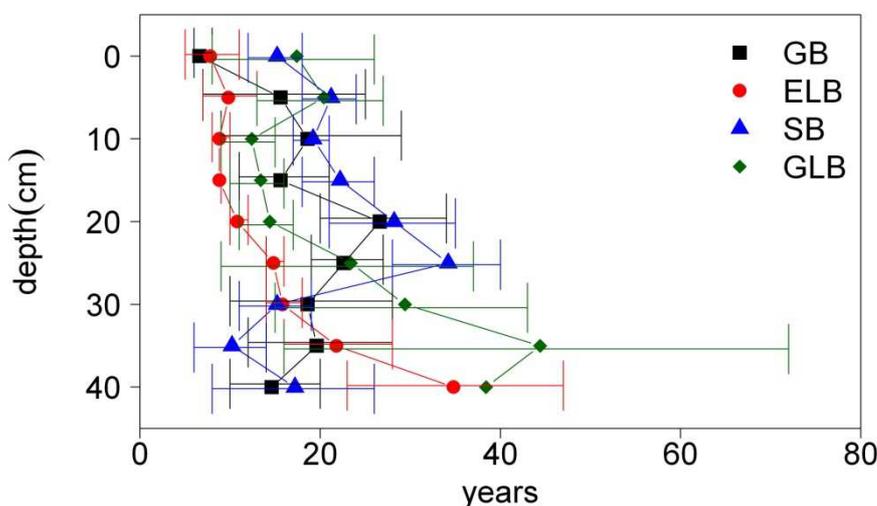
Fig. 3: Time span in years represented by peat segments over depth (cm) of 3 cores per bog; bars give standard deviation.

While the upper layers can represent as little as 5 years, the lower layers comprised up to 70 years. This can be attributed to the ongoing peat mineralization and compaction of the lower layers. Moreover, the time span covered by segments sampled in identical depths

of the three replicate cores per bog was highly variable. This can be critical for the analysis of deposition peaks as there is the potential for substantial underestimation of maximum deposition rates during peak periods which are "diluted" by a period of lower deposition rates represented within the same core segment. Overall, based on our results we conclude that dating inaccuracies can mainly be attributed to the coarse resolution of the 5 cm segments rather than to a general inapplicability of the ^{210}Pb method in bogs.

3.1.5 Reconstruction of historical deposition rates (study 2, 3 and 4)

The maximum $\sum_{12}$ PAH deposition rates ranged from 180 µg m^{-2}a^{-1} in GB to 59 µg m^{-2}a^{-1} in GLB. Although the 5 cm sections represent differing time spans, the deposition rates of the 3 cores per bog had maxima dated to 1880 – 1940 (see Fig. 4). The reconstructed historical deposition trends derived at the five bogs show increasing PAH deposition after 1870. This is consistent with the beginning of smelting operations in Sudbury, a city located upwind of the bogs, and the general onset of industrial development in Canada. Decreasing deposition rates after 1940 might reflect the installation of filters and replacement of the blast furnaces and roast yards by multi-hearth roasters and reverberatory furnaces for smelting (SARA, 2008).
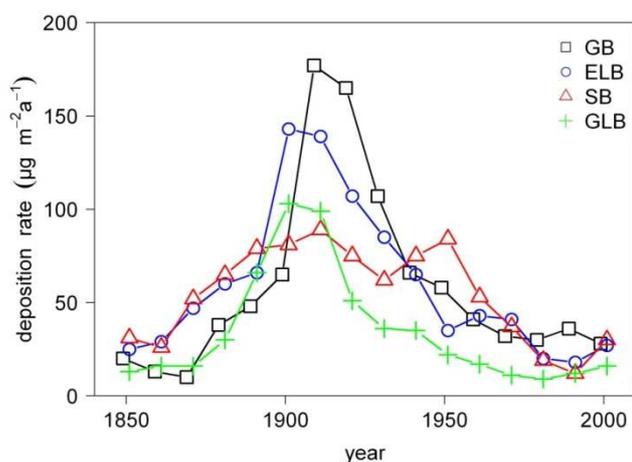
Fig. 4: Deposition rates of $\sum_{12}$ PAHs averaged to decades in sampled bogs (n = 3).

As discussed in the following the mobility of PCBs and PFAS results in biased deposition rates of these compounds. They are given here for completeness.

For all four peat bogs sampled comparable historical maximum deposition rates of PCBs were determined (between 600 to 1100 ng m^{-2}a^{-1}). The dominant isomer groups found in the peat samples were Tetra- (mean value = 39 %), Penta- (15 %) and Hexa-

chlorobiphenyls (22%). No peat bog contained significantly higher concentrations of PCBs. Therefore, they seem to reflect regional deposition and no local contamination.

Total PFAS concentrations increased from the most recent samples (surface) towards depths of 10-20 cm (1980s) and declined afterwards. The calculated PFAS deposition rates of Mer Bleue varied between 35 and 250 ng m^{-2} a^{-1} for PFOS, 50 and 140 ng m^{-2} a^{-1} for PFOA. Mostly, calculated PFAS deposition was fairly low and was rather in the range of that determined in remote or Arctic than of near urban samples.

3.1.6 Mobility within peat cores (study 2, 3 and 4)

To use peat cores as archives of atmospheric pollution, the contaminants have to be immobile within the profile. This has been questioned by Malawska et al.(2006) who determined more low molecular weight PAH in deeper depth than high molecular weight PAHs and therefore assumed a downward movement of the lighter ones. However, we did not observe such a difference in the distribution within the profiles as the deposition rates of all PAHs correlate significantly.

All cores had PCBs in sections that were dated before the onset of PCB production and use (1930s). Between 6.2 % (SB 2) to 55 % of $\sum_{11}$PCBs in GB1 are pre-production (23 % of $\sum_{11}$PCBs in average of all cores). In these sections the congeners with 4 to 7-Cl isomers dominated. This is similar to the findings of Sanders et al. (1995a) and Rapaport and Eisenreich (1988) who found 30 % and between 6 to 30 % of PCB residues, respectively, below depth corresponding to 1930. They assumed that this was partly caused by post-depositional mobility since the PCB pattern was dominated by the 3- and 4-C1 species. The low chlorinated congeners are more water soluble and therefore might get down washed to older sections.

The temporal resolution of the peat cores is relatively low. Certain events like maximum deposition rates might appear too late or too early, as the 5 cm segments reflect up to 30 years of deposition. Nevertheless, in 8 out of the 12 cores, the maximum deposition rates occurred 5 to 15 cm below the layer dated to the maximum production of PCBs (around 1970).
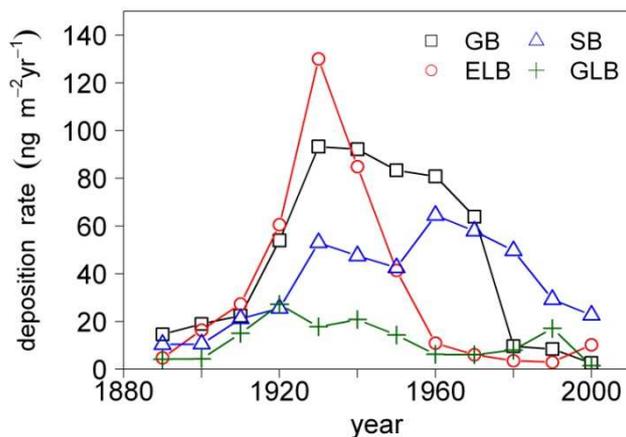
Fig. 5: Deposition rates of PCB 209 averaged to decades in sampled bogs (n = 3).

A high mobility of compounds causes an evenly distribution along a profile. Almost all PCB profiles analyzed in this study have one or two maxima at a certain depth and the deposition trends are still visible (see Fig. 5). Therefore, mobility occurs at a low rate or other mechanisms cause this shift.

Of 25 PFAS analyzed in the present study, 12 were detected consistently in peat core samples. Compared to reported production maxima, PFAS concentration maxima in peat appear 20 to 30 years too early which indicates a PFAS movement downwards the peat profile or uncertainties involved in the applied ^{210}Pb dating. Furthermore, PFAS were detected even in the oldest peat samples taken in this study. The shape of the deposition chronology more or less matches that of the estimated production volumes whereas its absolute timing does not. The shorter the length of the perfluorinated chain, the more evenly distributed within the peat core were the compounds. This may be interpreted similar to a chromatographic separation with strongest retention of longer-chained PFAS. As there is no substantial vertical transport of water and solutes in the peat, we attribute the obvious downward movement of shorter-chain compounds to redistribution by water table fluctuations and diffusive processes. Overall, our results indicate that (if at all) peat bogs may be suitable archives for the historical contamination by long-chain PFAS, but not for the other groups of PFAS studied here.

3.1.7 Comparison with lake sediment core (study 2 and 3)

In the sediment of OPL we found $\sum_{11}$PCB concentrations up to 42 ng g^{-1} (1984-1991) and 14 ng g^{-1} in the surface section. The deposition rates were up to 1344 ng m^{-2}a^{-1} at maximum and 336 ng m^{-2}a^{-1} at the surface. This is comparable to the rates we found in

cores from SB. Rapaport and Eisenreich (1988) also reported similar PCB deposition rates from lake sediments and bogs.

The $\sum_{12}$ PAH deposition rates derived from the Opeongo Lake sediment core peaked around 1920 with 571 µg m^{-2}a^{-1} and again around 1960 with 868 µg m^{-2}a^{-1}, followed by decreasing rates up to present time. Thanks to higher concentrations of PAHs in sediment and a matrix which can be sectioned more easily, thinner sections can be sampled in sediment. Therefore, the temporal resolution of the sediment is higher for the results of the sediment core and the peat core sampled close by (SB).

The distance between Opeongo Lake and Spruce Bog is only 16 km, so it is reasonable to assume that both sites received a similar atmospheric deposition of PAHs in the past. The deposition rates and the inventory of PAHs reconstructed from the sediment core were four times higher than those inferred from the SB cores for all compounds at all times. Higher inventories and consequently higher reconstructed deposition rates for lake sediments than for bogs were also reported for Pb and Hg (Farmer et al., 1997; Norton et al., 1997). While Farmer et al. assumed a certain loss within the bog but no mobility, Norton et al. (1997) and Bindler et al. (2004) supposed that a peat core may better reflect atmospheric deposition rates than lake sediments because no watershed is involved in the delivery of the pollutants and because of the greater complexity of lake basins and sedimentation processes. The relative synchronicity of the temporal deposition trends indicate that the differences in quantity are caused by deposition to the catchment and sedimentation, and not by mobility within the sediment. Further studies are necessary to determine the reason for the higher deposition rates reconstructed from sediments, but also to investigate whether OPL was contaminated by local sources.

3.2 Application of peat cores to determine the travel distance (study 5)

3.2.1 ETD

The maximum deposition rates of several PAHs as well as of Cu and Zn declined exponentially with distance from Sudbury (Fig.6). The ETDs determined for PAHs, Cu, and Zn range from 173 to 321 km with relative uncertainties between 26 and 46 %. The ETDs of the two metals were shorter than those of the PAHs. The discrepancy between the two metal ETDs reflects the overall uncertainty of our approach. Their average ETD (198 ± 45 km) was used to calculate the r_{metal}-ETD of PAHs.
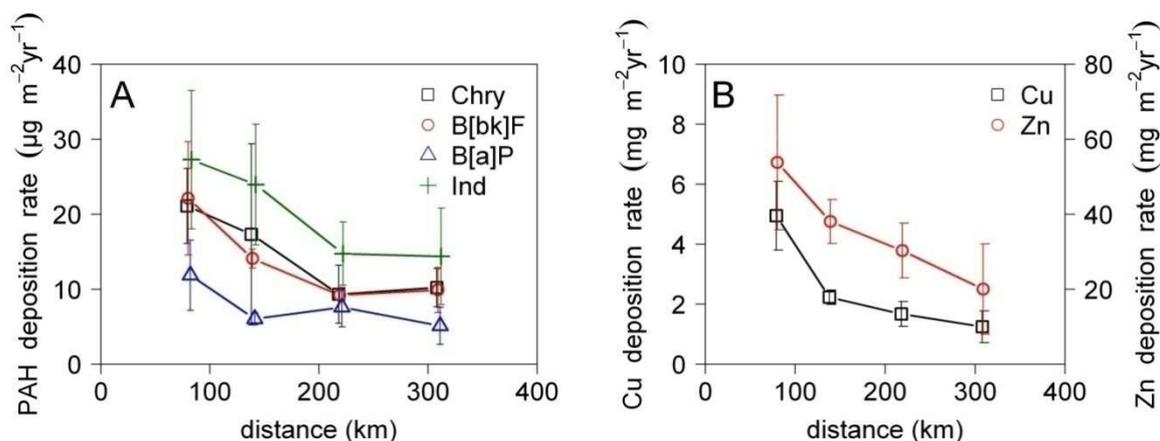
Fig.6: Average maximum deposition rates of (A) PAHs and (B) metals as a function of distance from the Greater Sudbury source area. The error bars represent the standard deviation of the three replicate peat cores.

3.2.2 CTD

When using the default settings of The Tool, CTDs up to 2860 km were calculated. After adjusting the settings and input parameters to the conditions in the Sudbury region the estimated CTDs were lower by a factor of 7.5. Using The Tool, the CTD of particles was longer than the CTDs of the PAHs except for the CTD of Phen and Flt in winter. The p-PAHs had almost the same CTD as the metals, while those of g- and c-PAHs were substantially shorter. B[a]A had the shortest CTD.

With default settings, CTDs up to 700 km were calculated with ELPOS. With region-specific settings, CTDs between 142 km (B[a]A) and 517 km (particles) were estimated for the annual average temperature of 4 °C. The $r_{particle}$-CTDs for all PAHs covered the range from 0.10 to 4.6 under the three temperature scenarios. B[a]A had the shortest $r_{particle}$-CTD due to its high degradation rate in air in summer, Phen had the longest in winter.

When the same degradation half-lives and temperature-adjusted partition coefficients were used in both models, the CTDs calculated by both models agreed reasonably well and were significantly correlated. However, ELPOS systematically estimated longer CTDs than The Tool. CTDs normalized to that of the metals agreed very well between both models.

3.2.3 Comparison of ETD and CTD

The absolute ETDs of PAHs derived from the peat transect were between 281 and 321 km, whereas the absolute CTDs with regional settings were between 44 and 480 km. By

normalizing the ETDs and CTDs to the travel distances of metals or particle bound PAHs effects of radial dilution, wind speed, and a changing wind direction were eliminated. This was important to exclude these natural factors which are not taken into account by the models. The comparison of the normalized distances is illustrated in Fig.7. When normalized to metals, the r_{metal}-CTDs of both models agreed very well, and the r_{metal}-CTDs of the three p-PAHs were close to 1, whereas the r_{metal}-CTD of Chry was substantially lower. However, the measured r_{metal}-ETD for all four compounds was much higher and around 1.5 for all compounds (see Fig.7). Thus, the agreement between measured and modeled relative-to-metal transport distances was not very good. This might be attributed to a different atmospheric behavior of the particles that metals and PAHs are associated with, or to some inaccuracy of the estimated metal-CTDs.

All r-ETDs are similar while the r-CTDs differ. Although it is very likely that PAHs and metals in historic samples shared the same dominant source in the Greater Sudbury area, they might be associated with different aerosol size classes which undergo different atmospheric transport, i.e., metals might be associated with somewhat larger particles than PAHs and consequently are removed from the atmosphere faster. Alternatively, PAHs might not be as reactive as the models assume. Which of the factors explains the discrepancy between r_{metal}-ETDs and r_{metal}-CTDs of PAHs cannot be decided based on the currently available knowledge.
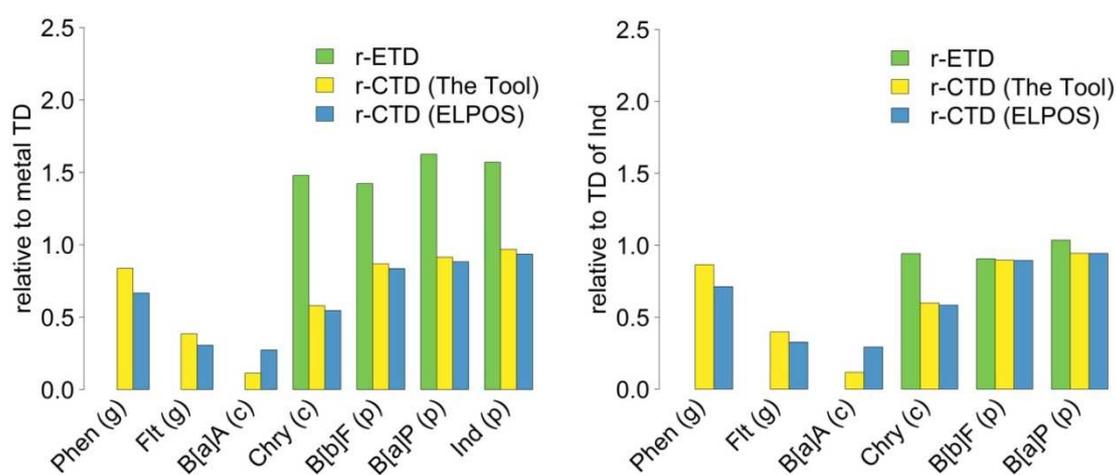
Fig.7: Comparison of relative ETDs and CTDs of PAHs at 4° C (left: relative to metals; right: relative to Ind).

To further reduce uncertainty, the CTD of PAHs can be normalized to the travel distance of Ind instead of metals (Fig.7), thereby referencing the transport distance to a compound with identical emission behavior and that is association with particle of similar size. This yielded a very good agreement between measurement and model for B[b]F and B[a]P, while the estimated r_{Ind}-CTDs for Chrysene were lower than the actually measured r_{Ind}-ETD.

4. Summary and Conclusion

This study demonstrated that peat bogs can be used as natural passive samplers and give reliable estimates for PAH deposition time trends. This is not the case for PCBs and PFAS as they seem to be mobile within the peat profile. No degradation of PAHs or PCBs in peat was observed within this study. Deposition rates to a lake determined in a sediment core were comparable to the ones obtained from the peat cores for PCBs but up to four times higher for PAHs. The dating and large time spans of the 5 cm segments are additional limitations this method. As the concentrations of the studied pollutants are too low or the detection limit too high, we could not sample thinner layers. Concerning heterogeneity of concentrations within one bog with up to 70 %, the results should be interpreted with care.

Nevertheless, we were able to obtain reliable results for the PAHs and calculate travel distances for them. These travel distances are suitable to experimentally evaluate predicted CTDs of PAHs if data are normalized to a reference compound. The comparison of these travel distances to the distances calculated using computer models worked out relatively fine and indicates that the models give realistic results and can be used to predict the environmental behavior of new pollutants.

We conclude that peat cores are suitable archives for inferring atmospheric deposition trends of PAHs, but due to the relatively low temporal resolution short-term events might not be visible. The analysis of more than one core per site is suggested to provide a realistic of the reconstructed deposition trends and total inventories.

5. References

Abramowicz, D.A., 1990. Aerobic and Anaerobic Biodegradation of PCBs: A Review. Critical Reviews in Biotechnology 10, 241-251.

Appleby, P.G., Oldfield, F., 1978. The calculation of lead-210 dates assuming a constant rate of supply of unsupported ^{210}Pb to the sediment. CATENA 5, 1-8.

Badsha, K., Eduljee, G., 1986. PCB in the U.K. environment - A preliminary survey. Chemosphere 15, 211-215.

Baek, S.O., Field, R.A., Goldstone, M.E., Kirk, P.W., Lester, J.N., Perry, R., 1991. A Review of Atmospheric Polycyclic Aromatic-Hydrocarbons - Sources, Fate and Behavior. Water Air and Soil Pollution 60, 279-300.

Bauer, M., Fulda, B., Blodau, C., 2008. Groundwater derived arsenic in high carbonate wetland soils: Sources, sinks, and mobility. Science of the Total Environment 401, 109-120.

Berset, J.D., Kuehne, P., Shotyk, W., 2001. Concentrations and distribution of some polychlorinated biphenyls (PCBs) and polycyclic aromatic hydrocarbons (PAHs) in an ombrotrophic peat bog profile of Switzerland. Science of the Total Environment 267, 67-85.

Beyer, A., Biziuk, M., Whitacre, D.M., 2009. Environmental Fate and Global Distribution of Polychlorinated Biphenyls

Reviews of Environmental Contamination and Toxicology Vol 201. Springer US, pp. 137-158.

Beyer, A., Matthies, M., 2001. Criteria for atmospheric long-range transport potential and persistence of pesticides and industrial chemicals. German Federal Environmental Agency, Berlin, Germany., Technical Report FKZ 299 265 402.

Beyer, A., Wania, F., Gouin, T., Mackay, D., Matthies, M., 2003. Temperature dependence of the characteristic travel distance. Environmental Science & Technology 37, 766-771.

Bindler, R., Klarqvist, M., Klaminder, J., Förster, J., 2004. Does within-bog spatial variability of mercury and lead constrain reconstructions of absolute deposition rates from single peat records? The example of Store Mosse, Sweden. Global Biogeochem. Cycles 18, GB3020.

Björseth, A., Lunde, G., Lindskog, A., 1979. Long-range transport of polycyclic aromatic hydrocarbons. Atmospheric Environment (1967) 13, 45-53.

Calafat, A.M., Needham, L.L., Kuklenyik, Z., Reidy, J.A., Tully, J.S., Aguilar-Villalobos, M., Naeher, L.P., 2006. Perfluorinated chemicals in selected residents of the American continent. Chemosphere 63, 490-496.

Cerniglia, C.E., 1992. Biodegradation of polycyclic aromatic hydrocarbons. Biodegradation 3, 351-368.

Dawn Pier, M., Zeeb, B.A., Reimer, K.J., 2002. Patterns of contamination among vascular plants exposed to local sources of polychlorinated biphenyls in the Canadian Arctic and Subarctic. Science of the Total Environment 297, 215-227.

Dreyer, A., Radke, M., 2005. Evaluation and optimization of extraction and clean-up methods for the analysis of polycyclic aromatic hydrocarbons in peat samples. International Journal of Environmental Analytical Chemistry 85, 423-432.

Dreyer, A., Radke, M., Turunen, J., Blodau, C., 2005. Long-term change of polycyclic aromatic hydrocarbon deposition to peatlands of eastern Canada. Environmental Science & Technology 39, 3918-3924.

Dreyer, A., Thuens, S., Kirchgeorg, T., Radke, M., 2012. Ombrotrophic Peat Bogs Are Not Suited as Natural Archives To Investigate the Historical Atmospheric Deposition of Perfluoroalkyl Substances. Environmental Science & Technology 46, 7512-7519.

Environment Canada, 2011. Canadian Climate Normals for North Bay -A, WMO ID: 71731, period 1971-2000. www.climate.weatheroffice.gc.ca.

Eriksson, M., Dalhammar, G., Borg-Karlson, A.K., 2000. Biological degradation of selected hydrocarbons in an old PAH/creosote contaminated soil from a gas work site. Applied Microbiology and Biotechnology 53, 619-626.

Farmer, J.G., Mackenzie, A.B., Sugden, C.L., Edgar, P.J., Eades, L.J., 1997. A Comparison of the Historical Lead Pollution Records in Peat and Freshwater Lake Sediments from Central Scotland. Water, Air, & Soil Pollution 100, 253-270.

Field, J.A., Sierra-Alvarez, R., 2008. Microbial transformation and degradation of polychlorinated biphenyls. Environmental Pollution 155, 1-12.

Haritash, A.K., Kaushik, C.P., 2009. Biodegradation aspects of Polycyclic Aromatic Hydrocarbons (PAHs): A review. Journal of Hazardous Materials 169, 1-15.

Harrad, S.J., Sewart, A.P., Alcock, R., Boumphrey, R., Burnett, V., Duarte-Davidson, R., Halsall, C., Sanders, G., Waterhouse, K., Wild, S.R., Jones, K.C., 1994. Polychlorinated biphenyls (PCBs) in the British environment: Sinks, sources and temporal trends. Environmental Pollution 85, 131-146.

Himberg, K.K., Pakarinen, P., 1994. Atmospheric PCB deposition in Finland during 1970s and 1980s on the basis of concentrations in ombrotrophic peat mosses (Sphagnum). Chemosphere 29, 431-440.

Hung, H., Blanchard, P., Halsall, C.J., Bidleman, T.F., Stern, G.A., Fellin, P., Muir, D.C.G., Barrie, L.A., Jantunen, L.M., Helm, P.A., Ma, J., Konoplev, A., 2005. Temporal and spatial variabilities of atmospheric polychlorinated biphenyls (PCBs), organochlorine (OC) pesticides and polycyclic aromatic hydrocarbons (PAHs) in the Canadian Arctic: Results from a decade of monitoring. Science of the Total Environment 342, 119-144.

IARC, 1998. Volume 32, Polynuclear Aromatic Compounds, Part 1, Chemical, Environmental and Experimental Data.

Jacob, J.r., Grimmer, G., Hildebrandt, A., 1993. The use of passive samplers for monitoring polycyclic aromatic hydrocarbons in ambient air. Science of the Total Environment 139â€"140, 307-321.

Jartun, M., Ottesen, R.T., Steinnes, E., Volden, T., 2009. Painted surfaces - Important sources of polychlorinated biphenyls (PCBs) contamination to the urban and marine environment. Environmental Pollution 157, 295-302.

Johnsen, A., Karlson, U., 2007. Diffuse PAH contamination of surface soils: environmental occurrence, bioavailability, and microbial degradation. Applied Microbiology and Biotechnology 76, 533-543.

Johnsen, A.R., Wick, L.Y., Harms, H., 2005. Principles of microbial PAH-degradation in soil. Environmental Pollution 133, 71-84.

Lee, W., 1991. The determination of dry deposition velocities for ambient gases and particles.

Lei, L., Khodadoust, A.P., Suidan, M.T., Tabak, H.H., 2005. Biodegradation of sediment-bound PAHs in field-contaminated sediment. Water Research 39, 349-361.

Li, A., Rockne, K.J., Sturchio, N., Song, W., Ford, J.C., Wei, H., 2009a. PCBs in sediments of the Great Lakes - Distribution and trends, homolog and chlorine patterns, and in situ degradation. Environmental Pollution 157, 141-147.

Li, Y.-F., Harner, T., Liu, L., Zhang, Z., Ren, N.-Q., Jia, H., Ma, J., Sverko, E., 2009b. Polychlorinated Biphenyls in Global Air and Surface Soil: Distributions, Air-Soil Exchange, and Fractionation Effect. Environmental Science & Technology 44, 2784-2790.

Lima, A.L.C., Eglinton, T.I., Reddy, C.M., 2003. High-resolution record of pyrogenic polycyclic aromatic hydrocarbon deposition during the 20th century. Environmental Science & Technology 37, 53-61.

Malawska, M., Bojakowska, I., Wiłkomirski, B., 2002. Polycyclic aromatic hydrocarbons (PAHs) in peat and plants from selected peat-bogs in the north-east of Poland. Journal of Plant Nutrition and Soil Science 165, 686-691.

Malawska, M., Ekonomiuk, A., Wiłkomirski, B., 2006. Polycyclic aromatic hydrocarbons in peat cores from southern Poland: distribution in stratigraphic profiles as an indicator of PAH sources. International Mire Conservation Group, International Peat Society.

Mastran, T.A., Dietrich, A.M., Gallagher, D.L., Grizzard, T.J., 1994. Distribution of polyaromatic hydrocarbons in the water column and sediments of a drinking water reservoir with respect to boating activity. Water Research 28, 2353-2366.

Michelutti, N., Liu, H., Smol, J.P., Kimpe, L.E., Keatley, B.E., Mallory, M., Macdonald, R.W., Douglas, M.S.V., Blais, J.M., 2009. Accelerated delivery of polychlorinated

biphenyls (PCBs) in recent sediments near a large seabird colony in Arctic Canada. Environmental Pollution 157, 2769-2775.

Moore, T.R., Lafleur, P.M., Poon, D.M.I., Heumann, B.W., Seaquist, J.W., Roulet, N.T., 2006. Spring photosynthesis in a cool temperate bog. Global Change Biology 12, 2323-2335.

Moser, G.A., McLachlan, M.S., 2002. Modeling Digestive Tract Absorption and Desorption of Lipophilic Organic Contaminants in Humans. Environmental Science & Technology 36, 3318-3325.

Muir, D.C.G., Wang, X., Yang, F., Nguyen, N., Jackson, T.A., Evans, M.S., Douglas, M., Kock, G., Lamoureux, S., Pienitz, R., Smol, J.P., Vincent, W.F., Dastoor, A., 2009. Spatial Trends and Historical Deposition of Mercury in Eastern and Northern Canada Inferred from Lake Sediment Cores. Environmental Science & Technology 43, 4802-4809.

Niederer, M., Maschka-Selig, A., Hohl, C., 1995. Monitoring polycyclic aromatic hydrocarbons (PAHs) and heavy metals in urban soil, compost and vegetation. Environmental Science and Pollution Research 2, 83-89.

Norton, S.A., Evans, G.C., Kahl, J.S., 1997. Comparison of Hg and Pb fluxes to hummocks and hollows of ombrotrophic big heath bog and to nearby Sargent Mt. Pond, Maine, USA. Water Air and Soil Pollution 100, 271-286.

Pathirana, S., Connell, D.W., Vowles, P.D., 1994. Distribution of Polycyclic Aromatic Hydrocarbons (PAHs) in an Urban Roadway System. Ecotoxicology and Environmental Safety 28, 256-269.

Paul, A.G., Jones, K.C., Sweetman, A.J., 2008. A First Global Production, Emission, And Environmental Inventory For Perfluorooctane Sulfonate. Environmental Science & Technology 43, 386-392.

Rapaport, R.A., Eisenreich, S.J., 1988. Historical Atmospheric Inputs of High Molecular-Weight Chlorinated Hydrocarbons to Eastern North-America. Environmental Science & Technology 22, 931-941.

Safe, S., 1989. Polychlorinated biphenyls (PCBs) - Mutagenicity and Carcinogenicity. Mutation Research 220, 31-47.

Sanders, G., Jones, K.C., Hamilton-Taylor, J., Dorr, H., 1995a. PCB and PAH Fluxes to a Dated UK Peat Core. Environmental Pollution 89, 17-25.

Sanders, G., Jones, K.C., Hamiltontaylor, J., Dorr, H., 1995b. PCB and PAH Fluxes to a Dated UK Peat Core. Environmental Pollution 89, 17-25.

SARA, 2008. Volume I - Chapter 3 : Historical Review of Air Emissions from the Smelting Operations. http://www.sudburysoilsstudy.com/EN/media/volume_I.asp.

Schneider, A.R., Stapleton, H.M., Cornwell, J., Baker, J.E., 2001. Recent declines in PAH, PCB, and toxaphene levels in the northern Great Lakes as determined from high resolution sediment cores. Environmental Science & Technology 35, 3809-3815.

Shatalov, V., Breivik, K., Berg, T., Dutchak, S., Pacyna, J., 2004. Persistent organic pollutants. Norwegian Meteorological Institute, EMEP assessment, Part 1: European Perspective, 129-150.

Shotyk, W., 1996. Peat bog archives of atmospheric metal deposition: geochemical evaluation of peat profiles, natural variations in metal concentrations, and metal enrichment factors. Environ. Rev. 4, 149-183.

Shotyk, W., Norton, S.A., Farmer, J.G., 1997. Summary of the workshop on peat bog archives of atmospheric metal deposition. Water Air and Soil Pollution 100, 213-219.

Sturm, R., Ahrens, L., 2010. Trends of polyfluoroalkyl compounds in marine biota and in humans. Environmental Chemistry 7, 457-484.

Su, Y., Lei, Y.D., Wania, F., Shoeib, M., Harner, T., 2006. Regressing Gas/Particle Partitioning Data for Polycyclic Aromatic Hydrocarbons. Environmental Science & Technology 40, 3558-3564.

Tanabe, S., 1988. PCB problems in the future: Foresight from current knowledge. Environmental Pollution 50, 5-28.

Tuhácková, J., Cajthaml, T., Novák, K., Novotný, C., Mertelík, J., Sasek, V., 2001. Hydrocarbon deposition and soil microflora as affected by highway traffic. Environmental Pollution 113, 255-262.

Turunen, J., Roulet, N.T., Moore, T.R., Richard, P.J.H., 2004. Nitrogen deposition and increased carbon accumulation in ombrotrophic peatlands in eastern Canada. Global Biogeochemical Cycles 18.

UNEP, 2001. Final Act of the Conference of Plenipotentaries on the Stockholm Convention on Persistent Organic Pollutants. United Nations Environment Program: Stockholm, Sweden.

Urban, N.R., Eisenreich, S.J., Grigal, D.F., Schurr, K.T., 1990. Mobility and diagenesis of Pb and ^{210}Pb in peat. Geochimica Et Cosmochimica Acta 54, 3329-3346.

Usenko, S., Landers, D.H., Appleby, P.G., Simonich, S.L., 2007. Current and historical deposition of PBDEs, pesticides, PCBs, and PAHs to rocky mountain national park. Environmental Science & Technology 41, 7235-7241.

Vile, M.A., Wieder, R.K., Novak, M., 1999. Mobility of Pb in Sphagnum-derived peat. Biogeochemistry 45, 35-52.

Wania, F., Daly, G.L., 2002. Estimating the contribution of degradation in air and deposition to the deep sea to the global loss of PCBs. Atmospheric Environment 36, 5581-5593.

Wania, F., Dugani, C.B., 2003. Assessing the long-range transport potential of polybrominated diphenyl ethers: A comparison of four multimedia models. Environmental Toxicology and Chemistry 22, 1252-1261.

Wilcke, W., 2000. SYNOPSIS Polycyclic Aromatic Hydrocarbons (PAHs) in Soil — a Review. Journal of Plant Nutrition and Soil Science 163, 229-248.

Wild, S.R., Jones, K.C., 1995. Polynuclear aromatic hydrocarbons in the United Kingdom environment: A preliminary source inventory and budget. Environmental Pollution 88, 91-108.

Yunker, M.B., Macdonald, R.W., 2003. Alkane and PAH depositional history, sources and fluxes in sediments from the Fraser River Basin and Strait of Georgia, Canada. Organic Geochemistry 34, 1429-1454.

6. Contribution to different studies

Study 1
Application of XAD-resin based passive air samplers to assess local (roadside) and regional patterns of persistent organic pollutants

S. Thuens	20 % Laboratory work; Field work; Data analysis; Discussion of results; Manuscript preparation
P. Barthel	45 % Laboratory work; Data analysis; Discussion of results; Manuscript preparation
M. Radke	10 % Concept; Discussion of results; Manuscript preparation
F. Wania	10 % Concept; Discussion of results; Manuscript preparation
C. Shunthirasingham,	5% Laboratory work
JN. Westgate	5 % Data Analysis; Modelling
C. Blodau and C. Estop	5 % Installation of PAS

Study 2
How suitable are peat cores to study historical deposition of PAHs?

S. Thuens	70 % Laboratory work; Field work; Data analysis; Discussion of results; Manuscript preparation
M. Radke	20 % Concept; Field work; Discussion of results; Manuscript preparation
C. Blodau	10 % Concept; Field work; Discussion of results; Manuscript preparation

Study 3
Evaluation of peat cores as archives of polychlorinated biphenyl deposition rates

S. Thuens	70 % Laboratory work; Field work; Data analysis; Discussion of results; Manuscript preparation
M. Radke	20 % Concept; Field work; Discussion of results; Manuscript preparation
C. Blodau	10 % Concept; Field work; Discussion of results; Manuscript preparation

Study 4

Ombrotrophic peat bogs as natural archives to investigate the historical atmospheric deposition of perfluorinated compounds

S. Thuens   10 % Field work; Discussion of results; Manuscript preparation

A. Dreyer   60 % Concept; Laboratory work; Data analysis; Discussion of results; Manuscript preparation

T. Kichgeorg   20 % Laboratory work; Discussion of results; Manuscript preparation

M. Radke   10 % Discussion of results; Manuscript preparation

Study 5

Comparison of atmospheric travel distances of several PAHs and metals calculated by two fate and transport models (The Tool and ELPOS) with experimental values derived from a peat bog transect

S. Thuens   60 % Data analysis; Discussion of results; Manuscript preparation

M. Radke   20 % Data analysis; Discussion of results; Manuscript preparation

F. Wania   15 % Discussion of results; Manuscript preparation

C. Blodau   5 % Discussion of results; Manuscript preparation

APPENDIX

Study 1

Application of XAD-resin based passive air samplers to assess local (roadside) and regional patterns of persistent organic pollutants

Paul Barthel , Sabine Thuens , Chubashini Shunthirasingham ,
John N. Westgate , Frank Wania ,
Michael Radke

Contents lists available at SciVerse ScienceDirect

Environmental Pollution

journal homepage: www.elsevier.com/locate/envpol
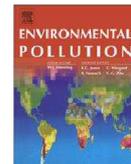
Application of XAD-resin based passive air samplers to assess local (roadside) and regional patterns of persistent organic pollutants

Paul Barthel [a], Sabine Thuens [a], Chubashini Shunthirasingham [b], John N. Westgate [b], Frank Wania [b], Michael Radke [a, c, *]

[a]Department of Hydrology, BayCEER, University of Bayreuth, 95440 Bayreuth, Germany
[b]Department of Physical and Environmental Sciences, University of Toronto Scarborough, 1265 Military Trail, Toronto, Ontario, Canada M1C 1A4
[c]Department of Applied Environmental Science, Stockholm University, 10691 Stockholm, Sweden

a r t i c l e   i n f o

*Corresponding author.
E-mail address: michael.radke@itm.su.se (M. Radke).

ABSTRACT

We used XAD-resin based passive air samplers (PAS) to measure atmospheric levels of polycyclic aromatic hydrocarbons (PAHs) and polychlorinated biphenyls (PCBs) at five ombrotrophic bogs in Eastern Canada. The aims of our study were to investigate the influence of local roads on contaminant levels in the bogs, to derive the regional pattern of atmospheric concentrations, and to assess the uncertainties of the method. Expanded uncertainties based on the duplicate PAS deployed at 24 sites were good for the PAHs, while the deployment period of approx. 100 days was too short to yield acceptable uncertainties for PCBs. The regional PAH distribution was in good agreement with the calculated source proximity of the sampled bogs. We conclude that XAD-resin based PAS deployed for comparatively short periods are well suited for measuring atmospheric concentrations of volatile PAHs, while in remote regions longer deployment is necessary for less volatile PAHs and for PCBs.

1. Introduction

Polycyclic aromatic hydrocarbons (PAHs) and polychlorinated biphenyls (PCBs) are semi-volatile, persistent and toxic organic pollutants, and as such have raised health and environmental concerns for several decades. PAHs are released to the atmosphere mainly by incomplete combustion of organic matter, notably burning of fossil fuels and biomass for industrial and domestic use, vehicle emissions, and forest fires (Ravindra et al., 2008). PCBs - which were banned worldwide in 2001 - are still emitted to the environment from old production facilities, from equipment still containing PCBs, and from waste disposal sites. Moreover, volatilization from soils and sediments is a potential secondary source for atmospheric PCBs (Bozlaker et al., 2008).

During the last decade, passive air samplers (PAS) have become a valuable tool for recording spatial and temporal trends in the air concentrations of persistent organic pollutants. Compared to active air samplers, their benefits are simplicity, low cost, and independence of a power supply. PAS can thus be deployed even in remote regions with no maintenance necessary beyond deployment and retrieval (Gouin et al., 2008; Harner et al., 2004). XAD-based PAS (Wania et al., 2003) have been successfully used to measure gas phase concentrations of organochlorine pesticides (Daly et al., 2007b), PAHs (Choi

et al., 2009; Westgate et al., 2010), and of PCBs and polybrominated diphenylethers (Shen et al., 2006) on various spatial scales.

In an ongoing study in Eastern Canada, we are using ombrotrophic bogs along a transect between Sudbury and Ottawa as archives for atmospheric deposition of PAHs and PCBs. The sampled bogs are located next to roads of various sizes. Since vehicular internal combustion engines are a potentially important PAH source, we have to verify that the sampling site in each bog is not influenced by direct roadside emissions of PAHs. Thus, the primary aim of this study was to determine the influence of traffic emissions on the bog sampling sites and to determine the distance from the road where the local PAH deposition becomes negligible relative to the regional background. While several authors have analyzed natural organic media like soil and leaf litter to study the distribution of PAHs next to roads (Glaser et al., 2005; Pathirana et al., 1994; Tuhácková et al., 2001), this is the first attempt to use passive air samplers for that purpose. Duplicate PAS were deployed at four bogs along transects from the road into the bog; one bog located close to the city of Ottawa was sampled with duplicate PAS. Moreover, we were aiming to compare differences in PAH and PCB concentrations along the investigated regional transect. Finally, the exceptionally high number of duplicate samplers deployed at each bog allows for a thorough uncertainty assessment of the whole method associated with the analysis of PAHs and PCBs using XAD-based passive air samplers.

2. Material and methods

2.1. Sampling

XAD-based PAS were used to determine the concentration of PAHs and PCBs in the air. These PAS consist of a stainless steel mesh cylinder filled with XAD-2 resin (Supelco, USA) which is suspended in a stainless steel can that serves as protective shelter. The can has an open bottom and small openings in the upper part to allow air exchange. For transport, the mesh cylinders were placed into aluminum tubes and sealed with PTFE-lined rubber stoppers. Mesh cylinders and transport tubes were baked overnight at 450 –C before use. A detailed description of sampler design and operation is provided elsewhere (Wania et al., 2003). In this study, however, a sampling cylinder only half as long as described in Wania et al. (2003) was used. As we assumed a net deposition of the target compounds to the bogs (high organic matter content, continuous growth) and the study was focusing on differences at the peat surface, samplers were mounted approx. 50 cm

above ground on steel poles. This comparatively low deployment height was also benefi-
cial from a practical point of view as anchoring longer poles would have been difficult in
the peat. The PAS were deployed from the end of May until early September 2009 (98-
104 days; see Supplementary material for exact periods).

We studied five bogs located along a west-east transect in Ontario, Canada, between the
cities of Sudbury and Ottawa: Giant Bog (GB; 46° 25.159`N, 79°56.001`W), Eagle Lake
Bog (ELB; 45°48.196`N, 79°26.397`W), Spruce Bog (SB; 45°35.172`N, 78°22.125`W),
Green Lake Bog (GLB; 45°41.056`N, 77°09.041`W), and Mer Bleue (MB; 45°24.375`N,
75°30.580`W) (Fig. 1). All bogs except MB are located in rural areas but relatively close
to roads. The traffic volume of these roads e two provincial highways (SB, GB) and two
smaller, unpaved roads (ELB, GLB) e is markedly different. Traffic rates in the months
July and August 2006 on Highway 60 next to Spruce Bog and on Highway 64 next to
Giant Bog were 4050 and 1750 vehicles per day, respectively, with a percentage of
commercial truck traffic of 15% counts were available, but traffic volumes there are as-
sumed minor. At GB the road was elevated by approx. 3 m above the bog surface,
whereas at the other sites the difference between road and bog was less than 1 m. Mer
Bleue, which was included in this study for comparison purposes, is located close to the
city of Ottawa but not directly next to a road. The average air temperatures obtained from
five official weather stations in the study area were relatively uniform and ranged from
15.5° C to 18.9°C for the whole the deployment period.

At each bog except MB, duplicate PAS were deployed along a transect from the road into
the bog. GB was sampled most intensely with PAS being deployed at distances of 2.5 m,
5 m, 20 m, 50 m, 100 m, 200 m, 440 m, and 550 m from the road. At SB, PAS were de-
ployed at 3 m, 5 m, 100 m, 400 m, and 500 m, and at Eagle Lake Bog (ELB) and Green
Lake Bog (GLB) at about 3 m, 6 m, 100 m, 150 m, and 250 m. The second-most distant
site corresponded to the site where peat samples were taken in the concurrent study. At
MB, duplicate PAS were deployed in the ombrotrophic section of the bog.
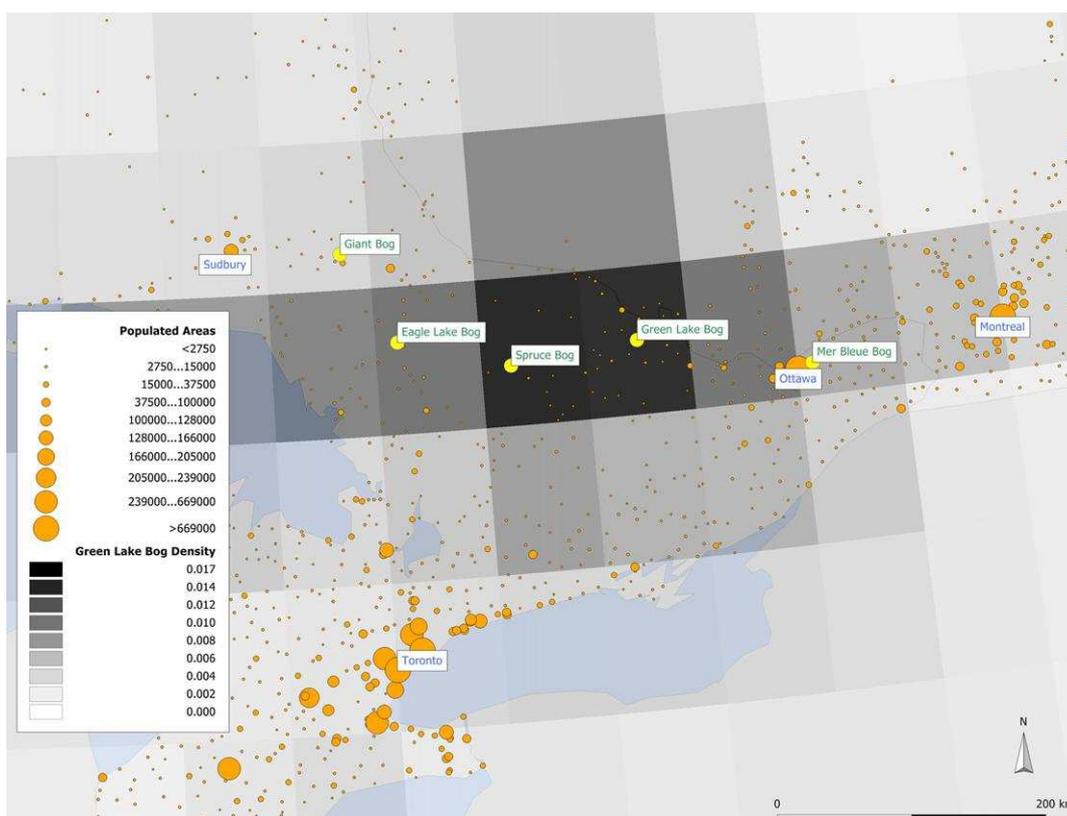
Fig. 1. Locations of sampled bogs (yellow), cities (orange), and back trajectory airshed for Green Lake Bog. The density is the fraction of air-mass back trajectory endpoints that fall within a given 1 degree of latitude by 1 degree of longitude quadrangle, and can be regarded as the relative contribution of each quadrangle to the air that was sampled at Green Lake Bog. (For interpretation of the references to colour in this figure legend, the reader is referred to the web version of this article.)

2.2. Extraction and analysis

Details on the analytical method are available as Supplementary material. Briefly, the XAD-2 resins were Soxhlet extracted, the extracts were then concentrated by a rotary evaporator and under a stream of nitrogen, and finally analyzed with GC-MS (PAHs) and High-Resolution GC-MS (PCBs). Internal standards (see below) were used to correct for recovery, and Mirex was used as injection standard for both PAHs and PCBs. PCB results were blank corrected based on the average of four solvent blanks and seven XAD-2 blanks. Blank correction for PAH was based on the average of seven XAD-2 blanks. Average recovery rates ($\pm$ standard deviations) of the internal PAH standards were $49 \pm 10\%$, $88 \pm 15\%$, $90 \pm 12\%$, and $90 \pm 12\%$ for D_8-Naphthalene, D_{10}-Fluorene, D_{10}-Phenanthrene, and D_{10}-Fluoranthene, respectively. For PCBs, average recovery rates ($\pm$ standard deviations) of the internal standards $^{13}C_{12}$-PCB-9, $^{13}C_{12}$-PCB-15, $^{13}C_{12}$-PCB-32, and PCB-198 were $96 \pm 28\%$, $108 \pm 27\%$, $101 \pm 30\%$, and $162 \pm 32\%$, respectively.

2.3. Calculations

Results are reported as sequestered amount of each compound per PAS (ng PAS^{-1}). For PAHs, these amounts were also converted into air concentrations (ng m^{-3}) using the length of the deployment period and compound specific sampling rates given in the Supplementary material. The uncertainties were calculated by error propagation from the standard deviation of the replicate PAS per site and the reported standard deviation of the sampling rates. To analyze the relation between PAH levels and distance to the road, the sequestered amounts were log transformed and regressed against the distance (m); a significance level of $p < 0.05$ was set. For the determination of the regional PAH levels along the transect, the results from all passive samplers were averaged at sites ELB, GLB, and MB, while at GB and SB only the results from the two most distant sampling sites ($\geq$ 400 m) were averaged. The resulting values are referred to as "regional background concentrations". For PCBs, the median of all samplers at one bog was used to calculate the regional concentration levels. Regional background concentrations were tested for significant differences using a Wilcoxon-Mann-Whitney test (U-test). To determine PCB chlorination profiles, we calculated the sum of the median concentrations of congeners with the same number of chlorine atoms.

Mean differences between duplicates were used as a measure of the precision of the results. The relative standard uncertainty and expanded relative standard uncertainty were calculated as described in the ISO 20988 guideline (International Organization for Standardization (ISO), 2007). A coverage probability of $p = 95\%$ was used for these calculations. The uncertainty analysis was based on sequestered amounts per passive sampler (ng PAS^{-1}).

Back trajectory probability maps, referred to as "airsheds", were calculated as described in Daly et al. (2007c) for the sampled bogs. These airsheds display probability densities of trajectories, indicating where the air parcels at the specific site are most frequently originating from. Cities and towns are also included in these maps.

The proximity of the bogs to probable sources of PAHs was estimated by adapting the Dispersion Pertingency Index (PI$_D$) from Westgate et al. (Westgate et al., 2010). Briefly, the population of each town or city in Ontario and Quebec was weighted with the inverse square of the distance to each bog, then summed and normalized to give a unique PI$_D$ for each bog. The scaling factor f from that work was set to unity. The locations and populations of the small towns of Ontario and Quebec were taken from the Canadian 1986 cen-

sus data, in which populations are expressed as a range (e.g., 500 to 4999 persons), and the middle value was used for the calculation (e.g. 2750) (see Natural Resources Canada, 2010). For large cities (e.g. Ottawa, Toronto, Montreal; a complete list is available as Supplementary material) the populations were taken from the 2006 Canadian Census database (Statistics Canada, 2010). Populations to the south beyond the border with the United States of America were ignored. Distances between the bogs and the towns and cities were determined using Manifold 8.0 GIS software using an Azimuthal Equidistant projection.

3. Results

3.1. Polycyclic aromatic hydrocarbons

Only the relatively volatile and abundant two- to four-ring PAHs naphthalene (Nap), fluorene (Flu), phenanthrene (Phe), and fluoranthene (Flt) were detected in quantifiable amounts in most samples. Generally, Nap was the most abundant compound with concentrations between 74 and 600 ng PAS^{-1}, followed by Phe (5.5 - 44 ng PAS^{-1}), Flu (4 - 25 ng PAS^{-1}), and Flt (not detected to 11 ng PAS^{-1}). The sequestered amounts of these compounds in each sampler are available as Supplementary material.

The spatial pattern as a function of distance to the road was different among the bogs (Fig. 2). At GB concentrations increased substantially within the first 20 m and then decreased significantly ($p < 0.05$) from 100 m onwards following a log-linear relationship. In contrast, at SB concentrations of all four PAH were highest directly next to the road and then followed e with the exception of Nap e a log-linear decrease ($p < 0.05$) along the transect into the bog. At ELB, no significant spatial trend was observed, while at GLB the concentrations of Flu and Phe increased significantly on a log-normal scale along the transect into the bog.
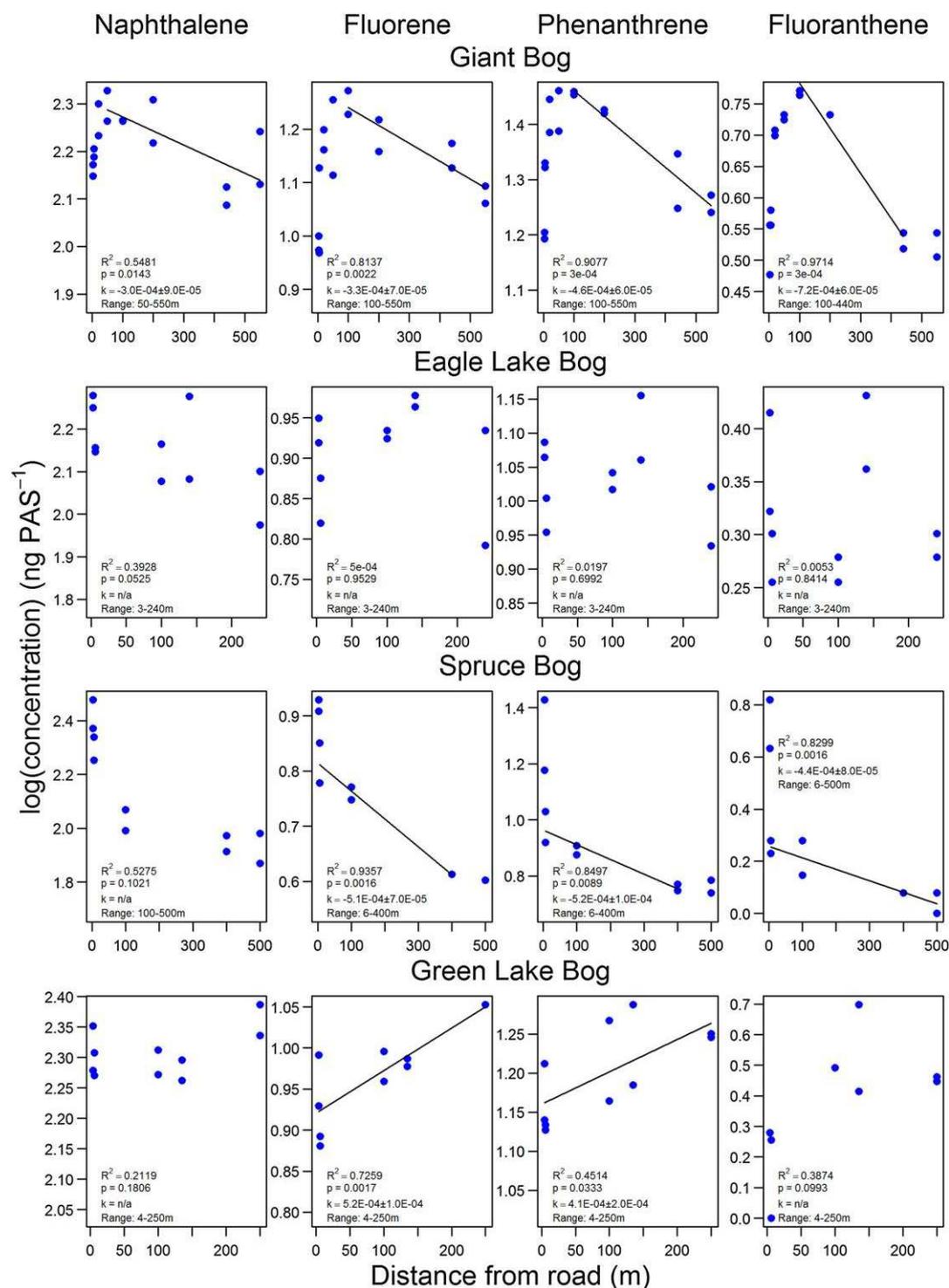
Fig. 2. Logarithmic sequestered amounts of PAHs as a function of distance to the road. The range used for calculating the regression is given in the individual plots, as well as the slope of the regression line (k) _ the error of the slope, the significance level (p), and the regression coefficient (R²). n/a: slope of regression line not significantly different from zero (p > 0.05). The regression line is only shown for significant cases.

The regional PAH background concentrations varied by a factor of 7 between the bogs (Fig. 3); with few exceptions concentrations were significantly different between bogs

(p < 0.05, 6 < n < 20; U-test; see Supplementary material for details). Concentrations were highest at MB which is located next to the city of Ottawa, while SB was the site with the lowest PAH concentrations. Along the first three bogs on the West-East transect, concentrations decreased and then increased again at the two Eastern sites which are located in more densely populated areas.
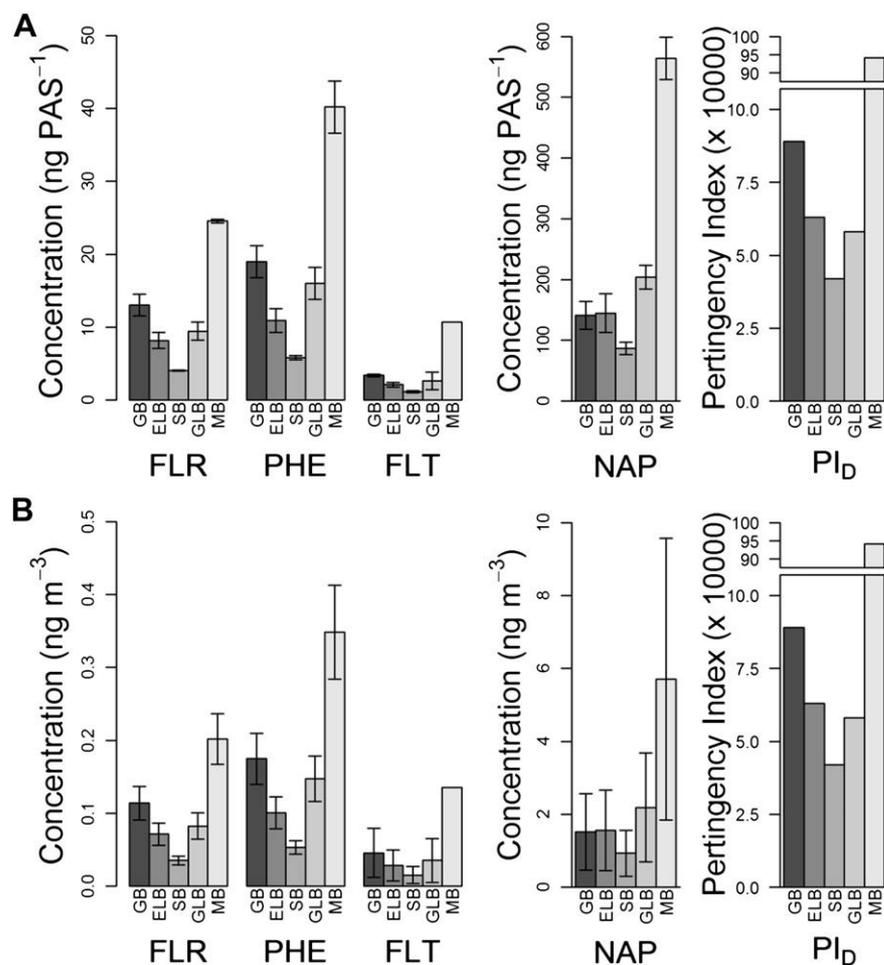
Fig. 3. Background concentrations (arithmetic means) of PAHs and Pertingency Index PI$_D$ along the bog transect. A. Concentration per passive sampler (ng PAS^{-1}); B. Air concentrations (ng m^{-3}) converted with sampling rates and length of deployment period. Number of observations: 4 (GB), 10 (ELB), 4 (SB), 10 (GLB), 2 (MB). Error bars represent standard deviations (A) and combined standard deviations from PAS and sampling rates (B). As only 2 samplers were deployed at MB, the error bars for the MB data represent the range of measured values instead of standard deviations; Fluoranthene data are only available for one of the samplers

The Dispersion Pertingency Index PI$_D$ reflects the same regional pattern as the PAH concentrations (Fig. 3); the value for the MB site is disproportionately high. The concentrations of Flt, Flr, and Phe were significantly correlated (p < 0.05) to PI$_D$ among the first three sites of the west-east transect (GB, ELB, SB); data for sites GLB and MB are outside this correlation (Fig. 4). No such correlation was observed for Nap. If all four bogs

are taken into account, a significant correlation ($p < 0.1$) is observed for Flr and Flt, while the Phe concentration does not correlate any more to PI_D (see Supplementary material for details).

The mean difference between duplicate samplers was 15% (n = 24), 10% (n = 24), 13% (n = 24), and 16% (n = 21) for Nap, Flu, Phe, and Flt, respectively, indicating good reproducibility of the results. Histograms illustrating the distribution of the relative differences of duplicates are available as Supplementary material. The expanded relative standard uncertainties calculated for a level of confidence of 95% (w_{95}) (International Organization for Standardization (ISO), 2007) based on all duplicate samplers were 25% (NAP), 21% (FLU), 32% (PHE), and 47% (FLT), respectively. Additional information is available as Supplementary material.

3.2. Polychlorinated biphenyls

The PCB congeners 101, 110, 95, 87, 52, 99, 149, 153, 44, and 138 were most abundant (in that descending order) and accounted on average of all samples for 84% of $\sum$PCB. Median concentrations of individual PCBs ranged from 0.17 ng PAS^{-1} to 6.1 ng PAS^{-1}. In Fig. 5A $\sum$PCB concentrations for each bog are displayed. The sequestered amounts of PCBs at GLB and MB were substantially higher than at the other sites. In contrast to the PAHs, PCB concentrations were highest at GLB.

The PCB chlorination profiles (based on the median concentrations of the individual compounds) (Fig. 5B) show a relative enrichment of penta- and hexa-CBs and a relative depletion of di-to tetra-CBs at GLB compared to the three more remote bogs. Results for Mer Bleue are not shown in Fig. 5B since median concentrations of only two replicates are highly uncertain.

The mean difference of PCB concentrations between duplicates was in the range of 50-60% and thus about three times as high as for the PAHs; the spread of the differences between duplicate samplers was substantial (see histograms provided as Supplementary material). Moreover, the expanded relative standard uncertainty w_{95} for the five compounds with the highest concentrations was substantially higher than for the PAH: 84% (PCB-52), 307% (PCB-87), 122% (PCB-95), 176% (PCB-101), and 340% (PCB-110) (see Supplementary material).

4. Discussion

4.1. Methodological aspects

The deployment period of approx. 3 months during summer was sufficient to determine reliable and robust estimates of the atmospheric levels of the studied PAHs also at the more remote sites. The expanded uncertainties for all four PAHs were lower than the 50% threshold value for the analysis of airborne PAH defined by the EU directive 2004/107/EC (The European Parliament and the Council of the European Union, 2005). Thus, we conclude that the PAS used in this study e which are usually deployed for longer periods e can also be used to determine seasonal trends for these compounds. Due to the shorter deployment period, the relatively volatile and abundant PAHs studied here did not reach equilibrium between ambient air and the XAD-2 resin, which may occur during a whole-year deployment period (Daly et al., 2007a). Flt was generally the compound present at the lowest concentrations. This is reflected in a higher uncertainty of Flt data ($w_{95} = 47\%$) compared to the other compounds ($w_{95} = 32\%$).

The deployment period was not sufficiently long to allow for the determination of PAHs with higher molecular weight. This is due to a combination of the lower gas phase concentrations of these compounds e they are bound to aerosol particles to a larger extent (St-Amand et al., 2008; Su et al., 2006), and aerosol particles are not accessible to the PAS (Wania et al., 2003) e and the detection limits of the analytical method.

The uncertainties for individual PCBs are much higher than the 50% threshold value for PAHs (The European Parliament and the Council of the European Union, 2005) and the theoretical w_{95} of 23.3% derived by Brown and Brown (Brown and Brown, 2008). The high uncertainty can be attributed to the short deployment period which resulted in concentrations in the final extracts close to the method detection limit. However, the availability of a high number of replicate samplers per site compensates for the poor side-by-side reproducibility since median concentrations are substantially more representative than single measurements. Therefore, we consider the general findings of this study still valid in spite of the comparatively high uncertainty. However, this is different for MB where only two samplers were installed. To determine PCB levels at similarly remote sites with less uncertainty, longer PAS deployment periods than the three months used here should be applied.

4.2. Variability of airborne PAHs and PCBs on a local scale

A priori we expected to measure highest PAH levels directly next to the major roads, followed by a log-linear decrease with distance from the road due to dispersion and deposition processes. At Spruce Bog (SB) next to Highway 60, this general pattern was observed. However, the samplers closest to the road (3 m) sequestered disproportionately high amounts of PAH. This observation is similar to findings by Tuhácková et al. (2001) who reported a sharp decline of Phe and Flt concentrations in roadside soils within the first 1.5 m. An exponential decrease of PAH concentrations in leaf litter between 1 and 30 m distance from the road has previously been reported by Pathirana et al. (1994).

At SB, the difference between the two most distant sampling sites (400 and 500 m) was marginal and thus we conclude that these two sites are not influenced by roadside emissions. The concentration ratio between the roadside and the most distant sites (400 and 500 m) was <5, whereas Tuhácková et al. (2001) reported a PAH concentration next to the road which was 30 times higher than the background concentration at a distance of 500 m. This difference can be attributed to much higher emissions at the site studied by Tuhácková et al. (2001) which had a daily traffic volume of 90,000 cars. In comparison, the daily traffic volume on the highway at SB was only 4000 cars.

In contrast to SB, PAH concentrations along the transect into GB increased from 2.5 m to 50 m (Nap) and 100 m (Flu, Phe, Flt) before they decreased with increasing distance (Fig. 2). The unexpected concentration increase within the first 100 m of the transect is most probably due to the road being elevated approx. 3 m above the bog. The comparatively warm vehicle exhausts should move preferentially upwards after release, and thus we hypothesize that the PAS close to the road were not exposed to representative concentrations. A similar process has been reported to cause an enrichment of lighter PAHs with increasing height above the road (Bryselbout et al., 2000). Moreover, the PAS closest to the road was densely covered by tall grass at the end of the sampling period. As at SB, the concentration difference between the two most distant sampling sites at GB was marginal (except for Flu) and thus we conclude that the impact of roadside emissions on these sites was negligible. Generally, the ratio between highest and lowest concentrations was ≤ 2 and thus we conclude that the influence of roadside emissions on PAH levels was rather low.

PAH concentrations at ELB and GLB (Fig. 2), which both are located next to small roads did not decrease with increasing distance to the road. For the significant increase of Flu

and Phe concentrations with distance from the road at GLB, there are two possible explanations: i) At the time of retrieval the two samplers close to the road were found partly covered by vegetation and one of them inside a hedge of loose shrubs. Therefore, PAH concentrations in these samplers could be underestimated. ii) Several houses are located a few hundred meters from the installed samplers. Emissions from residential summer activities (e.g., barbecuing, bonfires) during the deployment period could have caused locally unequal PAH dispersion. However, this spatial pattern can also be considered relatively uncertain as it was only observed for two of the four compounds and the scattering of the data is rather high. The ratio of maximum to minimum concentrations of all compounds were ≤ 2 (ELB) and < 1.5 (GLB), with the exception of Flt at site GLB (5). The latter reflects the comparatively high uncertainty of the Flt data since especially at GLB, the concentrations scattered substantially.

For PCBs, no dependence of concentration on distance from the road was observed. This was to be expected since vehicular emissions are no source of atmospheric PCBs.

With respect to the primary aim of this study, we conclude that the sites where peat was sampled in the concurrent project were receiving regionally rather than locally (i.e., traffic related) emitted PAHs. Based on the results of this study, a sampling distance of 400 m from highways with a traffic volume of less than 4000 cars per day seems "safe" to determine regional concentrations of the comparatively volatile PAHs analyzed; for minor roads this distance should be at least 100 m.

4.3. Variability of airborne PAHs and PCBs on a regional scale

The regional PAH distribution along the East-West transect (Fig. 3) reflects the proximity of the bogs to urban areas and other important point sources. SB can be considered as representative for the regional PAH background concentrations since there are no other PAH sources than the highway (which does not influence the background samplers in 400 and 500 m distance) and a visitor center (800 m) in the vicinity of the site and the population density around SB is extremely low. In the studied region westerly winds are prevailing (see airshed for GLB, Fig. 1), and thus the decreasing concentrations from GB to SB (Fig. 3) reflect an increasing distance to a major emission source west of the studied bogs. As metal and aluminum production in general are known to be the largest sources of PAH to the North American atmosphere (Galarneau et al., 2007), this emission source is most probably the Sudbury mining complex with its large nickel and cop-

per smelters located approx. 80 km east of GB. Traffic influence can be ruled out as cause for the significantly higher background concentrations at GB compared to SB since the traffic volume on the GB highway is lower than that on the SB highway and the background sites at the bogs were not influenced by the roadside emissions. Moreover, as temperatures in the studied region were comparatively uniform, temperature-dependent differences in sampling efficiency (Gouin et al., 2008) of the PAS at the individual bogs can also be excluded as cause for the observed concentration differences.
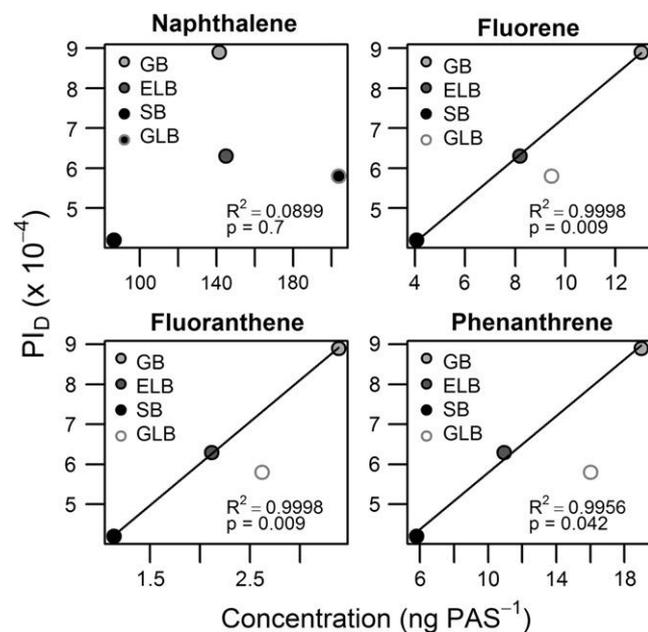
Fig. 4. Correlation between Dispersion Pertinency Index (PI_D) and the PAH back-ground concentrations. Site MB is not shown. Only data points shown in filled circles were included in the correlation analysis.

As expected, PAH concentrations were highest at MB which is located next to the city of Ottawa. SB was the most pristine site with respect to PAH concentrations. The correlation ($p < 0.05$) between the measured background concentrations of Flr, Flt, and Phe to the calculated PI_D for the three westerly bogs (Fig. 4) confirms that the measured concentration at sites GB, ELB, and SB reflect the regional background concentration. If GLB is included in the analysis, the correlation between concentration and PI_D is still significant for FLR ($p < 0.05$) and FLT ($p < 0.1$). The deviation of the GLB site can most probably be attributed to a combination of the overall methodological uncertainties and to a minor local PAH source, as is indicated by the increasing air concentration with distance from the road (see above).

As no dependence of PCB concentrations from distance to the road was expected and observed, the results of all samplers per bog can be used to analyze PCB distributions. Because of the comparatively large uncertainties of the PCB concentrations (see above) and the only two replicates, the MB site is not considered here. The low sequestered PCB amounts at GB, ELB and SB reflect a large distance to major emission sources. In contrast, the comparatively high PCB concentrations at GLB indicate a closer proximity to sources of atmospheric PCBs. These sources could be related to the general population density and to the volatilization of PCBs from old transformers or contaminated sites. Moreover, the proximity to Chalk River Laboratories, a nuclear research facility approx. 45 km north-west of GLB, and the comparatively high density of generating stations in the GLB area (Natural Resources Canada, 2007) are other indicators for potential PCB sources as these compounds were heavily used in such operations in the past.
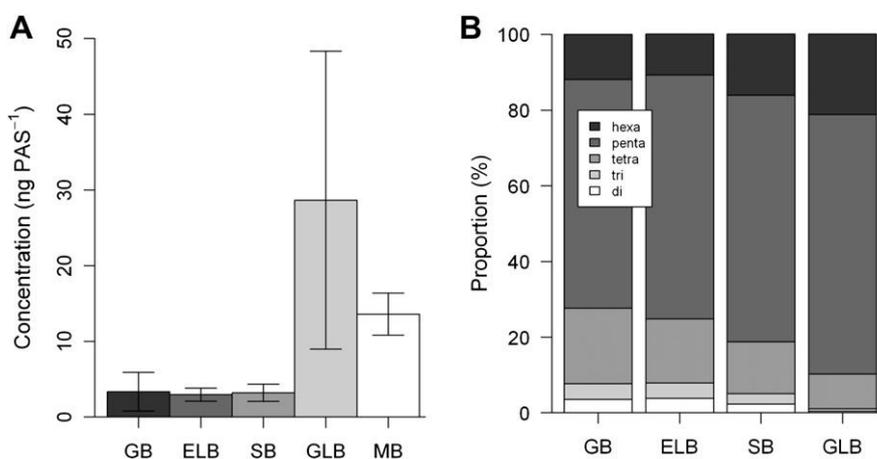
Fig. 5. A. Median SPCB concentrations along the bog transect. Number of observations: 16 (GB), 9 (ELB), 8 (SB), 9 (GLB), 2 (MB). Error bars represent standard deviations. B. PCB chlorination profiles at the sampled bogs based on the median concentrations of the individual congeners. Site MB not shown because of the low number of replicates.

The PCB chlorination profiles provide additional insight into proximities of the sampled bogs to potential sources. Airborne PCBs with low degree of chlorination are relatively more enriched in areas remote from urban/industrial sources compared to the higher chlorinated ones (Du et al., 2009; Harner et al., 2004). This is attributed to the gas-particle partitioning behavior of higher chlorinated PCB being associated with particles to a greater extent than lower chlorinated ones (Li et al., 2008) and differential removal processes in the atmosphere (von Waldow et al., 2010). Due to the faster deposition of particles, the higher chlorinated congeners consequently have a shorter atmospheric transport distance. This behavior is reflected in the chlorination profiles at the sampled

bogs (Fig. 5B) with a relative enrichment of penta- and hexa-CBs and depletion of di- to tetra-CBs at GLB compared to the three bogs to the west. This indicates a closer proximity of GLB to PCB sources and is in line with the observed elevated concentrations at GLB (Fig. 5).

Overall, we conclude that XAD-resin based PAS are well suited to monitor both local and regional patterns of atmospheric PAH concentrations on comparatively short time-scales with high reproducibility. However, this applies only to the more volatile and abundant low molecular weight PAHs which are predominantly present in the gas phase. The gas phase concentrations of PAHs with higher molecular weight were too low and did not allow detection; for PAS-based monitoring of such compounds in remote regions, longer deployment periods are necessary. For PCBs, some general trends could be derived, but longer deployment periods are advised due to the high overall uncertainties.

Acknowledgments

Appendix. Supplementary material

Supplementary material associated with this article can be found in the online version, at doi:10.1016/j.envpol.2012.03.026.

References

Bozlaker, A., Odabasi, M., Muezzinoglu, A., 2008. Dry deposition and soil-air gas exchange of polychlorinated biphenyls (PCBs) in an industrial area. Environmental Pollution 156, 784-793.

Brown, A.S., Brown, R.J.C., 2008. A study of the critical uncertainty contributions in the analysis of PCBs in ambient air. Journal of Automated Methods & Management in Chemistry 14. Article ID 179498.

Bryselbout, C., Henner, P., Carsignol, J., Lichtfouse, E., 2000. Polycyclic aromatic hydrocarbons in highway plants and soils. Evidence for a local distillation effect. Analusis 28, 290-293.

Choi, S.D., Shunthirasingham, C., Daly, G.L., Xiao, H., Lei, Y.D., Wania, F., 2009. Levels of polycyclic aromatic hydrocarbons in Canadian mountain air and soil are controlled by proximity to roads. Environmental Pollution 157, 3199-3206.

Daly, G.L., Lei, Y.D., Castillo, L.E., Muir, D.C.G., Wania, F., 2007a. Polycyclic aromatic hydrocarbons in Costa Rican air and soil: a tropical/temperate comparison. Atmospheric Environment 41, 7339-7350.

Daly, G.L., Lei, Y.D., Teixeira, C., Muir, D.C.G., Castillo, L.E., Jantunen, L.M.M., Wania, F., 2007b. Organochlorine pesticides in the soils and atmosphere of Costa Rica. Environmental Science & Technology 41, 1124-1130.

Daly, G.L., Lei, Y.D., Teixeira, C., Muir, D.C.G., Castillo, L.E., Wania, F., 2007c. Accumulation of current-use pesticides in neotropical montane forests. Environ-mental Science & Technology 41, 1118-1123.

Du, S., Wall, S., Cacia, D., Rodenburg, L., 2009. Passive air sampling for polychlorinated biphenyls in the Philadelphia Metropolitan area. Environmental Science & Technology 43, 1287-1292.

Galarneau, E., Makar, P.A., Sassi, M., Diamond, M.L., 2007. Estimation of atmospheric emissions of six semivolatile polycyclic aromatic hydrocarbons in southern Canada and the United States by use of an emissions processing system. Environmental Science & Technology 41, 4205-4213.

Glaser, B., Dreyer, A., Bock, M., Fiedler, S., Mehring, M., Heitmann, T., 2005. Source apportionment of organic pollutants of a highway-traffic-influenced urban area in Bayreuth (Germany) using biomarker and stable carbon isotope signatures. Environmental Science & Technology 39, 3911-3917.

Gouin, T., Wania, F., Ruepert, C., Castillo, L.E., 2008. Field testing passive air samplers for current use pesticides in a tropical environment. Environmental Science & Technology 42, 6625-6630.

Harner, T., Shoeib, M., Diamond, M., Stern, G., Rosenberg, B., 2004. Using passive air samplers to assess urbanerural trends for persistent organic pollutants. 1. Polychlorinated biphenyls and organochlorine pesticides. Environmental Science & Technology 38, 4474-4483.

International Organization for Standardization (ISO), 2007. ISO 20988: Air Quality - Guidelines for Estimating Measurement Uncertainty.

Li, Y., Jiang, G., Wang, Y., Wang, P., Zhang, Q., 2008. Concentrations, profiles and gas-particle partitioning of PCDDFs, PCBs and PBDEs in the ambient air of an E-waste dismantling area, southeast China. Chinese Science Bulletin 53, 521-528.

Natural Resources Canada, 2007. The Atlas of Canada. Generating Stations Map. Natural Resources Canada, 2010. The Atlas of Canada: Digital Base Map Data. Ontario Ministry of Transportation, 2006. Ontario Provincial Highways Traffic Volumes 1988-2006.

Pathirana, S., Connell, D.W., Vowles, P.D., 1994. Distribution of polycyclic aromatic hydrocarbons (PAHs) in an Urban Roadway System. Ecotoxicology and Envi-ronmental Safety 28, 256-269.

Ravindra, K., Sokhi, R., Van Grieken, R., 2008. Atmospheric polycyclic aromatic hydro-carbons: source attribution, emission factors and regulation. Atmospheric Environment 42, 2895-2921.

Shen, L., Wania, F., Lei, Y.D., Teixeira, C., Muir, D.C.G., Xiao, H., 2006. Polychlorin-ated biphenyls and polybrominated diphenyl ethers in the North American atmosphere. Environmental Pollution 144, 434-444.

St-Amand, A.D., Mayer, P.M., Blais, J.M., 2008. Seasonal trends in vegetation and at-mospheric concentrations of PAHs and PBDEs near a sanitary landfill. Atmospheric En-vironment 42, 2948-2958.

Statistics Canada, 2010. Population and Dwelling Counts, for Canada, Provinces and Territories, and Census Subdivisions (municipalities), 2006 and 2001 Censuses. 100% data, 2010-01-06 ed.

Su, Y., Lei, Y.D., Wania, F., Shoeib, M., Harner, T., 2006. Regressing gas/particle par-titioning data for polycyclic aromatic hydrocarbons. Environmental Science & Technol-ogy 40, 3558-3564.

The European Parliament and the Council of the European Union, 2005. Directive 2004/107/EC of the European Parliament and of the Council of 15 December 2004 relat-ing to arsenic, cadmium, mercury, nickel and polycyclic aromatic hydrocarbons in ambi-ent air. Official Journal of the European Union.

Tuhácková, J., Cajthaml, T., Novák, K., Novotný, C., Mertelík, J., Sasek, V., 2001. Hy-drocarbon deposition and soil microflora as affected by highway traffic. Environmental Pollution 113, 255-262.

von Waldow, H., MacLeod, M., Jones, K., Scheringer, M., Hungerbuhler, K., 2010. Re-moteness from emission sources explains the fractionation pattern of Polychlorinated Biphenyls in the Northern hemisphere. Environmental Science & Technology 44, 6183-6188.

Wania, F., Shen, L., Lei, Y.D., Teixeira, C., Muir, D.C.G., 2003. Development and cali-bration of a resin-based passive sampling system for monitoring persistent organic pollu-tants in the atmosphere. Environmental Science & Technology 37,1352-1359.

Westgate, J.N., Shunthirasingham, C., Oyiliagu, C., von Waldow, H., Wania, F., 2010. Three methods for quantifying proximity of air sampling sites to spatially resolved emis-sions of semi-volatile organic contaminants. Atmospheric Envi-ronment 44, 4380-4387.

SUPPLEMENTARY MATERIAL

Application of XAD-resin based passive air samplers to assess local (roadside) and regional patterns of persistent organic pollutants

Paul Barthel [a], Sabine Thüns [a], Chubashini Shunthirasingham [b], John N. Westgate [b], Frank Wania [b], Michael Radke [a,c]*

[a] Department of Hydrology, BayCEER, University of Bayreuth, 95440 Bayreuth, Germany

[b] Department of Physical and Environmental Sciences, University of Toronto Scarborough, 1265 Military Trail, Toronto, Ontario, Canada M1C 1A4

[c] Department of Applied Environmental Science, Stockholm University, 10691 Stockholm, Sweden

[*] Corresponding author: Michael Radke Stockholm University

       Department of Applied Environmental Science 10691 Stockholm

       Sweden

E-Mail: michael.radke@itm.su.se

Experimental Methods

Deployment periods of the PAS

Table S 1: Deployment periods of PAS

Giant Bog	2009/05/27 – 2009/09/02
Eagle Lake Bog	2009/05/28 – 2009/09/03
Spruce Bog	2009/05/28 – 2009/09/03
Green Lake Bog	2009/05/29 – 2009/09/04
Mer Bleue	2009/05/23 - 2009/09/04

Analytical methods

All glassware was solvent-rinsed several times or baked overnight at 450°C before use. Four solvent blanks and seven XAD-2 blanks were extracted and analyzed together with the samples. Prior to extraction, samples were spiked with 30 ng of deuterated PAHs (containing the 16 EPA PAHs) and 25 ng of a PCB recovery standard ($^{13}C_{12}$-PCB-9 and $^{13}C_{12}$-PCB-15, $^{13}C_{12}$-PCB-32, PCB-198) dissolved in isooctane. The XAD-2 filled sampling cylinders were then Soxhlet extracted for 24 h with 250 mL of dichloromethane (DCM) (99.96%, EMD, USA).

The extracts were concentrated on a rotary evaporator (Büchi, Switzerland), transferred to test tubes, and further reduced to approximately 1 mL under a stream of nitrogen (Organomation Associates, USA). Water in the extracts was removed by filtration through columns filled with 2 mL of baked sodium sulfate (Fisher Scientific, India). Subsequently, the solvent was exchanged to isooctane by adding 2 mL of isooctane to the concentrated extracts which were subsequently reduced to 1 mL in a gentle stream of dry nitrogen and transferred into GC-vials. 100 ng of mirex (>98%, Cambridge Isotope Labs, USA), which was used as injection standard for GC analyses, was added, and samples were further concentrated to a final volume of about 0.3 mL.

For PAH analysis, ten calibration standards at concentrations from 0.27 ng mL^{-1} to 540 ng mL^{-1} were diluted in isooctane from a 16 EPA priority PAH stock solution (99%, Cerilliant Corporation, USA). For recovery calibration, five standards of the deuterated PAHs were prepared at concentrations between 12 ng mL^{-1} and 43 ng mL^{-1}. PAHs were analyzed on a 7890A gas chromatograph (GC) coupled to a 5975C mass spectrometric detector (MSD; both instruments from Agilent, Santa Clara, USA) operated in electron impact ionization mode. PAHs were separated on a DB-5MS column (60 m $\Box$ 0.25 mm $\Box$ 0.10 µm; Agilent) using helium as carrier gas (flow rate: 1.0 mL min^{-1}). The measured data were corrected for recovery using the respective deuterated compounds; for blank correction, the average concentration of the seven resin blanks was subtracted from each sample. Average recovery rates ($\Box$ standard deviations) of the internal standards were 49 $\Box$ 10 %, 88 $\Box$ 15 %, 90 $\Box$ 12 %, and 90 $\Box$ 12 % for D$_8$-Naphthalene, D$_{10}$-Fluorene, D$_{10}$-Phenanthrene, and D$_{10}$-Fluoranthene, respectively.

PCB were analyzed on an HP 6890 plus Series high-resolution GC (Agilent,) coupled to an Autospec Ultima magnetic sector mass spectrometer (Micromass, Ultricham, UK). Electron impact ionization (EI) was used at 34 eV, and detection was carried out in selected ion monitoring (SIM) mode. The transfer line and ion source temperatures were 200°C and 250°C, respectively. Target compounds were separated on a DB-5MS column (15 m × 250 µm × 0.25 µm; Agilent) with helium as carrier gas at constant pressure of 1kPa. Six calibration standards prepared in isooctane were used for quantification at concentrations between 0.2 and 10 ng mL^{-1} (target compounds) and 0.5 to 3.5 ng mL^{-1} (recovery standards), respectively. Due to the sensitivity and linearity of the instrument, the calibration curve could be extrapolated down to 0.05 ng mL^{-1} which was used as limit of quantification. Concentrations < 0.05 ng mL^{-1} were set to 0.025 ng mL^{-1} for further calculations. Samples were analyzed for 56 congeners listed in Table S 2, out of which 26 were present in the samples at sufficiently high concentrations. The sum of these 26 congeners is subsequently referred to as ΣPCB. Results were blank corrected using the mean value of the 4 laboratory blanks and 7 resin blanks. Dichlorinated congeners were recovery corrected with the averaged recovery rate of $^{13}C_{12}$-PCB-9 and $^{13}C_{12}$-PCB-15, trichlorinated congeners with the recovery rate of $^{13}C_{12}$-PCB-32, and tetra- to hexachlorinated congeners with the average recovery rate of $^{13}C_{12}$-PCB-32 and PCB-198. Average recovery rates (± standard deviations) of the internal standards $^{13}C_{12}$-PCB-9, $^{13}C_{12}$-PCB-15, $^{13}C_{12}$-PCB-32, and PCB-198 were 96 ± 28 %, 108 ± 27 %, 101 ± 30 %, and 162 ± 32 %, respectively.

Table S 2: In PAS samples detected PCB congeners grouped according to the number of chlorine atoms

Group	congeners (Ballschmiter number)
Di-CBs	8, 15
Tri-CBs	16, 28, 31, 32, 33
Tetra-CBs	44, 49, 52, 56, 60, 66, 70, 74
Penta-CBs	87, 95, 99, 101, 105, 110
Hexa-CBs	128, 138, 149, 151, 153

Table S 3: Populations of larger Ontario and Quebec cities used to calculate *PI_D*.

City Name	Population	City Name	Population
Ajax	93104	Mississauga	668549
Barrie	128430	Montreal	2921357
Brampton	433806	Newmarket	74295
Brantford	90192	Oakville	165613
Burlington	164415	Oshawa	141590
Cambridge	120372	Ottawa	819263
Clarington	77820	Pickering	100273
Gatineau	242124	Quebec	603267
Guelph	114943	Richmond Hill	181000
Hamilton	504559	Toronto	3427168
Kingston	152358	Vaughan	238866
Kitchener	204668	Waterloo	97475
London	457720	Whitby	111184
Milton	53939	Windsor	216473

Table S 4: Sampling rates (m^3 d^{-1}) for polycyclic aromatic hydrocarbons obtained from a year-long calibration study at Egbert, Ontario as described in Hayward (2010). As the PAS were deployed over the summer, we used the summer rates to convert the amount of sequestered PAH per PAS (ng PAS^{-1}) to air concentrations (ng m^{-3}).

Compound	R (m^3 d^{-1})
naphthalene	0.95 ± 0.64
fluorene	1.17 ± 0.20
phenanthrene	1.11 ± 0.18
fluoranthene	0.76 ± 0.56

Results

Table S 5: Sequestered PAH concentrations (ng PAS^{-1}) of all samplers; results of the replicate samplers are shown in separate columns; N.D. = not detected

	distance	naphthalene		flourene		phenanthrene		flouranthene	
Giant Bog	2.5 m	149	141	10.0	9.4	16.0	15.6	3.65	3.05
	5 m	160	154	13.4	9.3	21.4	21.0	3.76	3.65
	20 m	171	199	14.5	15.8	24.3	27.9	4.99	5.14
	50 m	184	213	13.0	18.0	24.4	28.9	5.39	5.27
	100 m	184	183	18.7	16.9	28.4	28.8	5.87	5.77
	200 m	204	165	14.4	16.5	26.7	26.3	5.44	5.43
	440 m	133	122	14.9	13.4	22.2	17.7	3.54	3.32
	550 m	135	175	11.5	12.4	18.7	17.4	3.18	3.50
Eagle Lake Bog	3 m	190	178	8.3	8.9	11.6	12.2	2.08	2.62
	6 m	140	143	7.5	6.6	10.1	9.0	2.00	1.78
	100 m	120	146	8.4	8.6	11.0	10.4	1.91	1.84
	140 m	121	189	9.2	9.5	11.5	14.3	2.30	2.69
	240 m	94	126	6.2	8.6	8.6	10.5	2.00	1.93
Spruce Bog	3 m	301	235	8.1	8.5	26.8	15.0	6.57	4.26
	6 m	218	179	7.1	6.0	10.7	8.3	1.95	1.67
	100 m	98	117	5.6	5.9	8.1	7.5	1.89	1.37
	400 m	82	94	4.1	4.1	5.9	5.6	1.21	1.18
	500 m	74	96	4.0	4.0	5.5	6.1	0.96	1.20
Green Lake Bog	3.5 m	190	225	8.5	9.8	16.3	13.8	1.86	N.D.
	5.5 m	203	186	7.6	7.8	13.4	13.6	1.77	0.98
	100 m	187	205	9.9	9.1	18.5	14.6	N.D.	3.12
	135 m	183	197	9.5	9.7	19.4	15.3	4.95	2.59
	250 m	244	217	11.3	11.3	17.8	17.6	2.82	2.86
Mer Bleue		599	530	24.8	24.3	43.8	36.6	10.67	N.D.

Table S 6: Details of uncertainty analysis for the four PAHs and the five PCBs with highest sequestered amounts. For details on the individual parameters and calculations please refer to the ISO 20988 guideline (International Organization for Standardization (ISO), 2007). Differences in the number of measurements between the individual compounds are due to samples below the limit of quantification.

	NAP	FLU	PHE	FLT	PCB 52	PCB 87	PCB 95	PCB 101	PCB 110
average rel. difference between duplicates (-)	0.15	0.10	0.13	0.16	0.40	0.62	0.47	0.52	0.63
number of measurements (-)	24	24	24	21	20	22	21	22	22
coverage factor k_{95} (-)	2.09	2.09	2.09	2.09	2.09	2.09	2.09	2.09	2.09
min. range of application (ng PAS^{-1})	74.2	4.0	5.5	1.0	0.03	0.10	0.20	0.33	0.25
max. range of application (ng PAS^{-1})	599.0	24.8	43.8	6.6	0.34	7.30	4.85	13.00	15.80
relative std. uncertainty w (-)	0.12	0.10	0.15	0.22	0.40	1.47	0.59	0.84	1.63
relative expanded 95% uncertainty w_{95} (-)	0.25	0.21	0.32	0.47	0.84	3.07	1.22	1.76	3.40

Figure S 1: Histograms summarizing the distribution of relative differences between concentrations of PAHs and PCBs derived from duplicate PAS.
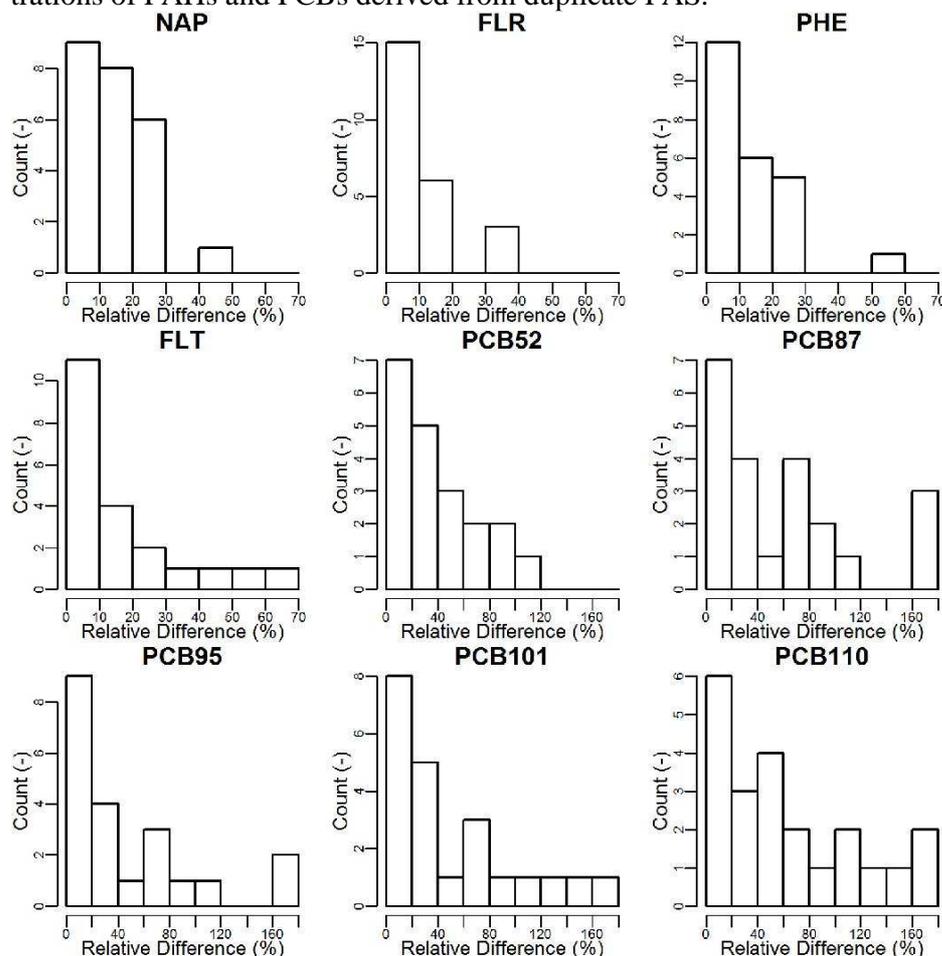
Table S 7: Correlation matrix (U-test) between sequestered amounts of PAHs at the five sites. Flt at site MB could not be analyzed since only one replicate sampler contained this compound at a concentration above the limit of detection. Please note: the results for statistical tests of MB data suffer from the low number of replicate samplers there and thus should be treated with caution.

NAP

	ELB	SB	GLB	MB
GB	0.84	0.03	<0.01	0.13
ELB	1	<0.01	<0.01	0.03
SB		1	<0.01	0.13
GLB			1	0.03

FLU

	ELB	SB	GLB	MB
GB	0.01	0.03	<0.01	0.13
ELB	1	<0.01	0.034	0.04
SB		1	<0.01	0.10
GLB			1	0.04

PHE

	ELB	SB	GLB	MB
GB	0.00	0.03	0.11	0.13
ELB	1	<0.01	<0.01	0.03
SB		1	<0.01	0.13
GLB			1	0.03

FLT

	ELB	SB	GLB	MB
GB	<0.01	0.03	0.05	
ELB	1	<0.01	0.28	
SB		1	0.04	
GLB			1	

Figure S 2: Correlation between Dispersion Pertingency Index (PI$_D$) and the PAH background concentrations. Site MB is not shown. All data points were included in the correlation analysis. Significant correlations ($p<0.1$) are indicated by the lines in the individual graphs.
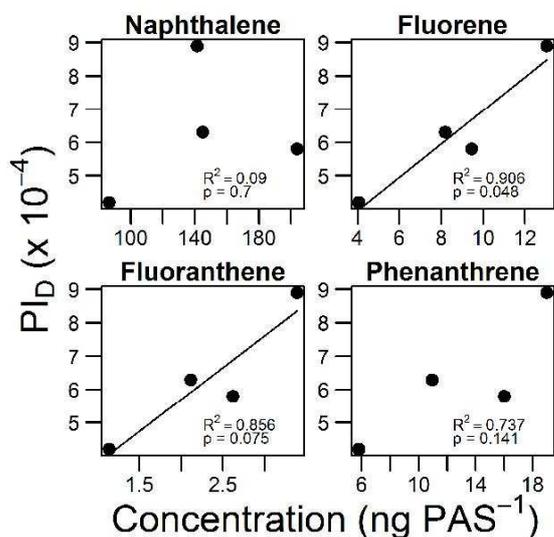
References

International Organization for Standardization (ISO), 2007. ISO 20988: Air quality - Guidelines for estimating measurement uncertainty.

Hayward, S.J., 2010. Fate of Current-Use Pesticides in the Canadian Atmosphere. Ph.D. thesis, University of Toronto, Department of Chemical Engineering and Applied Chemistry, 227 pages.

Study 2

How suitable are peat cores to study historical deposition of
PAHs?

Sabine Thuens, Christian Blodau, and Michael Radke

How suitable are peat cores to study historical deposition of PAHs?

Sabine Thuens [a], Christian Blodau [a,b], Michael Radke [a,c,]

[a] Department of Hydrology, BayCEER, University of Bayreuth, Bayreuth, Germany
[b] Hydrology Group, Institute of Landscape Ecology, University of Muenster, Muenster, Germany
[c] Department of Applied Environmental Science (ITM), Stockholm University, Sweden

HIGHLIGHTS

► We critically evaluate bogs as natural archives of atmospheric PAH deposition.

► PAHs are not degraded in the peat and there are no signs of their vertical mobility.

► Time trends compared to a sediment core, but deposition rates to peat are lower.

► Bogs are suitable to infer long-term time trends, short events might be missed.

► The low depth resolution of peat sampling methods is a major source of uncertainty.

GRAPHICAL ABSTRACT
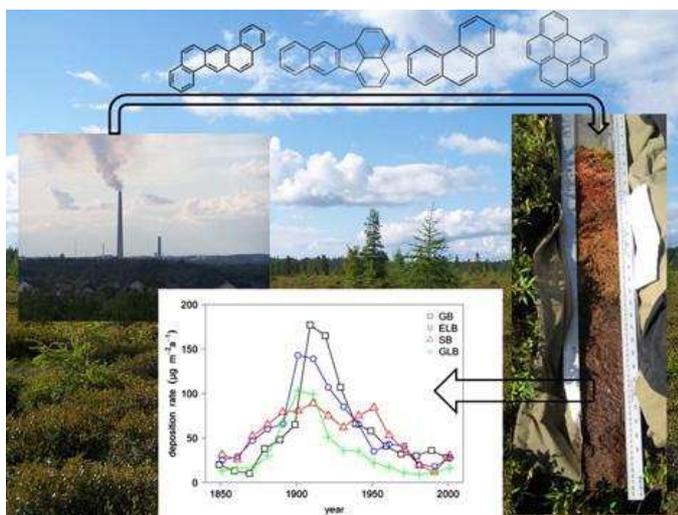
Corresponding author at:
Department of Applied Environmental Science (ITM),
Stockholm University, Sweden. Tel.: +46 86747136.
E-mail address: michael.radke@itm.su.se (M. Radke).

ABSTRACT

Ombrotrophic peat bogs are natural archives of atmospheric pollution, their depth profiles can be used to study the deposition chronology of harmful contaminants. Prerequisites for deriving historical deposition rates from the peat archive are that contaminants are persistent and immobile in the peat and that the applied dating technique is accurate. To examine these requirements and the accuracy of peat archives for polycyclic aromatic hydrocarbons (PAHs) 12 peat profiles were sampled in 4 bogs in Ontario, Canada, as well as surface peat in one bog. Additionally we carried out laboratory incubations; no degradation occurred over a 3-year period in these experiments. The standard deviations of PAH concentrations in surface samples and of PAH inventories in whole cores was approximately 30%, and concentrations in surface peat were on average 50% higher in hollows than in hummocks. No indications for mobility of PAHs were observed in peat. Temporal deposition trends inferred from peat cores were generally in agreement with trends derived from a sediment core sampled close by but deposition rates to the sediment were substantially higher. A major source of uncertainty was the rather coarse vertical sampling resolution of 5 cm which introduced substantial uncertainty in the dating of the individual segments. This caused variations of the deposition rates up to 70% per PAH between three replicate cores, and it also impedes the identification of deposition peaks. Overall, we conclude that peat cores are suitable archives for inferring atmospheric deposition trends, but due to their relatively low temporal resolution short-term events may not be identified and the development of sampling methods that allow a higher vertical resolution would greatly improve the performance of the method. The analysis of more than one core per site is suggested to provide a realistic estimate of the historic deposition and total inventories.

1. Introduction

Polycyclic aromatic hydrocarbons (PAHs) are ubiquitously present in the environment and were one of the first groups of atmospheric pollutants to be identified as carcinogenic. They are formed by incomplete combustion or high temperature pyrolytic processes of fossil fuels and other organic materials (Wild and Jones, 1995). They are non-polar and have a high affinity to organic matter (Berset et al., 2001).

As the active sampling of environmental pollutants at high temporal and spatial resolution or over extended periods is highly cost and labor intensive, natural archives

such as snow and ice, marine and lacustrine sediments, various biological media (corals, tree rings, herbarium specimens), and peat bogs have been used to study atmospheric pollution with organic or inorganic contaminants. For the determination of temporal and spatial trends of atmospheric PAH contamination, the analysis of sediment cores is well established as lake sediments provide a high temporal resolution. Sediment cores have, for example, been used to study historical PAH contamination (Hites et al., 1980; Laflamme and Hites, 1978; Schneider et al., 2001; Simcik et al., 1996; Wakeham et al., 1980). However, the concentration profiles obtained from sediment cores may be disturbed by seasonal mixing processes in the lake, bioturbation, and lake sediment focusing. The latter process considerably influences the sediment deposition rates and depends largely on the lake morphology (Blais and Kalff, 1995). Lake sediments also receive pollutants that are not deposited directly to the lake surface, but else-where in the catchment. This might lead to an overestimation of the deposition rates, as for example observed by Sanders et al. for the insecticide DDT (Sanders et al., 1995).

In contrast to sediments, ombrotrophic peat bogs only receive wet and dry deposition from the atmosphere and are not influenced by processes in the catchment. Because of the acidic and anoxic conditions prevailing below the water table, decomposition of biomass is slow. This leads to continuous growth of bogs (Zaccone et al., 2009a). The widespread distribution in the northern wet temperate and southern boreal zone and the similarity of peat bogs with respect to vegetation and hydrology thus provide an opportunity to establish spatial and historical patterns of atmospheric deposition based on this archive.

Organic pollutants are deposited to vegetation from the gaseous phase or bound to particles. From the gas phase they can enter vegetation by deposition onto the waxy cuticle of the leaves or by uptake through the stomata and subsequent translocation by the phloem. Particle-bound pollutants stick to the surface or a partly downwashed by rain, depending on particle size and leaf surface (Hosker and Lindberg, 1982). The pollutants accumulate in the living plants, which are decomposed to peat, an organic residue of varying composition and texture (Holoubek et al., 2000; Johnsen and Karlson, 2007). Due to its high organic matter content peat is a promising archive for atmospheric PAHs. As PAHs are highly sorptive to organic matter, their post-depositional mobility is assumed to be negligible (Sanders et al., 1995). Moreover, because of their low water solubility and the strong sorption PAHs are poorly available for microorganisms (Breedveld and Sparrevik, 2000; Shuttleworth and Cerniglia,

1995). In combination with the acidic and anoxic conditions and consequently a low overall metabolic activity in zones below the water table, the degradation of PAHs in peat is assumed to be very slow. Several studies have previously used peat cores to determine historical deposition rates and concentrations of PAHs (Berset et al., 2001; Dreyer et al., 2005a; Sanders et al., 1995).

A critical factor for establishing depositional records is the accurate dating of the stratified peat deposits. To this end radioisotopes such as ^{210}Pb have been used together with the constant rate of supply (CRS) model. The CRS model has been widely used to determine carbon, nitrogen, and metal accumulation rates in peat (Moore et al., 2004; Norton et al., 1997; Turetsky et al., 2004; Turunen et al., 2004). The slope gives then the accumulation rate (g cm^{-2}a^{-1}) which can be used to calculate the age of the samples. Dating through ^{210}Pb should be verified by independent chronostratigraphic markers (Urban et al., 1990); to this end, the peak of ^{241}Am deposition resulting from the peak of the nuclear bomb testing in 1962/1963 has been proposed as well as pollen records or other characteristic markers.

Although peat cores have been used previously as archives of atmospheric pollutant deposition, to our knowledge the suitability of bogs as archives for organic pollutants and the uncertainties inherent to this archive have not been systematically scrutinized. Such a critical evaluation is the objective of the present study. This study is based on 12 peat profiles sampled in 4 bogs in Ontario, Canada, on samples of surface peat at another bogs, and on one sediment core from a lake in the vicinity of one of the bogs. We studied PAH degradation in peat under aerobic and anaerobic conditions, analyzed the heterogeneity of PAH records within sites and with reference to the microtopography within a bog. Finally, we compared the PAH deposition rates derived from the peat archives to those derived from the sediment core.

2. Material and methods

2.1. Sampling

In 2007 and 2008 five peat bogs in eastern Ontario, Canada were sampled: Giant Bog (GB, this name was assigned to this site as no previous description and thus no established name was available), Eagle Lake Bog (ELB), Spruce Bog (SB), Green Lake Bog (GLB), and Mer Bleue Bog (MB) (coordinates are given in Table S1, a map is available as Fig. S1 in the Supplementary material). All peatlands had a hummock-

hollow microtopography. The vegetation was dominated by Sphagnum with ericaceous scrubs, characteristic for most ombrotrophic bogs in eastern Canada (Turunen et al., 2004). The pore water pH of the sampled bogs ranged from 3.5 to 4.5, which is typical for ombrotrophic bogs (Coggins et al., 2006). Samples were taken at the domed ombrotrophic section of the bogs at the largest possible distance to nearby roads. Triplicate peat cores were sampled with a box corer (87×90.6×1000 mm) from undisturbed hollows (10 m distance between sampling locations), avoiding peat compaction as far as possible. Below the living vegetation which was discarded, the cores were cut into 5 cm segments with a knife in the field; each segment was wrapped in aluminum foil, transferred to a plastic bag and stored in a cooler. The box corer and the knife were rinsed with distilled water and ethanol before each sample. At the MB site, we sampled surface peat by cutting it with a knife just below the living vegetation at 5 hollows and hummocks, respectively. Each sample was individually wrapped in aluminum foil and stored in a sealed plastic bag in a cooler.

One sediment core was sampled with a gravity corer at the deepest point of Opeongo Lake (location and details are given in Muir et al. (2009) and in the Supplementary material). It was sectioned in 1 cm intervals. All samples were frozen directly after arrival in the laboratory.

2.2. Degradation experiments

A sufficiently large amount of peat was sampled at Mer Bleue from the layer directly below the active vegetation (aerobic) and from the catotelm (anaerobic peat sampled from approx. 10 cm below the water table), respectively. These samples were homogenized and split into aliquots which were used for the incubation experiments.

Peat samples were incubated under controlled aerobic and anaerobic conditions in the laboratory at optimal degradation conditions to simulate a longer degradation time. For anaerobic incubations, 50 g of fresh wet peat sampled from the catotelm was weighed into crimp vials (120 mL), and the vials were capped with a gas-tight rubber/ PTFE septum. The gas phase was replaced by N_2 immediately after cap-ping and subsequently once a week. By this a limitation of degradation by the accumulation of CO_2 and CH_4 in the gas phase was avoided (Goldhammer and Blodau, 2008). The concentrations of oxygen, CO_2, and CH_4 in the headspace were determined regularly by gas chromatography with thermal conductivity and flame ionization detection to ensure that anaerobic conditions and an active microbial consortium were prevalent (method described by

Goldhammer and Blodau (2008)). Rates of CO_2 and CH_4 release were determined by linear regression of the concentration increase over a period of 5 days at 11 sampling events over 2 years.

Aerobic incubations were carried out accordingly with peat from the aerobic zone, but with a permeable filter membrane instead of the rubber septum and without replacing the gas phase. The gravimetric water content was kept constant at around 90%, similar to the original content of fresh aerobic peat; it was controlled regularly by weighing the vials and re-adjusted if necessary by adding distilled water.

Both aerobic and anaerobic incubations were carried out at 15 °C in the dark. Three replicates were sampled after 2, 5, 9, 13, 20, 26, and 33 months and analyzed for their PAH content. All concentrations reported for the aerobic incubation experiments were normalized to the weight of dry peat at the beginning of each experiment. In order to not disturb anaerobic microbial consortia we did not dry the anaerobic peat in the beginning. Therefore, concentrations in the anaerobic peat are normalized to the weight of dry peat at the end.

2.3. Analytical methods

All solvents were of residue analysis quality (nonane and dichloromethane purchased from Promochem, Wesel, Germany; hexane from J.T. Baker, Griesheim, Germany). Native and isotope-substituted PAHs (purity >98%) were purchased from Ultra Scientific (North Kingstown, USA), Cambridge Isotopes (Andover, USA), and Dr. Ehrenstorfer (Augsburg, Germany). Glassware was machine washed, solvent rinsed, and baked at 280 °C overnight.

Peat and sediment samples were freeze dried, milled to a fine powder in a pebble mill and kept frozen until extraction with pressurized liquid extraction. Extraction cells had glass fiber filters from Whatman (Whatman GF/B, Maidstone, UK) at both ends and were filled with 5 g of dry peat or sediment. A solution containing isotope-substituted PAHs as recovery standards (60 ng each of phenanthrene-d10, fluoranthene-d10, pyrene-d10, chrysene-d12, benzo[a]pyrene-d12) was spiked directly onto the peat. The cells were filled with diatomaceous earth (Celite545 coarse, Sigma-Aldrich, Munich, Germany) and extracted with pressurized liquid extraction (ASE 200, Dionex Co., Sunnyvale, USA). Cells were filled with hexane, pressurized to 14 MPa, and heated to 120 °C within 6 min. Pressure and temperature were held for 5 min, followed by rinsing with cold solvent (60% of the cell volume) and purging with argon for 90 s. This

extraction cycle was repeated once. The extract was reduced to about 1 mL with a rotary evaporator (Büchi, Switzerland). For extract clean-up, 3 g of aluminum oxide (aluminum oxide 90, neutral, deactivated with 15 wt.% water, 70–230 mesh from Merck, Darmstadt, Germany) upon 5 g of silica gel (silica gel 60, 200 mesh; Merck), was filled into glass columns of 1 cm diameter and equilibrated with hexane. The extracts were then quantitatively transferred to the columns and eluted with 35 mL of hexane followed by 30 mL of hexane/dichloromethane 3/1 (v/v) as described by Dreyer and Radke (2005). The combined extracts were evaporated to approx. 1 mL by the use of a rotary evaporator and then subjected to size exclusion chromatography for further clean-up. To this end, columns of 2.2 cm diameter filled with Bio-Beads (S-X-3, Bio-Rad, Hercules, USA) equilibrated with hexane/dichloromethane 1/1 were used. The extracts were quantitatively transferred to the columns and eluted with 60 mL of hexane/dichloromethane 1/1. This fraction was discarded. The target compounds were then eluted with 120 mL of hexane/ dichloromethane. The column was subsequently rinsed with additional 100 mL of the solvent mixture and re-used. The extracts were evaporated to 1 mL by a rotary evaporator and finally evaporated to dryness under a gentle stream of nitrogen. Prior to injection, samples were redissolved in 200 μL of a solution containing two deuterated PAH (anthracene-d10 and benzo[a]anthracene-d12) in nonane and transferred to glass vials.

We quantified the following 10 out of the 16 EPA-PAHs: phenanthrene (Phen), fluoranthene (Flt), pyrene (Pyr), benzo[a]anthracene (B[a]A), chrysene (Chry), benzo[b]fluoranthene (B[b]F), benzo[k]fluoranthene (B[k]F), benzo[a]pyrene (B[a]P), indeno[1,2,3-cd]pyrene (Ind), and benzo[ghi]perylene (B[ghi]P), and additionally benzo[e]pyrene (B[e]P), and benzo[j]fluoranthene (B[j]F). However, due to incomplete chromatographic separation of B[b]F, B[k]F and B[j]F in many chromatograms, the sum of the three compounds is reported as B[b+k+j]F. The total concentration of all PAHs is referred to as $\sum_{12}$ PAH throughout the manuscript.

One part of the samples was analyzed by a ion trap GC/MS (CP-3800 and Saturn 2000, Varian, Darmstadt, Germany) and the other part was analyzed on a quadrupole GC/MS (GC 8000 MS, Finnigan, Austin, USA). The chromatographic conditions are listed in the Supplementary material.

PAH calibration solutions (native compounds and recovery standards (see above): 50 ng mL^{-1}–2000 ng mL^{-1}; injection standards anthracene-d10 and benzo[a]anthracene-d12: 200 ng mL^{-1}) were prepared by diluting stock solutions in nonane. They were measured

with each set of samples.

The analytical procedure was evaluated by analyzing commercially available certified reference material (IAEA-159, Sediment; n=5) as well as diatomaceous earth spiked with a known concentration of all native PAHs (n=5). Laboratory blank samples (n=13) were analyzed with every set of samples.

Dry-milled subsamples (approximately 1 g from each 5 cm peat segment, 200 mg of each 1 cm sediment segment) were submitted to Flett Research Ltd (Winnipeg, Canada) or to the Institute of Environmental Geochemistry (University of Heidelberg, Germany) for ^{210}Pb analysis. In 4 cores the activity of In 4 cores the activity of ^{241}Am was measured as additional chronostratigraphic marker.

2.4. Calculations

All PAH concentrations were normalized to the dry weight (dw) of the peat sample.

The inventories of the PAHs were calculated as the total integrated mass of a compound per unit area as described by Schneider et al. (2001). Only layers younger than 1880 were taken into account so that all peat profiles represent the same time span.

Deposition rates of the individual PAHs (ng m^{-2} a $^{-1}$) were calculated by dividing the measured mass of PAHs per peat segment by the number of years covered by this segment and the surface area sampled. To derive average deposition rates from the three cores sampled in each bog, the deposition rates derived from each core were aver-aged to 10 year periods as described by Dreyer et al. (2005b).

Deposition rates determined for Opeongo Lake were corrected by division with a sediment particle focusing factor of 2.66. We obtained this factor by multiplying the excess ^{210}Pb inventory with the decay constant of ^{210}Pb and dividing it by the excess ^{210}Pb atmospheric deposition rate estimated for this longitude by Muir et al. (2009).

Statistical analysis was conducted with the software R (R Development Core Team, 2011).

3. Results and discussion

3.1. Evaluation of the analytical methods

The mean recovery rates of the isotope-labeled internal standards were between 48±27% (Phen-d10) and 86±29% (Pyr-d10) (n=126). The operational limit of

quantification (LOQ) determined according to DIN 32645 (1994) ranged from 2 ng g^{-1} (Phe) to 11 ng g^{-1} (Chry); details are summarized in Table S2 in the Supplementary material. As concentrations in peat and sediment were generally $>$ LOQ, we did not determine the limit of detection (LOD). Some blank samples contained individual PAHs at concentrations $>$ LOQ (given in Table S3). However, we did not observe a systematic contamination pattern in the blanks. Except for Chry in one blank sample, concentrations in the blanks were at least one order of magnitude lower than in the field samples. Therefore, the results were not blank corrected.

Recovery of the PAHs spiked to diatomaceous earth ranged from 95% (B[a]A) to 136% (Pyr), and PAH concentrations measured in the reference sediment (IAEA-159, Sediment) were comparable to the concentrations given by the distributor (shown in Fig. S2). Thus, the clean-up procedure was suitable to separate the interfering and complex matrix of peat from the PAHs at acceptable recovery of the analytes, and the overall analytical method can be considered appropriate for the purpose of this study.

3.2. PAH degradation in peat

The CO_2 and CH_4 production rates determined in our degradation experiments (1.37±1.13 (n=24) and 1.06±0.98 (n=15) µmol g^{-1} dw peat d^{-1}, respectively) are within the range of rates determined by Moore and Dalva (1997) in similar incubation experiments. These production rates indicate an active peat degrading microbial community.

In the samples incubated at aerobic conditions, the PAH concentrations did not change significantly ($p \leq 0.1$) over time as shown in Fig. 1 (other compounds are presented in Fig. S3 as Supplementary material). Similarly, in the anaerobic incubations there was no significant concentration trend ($p \leq 0.1$) for any PAH (Fig. 1 and Fig. S4 (Supplementary material)). Although there is some scatter in the data, we consider these interpretations valid based on the large number of samples and replicates they are based on.

Although the incubation period was much shorter than the period covered by the peat cores (up to 200 years) we think that this finding can be extrapolated to somewhat longer time scales as we maintained optimal degradation conditions throughout the incubation period.

A.
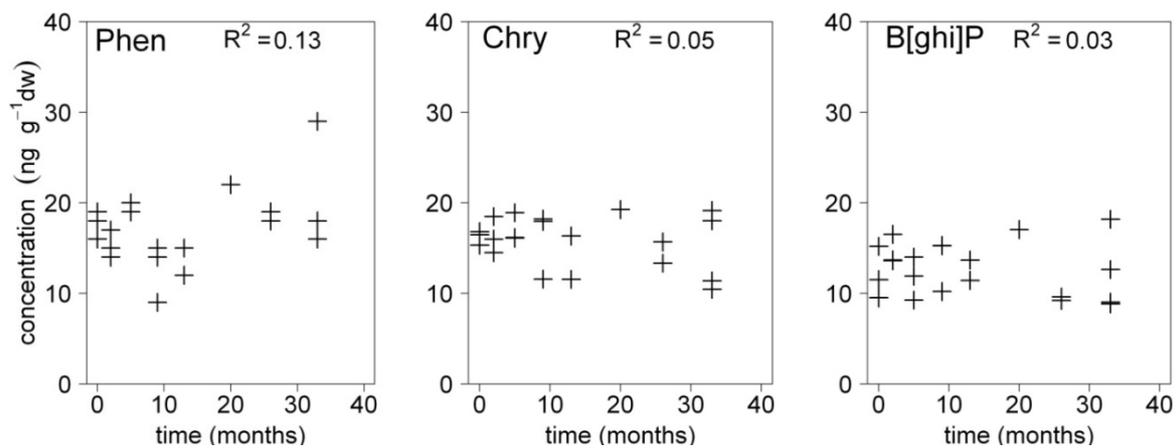
B.
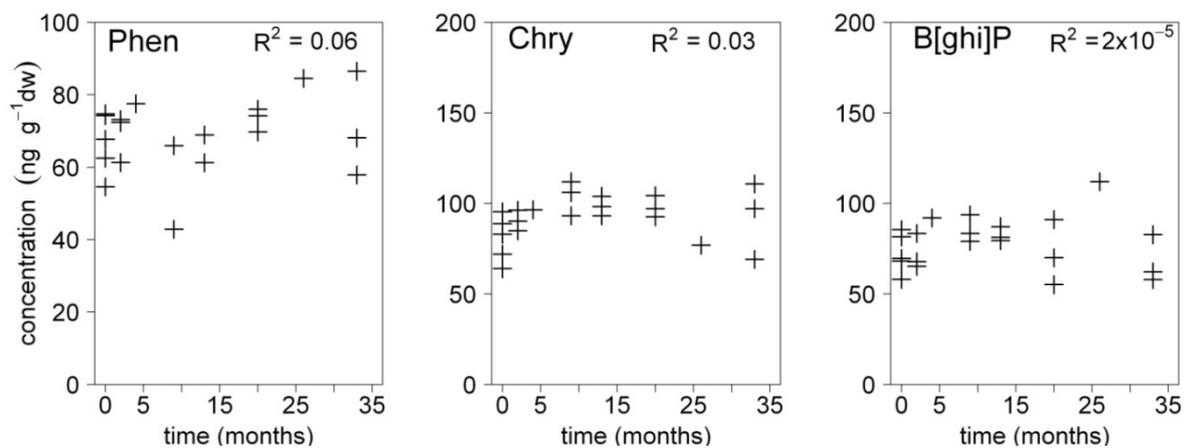
Fig. 1: Concentration time trend of Phenanthrene, Chrysene, and Benzo[ghi]perylene in the aerobic (A) and anaerobic (B) degradation experiments.

Therefore, degradation rates in the incubation experiments should be higher than in the field. This is based on the following reasons: i) the time while PAHs are present in the aerobic part of the peat is limited (although still in the range of 50–100 years in the studied bogs); ii) the anaerobic incubation experiments were carried out at relatively high temperature (15 °C) while turnover in the field is limited by colder temperatures (mean annual temperature 6 °C, 4 months a year below 0 °C (Moore et al., 2006)), and iii) the anaerobic incubations were not limited by an accumulation of the decomposition products CO_2 and CH_4, which in undisturbed bogs limits the overall microbial turnover in deeper peat layers (Blodau et al., 2011).

The stability of PAHs against degradation has also been studied in other media. Schneider et al. (2001) reported no degradation of PAHs in sediment cores sampled in the Great Lakes. In contrast to their and our findings, Lei et al. (2005) observed a 50–80% removal of 2- to 5-ring PAHs in field-contaminated sediment during 24 weeks of

incubation under aerobic conditions. This discrepancy to our observations can at least partly be explained by the high organic matter content of peat and thus a very high adsorbed PAH fraction, for which degradation should be very slow or does not occur (Eriksson et al., 2000; Johnsen et al., 2005) due to a lack of bioaccessibility (Johnsen and Karlson, 2007). In the experiments by Lei et al. (2005) degradation was inhibited when the pH was below 4.5, and no degradation of PAHs was observed under anaerobic conditions. These two conditions apply to the anaerobic parts of ombrotrophic bogs and thus limit the PAH degradation there. Based on the results of our incubation experiments and these findings, we conclude that post-depositional degradation of PAHs in peat is not significant on the time-scale of our experiments (3 years) and that it is likely that such a degradation is quantitatively of limited importance also on longer timescales.

3.3. Dating

Mean total residual unsupported ^{210}Pb activity in the dated peat cores was 0.64±0.17 Bq cm^{-2}, which is higher than the average activity of 0.35±0.11 Bq cm^{-2} measured by Turunen et al. (2004) in Canadian bogs but in the range of soil inventories reported for North America (0.31–0.84) by Urban et al. (1990). The CRS model was exclusively applied as all cores reached background activities and because it provided reasonable age predictions for each section even though the peat accumulation rate was changing with time.

The ^{210}Pb method is based on the assumption of post-depositional immobility of atmospherically derived constituents (Shotyk et al., 1997; Vile et al., 1999). However, the mobility of ^{210}Pb is discussed controversially in the literature. On the one hand Urban et al. (1990) concluded that ^{210}Pb is mobilized by the organic-rich waters of peatlands and inventories of ^{210}Pb in hummocks are depleted compared to peatland hollows. On the other hand, Vile et al. (1999) and MacKenzie et al. (1997) demonstrated the immobility of ^{210}Pb in peat profiles. One way of assessing the mobility of lead in individual peat profiles is the interpretation of the lead distribution with respect to the water table. Fluctuations of the redox potential caused by water table movements can affect metal solubility and mobility. When lead is dissolved in the pore water, it is mobilized and accumulates in the depth of the water table (Vile et al., 1999). Consequently, the activity of ^{210}Pb should be enhanced in this depth if a substantial

relocation of lead occurs at the specific site. However, none of the peat cores sampled in this study showed a maximum of ^{210}Pb activity in the depth of the water table at the time of sampling. Instead, the ^{210}Pb activity in the peat cores as well as in the sediment core decreased exponentially as a function of cumulative dry weight (R^2 >0.8; see Fig. S5 in the Supplementary material), indicating a low mobility of lead in the sampled cores. However, even if post-depositional mobility of ^{210}Pb in peat cannot be excluded, it does not affect the dating results obtained through the CRS model as long as it occurs at a uniform rate from year to year throughout the entire profile (Urban et al., 1990).

In four of our peat cores we measured the ^{241}Am activity to assess the dating accuracy. In core GB 2 the ^{241}Am peak appears in the segment dated to 1944–1962. This coincides with the maximum of the nuclear bomb testing activities in 1963. One core (SB 1) did not show a clear maximum of ^{241}Am activity, although the ^{210}Pb activity in this profile decreased exponentially with depth which indicates an intact core. In the two other cores the ^{241}Am activity peaked in layers dated to 1937–1956 (SB 2) and 1909–1933 (GB 1). Overall, ^{241}Am seems to appear slightly too early in most cores. However, it has to be taken into ac-count that ^{241}Am itself might be somewhat mobile in peat as observed by Mitchell et al. (1992). Moreover, as the temporal resolution of the peat profile is rather low individual segments can cover several decades. This is reducing the temporal resolution necessary to detect a sharp ^{241}Am peak, and depending on the segment borders a peak might even appear in an older peat layer. This possible peak shift is illustrated in the Supplementary material with a synthetic dataset (Fig. S6). Based on these results, we conclude that the findings by Urban et al. (1990) that dates based on ^{210}Pb can be inaccurate by as much as 30 years are likely to be applied to this study. However, other authors have reported a substantially lower dating inaccuracy. Appleby et al. (1997) used Cannabis pollen and ^{241}Am as independent chronostratigraphic maker for ^{210}Pb dating and found good agreement. Turunen et al. (2004) used a charcoal horizon resulting from a peat fire to validate the ^{210}Pb dating and reported a difference of only 4–8 years. Such differences might be due to site- or core-specific factors and are thus difficult to generalize.

The temporal resolution of the segments within individual cores varied considerably, i.e. the 5 cm segments represented very different time spans. While the upper layers can represent as little as 5 years, the lower layers comprised up to 70 years. This can be attributed to the ongoing peat mineralization and compaction of the lower layers.

Moreover, the time span covered by segments sampled in identical depths of the three replicate cores per bog was highly variable as shown in Fig. 2A. This can be critical for the analysis of deposition peaks as there is the potential for substantial underestimation of maximum deposition rates during peak periods which are "diluted" by a period of lower deposition rates represented within the same core segment.
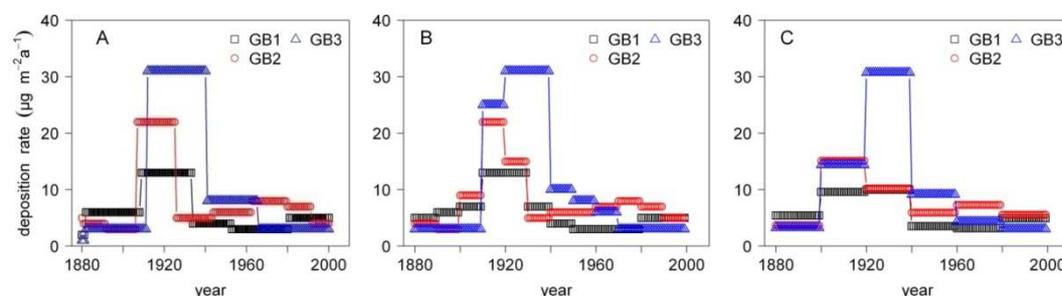
Fig. 2: Deposition time trend of Phen in three replicate cores at GLB presented in original data (i.e., the concentration of each segment is plotted for the entire period covered by this segment) (A) and averaged to segments of 10 years (B) and 20 years (C).

One difficulty regarding the interpretation of three replicate cores from one bog arises from the different periods covered by each individual segment. This precludes direct averaging of the three deposition profiles. To alleviate this problem, we generated 10 year average values as described in Dreyer et al. (2005b).

As shown in Fig. 2B, this approach usually preserves the maximum deposition rates while generating somewhat sharper deposition peaks. We examined several modifications of this method. Increasing the aggregation period from 10 to 20 or 30 years did not lower the variation between the deposition rates of the 3 cores, but lowered the maximum deposition rates considerably as shown in Fig. 2C. Decreasing the aggregation period to less than 10 years created sharp deposition peaks that were unrelated to measured data. Therefore, we consider the aggregation to 10 year-periods as most appropriate. To improve the temporal resolution of the method and to allow a better comparability of replicate cores, it would be necessary to sample thinner peat segments. This has been successfully used by Givelet et al. (2004) for the analysis of several elements (mainly metals) in 1 cm subsections of peat cores. However, given the dimensions of currently available peat corers, such thin slices will not provide the peat mass which is necessary to meet the detection limits of the analytical method for PAHs in all of the sections, and consequently this higher vertical resolution was not applicable in the current study.

Overall, based on our results we conclude that dating inaccuracies can mainly be attributed to the coarse resolution of the 5 cm segments rather than to a general inapplicability of the ^{210}Pb method in bogs.

3.4. Vertical mobility of PAHs

To use peat cores as archives of atmospheric pollution, the contaminants have to be immobile within the profile. This has been questioned by Malawska et al. (2006) who determined more LMW PAH in deeper depth than HMW PAHs in peat profiles and therefore assumed a down-ward movement of LMW PAHs. However, we did not observe such a difference in the distribution of LMW and HMW PAH within the profiles as the deposition rates of all PAHs correlate significantly (p < 0.1; see Fig. S7 in the Supplementary material). Moreover, the PAH concentration profiles and reconstructed deposition rates show a relatively sharp increase after 1870, which is the time of a substantial increase of industrial emissions (see Section 3.7 for details) in the study region (see Figs. S8 and S9 in the Supplementary material for concentrations of Phen (LMW) and Ind (HMW), and Fig. 3 for deposition rates of Σ_{12} PAH). For compounds undergoing vertical transport in the peat, an apparent increase of deposition rates should be detected before the actual increase of emissions. This indicates that the PAHs were not transported downward along the peat profile to a large extent.

3.5. Reconstructed deposition rates

Statistical analysis did not reveal significant differences between concentrations of the individual PAHs over depth (p < 0.1). This indicates that the compounds behave similar in all cores. Therefore, analyzing the sum of all compounds does not mask any trends of individual compounds and consequently we present the results mostly as Σ_{12} PAH in the following. The most abundant compounds were Phen, Flt, Chry, Pyr, Ind and B[ghi]P. The maximum Σ_{12} PAH deposition rates ranged from 180 μg m^{-2}a^{-1} in GB to 59 μg m^{-2}a^{-1} in GLB (Table 1). These deposition rates are very similar to those reported by Dreyer et al. (2005a) who determined Σ_{11} PAH deposition rates to 17 bogs in eastern Canada. Except for one subset (group 2b) of their bogs which was characterized by higher PAH contamination they reported deposition rates in the range between 20 and 150 μg m^{-2}a^{-1}.

Table 1: Maximum $\sum_{12}$ PAH deposition rates with their years of occurrence and inventory per peat profile and average inventory per bog with standard deviation.

	max. deposition rate		inventory	average inventory (s.d.)
	year	$\sum_{12}$ PAHs ($\mu g\ m^{-2}a^{-1}$)	mg m^{-2}	mg m^{-2}
GB 1	1909-1933	180	6.1	7.4 (1.1)
GB 2	1907-1925	176	8.2	
GB 3	1912-1940	172	7.8	
ELB 1	1902-1919	171	9.5	7.5 (1.8)
ELB 2	1875-1911	119	6.3	
ELB 3	1898-1926	137	6.6	
SB 1	1940-1970	95	4.0	5.9 (1.9)
SB 2	1911-1936	115	7.8	
SB 3	1893-1923	85	6.0	
GLB 1	1883-1913	59	5.8	4.6 (1.1)
GLB 2	1893-1920	136	4.2	
GLB 3	1901-1926	120	3.8	
MB	1919-1935	202	15.4	
OPL	1961-1968	868	42.1	

Although the 5 cm sections represent differing time spans, the de-position rates of the 3 cores per bog had similar maxima dated to 1880–1940 (given in Fig. S10 in the Supplementary material). All 3 cores of ELB showed a small secondary maximum. In SB 1 this secondary maximum was higher and in SB 3 even equal to the first one. In SB 2 only one broad peak was observed. In the profile of GLB 1 two small peaks were displayed in contrast to high single ones in GLB 2 and 3. These differences can be caused by different deposition to the individual locations in the bog or more likely by the rather coarse resolution of the peat cores with 5 cm segments (see example for apparent time shift in Supplementary material Fig. S6 and discussion above). By sampling of 5 cm sections or by subsequent averaging of the three cores, the two maxima may be merged into one and the information on these secondary maxima gets lost. The disparity between cores with one and two deposition maxima has also been observed previously. Dreyer et al. (2005b) found two maxima of PAH deposition in four out of fifteen sampled bogs. A difference in the intensity of the secondary peak has also been observed by Givelet et al. (2004) in Pb concentration profiles in peat. Secondary maxima of PAH deposition have also been observed by Schneider et al. (2001) in sediments from the Great Lakes, but not by Simcik et al. (1996). As shown above, a secondary and rather narrow peak of deposition might not be captured in cores

with a comparatively low temporal resolution. This should be taken to account when interpreting deposition time trends, and averaging of replicates has also to be used with caution. Deposition trends of each single core prior to any data aggregation should be presented in addition to the average trends per site (see Fig. S10 in the Supplementary material).
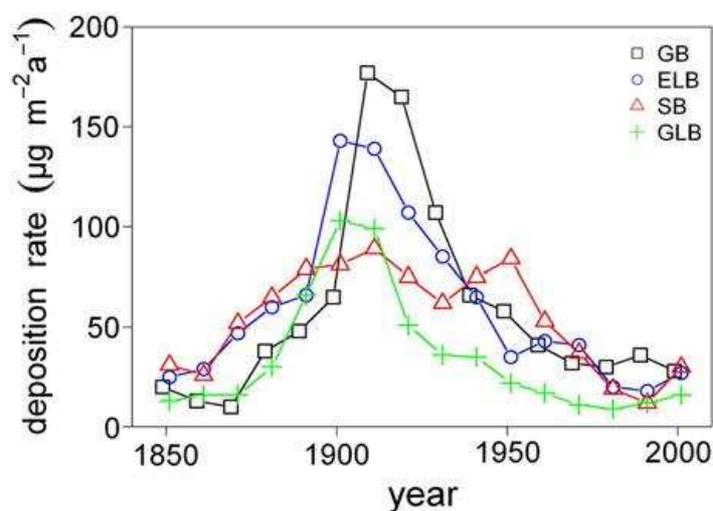
Fig. 3. Deposition rates of $\sum$12 PAHs to the sampled bogs averaged to decades (n=3).

The average deposition rates obtained from 10-year aggregated de-position trends of the three replicate cores per site are shown in Fig. 3 (the same figure including error bars is available as Fig. S11 in the Supplementary material). The reconstructed historical deposition trends derived at the five bogs show increasing PAH deposition after 1870. This is consistent with the beginning of smelting operations in Sudbury (SARA, 2008), a city located upwind of the bogs which has been a major source of airborne contaminants to this region, and with the overall steep increase of steel production and industrial coal consumption in Ontario between 1880 and 1900 (Donald, 1915). Other sources such as residential heating or wood burning have certainly also contributed to PAH immissions to the bogs, but these can be assumed to be comparatively small and especially their source strength can be assumed to be rather constant during this period if compared to the industrial emissions. Decreasing deposition rates after 1940 might reflect the installation of filters and replacement of the blast furnaces and roast yards by multi-hearth roasters and reverberatory furnaces for smelting (SARA, 2008) and other measures to reduce industrial emissions.

3.6. Heterogeneity within one bog

Except for Flt, the PAH concentrations in surface samples taken at Mer Bleue were significantly ($p < 0.05$; n=5) higher in hollows than in hummocks (Fig. 4, data are given in Table S3). The $\sum_{12}$ PAH concentration was 225±34 ng g^{-1} in hollows and 142±31 ng g^{-1} in hummocks. This finding illustrates the influence of microtopography on PAH concentrations in surface peat. A similar observation was made by Martens et al. (1997) at valleys and hills close to streets. Higher contaminant concentrations in hollows could be due to post-depositional transport of deposited particles following the microtopography of the bog during rain and snowmelt events. An alternative explanation is a reduced air velocity in hollows which might lead to an enhanced exchange between the gas phase and plant surfaces as well as to an increased deposition of particles. As it is not possible to determine the age of surface samples it might also be that the samples of hollows represent a longer accumulation period. Therefore, to avoid inconsistencies in the results it is important to exclusively sample either hollows or hummocks in studies that compare PAH inventories.
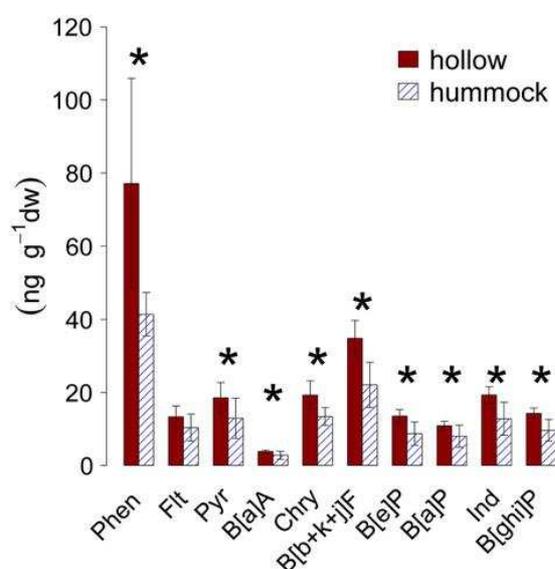

Fig. 4. Mean concentration of PAHs in surface peat samples of hollows and hummocks. Error bars represent standard deviations (n=5), a star marks compounds with significant difference between hummock and hollow.

A measure for the total historical deposition per surface area is the inventory of contaminants. Such inventories were calculated for the period from around 1880 to present for each individual core. As the age of the lowest peat segment varies somewhat between the cores, the actual lower age is within the range from 1867 (GB 1) to 1901 (GLB 1). The average $\sum_{12}$ PAH inventories of the four bogs ranged from 4.6 mg m^{-2} (GLB) to 7.5 mg m^{-2} (ELB; Table 1). The relative standard deviations of the $\sum_{12}$ PAH inventories at the four bogs with replicate cores were between 15 and 32% which is similar to the deviation of the surface samples. This reflects the heterogeneity of PAH concentrations between different hollows of an individual bog and the combined uncertainty of the sampling and analytical methods. The inventories determined here are comparable to the $\sum_{11}$ PAH inventory of 5.67 mg m^{-2} reported by Zaccone et al. (2009b) for a peat core sampled in the Jura Mountains, Switzerland, and also to the ones that can be calculated from the concentrations published by Dreyer et al. (2005b) for several Canadian bogs. For a peat core spanning the period 1886–1989 that was sampled in comparatively close proximity to large urbanizations in the UK, Sanders et al. (1995) determined a much higher inventory of $\sum_{14}$ PAH of 216 mg m^{-2}.

The relative standard deviations of the maximum deposition rates at the individual bogs, calculated from the three replicate cores, ranged up to 70% per compound and up to 41% for $\sum_{12}$ PAH. This deviation is caused both by differences in the absolute deposition rates and by some differences in the timing of the deposition peaks. The pre- and post-maximum rates also differ as the segments they are obtained from might still represent some years of pollution. Nevertheless they were all below 50 μg m^{-2}a^{-1}. The mean recent deposition rates ranged from 13 to 34 μg m^{-2}a^{-1} for $\sum_{12}$ PAH with relative standard deviations up to 70% (Table S4 in the Supplementary material) while the rates averaged to 10 years have standard deviations from 28 to 140% for $\sum_{12}$ PAH. This high deviation of the rates averaged to 10 years is an example of how averaging of replicate cores might enhance the uncertainty as discussed above. For the metals lead and mercury, Bindler et al. (2004) reported concentrations and inventories to vary in one bog by a factor of 2 and 4, respectively. In the current study, this variation was somewhat lower for PAHs, but we agree with Bindler et al. that a single core may not provide a representative record of atmospheric deposition for one bog as a whole.

3.7. Comparison with sediment core

The $\sum_{12}$ PAH deposition rates derived from the Opeongo Lake sediment core peaked around 1920 with 249 µg m^{-2}a^{-1} and again around 1960 with 379 µg m^{-2}a^{-1}, followed by decreasing rates up to the present time. The drop in deposition rates between the two peaks reflects general economic events such as the Great Depression, for example, or changes in dominant emission sources like the installation of filters. Christensen and Zhang (1993) determined maximum deposition rates of 2.8 mg m^{-2}a^{-1} for $\sum_{12}$ PAH to Lake Michigan for the year 1985, which is one order of magnitude higher than rates determined in remote lakes (Usenko et al., 2007). Schneider et al. (2001) determined $\sum_{33}$ PAH deposition rates in sediment cores of Lake Michigan between 250 and 520 µg m^{-2}a^{-1} and inventories of 21 to 78 mg m^{-2}. They dated maximum rates to the year 1942. Simcik et al. (1996) measured $\sum_{17}$ PAH deposition rates between 700 and 1500 µg m^{-2}a^{-1} and inventories of 50 to 70 mg m^{-2}. The reconstructed deposition rates of their study peaked on a plateau from 1930 to 1975. The latter two studies report inventories and historical trends comparable to the ones determined here for Opeongo Lake (inventory of 18.4 mg m^{-2}). This is surprising as Opeongo Lake is a rural site located in a Provincial Park and thus it should not be strongly impacted by local PAH sources, whereas Lake Michigan is impacted by direct anthropogenic PAH emissions from industry, power plants, households, and traffic. Muir et al. also reported Hg concentrations in surface sediment and the anthropogenic Hg flux to the sediment of Opeongo Lake to be elevated by a factor of 2 to 30 compared to other mid latitude lakes in eastern Canada (Muir et al., 2009). Based on these unexpected contaminant levels in OPL sediment, some historic or recent input of contaminants to the lake catchment from local or direct sources (e.g., forestry or tourism) can-not be completely excluded. On the other hand, atmospheric input stemming from long-range transport has been reported to be an important source of lead (Dillon and Evans, 1982) and other metals (Wong et al., 1984) to lakes in the study region. The uncertainty with respect to contaminant sources to OPL has to be taken into ac-count when comparing OPL and peat data.
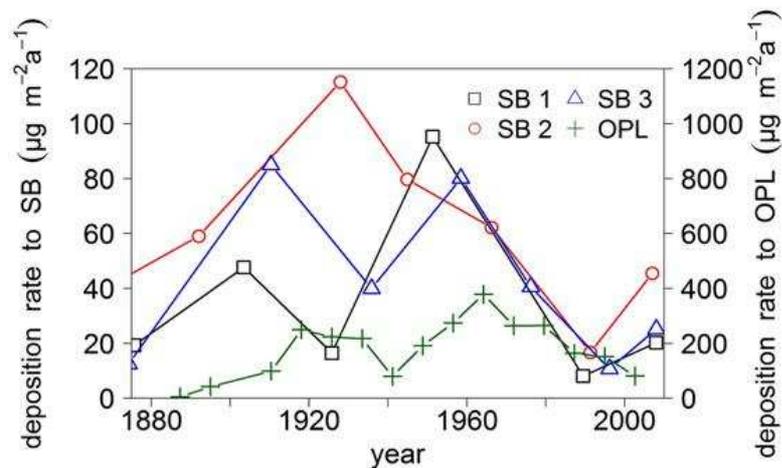
Fig. 5. Deposition rates of ∑12 PAHs to the sediment core (OPL) and to SB; deposition to SB is represented on the left y-axis, to OPL on the right y-axis.

Thanks to higher concentrations of PAHs in sediment and a matrix which can be sectioned more easily, thinner sections can be obtained from sediment cores. Therefore, the temporal resolution of the sediment is higher as demonstrated in Fig. 5 for the results of the sediment core and the peat core sampled close by (SB). The distance between Opeongo Lake and Spruce Bog is only 16 km, so it is reason-able to assume that both sites received a similar atmospheric deposition of PAHs in the past. The deposition time trends recorded in the OPL sediment core and in two of the SB peat cores are similar, while core SB2 was substantially different (as discussed above). In cores SB1 and SB3, the deposition peaks and the drop between these peaks appeared some 10–20 years earlier than in the OPL core (Fig. 5). This time shift might be caused by the time lag between de-position to lake and catchment and incorporation to the sediment. But most probably the early appearance of the peaks in SB 1 and 3 is due to the comparatively low temporal resolution of the peat pro-file. Still, the overall trends of PAH deposition are comparable. Good agreement in the temporal deposition trends between sediment and peat has already been demonstrated for Pb and Hg (Farmer et al., 1997; Norton et al., 1997).

The deposition rates and the inventory reconstructed from the sediment core were four times higher than those inferred from the SB cores (Table 1) for all compounds. Higher inventories and consequently higher reconstructed deposition rates for lake sediments than for bogs were also reported for Pb and Hg (Farmer et al., 1997; Norton et al., 1997). While Farmer et al. assumed a certain loss within the bog but no mobility, Norton et al. (1997) and Bindler et al. (2004) supposed that a peat core may better reflect atmospheric deposition rates than lake sediments because no watershed is

involved in the delivery of the pollutants and because of the greater complexity of lake basins and sedimentation processes. The relative synchronicity of the temporal deposition trends indicates that the differences in quantity are caused by deposition to the catchment and sedimentation, and are not caused by mobility within the sediment. Further studies are necessary to determine the reason for the higher deposition rates reconstructed from sediments and more specifically to investigate whether OPL was contaminated by local sources.

4. Conclusion

Based on the results of this study, we conclude that peat bogs fulfill the criteria for an archive for atmospheric PAH deposition. The results provide evidence that i) PAHs are not degraded over longer periods, ii) PAHs are immobile once they are deposited to the peat, and iii) that the temporal deposition trends inferred from the peat archives are generally in agreement with trends derived from sediment cores and across bogs in the same region. However, this study also shows the limitations of the peat archive, which are mainly related to the temporal resolution that can be achieved. Therefore, peat cores are not suitable to display short-time events as information on these might get lost due to methodological constraints. Moreover, the comparison of three replicate cores at four sites shows that the frequently used approach of analyzing only one core per bog might not provide adequate results, both regarding the absolute magnitude of reconstructed atmospheric deposition and the deposition time trends.

To overcome some of the limitations of reconstructing PAH deposition rates from peat profiles identified in this study, larger samplers could be developed and used to allow sampling of thinner peat slices. However, this might be impaired by logistical problems when sampling in remote areas as there are limits to hand-held operation of such corers.

Appendix A. Supplementary data

Supplementary data to this article can be found online at http://dx.doi.org/10.1016/j.scitotenv.2013.01.091.

References

Appleby PG, Shotyk W, Fankhauser A. Lead-210 age dating of three peat cores in the Jura Mountains, Switzerland. Water Air Soil Pollut 1997;100:223–31.

Berset JD, Kuehne P, Shotyk W. Concentrations and distribution of some polychlorinated biphenyls (PCBs) and polycyclic aromatic hydrocarbons (PAHs) in an ombrotrophic peat bog profile of Switzerland. Sci Total Environ 2001;267:67–85.

Bindler R, Klarqvist M, Klaminder J, Förster J. Does within-bog spatial variability of mercury and lead constrain reconstructions of absolute deposition rates from sin-gle peat records? The example of Store Mosse, Sweden. Global Biogeochem Cycles 2004;18:GB3020.

Blais JM, Kalff J. The influence of lake morphometry on sediment focusing. Limnol Oceanogr 1995;40:582–8.

Blodau C, Siems M, Beer J. Experimental burial inhibits methanogenesis and anaerobic decomposition in water-saturated peats. Environ Sci Technol 2011;45:9984–9.

Breedveld GD, Sparrevik M. Nutrient-limited biodegradation of PAH in various soil strata at a creosote contaminated site. Biodegradation 2000;11:391–9.

Christensen ER, Zhang X. Sources of polycyclic aromatic hydrocarbons to Lake Michigan determined from sedimentary records. Environ Sci Technol 1993;27:139–46.

Coggins AM, Jennings SG, Ebinghaus R. Accumulation rates of the heavy metals lead, mercury and cadmium in ombrotrophic peatlands in the west of Ireland. Atmos Environ 2006;40:260–78.

Dillon PJ, Evans RD. Whole-lake lead burdens in sediments of lakes in southern Ontario, Canada. Hydrobiologia 1982;91:121–30.

DIN 32645. Chemische Analytik: Nachweis-, Erfassungs- und Bestimmungsgrenze, Ermittlung unter Wiederholungsbedingungen, Begriffe, Verfahren, Auswertung. Beuth: Verlag; 1994.

Donald WJA. The Canadian iron and steel history. A study in the economic history of a protected industry. Dissertation, 1915, University of Chicago, US (http://www.archive. org/details/cu31924021085687, access date 2012-12-10).

Dreyer A, Radke M. Evaluation and optimization of extraction and clean-up methods for the analysis of polycyclic aromatic hydrocarbons in peat samples. Int J Environ Anal Chem 2005;85:423–32.

Dreyer A, Radke M, Turunen J, Blodau C. Long-term change of polycyclic aromatic hydro-carbon deposition to peatlands of eastern Canada. Environ Sci Technol 2005a;39: 3918–24.

Dreyer A, Blodau C, Turunen J, Radke M. The spatial distribution of PAH depositions to peatlands of Eastern Canada. Atmos Environ 2005b;39:3725–33.

Eriksson M, Dalhammar G, Borg-Karlson AK. Biological degradation of selected hydro-carbons in an old PAH/creosote contaminated soil from a gas work site. Appl Microbiol Biotechnol 2000;53:619–26.

Farmer JG, Mackenzie AB, Sugden CL, Edgar PJ, Eades LJ. A comparison of the historical lead pollution records in peat and freshwater lake sediments from central Scotland. Water Air Soil Pollut 1997;100:253–70.

Givelet N, Le Roux G, Cheburkin A, Chen B, Frank J, Goodsite ME, et al. Suggested protocol for collecting, handling and preparing peat cores and peat samples for physical, chemical, mineralogical and isotopic analyses. J Environ Monit 2004;6: 481–92.

Goldhammer T, Blodau C. Desiccation and product accumulation constrain heterotrophic anaerobic respiration in peats of an ombrotrophic temperate bog. Soil Biol Biochem 2008;40:2007–15.

Hites RA, Laflamme RE, Windsor JG, Farrington JW, Deuser WG. Polycyclic aromatic-hydrocarbons in an anoxic sediment core from the Pettaquamscutt River (Rhode-Island, USA). Geochim Cosmochim Acta 1980;44:873–8.

Holoubek I, Korínek P, Seda Z, Schneiderová E, Holoubková I, Pacl A, et al. The use of mosses and pine needles to detect persistent organic pollutants at local and re-gional scales. Environ Pollut 2000;109:283–92.

Hosker RP, Lindberg SE. Review: atmospheric deposition and plant assimilation of gases and particles. Atmos Environ 1982;16:889–910.

Johnsen A, Karlson U. Diffuse PAH contamination of surface soils: environmental occur-rence, bioavailability, and microbial degradation. Appl Microbiol Biotechnol 2007;76:533–43.

Johnsen AR, Wick LY, Harms H. Principles of microbial PAH-degradation in soil. Environ Pollut 2005;133:71–84.

Laflamme RE, Hites RA. The global distribution of polycyclic aromatic hydrocarbons in recent sediments. Geochim Cosmochim Acta 1978;42:289–303.

Lei L, Khodadoust AP, Suidan MT, Tabak HH. Biodegradation of sediment-bound PAHs in field-contaminated sediment. Water Res 2005;39:349–61.

MacKenzie AB, Farmer JG, Sugden CL. Isotopic evidence of the relative retention and mo-bility of lead and radiocaesium in Scottish ombrotrophic peats. Sci Total Environ 1997;203:115–27.

Malawska M, Ekonomiuk A, Wiłkomirski B. Polycyclic aromatic hydrocarbons in peat cores from southern Poland: distribution in stratigraphic profiles as an indicator of PAH sources. International Mire Conservation Group, International Peat Society; 2006.

Martens D, Maguhn J, Spitzauer P, Kettrup A. Occurrence and distribution of polycyclic aromatic hydrocarbons (PAHs) in an agricultural ecosystem. Fresenius J Anal Chem 1997;359:546–54.

Mitchell P, Schell W, McGarry A, Ryan T, Sanchez-Cabeza J, Vidal-Quadras A. Studies of the vertical distribution of 134Cs, 137Cs, 238Pu, 239,240Pu, 241Pu, 241Am and 210Pb in ombrogenous mires at mid-latitudes. J Radioanal Nucl Chem 1992;156:361–87.

Moore TR, Dalva M. Methane and carbon dioxide exchange potentials of peat soils in aerobic and anaerobic laboratory incubations. Soil Biol Biochem 1997;29:1157–64.

Moore TR, Blodau C, Turunen J, Roulet NT, Richard PJH. Recent rates of N and S accumulation in peatlands, eastern Canada. Glob Chang Biol 2004;11:356–67.

Moore TR, Lafleur PM, Poon DMI, Heumann BW, Seaquist JW, Roulet NT. Spring photo-synthesis in a cool temperate bog. Glob Chang Biol 2006;12:2323–35.

Muir DCG, Wang X, Yang F, Nguyen N, Jackson TA, Evans MS, et al. Spatial trends and historical deposition of mercury in eastern and northern Canada inferred from lake sediment cores. Environ Sci Technol 2009;43:4802–9.

Norton SA, Evans GC, Kahl JS. Comparison of Hg and Pb fluxes to hummocks and hollows of ombrotrophic big heath bog and to nearby Sargent Mt. Pond, Maine, USA. Water Air Soil Pollut 1997;100:271–86.

R Development Core Team. R: a language and environment for statistical computing. Vienna, Austria: R Foundation for Statistical Computing; 2011 [http://www. r-project.org/].

Sanders G, Jones KC, Hamiltontaylor J, Dorr H. PCB and PAH fluxes to a dated UK peat core. Environ Pollut 1995;89:17–25.

SARA. Volume I — chapter 3: historical review of air emissions from the smelting oper-ations. http://www.sudburysoilsstudy.com/EN/media/volume_I.asp. 2008. [access date: 2012-07-03].

Schneider AR, Stapleton HM, Cornwell J, Baker JE. Recent declines in PAH, PCB, and toxaphene levels in the northern Great Lakes as determined from high resolution sediment cores. Environ Sci Technol 2001;35:3809–15.

Shotyk W, Norton SA, Farmer JG. Summary of the workshop on peat bog archives of atmospheric metal deposition. Water Air Soil Pollut 1997;100:213–9.

Shuttleworth K, Cerniglia E. Environmental aspects of PAH biodegradation. Appl Biochem Biotechnol 1995;54:291–302.

Simcik MF, Eisenreich SJ, Golden KA, Liu S-P, Lipiatou E, Swackhamer DL, et al. Atmo-spheric loading of polycyclic aromatic hydrocarbons to Lake Michigan as recorded in the sediments. Environ Sci Technol 1996;30:3039–46.

Turetsky MR, Manning SW, Wieder RK. Dating recent peat deposits. Wetlands 2004;24: 324–56.

Turunen J, Roulet NT, Moore TR, Richard PJH. Nitrogen deposition and increased carbon accumulation in ombrotrophic peatlands in eastern Canada. Global Biogeochem Cycles 2004:18.

Urban NR, Eisenreich SJ, Grigal DF, Schurr KT. Mobility and diagenesis of Pb and 210Pb in peat. Geochim Cosmochim Acta 1990;54:3329–46.

Usenko S, Landers DH, Appleby PG, Simonich SL. Current and historical deposition of PBDEs, pesticides, PCBs, and PAHs to rocky mountain national park. Environ Sci Technol 2007;41:7235–41.

Vile MA, Wieder RK, Novak M. Mobility of Pb in Sphagnum-derived peat. Biogeochemistry 1999;45:35–52.

Wakeham SG, Schaffner C, Giger W. Polycyclic aromatic hydrocarbons in recent lake sediments—I. Compounds having anthropogenic origins. Geochim Cosmochim Acta 1980;44:403–13.

Wild SR, Jones KC. Polynuclear aromatic hydrocarbons in the United Kingdom environment: a preliminary source inventory and budget. Environ Pollut 1995;88:91-108.

Wong HKT, Nriagu JO, Coker RD. Atmospheric input of heavy metals chronicled in lake sediments of the Algonquin Provincial Park, Ontario, Canada. Chem Geol 1984;44: 187–201.

Zaccone C, D'Orazio V, Shotyk W, Miano T. Chemical and spectroscopic investigation of porewater and aqueous extracts of corresponding peat samples throughout a bog core (Jura Mountains, Switzerland). J Soils Sediment 2009a;9:443–56.

Zaccone C, Gallipoli A, Cocozza C, Trevisan M, Miano T. Distribution patterns of selected PAHs in bulk peat and corresponding humic acids from a Swiss ombrotrophic bog profile. Plant Soil 2009b;315:35–45.

Supplementary Material

How suitable are peat cores to study historical deposition of PAHs?

Sabine Thuens[1], Christian Blodau[1, 2], and Michael Radke[1, 3] *

[1] Department of Hydrology, BayCEER, University of Bayreuth, Bayreuth, Germany

[2]Hydrology Group, Institute of Landscape Ecology, University of Muenster, Muenster, Germany

[3]Department of Applied Environmental Science (ITM), Stockholm University, Sweden

[*]Correspondence: michael.radke@itm.su.se

Table S1: Coordinates of Greater Sudbury and sampling locations

Site Name	Latitude (N)	Longitude (W)	Extension of bog (km^2)	pH of bog water	Distance of sampling location to nearest road (m)
Mer Bleue (MB)	45.41042	75.516117	20	3.5	600
Giant Bog † (GB)	46.42422	79.937056	0.7	3.5	450
Eagle LakeBog (ELB)	45.80572	79.444830	1.35	3.7	125
Spruce Bog (SB)	45.59050	78.373055	0.3	4.3	385
Green LakeBog (GLB)	45.68517	77.151194	0.45	3.7	125
OpeongoLake (OPL)	45.41042	78.317483	-	-	-

† the name Giant Bog was assigned to this site as no previous description and thus no established name was available

Fig. S1: Locations of sampled peat bogs and Opeongo Lake in Ontario, Canada, in relation to North America

GC Conditions

CP-3800 and Saturn 2000, Varian:
cool on-column injection; injection volume 3 µL; injector program 130 °C held for 0.5 min, 200 °C min^{-1} to 320 °C, held for 30 min, 200 °C min^{-1} to 205 °C, held for 36 min; column VF-5ms (Varian; 50 m × 0.25 mm × 0.25 µm); carrier gas flow (He) 1.2 mL min^{-1}; temperature program 0.5 min at 130 °C, 3 °C min^{-1} to 320 °C, and held for 5 min.

GC 8000 MS, Finnigan:

split/splitless injection; injection volume 1 µL; injector program 130 °C held for 0.5 min, 200 °C min^{-1} to 320 °C, held for 30 min, 200 °C min^{-1} to 205 °C, held for 36 min; column DB-5ms (Agilent; 30 m × 0.25 mm × 0.25 µm); carrier gas flow (He) 1.2 mL min^{-1}; temperature program 2 min at 100 °C, 10 °C min^{-1} to 300 °C, and held for 18 min.
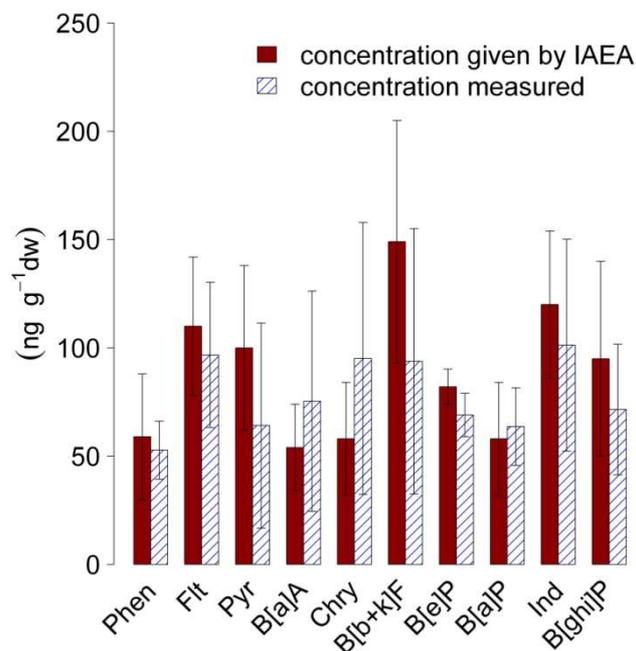
Fig. S2: Fig. 1: Comparison of measured (n = 5) and nominal PAH concentrations in the reference material; the columns represent the average value, error bars represent the 95 % confidence interval.

Table S2: Limit of Quantification and maximum concentrations in blanks in ng g^{-1}dw peat or sediment

	Phen	Flt	Pyr	B[a]A	Chry	B[b+k+j]F	B[a]P	B[e]P	Ind	B[ghi]P
LOQ	2	2	2	4	3	4	4	3	11	7
Max. conc. in blank	0	4	5	2	48	8	3	5	2	2
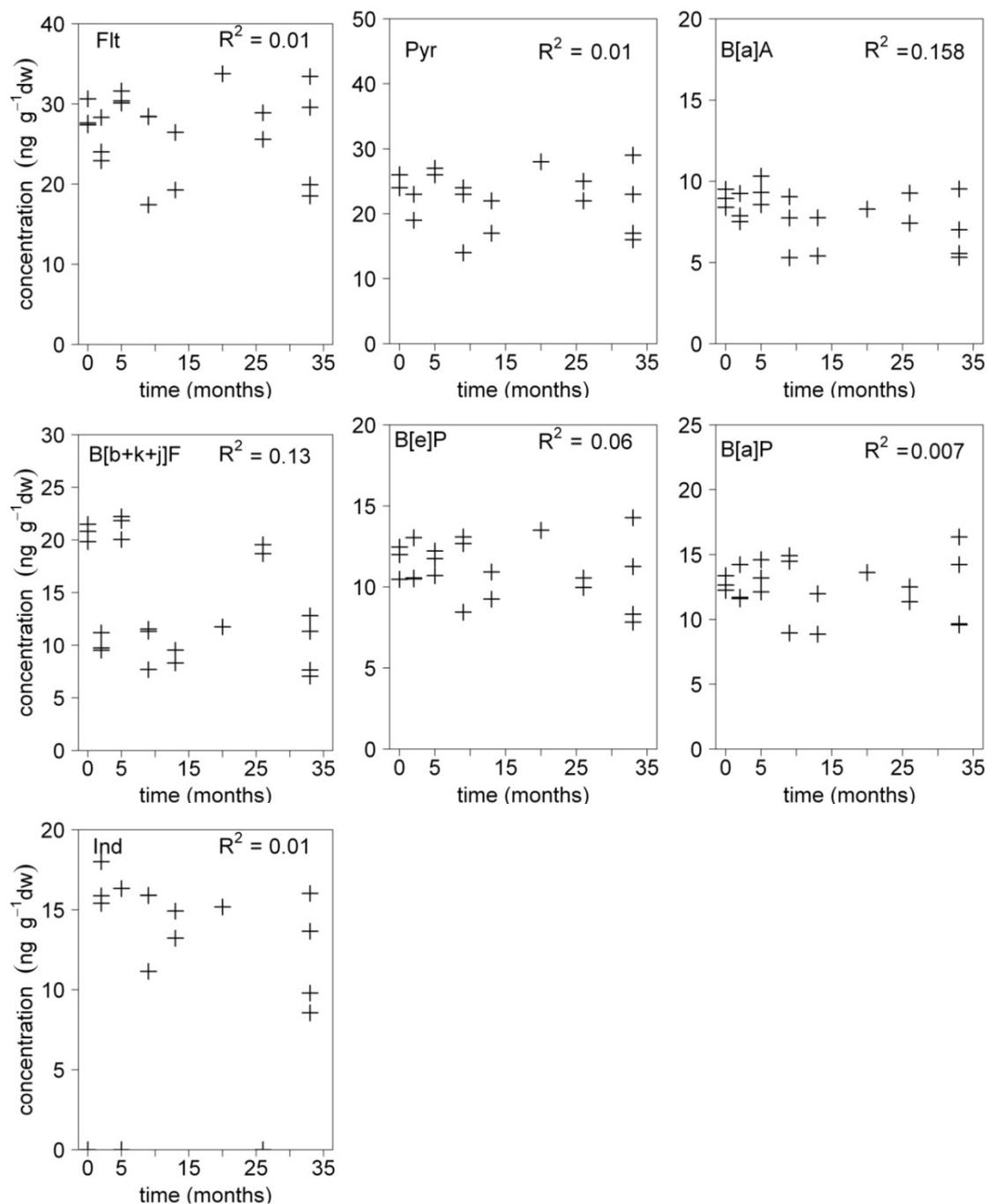
Fig. S3: Concentration of PAHs in ng g^{-1}dw peat over 33 months (n = 3) in aerobic incubations with coefficient of determination.
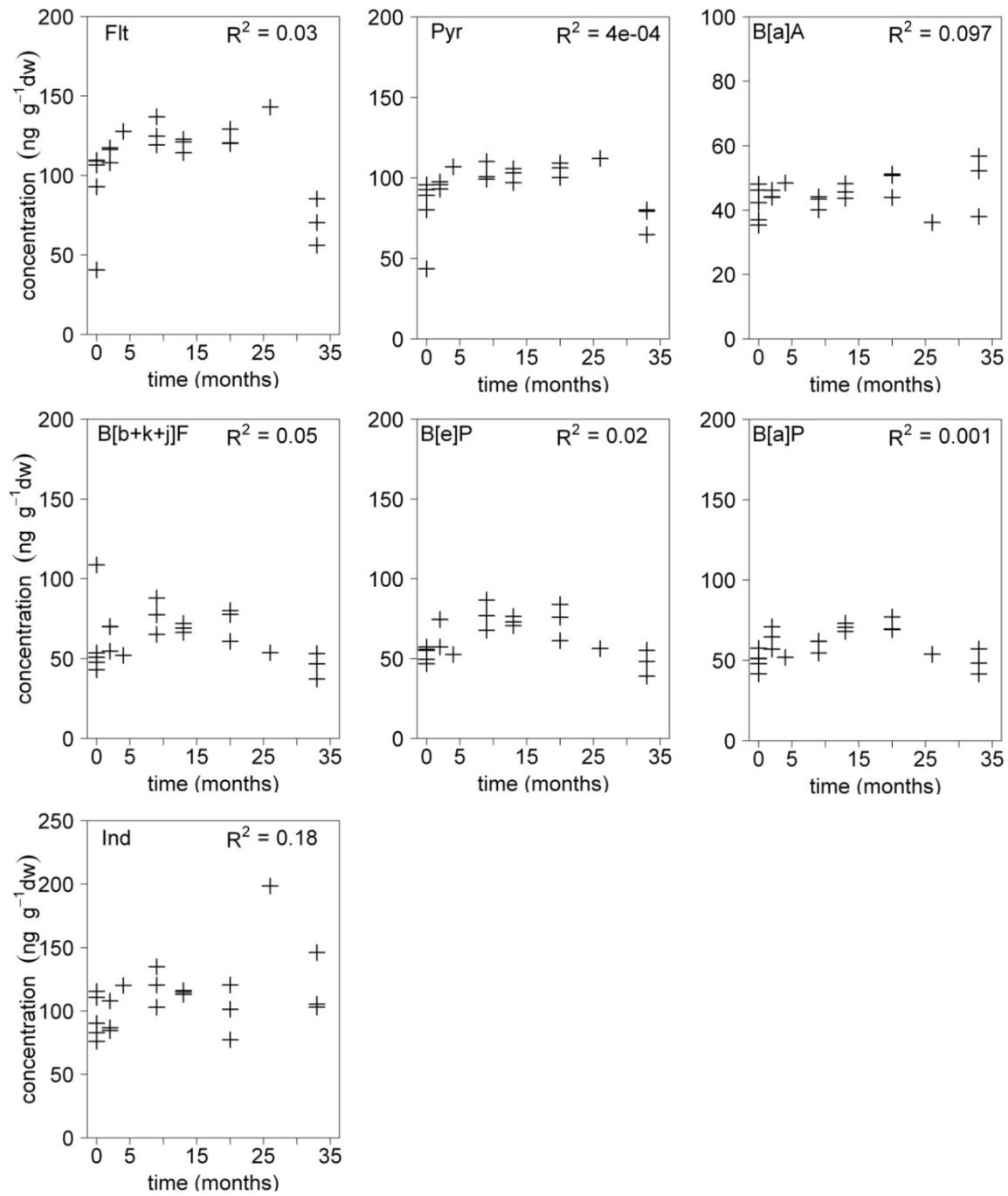
Fig. S4:Concentration of PAHs in ng g^{-1}dw peat over 33 months (n = 3) in anaerobic incubations with coefficient of determination.
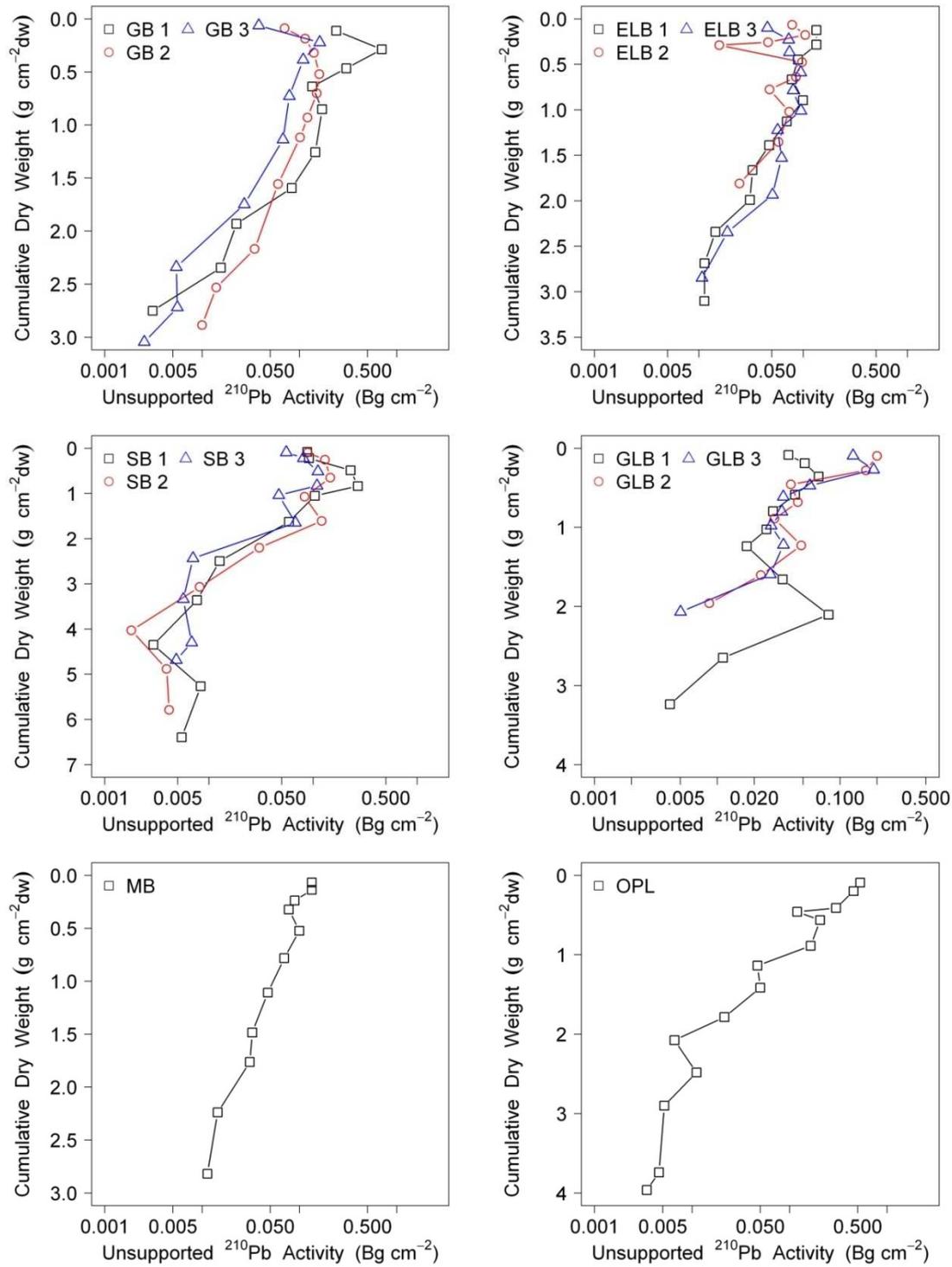
Fig. S5: Regression of unsupported ^{210}Pb activity versus accumulated dry weight of all profiles.
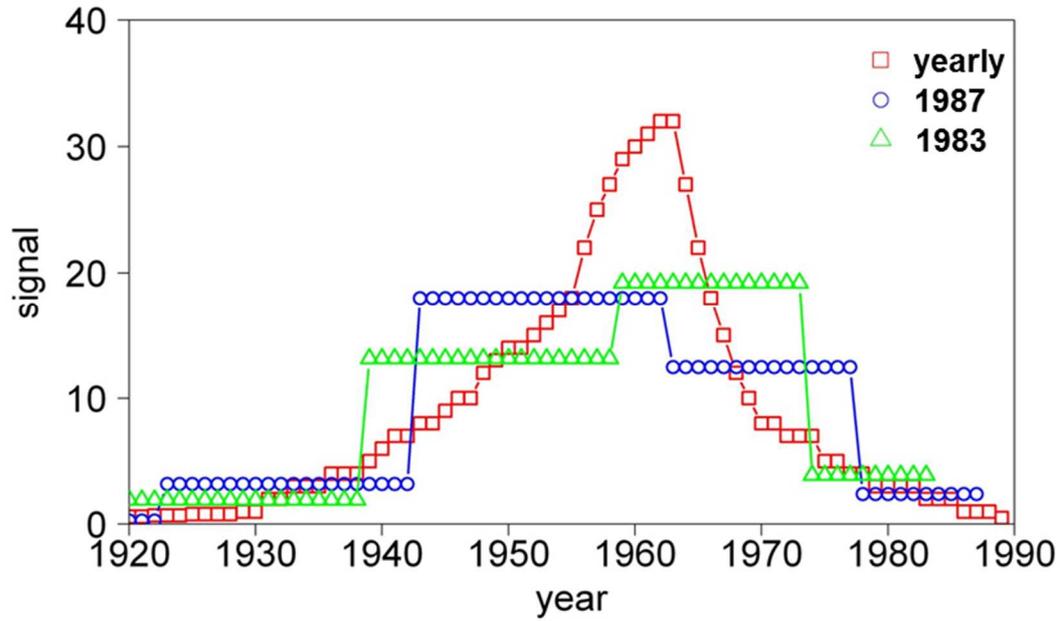
Fig. S6: Synthetic dataset for a parameter measured at yearly resolution and covered by different peat profiles *.

*The segment length is (from youngest to oldest): 10, 15, 20, 20, 25 years. The dataset labeled "1987" (blue) represents results that would be obtained from a core starting in 1987, while the dataset "1983" (green) represents a core starting in 1983. Both cores have the same time resolution of the individual segments. Maximum in the yearly data series is in year 1962. While the green core captures this maximum well (it falls into the period 1959-1973), the maximum is shifted to an earlier period (1943-1962). This illustrates apparent uncertainties in using the [241]Am peak as an independent dating reference.
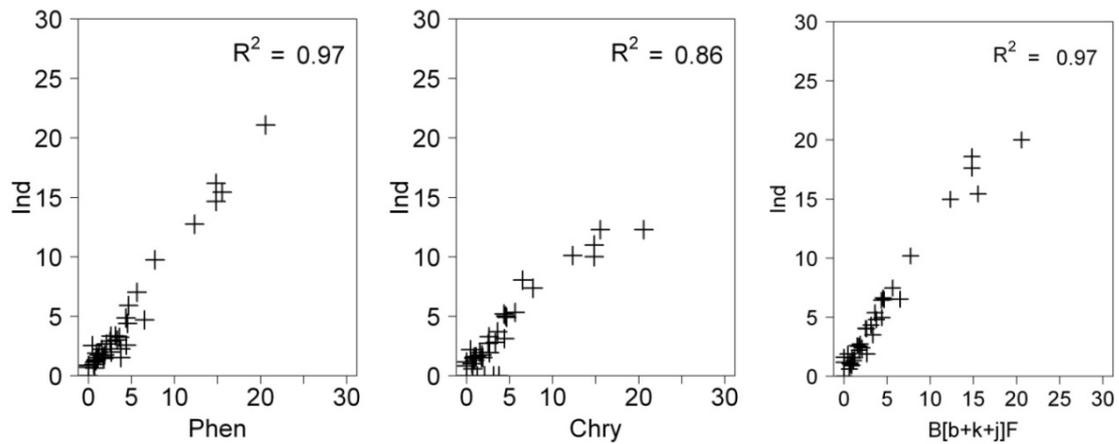
Fig. S7: Deposition rates in µg m^{-2}a^{-1} of Ind plotted against deposition rates of Phen, Chry and B[b+k+j]F at GLB with coefficient of determination.
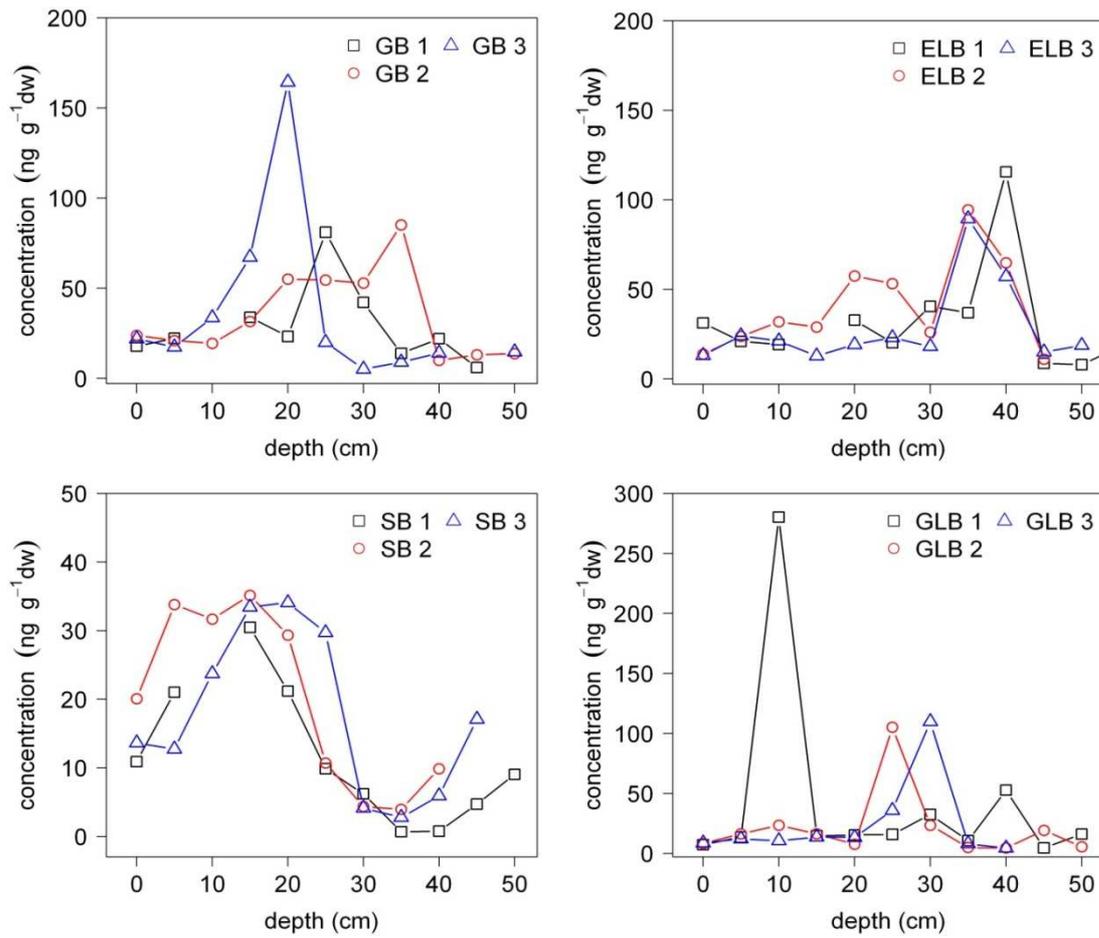
Fig. S8: Concentration of Phen over depth (cm) of three peat cores per bog
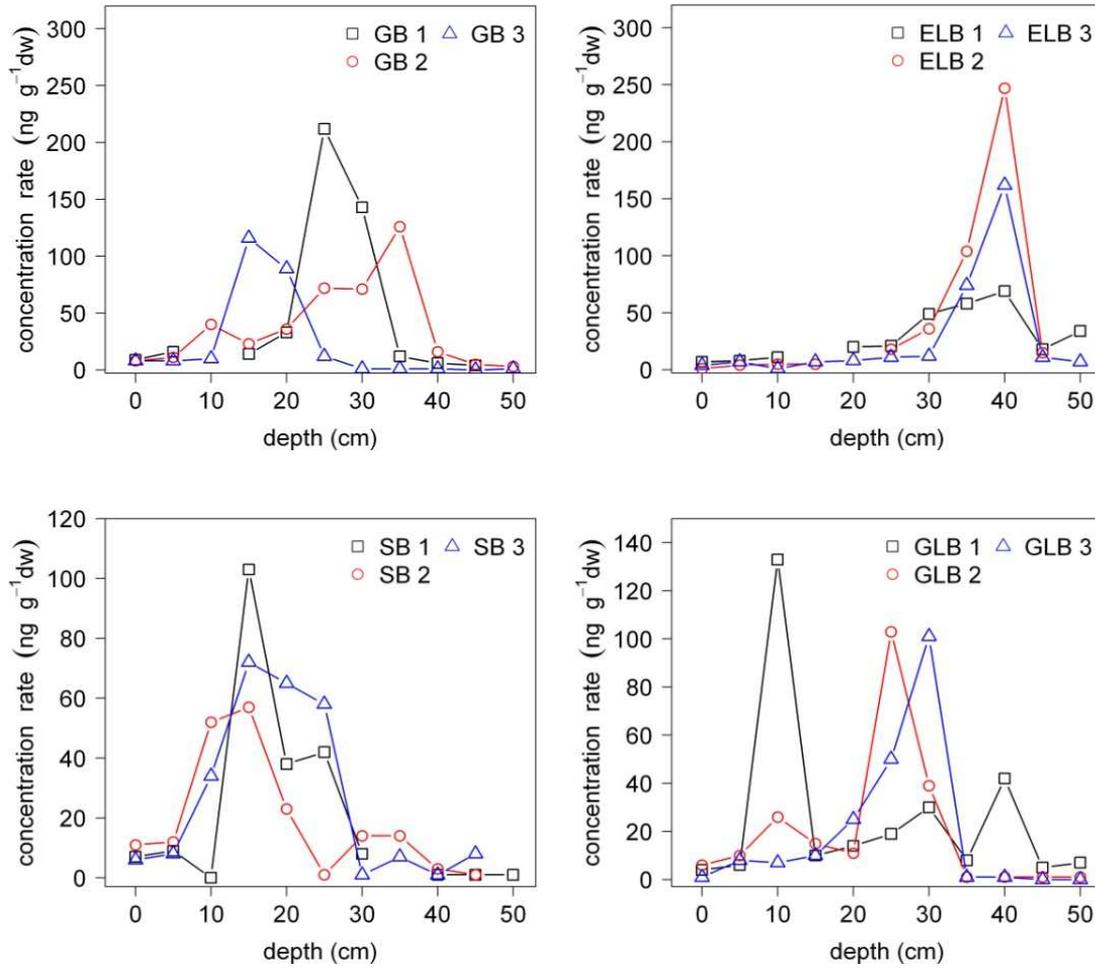
Fig. S9: Concentration of Ind (ng g $^{-1}$ dw) over depth (cm) of three peat cores per bog
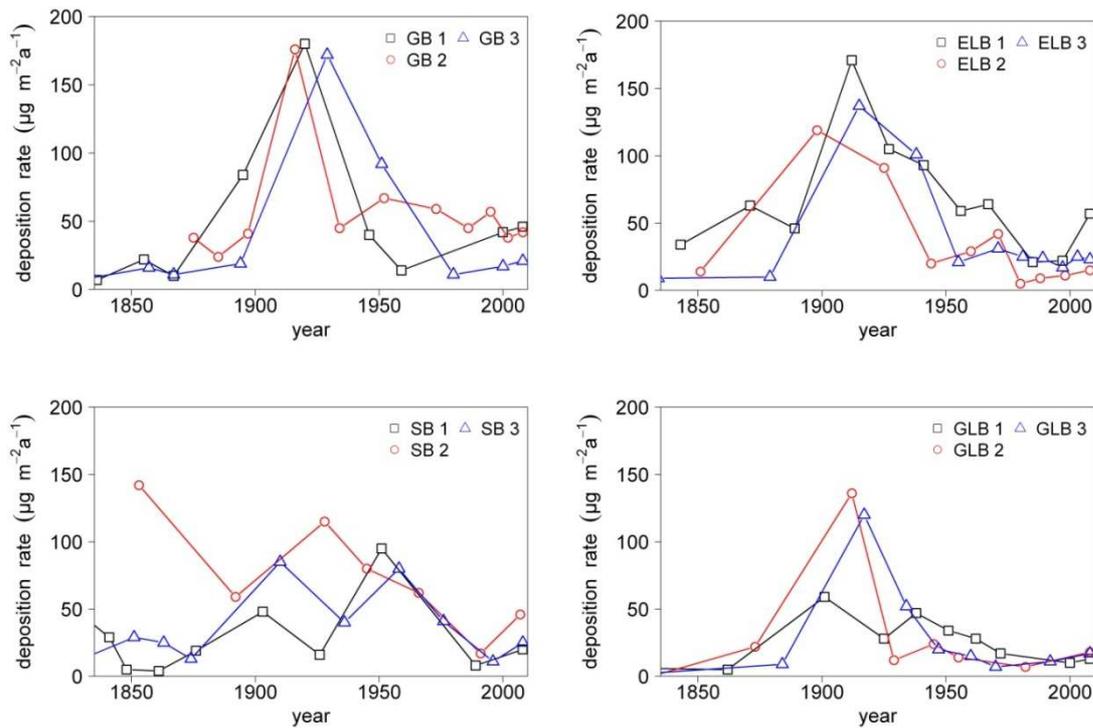
Fig. S10: Deposition rates of ∑12 PAH to three peat cores per bog between 1840 and 2000.
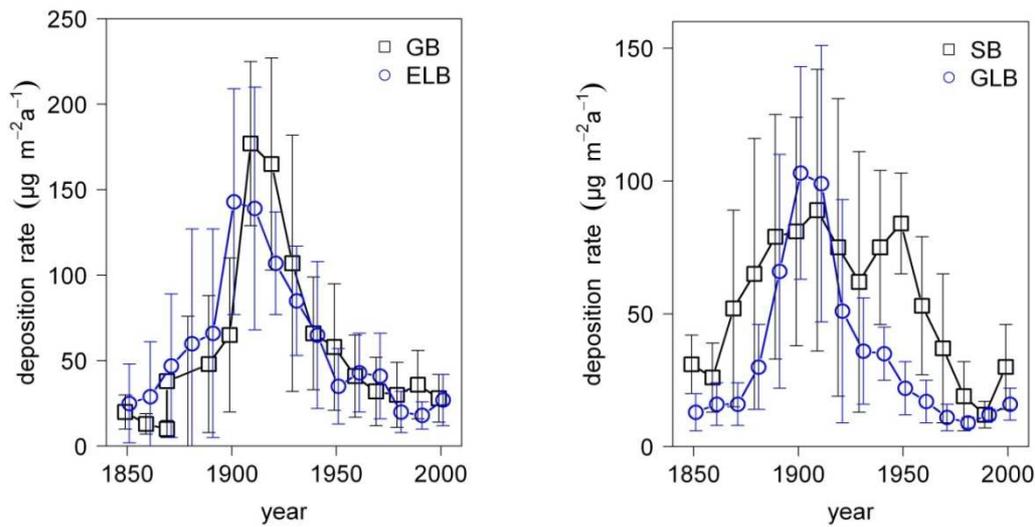
Fig.S11: Deposition rates of $\sum_{12}$ PAHs in µg m^{-2}a^{-1} averaged to decades in sampled bogs, error bars represent standard deviation of the three cores sampled.

Table S3: Concentration of PAHs in surface samples of Mer Bleue in ng g^{-1} (n = 5) in hollows and hummocks with standard deviation

	Phen	Flt	Pyr	B[a]A	Chry	B[b+k+j]F	B[a]P	B[e]P	Ind	B[ghi]P
hollow	77.1	13.4	18.5	3.9	19.3	34.9	13.6	10.9	19.3	14.3
Sd.	28.8	3.0	4.2	0.4	3.9	4.9	1.8	1.2	2.2	1.5
hummock	41.4	10.4	12.9	2.8	13.4	22.1	8.7	8.0	12.8	9.6
Sd.	5.9	3.7	5.5	1.1	2.5	6.2	3.2	3.0	4.5	3.0

Table S4: Mean recent deposition rates (µg m^{-2} yr^{-1}) per bog of single PAHs and $\sum_{12}$ PAH with standard deviation (s.d.; n = 3).

	Phen	Flt	Pyr	BaA	Chry	BbkF	BjF	BaP	BeP	Ind	BghiP	$\sum_{12}$ PAH	s.d
GB	6	4	10	0	5	3	1	2	1	2	2	36	22
ELB	7	4	5	1	4	4	1	2	1	1	2	32	22
SB	4	5	4	1	4	3	1	2	1	2	2	30	13
GLB	2	3	2	1	1	1	1	1	1	1	1	16	2

Study 3

Evaluation of peat cores as archives of polychlorinated biphenyl deposition rates

Sabine Thuens, Christian Blodau, and Michael Radke

To be submitted

Evaluation of peat cores as archives of polychlorinated biphenyl deposition rates

Sabine Thuens[1], Christian Blodau[1, 2], and Michael Radke[1, 3] [*]

[1] Department of Hydrology, BayCEER, University of Bayreuth, Bayreuth, Germany;

[2] Institute of Landscape Ecology, University of Muenster, Muenster, Germany

[3] Department of Applied Environmental Science (ITM), Stockholm University, Sweden

[*]Correspondence: michael.radke@itm.su.se

Abstract

To evaluate if peat bogs can be used as natural passive samplers for monitoring temporal and spatial trends of PCBs deposition 12 peat profiles in 4 bogs were sampled in Ontario, Canada. Anaerobic and aerobic degradation experiments of PCBs in peat were conducted over 3 years. Over this time span no degradation was observed. Maximum reconstructed deposition rates of $\sum_{11}$PCBs were up to 1.0 µg m^{-2}a^{-1}. The variation in the maximum deposition rates of $\sum_{11}$PCBs ranged from 15 to 29 % within one bog. In all cores PCBs were detected in sections that were dated before the onset of PCB production and use. In these sections the congeners with Di- to Hepta-PCB congeners dominated. Time trends and maximum deposition rates determined for a sediment core were comparable to those from the bog in the vicinity of the lake sampled. The concentrations of Di- to Hepta-PCB congeners were evenly distributed along the sediment profile, and also found in pre-production sections. Although peat profiles only receive atmospheric inputs and respond fast to changes in contaminant deposition they obtain several limitations to study historical deposition rates of PCBs. The low temporal resolution and potential PCB mobility limit the suitability of peat archives to study temporal trends and absolute deposition rates.

1. Introduction

In recent decades many environmental pollutants have been banned or their emissions have been restricted. The group of polychlorinated biphenyls (PCBs) is a prominent ex-

ample for a class of compounds that has been banned. To demonstrate that these regulations are effective, the current concentrations of such pollutants in the environment have to be compared to historical ones. The latter ones are not always available but can be obtained from natural archives of pollution such as sediment or peat cores. Ombrotrophic peat bogs have been shown to be suitable natural passive samplers for atmospheric pollutants as they only receive wet and dry atmospheric deposition but no terrestrial inputs. In combination with continuous growth, limited degradation, and the possibility of dating by ^{210}Pb, they can be used as archives of atmospheric deposition of multiple classes of organic contaminants and for recording temporal changes (Rapaport and Eisenreich, 1988). Nevertheless, some limitations of these archives have been found like mobility within the peat and low temporal resolution (Thuens et al., 2013).

In this study we evaluate the suitability of peat cores as archive for deposition of polychlorinated biphenyls (PCBs). PCBs are chemically very stable industrial compounds and have been used as dielectric and coolant fluids. As some PCBs are carcinogenic and teratogenic, their production and use is restricted. After an OECD control decision in 1973 PCB production was banned by the United States Congress in 1979 and finally by the Stockholm Convention on Persistent Organic Pollutants in 2001 (Himberg and Pakarinen, 1994; UNEP, 2001). They are lipophilic, consequently bioaccumulative, and due to their persistence they are still present in the environment (Berset et al., 2001). Rapaport and Eisenreich (1988) observed that the atmospheric PCB deposition rates derived from ombrotrophic peat closely correlate with PCB usage in the U.S. It is thus likely that atmospheric deposition rapidly reflects changes in the use pattern and that peat cores can be used to study historical PCB contamination trends (Himberg and Pakarinen, 1994). Schneider et al. (2001) assumed that PCBs are not degraded or remobilized within a peat core. But in both U.K. and U.S. peatlands, significant amounts of PCBs have been measured in peat sections originating from pre production times. This may be the result of immediate downward percolation of PCBs with rainfall (Rapaport and Eisenreich, 1988; Sanders et al., 1995). Movement of PCBs in peat has not been tested directly; however, field data suggest that PCB immobility may not be a reliable assumption (Turetsky et al., 2004). Therefore, it is necessary to study the reliability and the suitability of these records of atmospheric deposition (Berset et al., 2001).

The scope of this study is to analyze if peat bogs can be used as natural passive samplers to monitor the historical and regional trends of PCBs in the environment. Besides possi-

ble mobility the heterogeneity of PCB deposition within a bog was analyzed. We also evaluated if degradation in peat occurs over the time span of this study and compared time trends obtained from peat with trends obtained from a sediment core. To this end we sampled 12 peat profiles in 4 bogs in Ontario, Canada, and one sediment core from a lake in the vicinity of one bog.

2. Materials and Methods

2.1. Sampling

Four peat bogs in Eastern Ontario, Canada were sampled in 2007 and 2008: Giant Bog (GB), Eagle Lake Bog (ELB), Spruce Bog (SB), and Green Lake Bog (GLB) (coordinates are given Table S1 and Figure S1 in Supporting Information). Samples were taken at the domed ombrotrophic section of the bogs from undisturbed hollows (< 10 m distance between sampling locations). We sampled three peat cores per bog with a box corer ($87 \times 90.6 \times 1000$ mm) and used only cores that showed as less compaction as possible. Cores were cut into 5 cm segments in the field; each segment was wrapped in aluminum foil, transferred to a plastic bag and stored in a cooler. In Opeongo Lake (location and details given in Muir et al. (2009) and in SI) one sediment core was sampled with a gravity corer at the deepest point.. The sediment core was sectioned every 1 cm. All samples were frozen directly after arrival in the laboratory. More details on the sampling procedures are given in Thuens et al. (2013).

2.2. Degradation experiments

In Mer Bleue Bog (MB; location given in Supporting Information) we sampled aerobic and anaerobic peat which was transferred to incubation sets in Germany. Aerobic and anaerobic degradation experiments were conducted as described in Thuens et al. (2013) for PAHs. Three replicates containing aerobic or anaerobic peat of the lab incubations were analyzed on PCB concentrations after 2, 5, 9, 13, 20, 26, and 33 months, each. All concentrations reported for the aerobic incubation experiments were normalized to the weight of dry peat at the beginning of each experiment. As concentrations of several PCBs were below the limit of quantification, we were only able to determine concentrations of PCB 101, 138, 153, and 180 in the aerobic degradation experiments and PCB101,138, 153, 180 ,194, 195, and 209 in the anaerobic degradation experiments.

2.3. Chemicals and Analysis

All solvents were of residue analysis quality (nonane and dichloromethane purchased from Promochem, Wesel, Germany; hexane from J.T. Baker, Griesheim, Germany). Native and isotope-substituted PCBs (purity >98 %) were purchased from Ehrenstorfer, Augsburg, Germany.Glassware was machine washed, solvent rinsed, and baked at 280 °C overnight.

Peat and sediment samples were freeze dried, milled to a fine powder in a pebble mill and kept frozen until extraction with pressurized liquid extraction.Extraction cells were filled with 5 g of dry peat or sediment. A solution containing isotope-substituted PCBs as recovery standards (PCBs: 28, 52, 101, 138, 153, 180, 209) was spiked directly onto the peat. The cells were filled up with diatomaceous earth (Celite 545 coarse, Sigma-Aldrich, Munich, Germany) and extracted with pressurized liquid extraction (ASE Dionex 200, Dionex Co., Sunnyvale, USA). The extract was reduced to about 1 mL with a rotary evaporator (Büchi, Switzerland). For clean-up 3 g of aluminium oxide (aluminium oxide 90, neutral, deactivated with 15 wt % water, 70-230 mesh from Merck, Darmstadt, Germany) upon 5 g of silica gel (silica gel 60, 200 mesh; Merck)were filled into glass columns of 1 cm diameter. The extracts were then quantitatively transferred to the columns and eluted with 35 mL of hexane followed by30 mL of hexane/dichloromethane 3/1 (v/v). The combined extracts were evaporated to approx. 1 mL by use of a rotary evaporator and then subjected to size exclusion chromatography for further clean-up. To this end, columns of 2.2 cm diameter filled with Bio-Beads (S-X-3, Bio-Rad, Hercules, USA) and equilibrated with hexane/dichloromethane 1/1 were used. The extracts were quantitatively transferred to the columns and eluted with 60 mL of hexane/dichloromethane 1/1. This fraction was discarded. The target compounds were then eluted with 120 mL of hexane/dichloromethane. The column was subsequently rinsed with 100 mL of the solvent mixture and re-used. The extracts were evaporated to 1 mL by a rotary evaporator and finally evaporated to dryness under a gentle stream of nitrogen. Prior to injection, samples were redissolved in 200 µL of a solution containing ^{13}C labeled PCB 123 ^{13}C in nonane and transferred to glass vials.

We quantified the following 11 PCB congeners (Ballschmiter-numbers of the individual PCBs in brackets): Tetra (44, 52, 70), Penta (101), Hexa (138, 151, 153), Hepta (180), Octa (194 and 195) and Deca (209).The sum of all analyzed PCBs is referred to as $\sum_{11}$PCBs throughout the manuscript. The concentrations of PCBs were determined by

GC/MS (CP-3800 and Saturn 2000, Varian, Darmstadt, Germany, and GC 8000 MS, Finnigan, Austin, USA). The temperature programs are given in the Supporting Information. Stock solutions were prepared by diluting single compounds in nonane. Calibration solutions (native compounds and recovery standards (see above: 1 – 200 ng mL^{-1}; injection standards PCB 123 ^{13}C:100ng mL^{-1}) were prepared by dilution a mix of the stock solutions in nonane. They were measured daily with each set of samples. The analytical procedure was evaluated by analyzing commercially available certified reference material (IAEA-159, Sediment; n = 5).Laboratory blank samples (n = 13) were analyzed with every set of samples.

Dry-milled subsamples (approximately 1 g from each 5 cm peat segment, 200 mg of each 1 cm sediment segment) were submitted to Flett Research Ltd (Winnipeg, Canada) or to the Institute of Environmental Geochemistry (University of Heidelberg, Germany) for ^{210}Pb analysis. The CRS model of Appleby and Oldfield (1978) was applied for data evaluation as described in Thuens et al.(2013).

2.2 Concentrations and deposition rates in peat cores

Concentrations of PCBs were normalized to the dry weight (dw) of the peat samples. The PCB inventories were calculated as the total integrated mass of a compound per square meter as described by Schneider et al. (2001). To assure that all peat profiles represent the same time span, only layers younger than 1880 were taken into account as this time span was represented by all peat cores. Deposition rates of the individual compounds (ng m^{-2} a^{-1}) were calculated by dividing the measured amount per peat segment by the years represented by this segment and the surface sampled. Deposition rates determined for Opeongo Lake were corrected by division with a sediment particle focusing factor (2.66) taken from Thuens et al. (2013). Statistical analysis was conducted with the software R (R Core Team, 2012).

3. Results and discussion

3.1. Quality assurance

The limits of detection and of quantification for PCBs are given in Supporting Information (Table S2). The mean recovery rates of the isotope-substituted internal standards were between 60 ± 28 % (PCB 52) and 79 ± 26 % (PCB 209) (n = 129). More data is available in Fig. S2 as Supporting Information. Concentrations of PCBs measured in the

certified reference sediment were within the range given by the distributor (IAEA) (Fig. 1). Concentrations of PCB 209 determined in this study were low, but within the range of the standard deviation given by the IAEA.
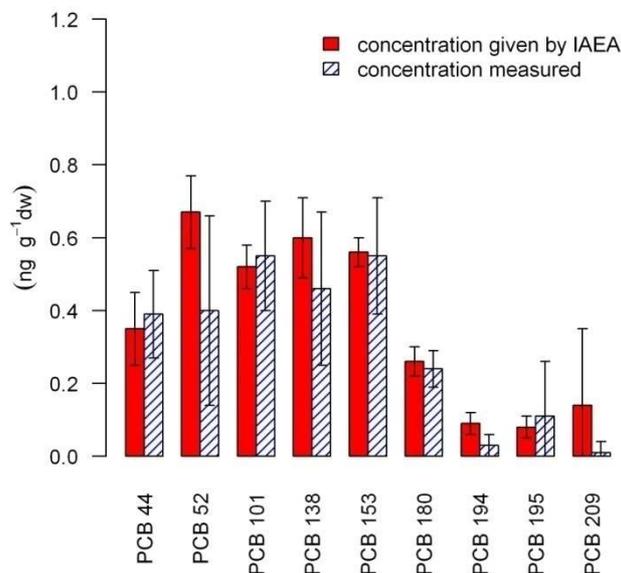
Fig. 1: concentration of PCBs in reference material, given by IAEA and measured; n = 5; error bars represent 95 % confidence interval.

Only in one blank sample we detected PCBs (<400 pg g^{-1}), in all other blank samples PCB concentrations were below the limit of detection. Therefore, we did not blank correct the results for PCBs.

3.2. PCBs in peat

3.2.1. Degradation

No obvious and statistically significant (p<0.05) concentration time trend of PCBs was seen in the aerobic and anaerobic degradation experiments (Fig S3 A and B). However, the scattering in the data is very high as the concentrations were close to the detection limit and probably also due to inhomogeneous material, and consequently it is difficult to provide a robust interpretation. As discussed in our previous paper on PAHs, the degradation experiments were conducted under conditions which favor degradation (higher temperature, no accumulation of CO_2 and CH_4) (Thuens et al., 2013). We therefore assume that the PCB degradation should not be important for the time scale represented by the peat cores (120 years).

It is not trivial to assess the stability of compounds over a long time scale in the environment, especially when emission still can occur. Malmquist et al. (2003) found PCB congener patterns in sediments of seven lakes in West Greenland that were almost identical to the congener patterns from a commercial PCBs mixture. This indicates that no degradation of any specific PCB congener and no formation of any specific less-chlorinated congener as degradation product has occurred in these sediments. On the other hand these results are indicating that no fractionation of the congeners has been taken place during atmospheric transport which is in contrast to many other studies. Nevertheless, Li et al. (2009) assumed evidence for in-situ degradation of sedimentary PCBs as they found the fraction of heavier congeners decreasing with depth. But they only detected this trend in Lake Ontario and not in Lake Michigan. They also discussed that several studies did not determine this trend.

Anaerobic dechlorination of PCBs has been observed in several studies on sediments. A major factor influencing the biodegradation is the bioavailability of PCBs, which is determined by adsorption and desorption processes. Over time, the so called process of aging of PCB contaminations leads to stronger adsorption and lower recovery rates of PCBs (Tiedje et al., 1993; Øfjord et al., 1994). As a high fraction of PCBs is adsorbed to peat due to the high content of organic matter of peat, bioavailability of PCBs in peat can be assumed to be low. The optimal pH for overall removal of chlorines of PCBs is around 7 (Wiegel and Wu, 2000). The low pH of < 4 in peat might therefore also reduce the dechlorination rates of PCBs.

Tiedje et al. (1993) determined anaerobic dechlorination rates of 3 µg Cl/g sediment per week of PCBs in sediments. This is totally in contrast to our results for the anaerobic degradation in peat. Therefore, we agree with Sanders et al. (1995) that the digenesis of higher chlorinated congeners by anaerobic dechlorination is not thought to be of any significance as the degradation rate is too low to influence the concentrations significantly.

3.2.2. Timing of historical deposition rates

Highest concentrations of $\sum_{11}$PCBs up to 6.8 ng g^{-1}were measured at a depth of 10-35 cm (dating from 1925 to 1986) in the peat cores. Maximum reconstructed deposition rates of $\sum_{11}$PCBs were up to 1.0 µg m^{-2}a^{-1}(Fig. 2 for ELB, see Fig. S4 to S6 in SI for profiles of other bogs).The dominant congener groups found in the peat samples were Tetra- (mean value = 39 %), Penta- (15 %) and Hexa-chlorobiphenyls (22%). Berset et al.(2001) and

Himberg and Pakarinen (1994) found Tri-, Tetra- and Penta-chlorobiphenyls to be the most dominant ones with 20, 33 and 20 %, and 30, 25 and 23 %, respectively.
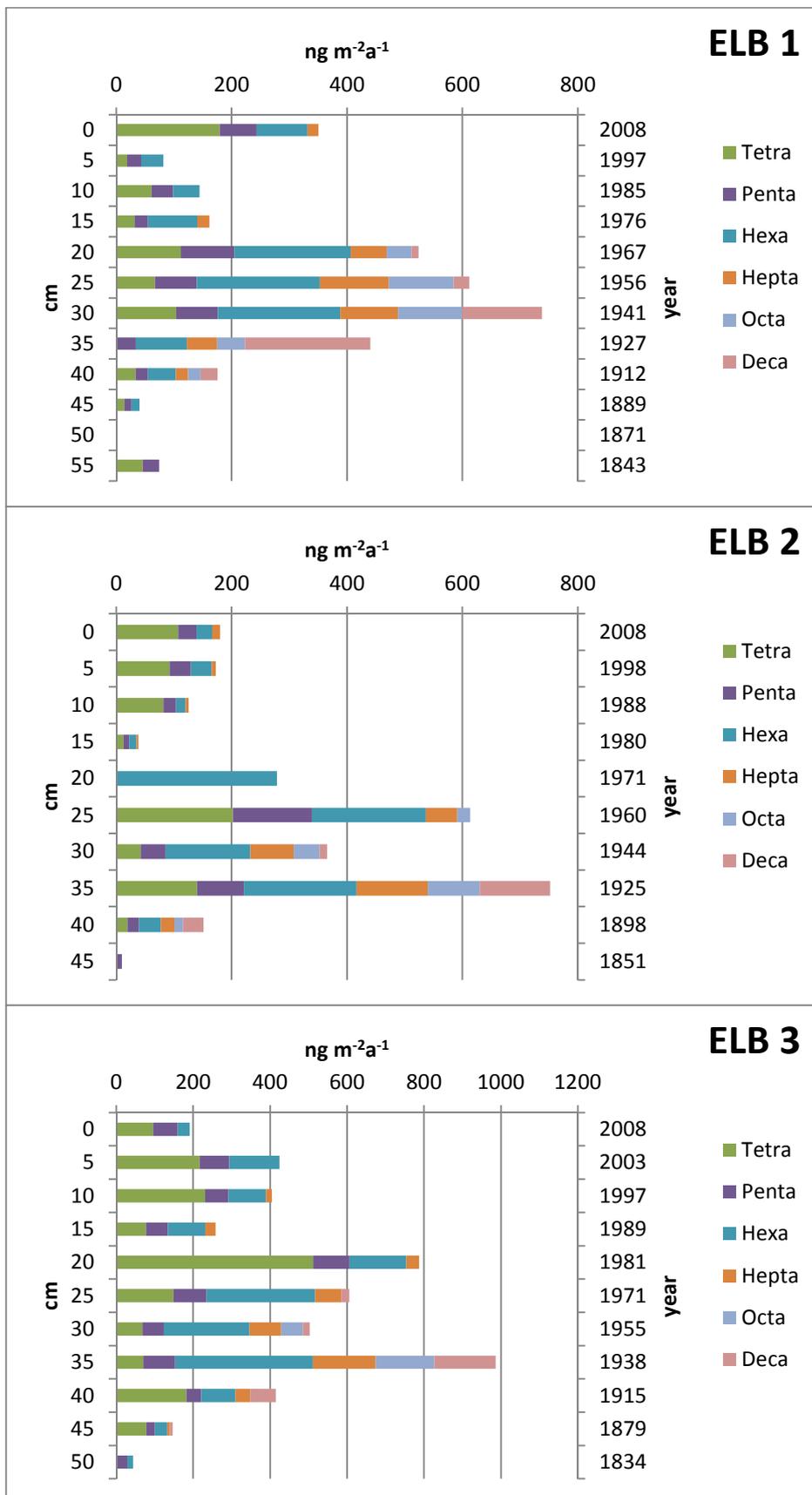
Fig. 2: Deposition rates of PCB congener groups to Eagle Lake Bog in 3 peat core profiles over depth (cm) and years.

All cores contained PCBs in sections that were dated before the onset of PCB production and use (1930s). Between 6.2 % (SB 2) to 55 % of $\sum_{11}$PCBs in GB1 are pre-production (23 % of $\sum_{11}$PCBs in average of all cores). This is similar to the findings of Sanders et al. (1995) and Rapaport and Eisenreich (1988) who found 30 % and between 6 to 30 % of PCB residues, respectively, below the depth corresponding to 1930. As Sanders et al. found almost exclusively Tri- and Tetra-congeners below 21 cm (pre 1945) they assumed that these concentrations were partly caused by post-depositional mobility. As the lower chlorinated congeners are more water soluble than the highly chlorinated ones, they might be preferentially translocated to older sections. In sections from pre-production periods analyzed in our cores, the congeners with 4 to 7-Cl congeners dominated.

The temporal resolution of the peat cores is relatively low as discussed in Thuens et al.(2013). Therefore, certain events like maximum deposition rates might appear too late or too early, as the 5 cm segments reflect up to 30 years of deposition. Nevertheless, in 8 out of the 12 cores the maximum deposition rates occurred 5 to 15 cm below the layer dated to the maximum production of PCBs (around 1970; usually resulting in maximum emission rates to the environment). This shift does not change when only analyzing Octa- and Deca-PCBs indicating that it is not caused by the different solubility of the congeners. Rapaport and Eisenreich concluded that mobility of PCBs is likely due to downward advective transport within the peat due to rainfall (Rapaport and Eisenreich, 1988).

3.2.3. Heterogeneity of deposition rates in peat cores

For all four peat bogs comparable historical maximum deposition rates were determined (between 600 to 1100 ng m^{-2}a^{-1}). No peat bog contained significantly higher concentrations of PCBs (p < 0.1). Therefore, they seem to reflect regional deposition and no local contamination. Barthel et al. (2012) found higher PCB concentrations in passive samplers deployed in GLB compared to concentrations of passive samplers deployed in the other bogs. The passive samplers reflect only recent concentrations which might not be reflected in the peat profiles yet.

One important aspect of the suitability of peat archives to study historical deposition rates is the heterogeneity within one bog. The standard deviation of the maximum deposition rates of $\sum_{11}$PCBs of the three cores per bog ranged from 15 % (SB) to 29 % (GB). This deviation is mainly caused by the different time span the layers represent and by the

possible mobility. If the layer of the maximum deposition is representing a relative long time period the maximum might get "diluted" by lower rates. Nevertheless, this variation is less than found for PAHs in the three cores (up to 41 %) (Thuens et al., 2013).

In case of mobile contaminants, inventories are suitable to analyze contamination patterns as long as the contaminants are not transported out of the system. The mean inventories of the three cores per bog of $\sum_{11}$PCBs ranged from 37.0 ± 5.4 to 47.2± 27.8 to µg m^{-2} (Table S3). This is 10 times lower than the inventory of $\sum_{25}$PCBs determined by Sanders et al. (1995) in a bog in the UK indicating a higher pollution of rural areas in the UK than in Ontario, Canada.

The standard deviation of the inventories of $\sum_{11}$PCBs given in Table 1 ranged from 15 % (GLB) to 59 % (GB). The 15 % are comparable with the deviation found for PAHs, but the deviation found for inventories of PCBs in GB is almost twice as high as the one for PAHs. In one core of GB we determined high concentrations of Tetra-PCBs, which cause this high deviation.

Table 1: Mean inventories since 1880 of PCBs in peat bogs in µg m^{-2} (n = 3) with standard deviation and in sediment of Opeongo Lake corrected with focusing factor (n.d. = not detected).

	Tetra	Penta	Hexa	Hepta	Octa	Deca	Sum
GB	16.0± 13.9	5.6± 2.3	11.7± 5.8	4.9± 2.4	3.5± 1.5	5.5± 2.0	47.2± 27.8
ELB	10.9± 7.4	5.7± 1.2	14.3± 8.6	5.3± 0.9	3.6± 1.7	4.8± 1.3	44.5± 21.2
SB	10.3± 5.0	5.3± 2.1	14.4± 8.8	4.6± 2.1	4.0± 1.4	3.6± 1.4	42.2± 20.8
GLB	11.3± 0.7	6.6± 1.0	10.7± 2.0	4.9± 1.1	1.7± 0.2	1.8± 0.5	37.0± 5.4
OPL	50.3	12.2	6.8	1.8	1.5	2.9	75.5

3.2.4. Comparison bogs and lake

In the OPL sediment core we found $\sum_{11}$PCB concentrations of maximum 42 ng g^{-1}(1984-1991) and deposition rates were up to 1344 ng m^{-2}a^{-1}at maximum. This is comparable to the rates we found in cores from SB which is located in the vicinity of OPL. Rapaport and Eisenreich (1988) also reported similar PCB deposition rates from lake sediments and bogs. The inventory of $\sum_{11}$PCB in OPL was 75.5 µg m^{-2} and almost 2 times higher than the one of SB. Taking into account the high standard deviation of the three invento-

ries of SB, they are still comparable. Muir et al. determined inventories of $\sum_{90}$PCB in sediments of three lakes in Ontario. Although they analyzed 90 congeners they found comparable inventories of up to 120 µg m^{-2}(Muir et al., 1996).

Di- to Hepta-PCB congeners were found in all sections in the sediment profile, even in layers dated to times before PCB production (Fig. 3). Malmquist et al.(2003) and Gevao et al. (1997) also determined lower chlorinated PCBs in preproduction sections in several lake sediments. Isosaari et al.(2002) measured concentrations of PCBs in sediment sections older than 8000 years, withTetra- and Penta-congeners dominating. They assumed that contamination by ambient air during sampling and extraction with the lower chlorinated PCBs might be an explanation for the concentrations in the deep sections. Kjeller and Rappe (1995) also found PCBs in depth dated before PCB production but did not see a enhancement in Tetra- and Penta-congeners. Yamashita et al. (2000) found the deepest sections in their sampled sediment core to be dominated by Tri- and Tetra-congeners. They assumed a selective movement or the existence of an unknown source, potentially natural.

The concentrations of Octa- and Deca-PCB congeners are below the detection limit in preproduction sections in the OPL core. The occurrence in deeper layers seems to be congener specific for the chlorination degree (Fig. 3). Therefore smearing of surface material into deeper sections during core extrusion can be excluded.

The PCB pattern in the sediment profile is dominated by Tetra-PCB congeners. This is in contrast to the congener pattern found in the peat cores. As the Tetra-congeners are detected in all depths of the OPL core it might be that they have natural sources (Gribble, 1992). As discussed by Alcock et al. (1994) it is more reasonable that these congeners are artefacts due to contamination. Gevao et al. (1997) assumed that contamination during sample preparation and analysis, and selective downward migration depending on the amount of chlorination are possible reasons. An enrichment of Tetra-PCBs in Hudson River sediment inoculated with a population enriched from an industrial sludge lagoon as products of dehalogenation by biodegradation has been seen by Tiedje et al. (1993).
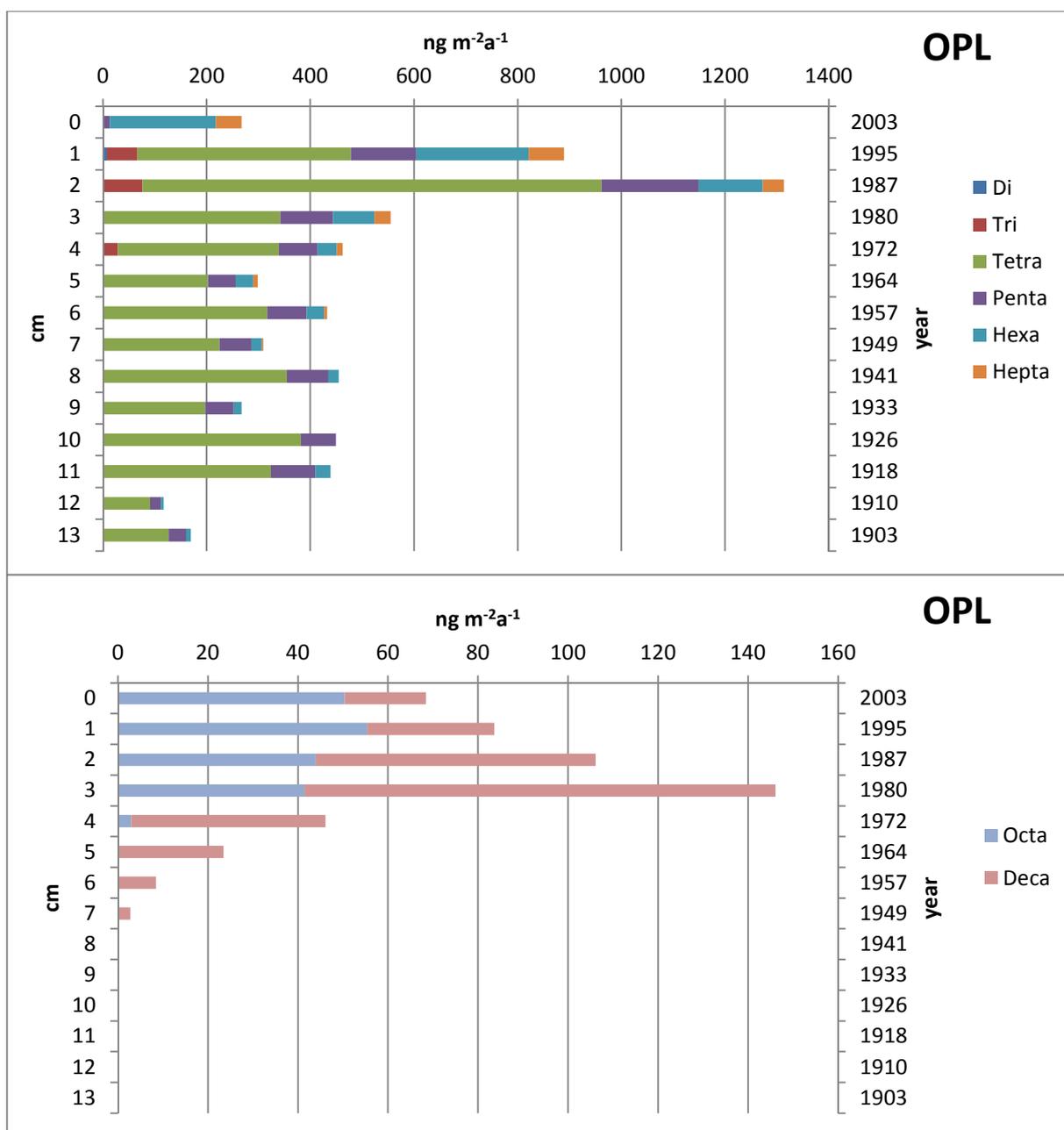
Fig. 3: Deposition rates of PCB congeners to OPL over depth and years.

Octa- and Deca-PCBs were mainly introduced in the environment with Aroclor 1260 which was only produced before 1950. Surprisingly their maximum deposition rate is at 1980 and recent rates are still elevated. Although new contamination can still occur through damage to old PCB-containing transformers and by disturbance of PCB-containing sludge and sediments or by ongoing transport of these congeners in the environment, this cannot explain this time shift. We did not detect any Octa- and Deca-congeners in the recent peat layers. As sediment is the slowest compartment in responding to a change in atmospheric pollutant deposition (Li et al., 2006) and it might take up to decades to see changes in load of contaminants in sediment (Nylund et al., 1992), it

might be that OPL reflects a former contamination pattern. In the sediment profiles of Muir et al. (1996) the peak in PCB concentrations also appears pretty late (1980 to 1984). Yamashita et al. (2000) also found a time lag between peak periods of production and usage and the deposition to marine environment. They explained this with the hydraulic residence times and particle deposition velocities.

Compared with the deposition profile of OPL, the deposition profiles of Octa- and Deca-PCB determined in SB have no time shift (see Supporting Information Fig. S5). In the sediment core deposition trends seem to be displayed with a certain delay. The lower chlorinated PCBs were evenly distributed along the profile and therefore are supposed to be mobile. For this reason sediment profiles should only be used to determine historical deposition pattern of higher chlorinated PCBs.

4. Suitability of peat cores to study PCB deposition rates

As discussed above the degradation of PCBs in peat is assumed to be low. Thus, degradation does not bias historical deposition rates. The advantage of peat profiles is that they only receive atmospheric inputs and respond fast to changes in contamination patterns. Nevertheless in the case of PCBs the low temporal resolution of the 5 cm segments used in this study and the potential mobility diminish this advantage. Due to the low concentrations of PCBs in peat it is difficult to sample thinner sections and still obtain detectable concentrations. The PCB deposition rates showed maxima 10 cm below the maximum production. This shift can be caused by translocation in peat. Partly, it can also be caused by the low temporal resolution of the 5 cm sections as discussed in Thuens et al.(2013). Nevertheless, the shift in maximum deposition rates was less for PAHs. Due to their planar structure PAHs might be incorporated better into the peat matrix and consequently less mobile.

Rapaport and Eisenreich (1988) observed that the atmospheric PCB deposition rates derived from ombrotrophic peat closely correlate with PCB usage in the U.S.. When looking at the results of this study and the mobility of PCBs in peat as discussed above it is surprisingly they obtained such comparable deposition rates.

Although peat profiles only receive atmospheric inputs and respond fast to changes in contamination patterns they obtain many limitations to study historical deposition rates of PCBs. The low temporal resolution and the potential mobility of most congeners might lead to incorrect temporal trends and absolute deposition rates.

Acknowledgements

References

Alcock, R.E., Halsall, C.J., Harris, C.A., Johnston, A.E., Lead, W.A., Sanders, G., Jones, K.C., 1994. Contamination of Environmental Samples Prepared for PCB Analysis. Environmental Science & Technology 28, 1838-1842.

Appleby, P.G., Oldfield, F., 1978. The calculation of lead-210 dates assuming a constant rate of supply of unsupported ^{210}Pb to the sediment. CATENA 5, 1-8.

Barthel, P., Thuens, S., Shunthirasingham, C., Westgate, J.N., Wania, F., Radke, M., 2012. Application of XAD-resin based passive air samplers to assess local (roadside) and regional patterns of persistent organic pollutants. Environmental Pollution 166, 218-225.

Berset, J.D., Kuehne, P., Shotyk, W., 2001. Concentrations and distribution of some polychlorinated biphenyls (PCBs) and polycyclic aromatic hydrocarbons (PAHs) in an ombrotrophic peat bog profile of Switzerland. Science of the Total Environment 267, 67-85.

Gevao, B., Hamilton-Taylor, J., Murdoch, C., Jones, K.C., Kelly, M., Tabner, B.J., 1997. Depositional Time Trends and Remobilization of PCBs in Lake Sediments. Environmental Science & Technology 31, 3274-3280.

Gribble, G.W., 1992. Naturally Occurring Organohalogen Compounds--A Survey. Journal of Natural Products 55, 1353-1395.

Himberg, K.K., Pakarinen, P., 1994. Atmospheric PCB deposition in Finland during 1970s and 1980s on the basis of concentrations in ombrotrophic peat mosses (Sphagnum). Chemosphere 29, 431-440.

Isosaari, P., Pajunen, H., Vartiainen, T., 2002. PCDD/F and PCB history in dated sediments of a rural lake. Chemosphere 47, 575-583.

Kjeller, L.-O., Rappe, C., 1995. Time Trends in Levels, Patterns, and Profiles for Polychlorinated Dibenzo-p-dioxins, Dibenzofurans, and Biphenyls in a Sediment Core from the Baltic Proper. Environmental Science & Technology 29, 346-355.

Li, A., Rockne, K.J., Sturchio, N., Song, W., Ford, J.C., Buckley, D.R., Mills, W.J., 2006. Polybrominated Diphenyl Ethers in the Sediments of the Great Lakes. 4. Influencing Factors, Trends, and Implications. Environmental Science & Technology 40, 7528-7534.

Li, A., Rockne, K.J., Sturchio, N., Song, W., Ford, J.C., Wei, H., 2009. PCBs in sediments of the Great Lakes - Distribution and trends, homolog and chlorine patterns, and in situ degradation. Environmental Pollution 157, 141-147.

Malmquist, C., Bindler, R., Renberg, I., vanBavel, B., Karlsson, E., Anderson, N.J., Tysklind, M., 2003. Time Trends of Selected Persistent Organic Pollutants in Lake Sediments from Greenland. Environ. Sci. Technol. 37, 4319-4324.

Muir, D.C.G., Omelchenko, A., Grift, N.P., Savoie, D.A., Lockhart, W.L., Wilkinson, P., Brunskill, G.J., 1996. Spatial Trends and Historical Deposition of Polychlorinated Biphenyls in Canadian Midlatitude and Arctic Lake Sediments. Environ. Sci. Technol. 30, 3609-3617.

Muir, D.C.G., Wang, X., Yang, F., Nguyen, N., Jackson, T.A., Evans, M.S., Douglas, M., Kock, G., Lamoureux, S., Pienitz, R., Smol, J.P., Vincent, W.F., Dastoor, A., 2009. Spatial Trends and Historical Deposition of Mercury in Eastern and Northern Canada Inferred from Lake Sediment Cores. Environmental Science & Technology 43, 4802-4809.

Nylund, K., Asplund, L., Jansson, B., Jonsson, P., Litzen, K., Sellstrom, U., 1992. Analysis of some polyhalogenated organic pollutants in sediment and sewage sludge. Chemosphere 24, 1721-1730.

Rapaport, R.A., Eisenreich, S.J., 1988. Historical Atmospheric Inputs of High Molecular-Weight Chlorinated Hydrocarbons to Eastern North-America. Environmental Science & Technology 22, 931-941.

Sanders, G., Jones, K.C., Hamilton-Taylor, J., Dorr, H., 1995. PCB and PAH Fluxes to a Dated UK Peat Core. Environmental Pollution 89, 17-25.

Schneider, A.R., Stapleton, H.M., Cornwell, J., Baker, J.E., 2001. Recent declines in PAH, PCB, and toxaphene levels in the northern Great Lakes as determined from high resolution sediment cores. Environmental Science & Technology 35, 3809-3815.

Team, R.C., 2012. R: A language and environment for statistical computing. R Foundation for Statistical Computin Vienna, Austria http://www.r-project.org/.

Thuens, S., Blodau, C., Radke, M., 2013. How suitable are peat cores to study historical deposition of PAHs? The Science of the Total Environment.

Tiedje, J.M., Quensen, J.F., Chee-Sanford, J., Schimel, J.P., Boyd, S.A., 1993. Microbial reductive dechlorination of PCBs. Biodegradation 4, 231-240.

Turetsky, M.R., Manning, S.W., Wieder, R.K., 2004. Dating recent peat deposits. Wetlands 24, 324-356.

UNEP, 2001. Final Act of the Conference of Plenipotentaries on the Stockholm Convention on Persistent Organic Pollutants. United Nations Environment Program: Stockholm, Sweden.

Wiegel, J., Wu, Q., 2000. Microbial reductive dehalogenation of polychlorinated biphenyls. FEMS Microbiology Ecology 32, 1-15.

Yamashita, N., Kannan, K., Imagawa, T., Villeneuve, D.L., Hashimoto, S., Miyazaki, A., Giesy, J.P., 2000. Vertical Profile of Polychlorinated Dibenzo-p-dioxins, Dibenzofurans, Naphthalenes, Biphenyls, Polycyclic Aromatic Hydrocarbons, and Alkylphenols in a Sediment Core from Tokyo Bay, Japan. Environ. Sci. Technol. 34, 3560-3567.

Øfjord, G.D., Puhakka, J.A., Ferguson, J.F., 1994. Reductive Dechlorination of Aroclor 1254 by Marine Sediment Cultures. Environmental Science & Technology 28, 2286-2294.

Supporting Information

Evaluation of peat cores as archives of polychlorinated biphenyl deposition rates

Sabine Thuens[1], Christian Blodau[1, 2], and Michael Radke[1, 3] [*]

[1] Department of Hydrology, BayCEER, University of Bayreuth, Bayreuth, Germany;

[2] Institute of Landscape Ecology, University of Muenster, Muenster, Germany

[3] Department of Applied Environmental Science (ITM), Stockholm University, Sweden

[*] Correspondence: michael.radke@itm.su.se

Table S1: Coordinates of Greater Sudbury and sampling locations

Site Name	Latitude (N)	Longitude (W)	Extension of bog (km^2)	pH of bog water	Distance of sampling location to road (m)
Mer Bleue (MB)	45.41042	75.516117	20	3.5	600
Giant Bog † (GB)	46.42422	79.937056	0.7	3.5	450
Eagle Lake Bog (ELB)	45.80572	79.444830	1.35	3.7	125
Spruce Bog (SB)	45.59050	78.373055	0.3	4.3	385
Green Lake Bog (GLB)	45.68517	77.151194	0.45	3.7	125
Opeongo Lake (OPL)	45.41042	78.317483	-	-	-

† the name Giant Bog was assigned to this site as no previous description and thus no established name was available

Fig. S1: Locations of sampled peat bogs and lake in Ontario, Canada, in relation to North America

Information about GC Method

<u>CP-3800 and Saturn 2000, Varian:</u>

cool on-column injection; injection volume 10 µL; injector program 130 °C held for 0.1 min, 200 °C min^{-1} to 320 °C, held for 30 min, 200 °C min^{-1} to 205 °C, held for 21 min; column VF-5ms (Varian; 50 m × 0.25 mm × 0.25 µm); carrier gas flow (He) 1.2 mL min^{-1}; temperature program 3.5 min at 130 °C, 4 °C min^{-1} to 320 °C, and held for 2 min.

<u>GC 8000 MS, Finnigan:</u>

split/splitless injection; injection volume 1 µL; injector program 130 °C held for 0.5 min, 200 °C min^{-1} to 320 °C, held for 30 min, 200 °C min^{-1} to 205 °C, held for 36 min; column DB-5ms (Agilent; 30 m × 0.25 mm × 0.25 µm); carrier gas flow (He) 1.2 mL min^{-1}; temperature program 2 min at 100 °C, 10 °C min^{-1} to 300 °C, and held for 18 min.

Table S2: Limits of detection (LOD) and limits of quantification (LOQ) for PCBs taking into account the uncertainty of the calibration as described by the DIN 32645 (DIN 32645, 1994).

	LOD pg µL^{-1}	LOD pg g^{-1} dw	LOQ pg µL^{-1}	LOQ pg g^{-1} dw
PCB 52	1.0	41	4.0	159
^{13}CPCB 52	1.2	49	4.5	182
PCB 44	1.1	45	4.2	166
PCB 70	0.9	38	3.5	141
PCB 101	0.7	27	2.6	104
^{13}CPCB 101	1.5	59	5.4	217
PCB 151	0.9	36	3.4	136
PCB 138	1.1	42	3.9	158
^{13}CPCB 138	1.4	56	5.1	204
PCB 153	1.0	42	3.8	153
PCB 180	1.0	39	3.5	142
^{13}CPCB 180	1.3	53	4.8	191
PCB 194	1.3	52	4.8	192
PCB 195	1.3	51	4.6	186
PCB 209	0.9	36	3.3	134
^{13}CPCB 209	1.8	72	6.4	258
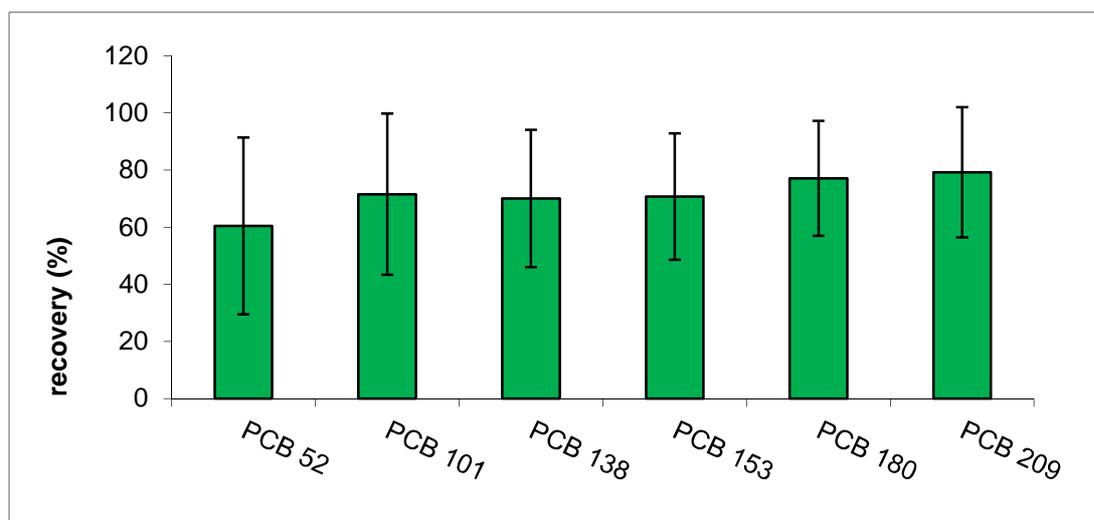
Fig. S2: Recovery rate of labeled PCBs (n = 127), error bars give standard deviation.

A.
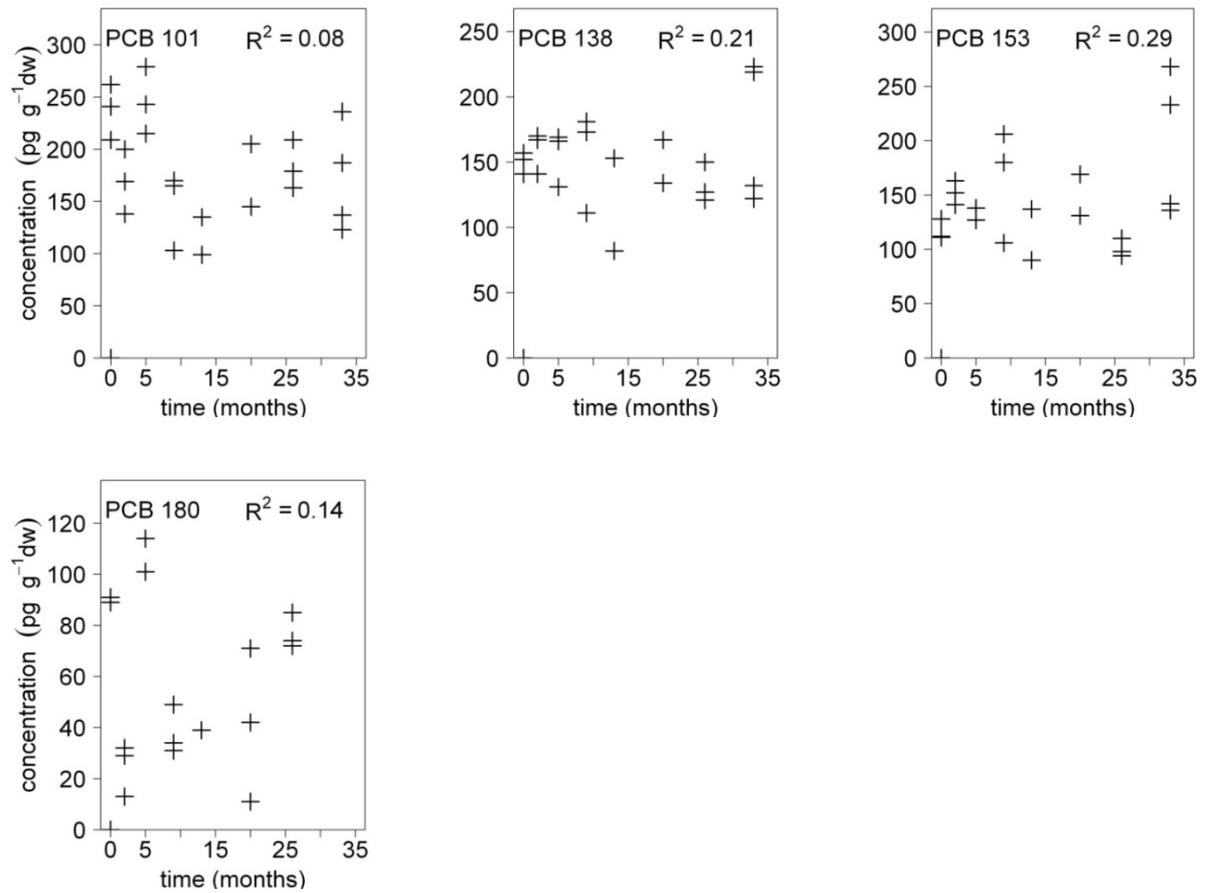
Fig. S3A: Concentrations time trend of PCBs in the aerobic degradation experiments with coefficient of determination.

B.
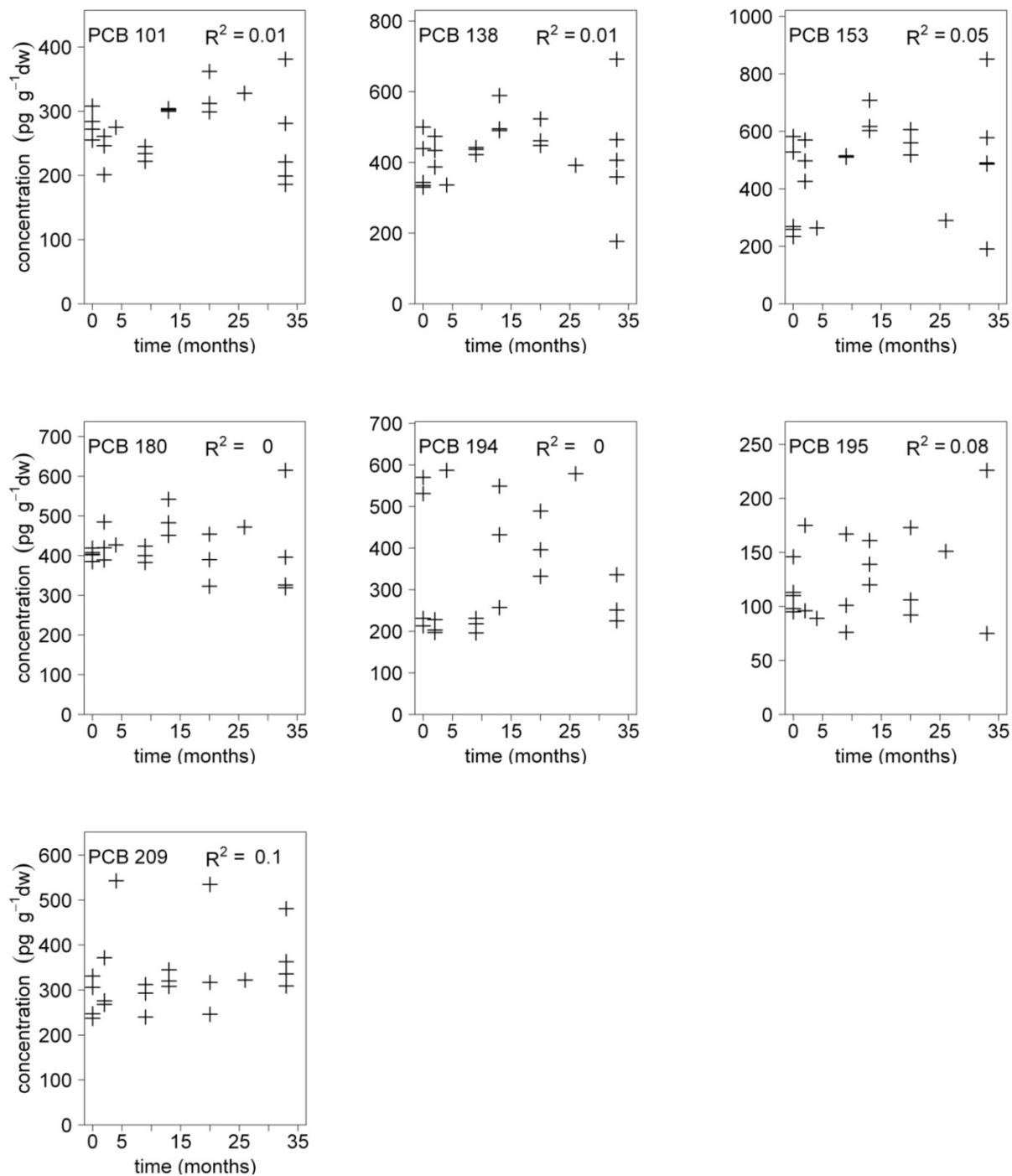
Fig. S3B: Concentrations time trend of PCBs in the anaerobic degradation experiments with coefficient of determination.
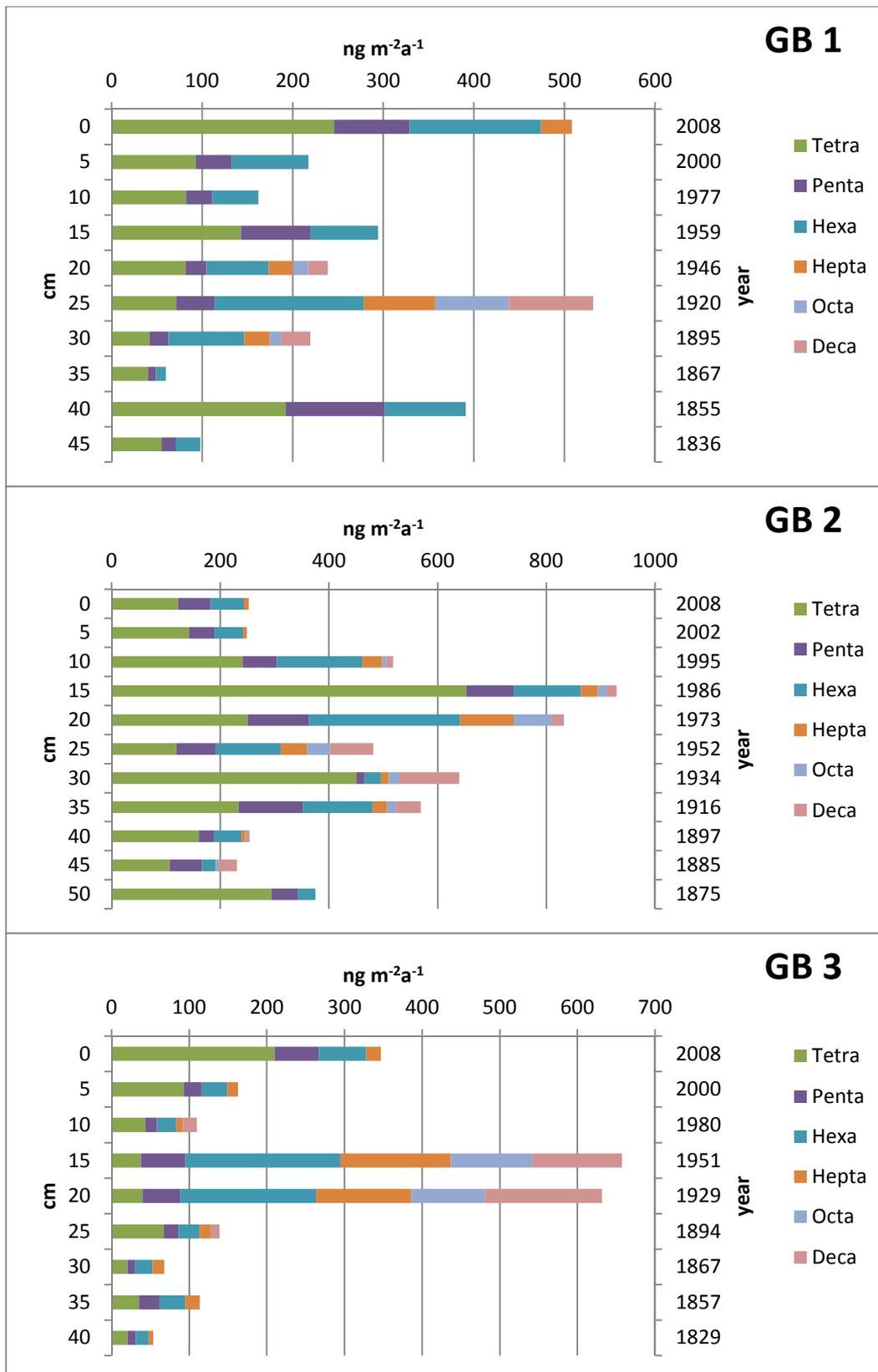
Fig. S4: Deposition rates of PCB congeners to Giant Bog in 3 peat core profiles over depth and years.
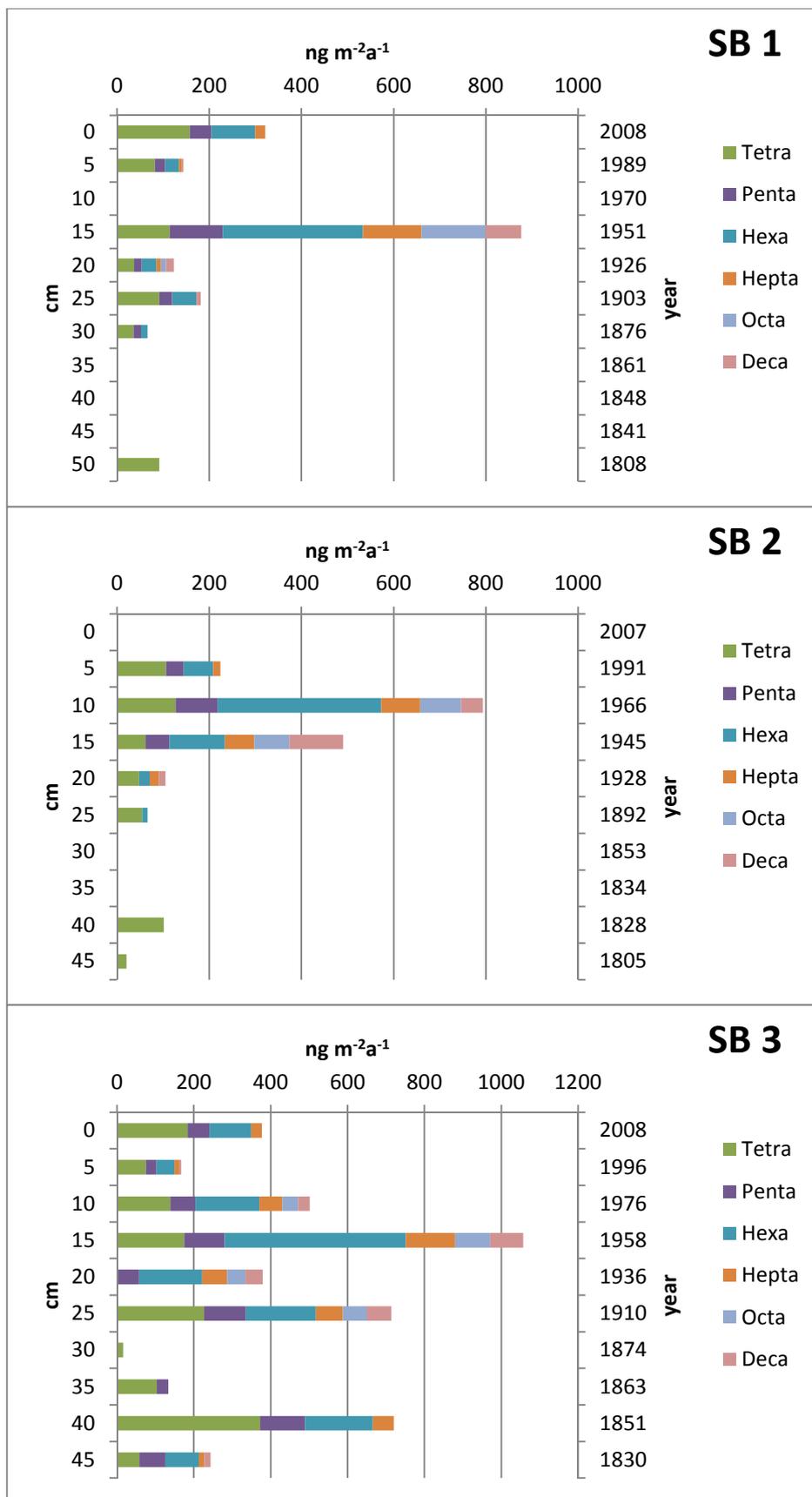
Fig. S5: Deposition rates of PCB congeners to Spruce Bog in 3 peat core profiles over depth and years.
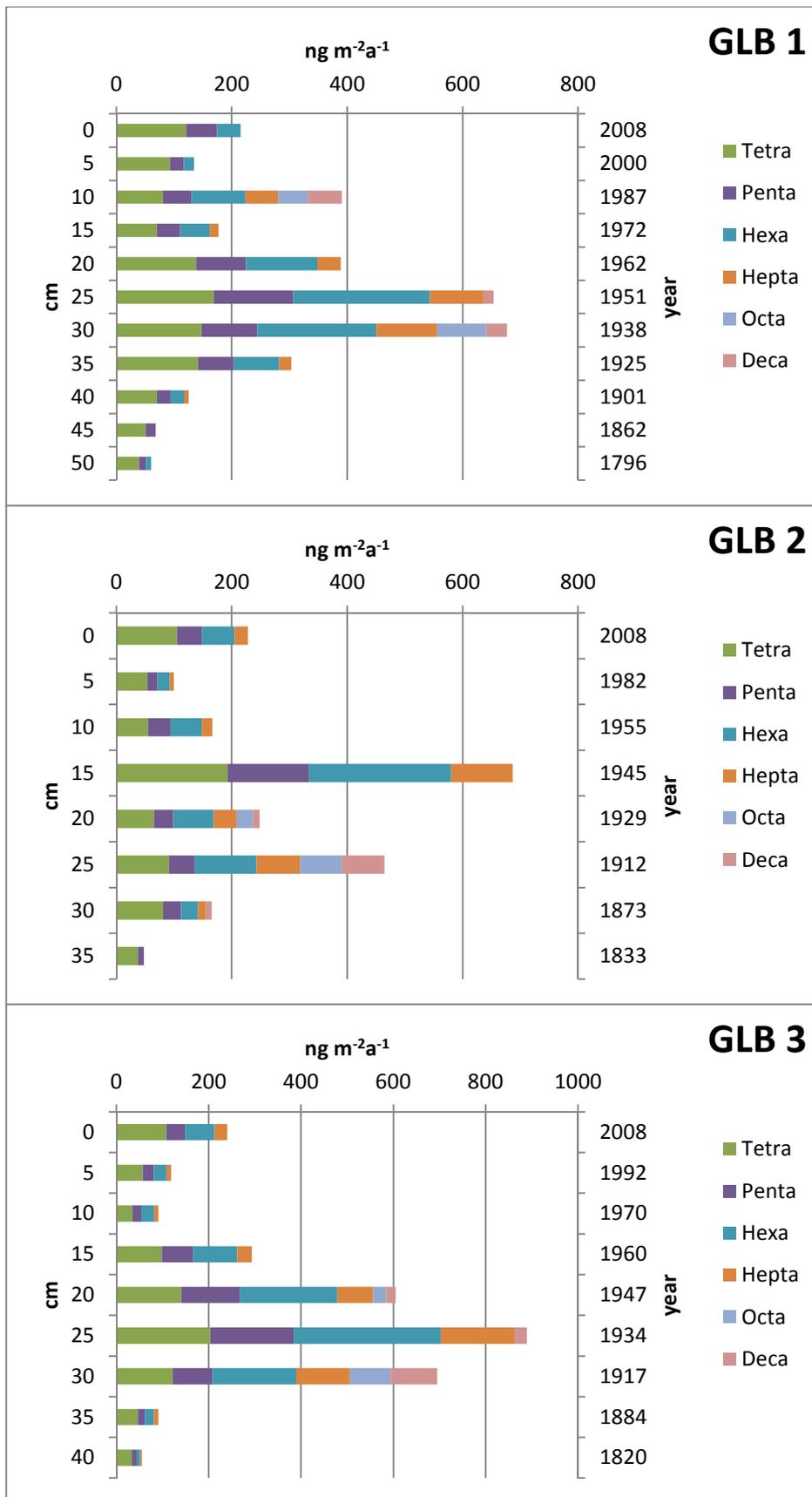
Fig. S6: Deposition rates of PCB congeners to Green Lake Bog in 3 peat core profiles over depth and years.
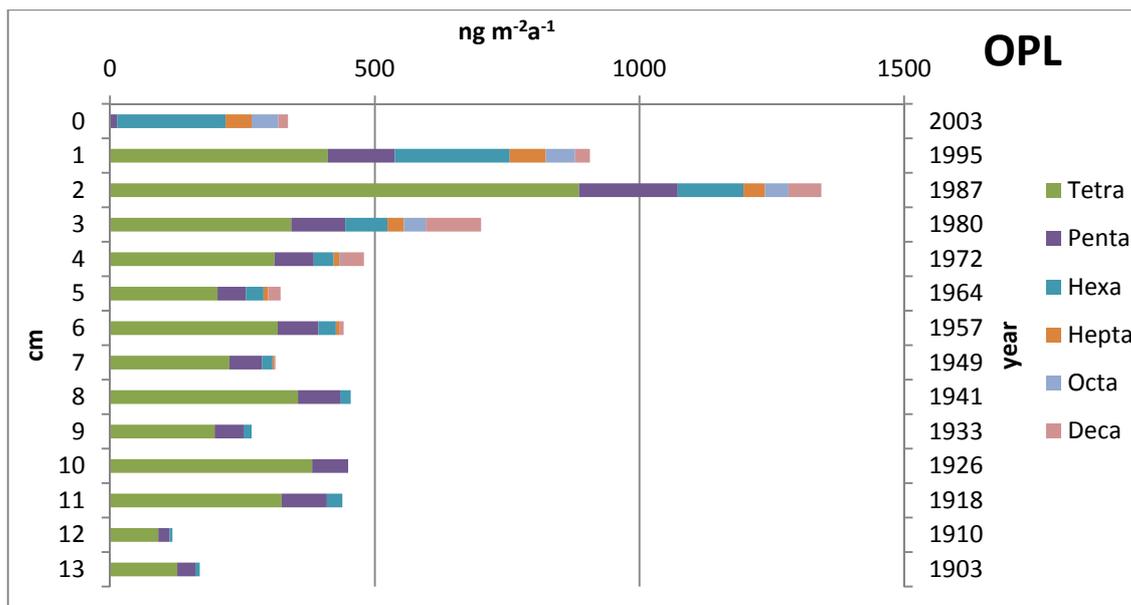
Fig. S7: Deposition rates of PCB congeners to Opeongo Lake in 3 peat core profiles over depth and years

Literature

DIN 32645, 1994. Chemische Analytik: Nachweis-, Erfassungs- und Bestimmungsgrenze, Ermittlung unter Wiederholungsbedingungen, Begriffe, Verfahren, Auswertung. Beuth: Verlag.

Study 4

Ombrotrophic peat bogs are not suited as natural archives to investigate the historical atmospheric deposition of perfluoroalkyl substances

Annekatrin Dreyer, Sabine Thuens, Torben Kirchgeorg, and Michael Radke

Ombrotrophic Peat Bogs Are Not Suited as Natural Archives To Investigate the Historical Atmospheric Deposition of Perfluoroalkyl Substances

Annekatrin Dreyer,*,[†, ‡] Sabine Thuens,[§] Torben Kirchgeorg,[‡, //] and Michael Radke[§, ⊥]

[†]Eurofins GfA, Air Monitoring, Hamburg, Germany

[‡]Department of Environmental Chemistry, Helmholtz-Zentrum Geesthacht, Institute for Coastal Research, Geesthacht, Germany

[§]Department of Hydrology, University of Bayreuth, BayCEER, Bayreuth, Germany

[//]Department of Environmental Sciences, Informatics and Statistics, University Ca′ Foscari of Venice, Venice, Italy

[⊥]Department of Applied Environmental Science, Stockholm University, Stockholm, Sweden

*Supporting Information

ABSTRACT:

As ombrotrophic peat bogs receive only atmospheric input of contaminants, they have been identified as suitable natural archives for investigating historical depositions of airborne pollutants. To elucidate their suitability for determining the historical atmospheric contamination with perfluoroalkyl substances (PFAS), two peat cores were sampled at Mer Bleue, a bog located close to Ottawa, Canada. Peat cores were segmented, dried, and analyzed in duplicate for 25 PFASs (5 perfluororalkyl sulfonates (PFSAs), 13 perfluoroalkyl carboxylates (PFCAs), 7 perfluororalkyl sulfonamido substances). Peat samples were extracted by ultrasonication, cleaned up using a QuEChERS method, and PFASs were measured by HPLC-MS/MS. Twelve PFCAs and PFSAs were detected regularly in peat samples with perfluorooctane sulfonate (85–655 ng kg^{-1}), perfluorooctanoate (150–390 ng kg^{-1}), and perfluorononanoate (45–320 ng kg^{-1}) at highest concentrations. Because of post depositional relocation processes within the peat cores, true or unbiased deposition fluxes (i.e., not affected by post depositional changes) could not be calculated. Apparent or biased deposition rates (i.e., affected by post depositional chang-

es) were lower than measured/calculated deposition rates for similar urban or near-urban sites. Compared to PFAS production, PFAS concentration and deposition maxima were shifted about 30 years toward the past and some analytes were detected even in the oldest segments from the beginning of the 20th century. This was attributed to PFAS mobility in the peat profile. Considerable differences were observed between both peat cores and different PFASs. Overall, this study demonstrates that ombrotrophic bogs are not suited natural archives to provide authentic and reliable temporal trend data of historical atmospheric PFAS deposition.

INTRODUCTION

Since the 1990s, an increasing number of scientific studies pointed at the environmental problems related to poly- and perfluoroalkyl substances (PFASs) and brought these chemicals into the focus of international public concern. Today, the ubiquitous occurrence of these substances in different environ-mental compartments has been recognized as an emerging issue in the field of environmental chemistry. As PFASs comprise toxic, bioaccumulating, and/or extraordinarily persistent compounds that have been detected worldwide in humans, wildlife, and the abiotic environment,[1–7] manufacturing and use of several PFASs has been legislatively restricted or voluntarily phased out by their producers.[8–11]

Several PFASs were identified to be atmospherically transported, among them primarily neutral substances such as fluorotelomer alcohols (FTOH), perfluororalkyl sulfonamides (FASA), or perfluororalkyl sulfonmidoethanols (FASE) in the gas phase but also perfluoroalkyl carboxylates (PFCA) and perfluoroalkane sulfonates (PFSA) partly as their degradation products in the particulate phase.[2,12,13] Laboratory experiments indicated wet and dry deposition to be significant loss mechanisms of certain PFASs from the atmosphere[14] which was confirmed by studies reporting several perfluoroalkyl acids (PFAAs) in precipitation.[15,16] PFASs in wet deposition have been monitored on short time scales; however, to the best of our knowledge, only two studies investigated long-term trends of airborne PFASs.[7,17] Both studies used ice core samples as archives which dated back to the mid 1990s. Studies covering longer time periods were usually conducted using archived biota samples.[1,5] However, these samples rather reflect the contamination of the diet (with all its uncertainties), discriminate compounds which are not bioaccumulative, and are mostly concerning the aquatic or marine environment. Similarly, investigations

on sediments[18–21] mainly refer to the aquatic or marine environment as separating atmospheric from non-atmospheric signals is difficult.[22] Also, sediment records display the contamination of the corresponding entire catchments and interpretation of temporal trends may be challenging as chemicals may be influenced by disturbances, bioturbation, or resuspension of the sediment as well as variable pH or redox conditions.[22]

In contrast to biota and sediment and alternatively to ice cores, ombrotrophic peat bogs can be used to determine the input of airborne contaminants such as metals, polycyclic aromatic hydrocarbons (PAHs), polychlorinated biphenyls (PCBs), and polybrominated diphenyl ethers (PBDEs) over time and space.[23–29] Ombrotrophic bogs are isolated from regional surface- or groundwater flow and receive inputs of nutrients, but also contaminants, by atmospheric deposition only.[26,28] Since up to 99% of peat consists of organic matter, adsorption of organic contaminants is enhanced, however, this may reduce their extractability.[26,30] As recently discussed by Rayne and Forrest,[31] long-chain PFAAs are expected to be rather immobile at such high organic carbon contents. In contrast to soils or sediments there is no strong turnover by fauna, and due to the prevailing anaerobic and acidic conditions in ombrotrophic bogs microbiological degradation is minimized.[26,32] Due to the acidity of bogs, sorption of PFASs to the peat may even be enhanced as sorption increases with decreasing pH because of protonation of surfaces, adduct formation, or protonation of PFASs themselves.[33] Furthermore, and in contrast to glaciers or ice shields, peatlands are widely distributed in boreal and temperate climate zones as well as in mountainous regions throughout the world allowing for studying the spatial distribution of historical contaminant depositions which may further help in characterizing and understanding PFAS input into soils and their distribution from source to pristine regions.[29,34] Therefore we aimed to analyze PFASs in peatlands in order to evaluate and discuss whether ombrotrophic bogs are suitable natural archives to reconstruct historical atmospheric PFAS pollution. To meet these aims, an analytical method was carefully optimized and applied to two peat cores collected in 2009 at Mer Bleue, an undisturbed ombrotrophic bog close to Ottawa, Canada.

EXPERIMENTAL SECTION

Chemicals. All chemicals and suppliers of native and mass-labeled PFASs as well as their acronyms and purities are given in Table S1 in the Supporting Information. Solvents used included methanol (MeOH; Picograde, Promochem, Ger-many) and acetonitrile

(ACN; Suprapur, Merck, Germany). Glacial acetic acid, formic acid, and ammonium hydroxide (all Suprapur) were purchased from Merck (Germany). For dispersive solid phase extraction, CHROMABOND QuECh-ERS (Quick, Easy, Cheap, Effective, Rugged, Safe) Mix I (containing 4 g of $MgSO_4$, 1 g of NaCl, 0.5 g of Na_2H-citrate·1.5 H_2O, 1 g of Na_4-citrate·2 H_2O), and Mix V (containing 0.15 g of CHROMABOND Diamino with 0.9 g of $MgSO_4$ and 45 mg of carbon) were obtained from Macherey & Nagel (Germany).

Sampling. Sampling was performed in October 2009 at Mer Bleue Bog (45.4° N, 75.5° W; mean annual temperature 5.8 °C; mean annual precipitation 910 mm [35]), an ombrotrophic peat bog located in the vicinity of Ottawa, Canada (Figures S9–S11). Mer Bleue was chosen because it is an undisturbed and well investigated (mostly regarding biogeochemical processes, but also organic pollutants) bog. The bog is part of the Mer Bleue Conservation Area and located in a meltwater channel of the postglacial Ottawa River. As an ombrotrophic bog, it receives water mainly from precipitation creating oligotrophic conditions. Overall, drainage is poor due to underlying clay deposits as well as numerous beaver dams, and the water level usually remains at or near the surface.[36] Sphagnum spp. are the dominant low lying form of vegetation in the bog.[36] Further details on vegetation and characteristics of such peatlands can be found elsewhere.[37]

Two peat cores were taken from undisturbed hollows of the ombrotrophic section of the bog using a steel box sampler (87 × 90.6 × 1000 mm). Compaction of peat cores was avoided as far as possible; sampling was repeated if compaction was excessive. After sampling, peat cores were cut into 5-cm segments. Coarse root fragments were removed. The first core (MBI) consisted of nine segments, and the second core (MBII) consisted of eight segments. The most recent and still active vegetation (mainly Sphagnum) was sampled as well (surface). For transport and storage, segmented samples were wrapped in aluminum foil and polyethylene bags. Additionally, peat water was sampled in 500-mL glass bottles. All samples were shipped refrigerated to the laboratory.

Analytical Protocol. Segmented peat samples were freeze-dried and ground with a pebble mill after drying. For extraction, 2 g of ground samples were weighed into 15-mL polypropylene (PP) tubes. Each segment was extracted and analyzed in duplicate so that PFASs were determined in four sets of samples (MBI-1, MBI-2, MBII-1, and MBII-2) consisting of nine/eight peat segments, the corresponding surface sample, and one analytical blank, each. This experimental setup enabled the determination of intracore and in-

tercore concentration variations later on. As Dreyer et al.[25] did not observe significant differences of PAH concentrations from two different Mer Bleue peat cores and the current study was intended as preliminary study on PFAS, dating (using the ^{210}Pb method) of the PFAS peat cores was transferred from a separate core taken by Thuens et al in 2009.[23] This may have resulted in the observed shifting timelines discussed in the Results and Discussion section. The peat cores roughly covered the past 100 years.

Sample extraction and cleanup was optimized (Supporting Information) and finally performed using ultrasonication and a QuEChERS method[38] that was modified to suit the needs of peat extract cleanup. Prior to the extraction, 50 µL of a standard solution containing mass-labeled PFASs ($^{18}O_2$ PFHxS, $^{13}C_4$ PFOS, $^{13}C_3$ PFBA, $^{13}C_2$ PFHxA, $^{13}C_4$ PFOA, $^{13}C_5$ PFNA, $^{13}C_2$ PFDA, $^{13}C_2$ PFUnDA, $^{13}C_2$ PFDoDA, $^{13}C_8$ FOSA, d_3 MeFOSA, d_5 EtFOSA, d_7 MeFOSE, d_9 EtFOSE; 5 ng abs.) were spiked directly to each peat sample. Samples were ultrasonic-extracted with 7.5 mL of ACN for 15 min. After extraction, samples were centrifuged (Hettich Universal 320, Hettich, Germany) at 5000 rpm for 5 min and supernatants were transferred into 25-mL glass flasks. The extraction procedure was repeated once, and corresponding supernatants were combined. For cleanup, sampling volume was reduced to 5 mL using rotary evaporators (Buechi R210, Buechi, Switzerland). Samples were transferred to 15-mL PP tubes containing 5 mL of Millipore water, and QuEChERS Mix I was added. PP tubes were shaken vigorously for 1 min and centrifuged (5000 rpm, 5 min) afterward. Supernatant ACN phases were transferred to new 1-mL PP tubes. Glacial acetic acid (400 µL) and QuEChERS Mix V were added to each sample. PP tubes were shaken vigorously for 1 min, centrifuged (5000 rpm, 5 min), and contents were transferred to 10-mL glass vials. ACN (5 mL) was again added to each of the PP tubes which were then softly shaken and centrifuged as described above. Supernatants were combined with corresponding previous ones. Samples were evaporated to 150 µL using a gentle stream of nitrogen and transferred to HPLC vials. Prior to the measurement, 50 µL of MeOH:H_2O 1:4 (v:v) was added to each vial.

The peat water sample was spiked with mass-labeled PFASs as described above and extracted by solid-phase extraction using Oasis WAX cartridges (6 cm^3, 150 mg, 30 mm; Waters, Germany). Briefly, cartridges were preconditioned with methanol and Millipore water prior to loading the cartridges with the sample. After the extraction, cartridges were washed with Millipore water and 0.1% formic acid, dried for 30 min, and eluted with 14 mL of ACN for neutral PFASs and 5 mL methanol and 0.1% ammonium hydroxide

for ionic PFASs. Samples were evaporated to 150 μL using a gentle stream of nitrogen and transferred to HPLC vials. Prior to the measurement, 50 μL of MeOH:H_2O 1:4 (v:v) was added to each vial. Further details are given elsewhere.[39]

Instrumental Analysis and Quantification. The following PFASs were determined by high-performance liquid chromatography electrospray ionization (negative mode) tandem mass spectrometry (HPLC-ESI-MS/MS): PFBS, PFHxS, PFHpS, PFOS, PFDS, PFBA, PFPeA, PFHxA, PFHpA, PFOA, PFNA, PFDA, PFUnDA, PFDoDA, PFTrDA, PFTe-DA, PFHxDA, PFOcDA, FOSA, MeFOSA, EtFOSA, MeFOSE, EtFOSE, MeFBSA, and MeFBSE (full names are given in the Supporting Information). PFASs were separated on a Synergi Hydro RP 80A column (Phenomenex, USA; 150×2 mm 2 μm). Details are given by Kirchgeorg et al.[39]

Quantification was based on peak areas. Analyte concentrations were calculated with the internal standards method and corrected by blank concentrations. Compounds were classified as not detected (n.d.) with a signal-to-noise ratio (S/N) below 3 and not quantified (n.q.) with a S/N below 10. Furthermore, analytes were not considered further when their concentrations were below the method detection limits (quantified as mean analytical blank + 3 * standard deviation, Table S8). This provided a conservative estimate to avoid false positives.

PFAS concentrations in peat (ng kg^{-1}) were calculated from the dry weight of the samples by dividing the absolute amount of PFASs by the weighted peat mass. Annual PFAS deposition rates (ng m^{-2} a^{-1} (annum)) were calculated by dividing the PFAS peat concentration by the area covered by the box sampler (7.9×10^{-3} m^2) and the number of years peat accumulated in the respective peat segment.

QA/QC. Perfluorinated materials or fluorinated polymers were avoided during sampling and sample preparation. Laboratory equipment and glassware were thoroughly cleaned before use. Mass-labeled internal standards were used to correct for losses during analysis and measurement. For the quantification of analytes in peat samples by this method, a nine-point calibration was run with each set of samples measured. Calibration curve linearity was always checked prior to and after running the sample series. With each set of samples, one analytical blank was analyzed. PFBA (71 ± 21 ng kg^{-1} on average $\pm$ S.D.) and PFOA (32 ± 21 ng kg^{-1} on average $\pm$ S.D.) were detected in all blank samples (n = 4). Most of the other analytes were occasionally detected (Table S15). Instrumental limits of detection calculated on the basis of standard signal-to-noise ratios (IDL) were

between 2 and 33 ng kg^{-1} (Table S8). Method detection (MDL) and quantification limits (MQL) calculated on the basis of analytical blanks were between 3.8 and 141 ng kg^{-1} and 11 and 282 ng kg^{-1}, respectively (Table S8). "Real" field blanks could not be analyzed due to practical reasons as there is no peat soil certified as being free of PFASs. However, we assume that any contamination rather originates from the analytical than from the sampling procedure. Thus, quantification on the basis of conservative MDL/MQLs will prevent that field blanks will be accounted for as false positive peat concentrations. Relative recovery rates of native PFASs (on average 98% ± 17%, Table S10) were calculated as well as the effect of the remaining sample matrix (Table S9). Analyte losses were also evaluated stepwise (Figures S2–S8). Furthermore, accuracy (Table S12), precision (Table S12), and method uncertainties according to EURACHEM/CITAC guidelines[40] and ISO-20988[41] were calculated and are discussed in the Supporting Information (Tables S13–S15).

RESULTS AND DISCUSSION

PFAS Presence in Peat Samples. Of 25 PFASs analyzed in the present study, 12 (PFHxS, PFOS, PFBA, PFHxA, PFHpA, PFOA, PFNA, PFDA, PFUnDA, PFDoDA, PFTriDA, and PFTeDA) were detected consistently in peat core samples. PFBS, PFHpA, and PFPeA were only detected once above the method detection limit and were not considered for any further evaluation. None of the investigated neutral PFASs were detected. Although detected consistently, PFBA is not evaluated in detail in the context of this study because of varying chromatographic peak performance and thus high uncertainties involved with the measurements.

PFAS concentrations of each peat core are presented in Tables S17–S20, and average PFAS concentrations (n = 4) are given in Figure 1. Depth segment averages (n = 4) of Σ11PFAS concentrations varied between 461 and 1898 ng kg^{-1}. With 85–655 ng kg^{-1} on average, PFOS was observed in highest concentrations (12–45% of the total PFAS concentration), followed by PFOA (150–390 ng kg^{-1}; 13–47%), PFNA (45– 320 ng kg^{-1}; 7–18%), and PFUnDA (10–225 ng kg^{-1}; n.d. − 16%). Whereas duplicate PFAS concentrations of each peat core differed only slightly, considerable differences were observed between both cores. PFAS concentrations at Mer Bleue were in the same range as PFAS soil concentrations published by Washington et al.[42] and at the lower PFAS concentration limit reported by Strynar et al.[43] for American soil samples. They were 3 orders of mag-

nitude lower than PAH concentrations[25] and at least 1 order of magnitude lower than PCB concentrations[24] observed in the same bog.
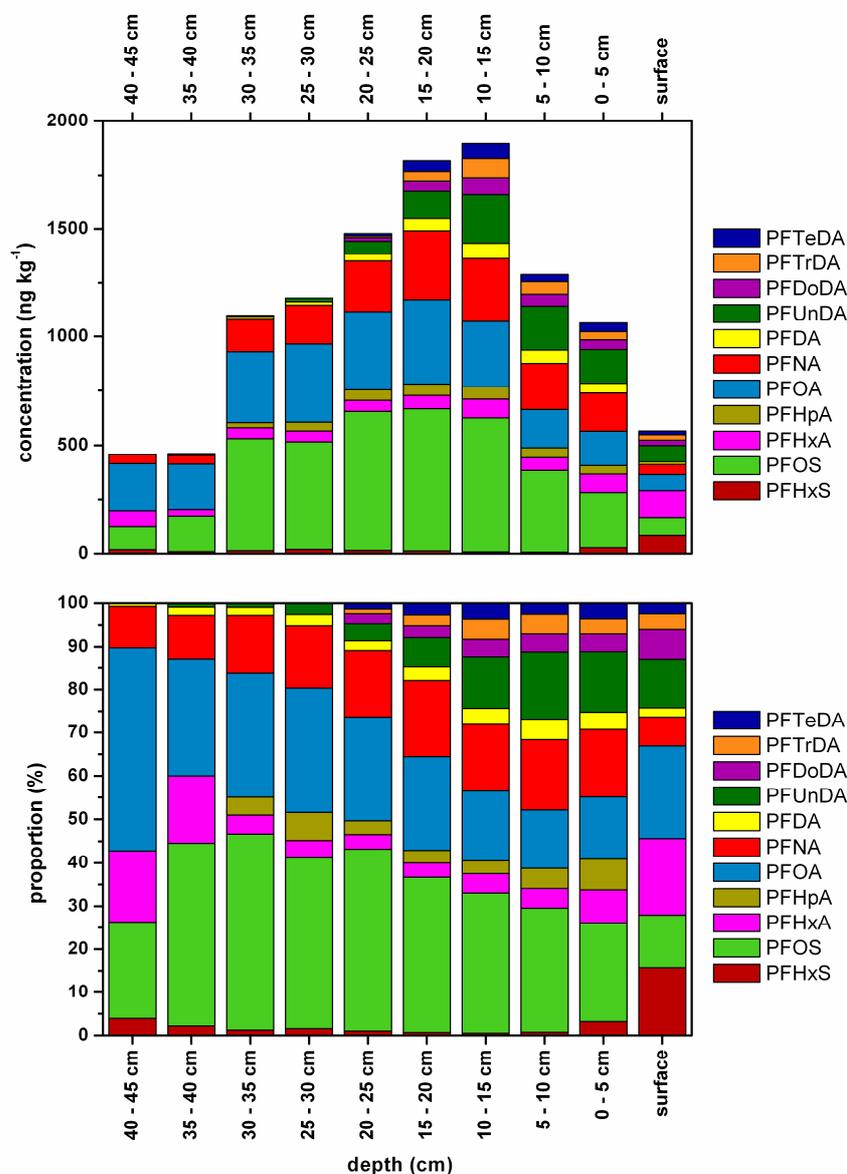
Figure 1. Average (n = 4) PFAS concentrations (ng kg^{-1}) and proportions (%) in peat segments. The average water table was at about 10 cm below the peat surface. Note: The surface segment represents the most recent contamination and may not be directly comparable to the underlying peat. Dating is from a separate core.

As results of this study indicate post-depositional trans-location of PFASs (see below) and the dating turned out to be uncertain it was not possible to reconstruct "true" deposition rates or even temporal deposition trends. For comparison to other studies, we calculated "biased" deposition rates ("biased" because these deposition rates are strongly influenced by PFAS mobility or the applied dating). These calculated (biased) average PFAS deposition rates varied between 35 and 250 ng m^{-2} a^{-1} for PFOS, 50 and

140 ng m^{-2} a^{-1} for PFOA, and between 15 and 90 ng m^{-2} a^{-1} for PFNA. Mostly, calculated (biased) PFAS deposition was fairly low compared to that obtained from measurements in precipitation (920 ng m^{-2} a^{-1} (PFOS, extrapolated),[15] 1550 ng m^{-2} a^{-1} (PFOA, extrapolated),[15] 2300–11400 ng m^{-2} a^{-1} (PFOA),[16] 600–12000 ng m^{-2} a^{-1} (PFNA)[16]) or ice cores (0–81 ng m^{-2} a^{-1} (PFOA),[7] 0–32 ng m^{-2} a^{-1} (PFOS), 40–285 ng m^{-2} a^{-1} (PFOA)[17]) and was rather in the range of that determined in remote or Arctic than of near urban samples. However, calculated (biased) PFOA deposition was similar to modeled annual deposition fluxes of 3–100 ng m^{-2} a^{-1} for continental American regions or 30–200 ng m^{-2} a^{-1} adjacent to sources.[44] Calculated (biased) PFNA deposition was still 10-fold lower than modeled values.[44]

Temporal Trends. Figure 1 depicts average PFAS concentrations as function of depth or corresponding age. Total PFAS concentrations increased from the most recent samples (surface) toward depths of 10–20 cm (1980s) and declined afterward. Compared to reported production maxima of C8-PFSA,[45–47] PFAS concentration maxima in peat appear 20–30 years too early which indicates a PFAS movement downward the peat profile or uncertainties involved in the applied ^{210}Pb dating.
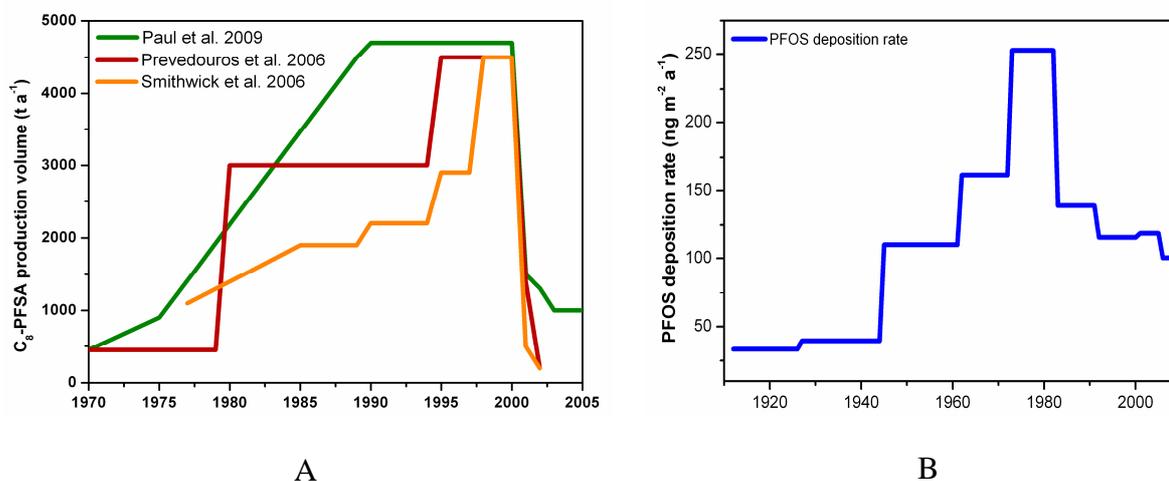
Figure 2. C8–PFSA (PFOS + derivatives) production volumes reported by Prevedouros et al.,[45] Paul et al.,[46] and Smithwick et al.[47] (A) and average PFOS deposition rates (B) determined at Mer Bleue Bog, Canada. Note that the step width of the PFOS deposition rate curve is influenced by the dating and thus its uncertainties. Note also the different time scales for reconstructed deposition rates (panel B) and production (panel A).

Furthermore, PFASs were detected even in the oldest peat samples taken in this study. This may be attributed to uncertainties involved in the dating (not expected, influence is estimated to be too low to explain such a big shift; see below), contamination during sampling (not expected, for reasons refer to the method section), or PFAS mobility (an-

ticipated, see below). Thus, as demonstrated for PFOS in Figure 2, the shape of the deposition chronology more or less matches that of the estimated C_8–PFSA production volumes[45–47] whereas its absolute timing does not. Therefore, the following discussion on temporal PFAS concentration variations will not be focused on their accurate position in time and values will be related to the depth of the peat core.

Depth-dependent variations of concentrations and proportions were different for PFAAs of different chain lengths (Figures 1, 3); e.g., long-chain PFCAs (C_{10}–C_{14}) were predominantly observed in the upper part of the peat core. Their curves were characterized by a distinct and narrow concentration peak in the upper peat segments (roughly in the 1990s). Except for PFDA and PFUnDA, these compounds were not observed in depths below 25 cm (1970s) and their appearances roughly coincide with the onset of FTOH production. On the contrary, concentration curves of shorter-chain PFCAs and PFSAs ($\leq C_9$) were rather flat and characterized by broad peaks. The shorter the perfluorinated chain lengths, the more evenly distributed within the peat core were the compounds. This behavior was most pronounced for PFHxA. As Mer Bleue is a long-term recharge system[48] and thus a downward net transport of water and solutes is prevailing, this may be conceptualized as being similar to a chromatographic separation with strongest retention of longer-chained PFCAs at the peat matrix. Although this analogy is somewhat simplistic given the complex hydraulic conditions with episodic flow reversals during periods of high evapotranspiration,[48] overall these results demonstrate that vertical mobility differs for PFCAs of different carbon chain lengths. This is supported by recent findings for PFAA eluting from a melting snowpack[49] or by results of leaching experiments in soil[50] and may also apply to other matrixes such as sediments. Overall, our results indicate that (if at all) peat bogs may be suitable archives for the historical contamination for long-chain PFCAs, but not for the other groups of PFASs studied here.
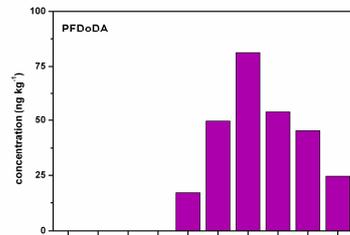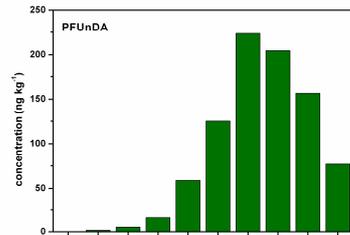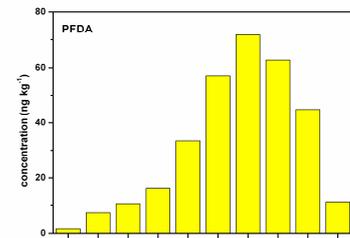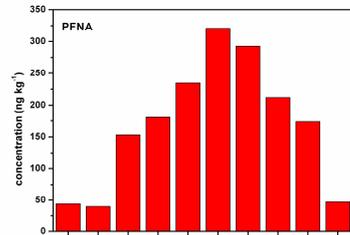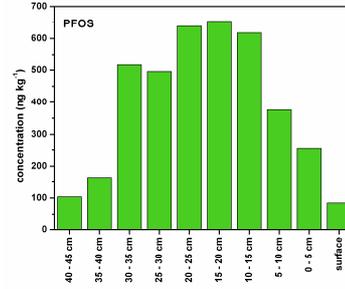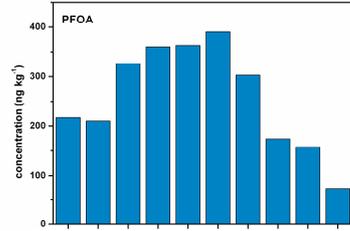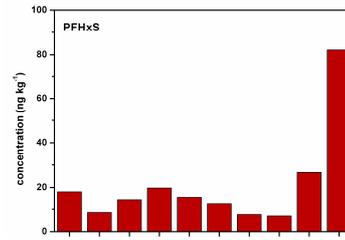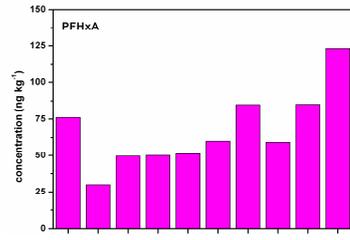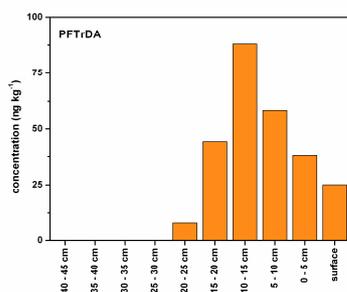
Figure 3. Average vertical distribution of PFCAs (left) and PFSAs (right) of different chain lengths in the peat profile. Note that the surface segment represents the most recent contamination and may not be directly comparable to the underlying peat.

Despite the different mobility, contamination of all PFASs comprising more than 7 perfluorinated carbon atoms declined recently (Figures 1, 3). Although being more mobile than long-chain PFASs, PFHxS and PFHxA were the only PFASs with increasing concentrations and proportions in the most recent samples (not statistically significant (U-test, $p < 0.05$)). Such shifts were also observed in ice core samples of high altitude environments in Europe[17] but were usually not reported in biota-based trend studies as short-chain PFASs do not bioaccumulate.[4] Our results may reflect a production shift from long-chain to short-chain PFASs as consequence of phase-out, manufacturing restrictions, and/or use regulations.[8,9,51,52]

Generally, there was/is a production shift from C8 sulfonate chemistry to C4 sulfonate chemistry whereas PFOA is replaced by PFHxA.[52] However, we are not aware of any production shift toward PFHxS in North America that would explain the observations in Mer Bleue.

Implication of This Study and Suitability of Peat Cores for PFAS Trend Studies. As mentioned above, two peat cores were taken and each peat segment was analyzed in duplicate to allow for the determination of intercore and intracore differences, respectively, and thus to provide a measure for the quality of the analytical method and suitability of peat cores as archives for the atmospheric PFAS contamination history. Concentration differences between the four sets of samples are exemplarily presented for PFOS and PFOA in Figure 4. The overall uncertainties according to ISO 20988[41] resulting from inter- and intracore paired measurements are given in Tables S14 and S15. Concentration differences between duplicate samples of each peat core were fairly low. In contrast, considerable differences were observed between both cores. Similarly, uncertainties for intracore measurements were lower than those for intercore measurements, revealing that

the analytical method to determine PFASs in peat samples is quite precise. However, it also demonstrates that each investigated peat core is different, either due to a dissimilar microtopography and specific microstructure and/or by variations during sampling (e.g., different degree of peat compaction). In turn, this also implies that temporal trend studies should only be performed when each peat core/ segment is dated. Applying the dating from a separate peat core as performed in this study may result in additional uncertainties of the observed temporal variations, particularly when reconstructing atmospheric deposition rates.
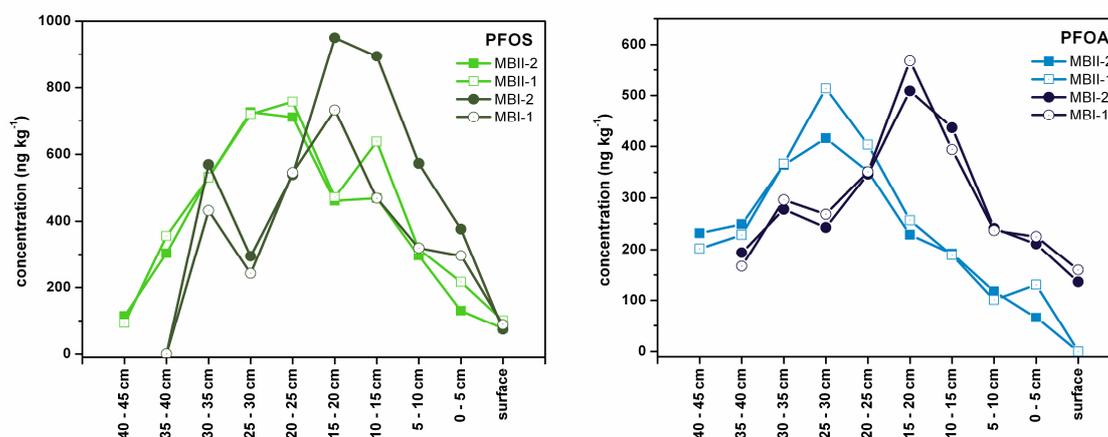
Figure 4. Intercore and intracore variations of PFOA and PFOS concentrations (ng kg^{-1}) over depth. The two cores are labeled MBI and MBII, the replicate analyses are indicated by the last digit (1/2).

Furthermore, incorrect reconstructed contamination histories may be a result of inaccurate dating as the dating itself might be imprecise because of the mobility of radioisotopes which can also be influenced by water table alterations or diagenetic processes.[53] Therefore, Urban et al.[53] estimated that dating using the ^{210}Pb method does not yield results with a resolution better than 10 years. Turunen et al.[37] reported differences of less than 8 years when comparing a charcoal horizon with dating in the same Canadian bog. In contrast, Thuens et al.[23] recently described ^{210}Pb dating in Canadian peat cores to be more uncertain. In several peat cores, they observed a time shift of the onset of [241]Am occurrence due to nuclear testing toward earlier periods. They attributed this to artifacts due to the comparatively coarse 5-cm resolution of the peat cores.

Regardless of core-to-core variations or dating uncertainties, (biased) PFAS deposition rates determined at Mer Bleue, a near urban site, were rather similar to those determined in measured data published for source-related, urban, or near urban areas[7,15,16] which may question the suitability of peat cores as natural archives to investigate the historical PFAS

deposition. In contrast to PFASs, Mer Bleue was characterized by the highest N deposition rate[37] and one of the highest PAH deposition rates of 23 bogs investigated in Eastern Canada[25] indicating that there must be strong "loss" mechanisms for PFASs at the site. Although low PFAS deposition rates (and concentrations) may be a result of non extractable bound residues (or insuffcient extraction effciency), several reasons suggest PFAS (here PFAA) mobility as being more important.

(1)   PFAAs were detected even in the deepest peat segments originating from the beginning of the 20th century, i.e. long before the onset of the industrial PFAS production. At a first glance, this is surprising because the water flow at Mer Bleue is rather horizontal than vertical as the vertical hydraulic conductivity is 1−3 orders of magnitude lower than the horizontal one.[48] However, changes in precipitation and evapotranspiration over the year lead to water table fluctuations of 20−30 cm which may result in a redistribution of certain chemicals (has been shown for nutrients).[35,48]

(2)   Sorption of PFASs to peat in bogs should be enhanced, as PFAS solid-water partitioning coeffcients (K_d values) increase with increasing organic matter content and decreasing pH.[31,33] However, our findings do not suggest that peat is a strong retaining matrix for most PFAAs which were at least partly expected to be immobile at soil organic carbon contents measured in the peat of Mer Bleue (46%). Also, bog pH (about 4) does not seem to be low enough to have a significant effect on PFAA adsorption to the peat. This consequently indicates a negligible presence of PFAAs in their nondissociated form which corresponds to recent findings[54] and may be supported by the occurrence of most PFAAs in the analyzed peat water in concentrations of up to 0.8 ng L^{-1} (PFOS, PFNA, Table S25) as well. This was expected for short-chain PFAAs but not for long-chain analogues, since K_d values generally increase with an increasing carbon chain length of the PFAA molecule.[33] However, Higgins and Luthy[33] assumed K_d values to drop at enhanced concentrations of dissolved organic matter (DOM, 26.9 mg L^{-1} in the present study's peat water sample) as PFAAs may occur DOM-associated. This was supported by a study of Jeon et al.[55] who observed higher PFOA and PFOS concentrations in water in the presence of DOM than in the absence of DOM. They attributed this either to competition between PFAAs and DOM for binding sites of the

sorbent or, more likely, to binding of PFAAs to DOM. A more detailed inter-
pretation of this aspect is not possible as we measured total aqueous PFAA
concentrations and thus cannot differentiate between freely dissolved and
DOM-associated PFAA.

(3)   PFAA transport and diffusion through the peat core may also be facilitated by
        the formation of micelles or micellular structures. The critical micellular con-
        centration (CMC) of PFOA and PFOS is around 3.6 and 4 g L^{-1},[56] respective-
        ly. However, formation of micellar or hemimicellar structures starts at about a
        factor of 100– 1000 below the CMC,[57] which is still higher than concentra-
        tions observed in bog water. On the basis of sediment analysis, Higgins and
        Luthy[33] suggested that the change in free energy due to sorption of an anionic
        PFAS surfactant monomer to a solid (sediment) is very similar to the free-
        energy change due to its movement from the bulk aqueous phase into a mi-
        celle. This would mean that the dissolved PFAS surfactant moves to a micelle
        or a micellar structure just as much as to an adsorbent. Still, Higgins and Lu-
        thy[33] found it unlikely that micelles or even hemimicelles are formed within
        the investigated sediment organic matter at local environ-mental conditions.
        Later, Cheng et al.[54] reported the formation of PFOA dimer ($(PFO)_2H^-$) clus-
        ters in laboratory studies at low concentrations and at pH values of about 4
        (roughly the pH of Mer Bleue Bog). Hypothetically (as it can neither be
        proved or disproved with our data), this would result in the existence of two
        "transportable" phases: the freely dissolved molecule on the one hand and the
        dimer structure on the other hand (which may be a part of some dissolved col-
        loidal micelle composed of PFAAs, dissolved organic matter, and/or other
        surfactants). The dissolved molecule or micellar aggregate can then be trans-
        ported through the pore water by molecular diffusion. This may be assumed
        to be a much slower process than leaching or drainage, but would be much
        quicker than pore water diffusion of PCBs or transport of highly "hydropho-
        bic" compounds such as PAHs through the pore water as the PFAA affnity for
        the particulate phase would be severely reduced. Such a mechanism might
        explain differences in mobility between the different compound classes.

Overall, this study demonstrates that ombrotrophic bogs are not suitable as natural ar-
chives for reconstructing atmospheric PFAS deposition accurately and reliably. This is in

contrast to findings for other contaminants.[25–28] As a further implication, this study reveals that PFAAs are only little retained in soils even if these have a high content of organic matter.

ASSOCIATED CONTENT

Supporting Information

Additional text, data, tables, and figures as mentioned in the text. This material is available free of charge via the Internet at http://pubs.acs.org.

AUTHOR INFORMATION

Corresponding Author

*E-mail: annekatrindreyer@eurofins.de; phone: +49 (0)40 69709655; mail: Stenzelring 14b, 21107 Hamburg, Germany.

Notes

The authors declare no competing financial interest.

ACKNOWLEDGMENTS

REFERENCES

(1)   Sturm, R.; Ahrens, L. Trends of Polyfluoroalkyl compounds in marine biota and in humans. Environ. Chem. 2010, 7, 457–484.

(2)   Dreyer, A.; Weinberg, I.; Temme, C.; Ebinghaus, R. Polyfluorinated compounds in the atmosphere of the Atlantic and Southern Oceans: Evidence for a global distribution.

Environ. Sci. Technol. 2009, 43, 6507−6514.

(3)   Lau, C.; Anitole, K.; Hodes, C.; Lai, D.; Pfahles-Hutchens, A.; Seed, J. Perfluoro-alkyl acids: A review of monitoring and toxicological findings. Toxicol. Sci. 2007, 99, 366−394.

(4) Conder, J. M.; Hoke, R. A.; De Wolf, W.; Russell, M. H.; Buck, R. C. Are PFCAs bioaccumulative? A critical review and comparison with regulatory lipophilic compounds. Environ. Sci. Technol. 2008, 42, 995− 1003.

(5) Houde, M.; Martin, J. W.; Letcher, R. J.; Solomon, K. R.; Muir, D. C. G. Biological monitoring of polyfluoroalkyl substances: A review. Environ. Sci. Technol. 2006, 40, 3463−3473.

(6)   Rayne, S.; Forest, K. Perfluoroalkyl sulfonic and carboxylic acids: A critical review of physicochemical properties, levels and patterns in waters and wastewaters, and treatment methods. J. Environ. Sci. Health, Part A 2009, 44, 1145−1199.

(7)   Young, C. J.; Furdui, V. I.; Franklin, J.; Koerner, R. M.; Muir, D. C. G.; Mabury, S. A. Perfluorinated acids in Arctic snow: New evidence for atmospheric formation. Environ. Sci. Technol. 2007, 41, 3455−3461.

(8)   European Community. . Directive 2006/122/Ec of the European Parliament and of the Council. Off. J. Eur. Union 2006, L 372, 32−34.

(9)   U.S.   EPA.   2010/15   PFOA   stewardship   program;   2006;   http://www.epa.gov/oppt/pfoa/pubs/stewardship/index.html.

(10)   U.S. EPA. Perfluoroalkyl sulfonates; significant new use rule; final rule and supplemental proposed rule. Fed. Regist. 2002, 67, 11008−11013

(11)   Stockholm Convention Stockholm Convention on Persistent Organic Pollutants (POPs); 2009; http://chm.pops.int/default.aspx.

(12)   Barber, J. L.; Berger, U.; Chaemfa, C.; Huber, S.; Jahnke, A.; Temme, C.; Jones, K. C. Analysis of per- and polyfluorinated alkyl substances in air samples from Northwest Europe. J. Environ. Monit. 2007, 9, 530−541.

(13)   Shoeib, M.; Harner, T.; Vlahos, P. Perfluorinated chemicals in the Arctic atmosphere. Environ. Sci. Technol. 2006, 40, 7577−7583.

(14) Hurley, M. D.; Andersen, M. P. S.; Wallington, T. J.; Ellis, D. A.; Martin, J. W.; Mabury, S. A. Atmospheric chemistry of perfluorinated carboxylic acids: Reaction with OH radicals and atmospheric lifetimes. J. Phys. Chem. A 2004, 108, 615−620.

(15) Dreyer, A.; Matthias, V.; Weinberg, I.; Ebinghaus, R. Wet deposition of poly- and perfluorinated compounds in Northern Germany. Environ. Pollut. 2010, 158, 1221−1227.

(16) Scott, B. F.; Spencer, C.; Mabury, S. A.; Muir, D. C. G. Poly and perfluorinated carboxylates in North American precipitation. Environ. Sci. Technol. 2006, 40, 7167–7174.

(17) Kirchgeorg, T.; Gabrieli, J.; Dreyer, A.; Xie, Z.; Schwikoski, M.; Barbante, C.; Boutron, C.; Ebinghaus, R. Perfluorinated compounds in ice core samples from the Alps. Poster at the SETAC Europe 31st annual Meeting, Milan, Italy 2011.

(18) Zushi, Y.; Tamada, M.; Kanai, Y.; Masunaga, S. Time trends of perfluorinated compounds from the sediment core of Tokyo Bay, Japan (1950s–2004). Atmos. Environ. 2010, 158, 756–763.

(19) Ahrens, L.; Yamashita, N.; Yeung, L. W. Y.; Taniyasu, S.; Horii, Y.; Lam, P. K. S.; Ebinghaus, R. Partitioning behavior of per- and polyfluoroalkyl compounds between pore water and sediment in two sediment cores from Tokyo Bay, Japan. Environ. Sci. Technol. 2009, 43, 6969–6975.

(20) Stock, N. L.; Furdui, V. I.; Muir, D. C. G.; Mabury, S. A. Perfluoroalkyl contaminants in the Canadian Arctic: Evidence of atmospheric transport and local contamination. Environ. Sci. Technol. 2007, 41, 3529–3536.

(21) De Silva, A.; Muir, D. C. G.; Mabury, S. A. Distribution of perfluorocarboxylate isomers in selects samples from the North American environment. Environ. Toxicol. Chem. 2009, 28, 1801–1814.

(22) Shotyk, W. Archives of environmental contamination. J. Environ. Monit. 2004, 6, 417.

(23) Thuens, S.; Blodau, C.; Radke, M. How suitable are peat cores to study historical deposition of PAHs? Environ. Int. 2012, in preparation.

(24) Thuens, S.; Blodau, C.; Radke, M. Limitations of Peat Cores for the Determination of PCB and PBDE deposition rates. Environ. Pollut. 2012, in preparation.

(25) Dreyer, A.; Radke, M.; Turunen, J.; Blodau, C. Long-Term change of polycyclic A aromatic hydrocarbon deposition to peatlands of Eastern Canada. Environ. Sci. Technol. 2005, 39, 3918–3924.

(26) Berset, J. D.; Kuehne, P.; Shotyk, W. Concentrations and distribution of some polychlorinated biphenyls (PCBs) and polycyclic aromatic hydrocarbons (PAHs) in an ombrotrophic peat bog profile of Switzerland. Sci. Total Environ. 2001, 267, 67–85.

(27) Cortizas, A. M.; Gayoso, E. G. R.; Weiss, D. Peat bog archives of atmospheric metal deposition. Sci. Total Environ. 2002, 292, 1–5.

(28) Sanders, G.; Jones, K. C.; Hamiltontaylor, J.; Dorr, H. PCB and PAH Fluxes to a

dated UK peat core. Environ. Pollut. 1995, 89, 17−25.

(29)   Dreyer, A.; Blodau, C.; Turunen, J.; Radke, M. The spatial distribution of PAH depositions to peatlands of Eastern Canada. Atmos. Environ. 2005, 39, 3725−3733.

(30) Gorham, E. Biotic impoverishment in northern peatlands. In The Earth in Transition: Patterns and Processes of Biotic Impoverishment; Woodwell, G. M., Ed.; Cambridge University Press: Cambridge, 1990; pp 65−98.

(31) Rayne, S.; Forest, K. Congener specific organic carbon normalized soil and sediment-water partitioning coefficients for the C1 through C8 perfluoroalkyl carboxylic and sulfonic acids. J. Environ. Sci. Health., Part A 2009, 44, 1374−1387.

(32)   Aamot, E.; Steinnes, E.; Schmid, R. Polycyclic aromatic hydrocarbons in Norwegian forest soils: Impact of long range atmospheric transport. Environ. Pollut. 1996, 92, 275−280.

(33)   Higgins, C. P.; Luthy, R. G. Sorption of perfluorinated surfactants on sediments. Environ. Sci. Technol. 2006, 40, 7251−7256.

(34)   Thuens, S.; Blodau, C.; Wania, F.; Radke, M. Comparison of the travel distance of PAHs and metals calculated by two fate and transport models (the Tool and ELPOS) to experimentally derived values using peat bogs as passive samplers. Environ. Sci. Technol. 2012, in preparation.

(35)   Moore, T. R.; Blodau, C.; Turunen, J.; Roulet, N. T.; Richard, P. J. H. Patterns of nitrogen and sulfur accumulation and retention in ombrotrophic bogs, Eastern Canada. Global Change Biol. 2004, 11, 356−367.

(36)   Wetlands International Canada 33: Mer Bleue conservation area. Information Sheet on Ramsar Wetlands; 2011; http://www. wetlands.org/reports/ris/4CA033en.pdf (accessed February 2011).

(37)   Turunen, J.; Roulet, N.; Moore, T. R.; Richard, P. J. H. Nitrogen deposition and increased carbon accumulation in ombrothrophic peatlands in Eastern Canada. Global Biogeochem. Cycles 2004, 18, GB3002/3001−GB3002/3012.

(38)   Anastassiades, M. Quechers: A Mini-Multiresidue Method for the analysis of pesticide residues in low-fat products; 2005; http://www.quechers.com/docs/quechers_en_oct2005.pdf (accessed February 2011).

(39)   Kirchgeorg, T.; Weinberg, I.; Dreyer, A.; Ebinghaus, R. Perfluorinated compounds in marine surface waters: Data from the Baltic Sea and methodological challenges for future studies. Environ. Chem. 2010, 7, 429−434.

(40)   EURACHEM/CITAC. Quantifying uncertainty in analytical measurement.

EURACHEM/CITAC guide CG 04; 2000; http://www.measurementuncertainty.org/mu/QUAM2000-1.pdf.

(41) ISO-20988, Air quality - Guidelines for estimating measurement uncertainty; 2007.

(42) Washington, J. W.; Henderson, W. M.; Ellington, J. J.; Jenkins, T. M.; Evans, J. J. Analysis of perfluorinated carboxylic acids in soils II: Optimization of chromatography and extraction. J. Chromatogr., A 2008, 1181, 21–32.

(43) Strynar, M.; Nakayama, S.; Helfant, L.; Lindstrom, A. Determination of perfluorinated compounds in surface soils. Chemosphere 2012, submitted.

(44) Yarwood, G.; Kemball-Cook, S.; Keinath, M.; Waterland, R. L.; Korzeniowski, S. H.; Buck, R. C.; Russell, M. H.; Washburn, S. T. High-resolution atmospheric modeling of fluorotelomer alcohols and perfluorocarboxylic acids in the North American troposphere. Environ. Sci. Technol. 2007, 41, 5756–5762.

(45) Prevedouros, K.; Cousins, I. T.; Buck, R. C.; Korzeniowski, S. H. Sources, fate and transport of perfluorocarboxylates. Environ. Sci. Technol. 2006, 40, 32–44.

(46) Paul, A. G.; Jones, K. C.; Sweetman, A. J. A first global production, emission, and environmental inventory for perfluorooctane sulfonate. Environ. Sci. Technol. 2009, 43, 386–392.

(47) Smithwick, M.; Norstrom, R. J.; Mabury, S. A.; Solomon, K.; Evans, T. J.; Stirling, I.; Taylor, M. K.; Muir, D. C. G. Temporal trends of perfluoroalkyl contaminants in polar bears (Ursus maritimus) from two locations in the North American Arctic, 1972–2002. Environ. Sci. Technol. 2006, 40, 1139–1143.

(48) Frazer, C. J. D.; Roulet, N. T.; Lafleur, M. Groundwater flow patterns in a large peatland. J. Hydrol. 2001, 246, 142–154.

(49) Plassmann, M.; Meyer, T.; Lei, Y. D.; Wania, F.; McLachlan, M. S.; Berger, U. Laboratory studies on the fate of perfluoroalkyl carboxylates and sulfonates during snow melt. Environ. Sci. Technol. 2011, 45 (16), 6872–6878.

(50) Gellrich, V.; Stahl, T.; Knepper, T. P. Behavior of perfluorinated compounds in soils during leaching experiments. Chemosphere 2012, 87, 1052–1056.

(51) Renner, R. The long and the short of perfluorinated replacements. Environ. Sci. Technol. 2006, 40, 12–13.

(52) Ritter, S. K. Fluorochemicals go short. Chem. Eng. News 2010, 88, 12–17.

(53) Urban, N. R.; Eisenreich, S. J.; Grigal, D. F.; Schurr, K. T. Mobility and diagenesis of Pb and Pb-210 in peat. Geochim. Cosmochim. Acta 1990, 54, 3329–3346.

(54) Cheng, J.; Psillakis, E.; Hoffmann, M. R.; Colussi, A. J. Acid dissociation versus

molecular association of perfluoroalkyl oxoacids: Environmental implications. J. Phys. Chem. A 2009, 113, 8152–8156.

(55) Jeon, J.; Kannan, K.; Lim, B. J.; An, K. G.; Kim, S. D. E☐ects of salinity and organic matter on the partitioning of perfluoroalkyl acid (PFAs) to clay particles. J. Environ. Monit. 2011, 13, 1803–1810.

(56) Harrad, S., Ed. Persistent Organic Pollutants; Wiley, 2010.

(57) Yu, Q.; Zhang, R.; Deng, S.; Huanga, J.; Yu, G. Sorption of perfluorooctane sulfonate and perfluorooctanoate on activated carbons and resin: Kinetic and isotherm study. Water Res. 2009, 43, 1150– 1158.

Supporting Information

Ombrotrophic peat bogs are not suited as natural archives to investigate the historical atmospheric deposition of perfluoroalkyl substances

Annekatrin Dreyer[1,2, #], Sabine Thuens[3], Torben Kirchgeorg[2,4], Michael Radke[3,5]

[1]   Eurofins GfA, Air Monitoring, Hamburg, Germany
[2]   Helmholtz-Zentrum Geesthacht, Institute for Coastal Research, Department of Environmental Chemistry, Geesthacht, Germany
[3]   University of Bayreuth, Department of Hydrology, BayCEER, Bayreuth, Germany
[4]   Department of Environmental Sciences, Informatics and Statistics, University Ca' Foscari of Venice, Venice, Italy
[5]   Stockholm University, Department of Applied Environmental Science, Stockholm, Sweden

[#] corresponding author: annekatrindreyer@eurofins.de
              phone: +49 (0)40 69709655
              Stenzelring 14b, 21107 Hamburg

Content

1. Chemicals

Table S 1: Standards used in the present study.

compound	acronym	producer (purity (%))
potassium perfluoro-n-butane sulfonate	(K-)PFBS	Well. Lab[a] (> 98 %)
sodium perfluoro-n-hexane sulfonate	(Na-)PFHxS	Well. Lab[a] (> 98 %)
sodium perfluoro-n-heptane sulfonate	(Na-)PFHpS	Well. Lab[a] (> 98 %)
sodium perfluoro-n-octane sulfonate	(Na-)PFOS	Well. Lab[a] (> 98 %)
sodium perfluoro-n-decane sulfonate	(Na-)PFDS	Well. Lab[a] (> 98 %)
perfluoro-n-butanoate	PFBA	Well. Lab[a] (> 98 %)
perfluoro-n-pentanoate	PFPA	Well. Lab[a] (> 98 %)
perfluoro-n-hexanoate	PFHxA	Well. Lab[a] (> 98 %)
perfluoro-n-heptanoate	PFHpA	Well. Lab[a] (> 98 %)
perfluoro-n-octanoate	PFOA	Well. Lab[a] (> 98 %)
perfluoro-n-nonanoate	PFNA	Well. Lab[a] (> 98 %)
perfluoro-n-decanoate	PFDA	Well. Lab[a] (> 98 %)
perfluoro-n-undecanoate	PFUnDA	Well. Lab[a] (> 98 %)
perfluoro-n-dodecanoate	PFDoDA	Well. Lab[a] (> 98 %)
perfluoro-n-tridecanoate	PFTrDA	Well. Lab[a] (> 98 %)
perfluoro-n-tetradecanoate	PFTeDA	Well. Lab[a] (> 98 %)
perfluoro-n-hexadecanoate	PFHxDA	Well. Lab[a] (> 98 %)
perfluoro-n-octadecanoate	PFOcDA	Well. Lab[a] (> 98 %)
perfluoro-1-octane sulfonamide	FOSA	Well. Lab[a] (> 98 %)
N-Methyl perfluoro-1-octane sulfonamide	MeFOSA	Well. Lab[a] (> 98 %)
N-Ethyl perfluoro-1-octane sulfonamide	EtFOSA	Well. Lab[a] (> 98 %)
2-(N-Methyl perfluoro-1-octane sulfonamido)-ethanol	MeFOSE	Well. Lab[a] (> 98 %)
2-(N-Ethyl perfluoro-1-octane sulfonamido)-ethanol	EtFOSE	Well. Lab[a] (> 98 %)
N-Methyl perfluoro-1-butane sulfonamide	MeFBSA	Well. Lab[a] (> 98 %)
2-(N-Methyl perfluoro-1-butane sulfonamido)-ethanol	MeFBSE	Well. Lab[a] (> 98 %)
perfluoro-1-hexane [$^{18}O_2$]-sulfonate	[$^{18}O_2$]-PFHxS	Well. Lab[a] (> 98 %)
perfluoro-1-[1,2,3,4-$^{13}C_4$]-octane sulfonate	[$^{13}C_4$]-PFOS	Well. Lab[a] (> 98 %)
perfluoro-n-[1,2,3,4-$^{13}C_4$]-butanoate	[$^{13}C_4$]-PFBA	Well. Lab[a] (> 98 %)
perfluoro-n-[1,2,3,4-$^{13}C_4$]-hexanoate	[$^{13}C_4$]-PFHxA	Well. Lab[a] (> 98 %)
perfluoro-n-[1,2,3,4-$^{13}C_4$]-octanoate	[$^{13}C_4$]-PFOA	Well. Lab[a] (> 98 %)
perfluoro-n-[1,2,3,4,5-$^{13}C_5$]-nonanoate	[$^{13}C_5$]-PFNA	Well. Lab[a] (> 98 %)
perfluoro-n-[1,2-$^{13}C_2$]-decanoate	[$^{13}C_2$]-PFDA	Well. Lab[a] (> 98 %)
perfluoro-n-[1,2-$^{13}C_2$]-undecanoate	[$^{13}C_2$]-PFUnDA	Well. Lab[a] (> 98 %)
perfluoro-n-[1,2-$^{13}C_2$]-dodecanoate	[$^{13}C_2$]-PFDoDA	Well. Lab[a] (> 98 %)
perfluoro-1-[$^{13}C_8$]-octane sulfonamide	[$^{13}C_8$]-FOSA	Well. Lab[a] (> 98 %)
N-Methyl d_3-perfluoro-1-octane sulfonamide	d_3-MeFOSA	Well. Lab[a] (> 98 %)
N-Ethyl d_5-perfluoro-1-octane sulfonamide	d_5-EtFOSA	Well. Lab[a] (> 98 %)
2-(N-deuteriomethyl perfluoro-1-octane sulfonamido)-1,1,2,2-tetradeuterioethanol	d_7-MeFOSE	Well. Lab[a] (> 98 %)
2-(N-deuterioethyl perfluoro-1-octane sulfonamido)-1,1,2,2-tetradeuterioethanol	d_9-EtFOSE	Well. Lab[a] (> 98 %)

[a] Wellington Laboratories, purchased via Campro Scientific, Berlin, Germany

2. Method optimization

The extraction of peat with common extraction methods yields a colourful (usually yellow to dark brown, for the most recent horizons also green) extract with more or less white to beige precipitation (probably plant waxes). Colour and thus matrix intensity depends on the extraction method and kind of solvent. Among accelerated solvent extraction (ASE), Soxhlet extraction (SE), fluidized bed extraction (FBE) and ultrasonic extraction (USE), heaviest matrix load after peat extraction was observed for ASE. Lowest visible matrix content was observed for USE. In general, extraction with acetonitrile (ACN) resulted in less visible matrix content than extraction with methanol (MeOH). However, after concentration to 150 µL, none of the extracts were of sufficient quality for injection and detection using HPLC-MS/MS. Therefore, a clean-up procedure had to be developed to obtain injectable and measurable samples. In the following, attempts to find a suitable clean-up method are briefly described. Usually, clean-up tests were performed with and without matrix. Some clean-up materials were part of test kits and thus only available in a small number. For these materials, matrix-based performance was investigated first. All matrix samples stemmed from a pool of combined peat extracts.

2.1 Solid Phase Extraction (SPE) using Envicarb

Table S 2: Clean-up using solid phase extraction (SPE) with EnviCarb as sorbent. 2mL S+IS: 2 mL of solvent [a] (S) spiked with 50 µL of an internal standard (IS, 5 ng abs.). 2mL M+IS: 2 mL of matrix[b] (M) spiked with 50 µL of an internal standard (IS, 5 ng abs.). R: absolute recovery rate (%). Ace: acetone. MeOH: methanol

2 mL S[a] + IS	2 mL M[b]+IS	Clean-Up	R_{PFOS} (%)	R_{PFOA} (%)	observations/remarks
X		SPE: EnviCarb (Supelco, 3 mL, 0.25 g), Elution 3 x 3 mL MeOH, 1 x MeOH:Ace 1:1	78	49	
	X	SPE: EnviCarb (Supelco, 3 mL, 0.25 g), Elution 3 x 3 mL MeOH, 1 x MeOH:Ace 1:1	not measurable		yellow to brown, precipitation (depending on collected fraction)
X		SPE: EnviCarb (Supelco, 2g self-packed); Elution 4 x 6 mL MeOH	78	46	
	X	SPE: EnviCarb (Supelco, 2g self-packed); Elution 4 x 6 mL MeOH	25	25	light yellow to yellow (depending on collected fraction)

[a]   methanol
[b]   50 mL matrix extract were concentrated to 2 mL,

Conclusions
- Matrix-free experiments yielded acceptable absolute recovery rates.
- Clean-up with 0.25 g EnviCarb cartridges did not yield sufficiently clean matrix extracts
- Clean-up with 2 g self-packed EnviCarb cartridges yielded measurable matrix extracts, however, with low recovery rates, only.
  ➔ Clean-up is not suited in present form

2.2 Solid Phase Extraction (SPE) using C18

Table S 3: Clean-up using solid phase extraction (SPE) with C18 as sorbent. 2mL S+IS: 2 mL of solvent[a]

(S) spiked with 50 µL of an internal standard (IS, 5 ng abs.). 2mL M+IS: 2 mL of matrix[b] (M) spiked with 50 µL of an internal standard (IS, 5 ng abs.). R: absolute recovery rate (%). MeOH: methanol.

2 mL S[a] + IS	2 mL M[b]+IS	Clean-Up	R_{PFOS} (%)	R_{PFOA} (%)	observations/remarks
X		SPE: C18 (Supelco, 2g self-packed); Elution 4 x 6 mL MeOH	38	26	
	X	SPE: C18 (Supelco, 2g self-packed); Elution 4 x 6 mL MeOH	not measurable		light yellow to yellow (depending on collected fraction))

[a] methanol
[b] 50 mL matrix extract were concentrated to 2 mL,

Conclusions
- Matrix-free experiments yielded low absolute recovery rates, only.
- Clean-up with 2 g self-packed C18 cartridges did not yield sufficiently clean matrix extracts
- → Clean-up is not suited

2.3. Solid Phase Extraction (SPE) using anion exchange resins – direct approach

Table S 4: Clean-up using solid phase extraction (SPE) with anion exchange materials as sorbents. 2mL S+IS: 2 mL of solvent[a] (S) spiked with 50 µL of an internal standard (IS, 5 ng abs.). 2mL M+IS: 2 mL of matrix[b] (M) spiked with 50 µL of an internal standard (IS, 5 ng abs.). R: absolute recovery rate (%).

2 mL S[a] + IS	2 mL M[b]+IS	Clean-Up	R_{PFOS} (%)	R_{PFOA} (%)	observations/remarks
	X	SPE: DMA[c] (CHROMABOND DMA, M&N; 3 mL, 0.5g), Elution 3 mL MeOH, 3 mL MeOH:Ace (1:1), 3 mL Ace, 3 mL Ace:Hex (1:1), 3 mL Hex	not measurable		yellow to green (all fractions)
	X	SPE: SB[d] (CHROMABOND SB, M&N; 3 mL, 0.5 g), Elution 3 mL MeOH, 3 mL MeOH:Ace (1:1), 3 mL Ace, 3 mL Ace:Hex (1:1), 3 mL Hex	not measurable		yellow to green (allfractions)
	X	SPE: PS-OH[e] (CHROMABOND PS-OH, M&N; 3 mL, 0.5g), Elution 3 mL MeOH, 3 mL MeOH:Ace (1:1), 3 mL Ace, 3 mL Ace:Hex (1:1), 3 mL Hex	not measurable		yellow to green (all fractions)

[a] methanol
[b] 50 mL matrix extract were concentrated to 2 mL
[c] DMA is a weak anion exchange material
[d] SB is a strong anion exchange material. Since there was only a limited number of SB-SPE cartridges available, performance with matrix was tested first. As the clean-up did not yield a measurable extract, further matrix-free clean-ups were not performed.
[e] PS-OH is a strong polymer-based anion exchange material. Since there was only a lim-

ited number of PS-OH-SPE cartridges available, performance with matrix was tested first. As the clean-up did not yield a measurable extract, further matrix-free clean-ups were not performed.

Conclusions
- ▪ Clean-ups with anion exchange materials did not yield sufficiently clean matrix extracts in a direct approach (i.e. extracts were transferred directly to the SPE cartridges).
  - ➔ Clean-ups are not suited

- ▪ *2.4 Solid Phase Extraction (SPE) using anion exchange resins – indirect approach*

Table S 5: Clean-up using solid phase extraction (SPE) with anion exchange materials as sorbents after the samples were diluted in 100 mL Millipore water (indirect approach). 2mL S+IS: 2 mL of solvent[a] (S) spiked with 50 µL of an internal standard (IS, 5 ng abs.). 2mL M+IS: 2 mL of matrix[b] (M) spiked with 50 µL of an internal standard (IS, 5 ng abs.). R: absolute recovery rate (%). MeOH methanol. ACN: acetonitrile.

2 mL S[a] + IS	2 mL M[b]+IS	Clean-Up	RPFO S (%)	RPFO A (%)	observations/remarks
X		SPE: HR-XAW (CHROMABOND HR-XAW, M&N, 3 mL, 60 mg), acidic wash, Elution 2 mL MeOH 5% NH$_4$OH	104	111	
	X	SPE: HR-XAW (CHROMABOND HR-XAW, M&N, 3 mL, 60 mg), acidic wash, Elution 2 mL MeOH 5% NH4OH	not measurable		precipitation clogged cartridge, brown
X		SPE: Oasis WAX (Waters, 6 mL, 0.5 g), wash, dry, Elution 5 mL MeOH 0.1% NH4OH, 14 mL ACN	23	1	
	X	SPE: Oasis WAX (Waters, 6 mL, 0.5 g), wash, dry, Elution 5 mL MeOH 0.1% NH4OH, 14 mL ACN	not measurable		brown, lots of precipitation
	X	SPE: Oasis HLB$_c$ (Waters, 6 mL, 0.5 g), wash, dry, Elution 5 mL MeOH 0.1% NH4OH, 14 mL ACN	not measurable		reddish brown, lots of precipitation

[c]   methanol, diluted in 100 mL Millipore water (indirect approach)
[d]   50 mL matrix extract were concentrated to 2 mL, diluted in 100 mL Millipore water (indirect approach)
[e]   Oasis HLB is not a weak ion exchange resin but a polymer-based material sometimes used for water analysis. Therefore, it was tested here as well.

Conclusions
- ▪ Matrix-free experiments yielded in acceptable recovery rates for HR-XAW but not for Oasis WAX. The reason for this finding remained unclear.
- ▪ Clean-ups with anion exchange materials did not yield sufficiently clean matrix extracts in the indirect approach (i.e. extracts were diluted in 100 mL Millipore water and then transferred to the SPE cartridges).
  - ➔ Clean-ups are not suited

2.5 Acidic clean-ups

Table S 6: Acidic clean-up in combination with solid phase extraction (SPE). 2mL S+IS: 2 mL of solvent[a] (S) spiked with 50 µL of an internal standard (IS, 5 ng abs.). 2mL M+IS: 2 mL of matrix[b] (M) spiked with 50 µL of an internal standard (IS, 5 ng abs.). R: absolute recovery rate (%). MeOH: methanol. ACN: acetonitrile. HAc: acetic acid.

2 mL S[a] + IS	2 mL M[b]+IS	Clean-Up	R$_{PFOS}$ (%)	R$_{PFOA}$ (%)	observations/remarks
	X	10 mL 1%-HAc, SPE: C18, wash, dry, elution 4 mL MeOH (Higgins et al., 2005)	not measurable		grey-brown precipitation
	X	4000 µL highly concentrated H$_2$SO$_4$, + 100mL H$_2$O, filter precipitation, pH adjustment with NH$_3$ to pH7, SPE Oasis Wax (Waters, 6 mL, 0.5 g), wash, dry, elution 5 mL MeOH0.1 NH$_3$ %, 14 mL ACN	n.d.	n.d.	clear and clean n.d. because of too much H$_2$SO$_4$ (see below)
X		50 µL highly concentrated H$_2$SO$_4$, same as above	28	4	
X		100 µL highly concentrated H$_2$SO$_4$, same as above	5		
X		250 µL highly concentrated H$_2$SO$_4$, same as above	10		
X		500 µL highly concentrated H$_2$SO$_4$, same as above	1		
X		1000 µL highly concentrated H$_2$SO$_4$, same as above	n.d.		
X		2000 µL highly concentrated H$_2$SO$_4$, same as above	n.d.		
X		1000 µL highly concentrated H$_2$SO$_4$, same as above but Oasis Wax is coupled to - SO$_4^{2-}$-cartridge (M&N)	25		
X		Same as above but 2 - SO$_4^{2-}$- cartridges (M&N)	22		
X		1000 µL highly concentrated H2SO4, 100 mL H2O, pH adjustment to 7, SPE: Oasis HLB (Waters, 6 mL, 0.5 g), wash, dry, Elution 5 mL MeOH, 5mL 0.1 NH3 % in MeOH	16		
X		same as above but pH 2	21		
X		same as above but pH 2 and elution with 3 x 5mL MeOH	30		
X		same as above but pH 4	25		
X		same as above but pH 8	29		

[a] methanol, diluted
[b] 50 mL matrix extract were concentrated to 2 mL

Conclusions
- The clean-up developed by Higgins et al. (2005) for sludge is not suited because it did not result in measurable extracts
- Clean-ups using concentrated H$_2$SO$_4$ are promising since they removed almost all visible matrix contents. However, recoveries did not rise above ~30 % in matrix-free experiments. SPE materials developed in future may improve this clean-up.
    - ➔ Clean-ups are not suited yet

2.6 Clean-ups using dispersive Solid Phase Extraction (SPE)

Table S 7: Clean-Up using dispersive SPE. R: recovery rate (%). S: solvent. M: matrix. HAc: acetic acid.

S + IS	M+IS	Clean-Up	R_{PFOS} (%)	R_{PFOA} (%)	observations/remarks
	X	5 g peat, USE with ACN, concentration to 1 mL, disp. SPE with 30 mg Envi-Carb+50 mL HAc	not measurable		dark brown, precipitation
	X	5 g peat + 15 mL ACN + 15 mL H2O, shaking + Mix MN1[a], shaking, centrifuge, transfer to vial, N2	not measurable		dark brown, precipitation
	X	MN1a, shaking, centrifuge, ACN phase + MN4[b], shaking, centrifuge, transfer to vial, N2	n.d.	2	yeallowish brown, clear
	X	5 g Torf + 15 mL ACN + 15 mL H2O, shaking, Mix MN1[a], shaking, centrifuge, ACN phase + MN5[c], shaking, centrifuge, transfer to vial, N2	15	6	yellow, clear; *suited best*
	X	5 g Torf + 15 mL ACN + 15 mL H2O, shaking, Mix MN1[a], shaking, centrifuge, ACN phase + MN6[d], shaking, centrifuge, transfer to vial, N2	12	3	brownish yellow, clear
	X	5 g peat + 15 mL ACN + 15 mL H2O, shaking, centrifuge, + Mix SA2[e], shaking, centrifuge, transfer to vial, N2	not measurable		dark brown, precipitation
	X	5 g peat + 15 mL ACN + 15 mL H2O, shaking, Mix SA2[e], shaking, centrifuge, ACN phase + SA4[f], shaking, centrifuge, transfer to vial, N2	not measurable		brown, precipitation
	X	5 g peat + 15 mL ACN + 15 mL H2O, shaking, Mix SA1[g], shaking, centrifuge, ACN phase + SA4[f], shaking, centrifuge, transfer to vial, N2	7	3	light brown, clear
	X	5 g peat + 15 mL ACN + 15 mL H2O, shaking, Mix SA1[g], shaking, centrifuge, ACN phase + SA5[h], shaking, centrifuge, transfer to vial, N2	5	1	brown, clear
X		1 g peat + 1 mL 200 mmol NaOH in MeOH for 1/2 h, + 200 μL HCl 1 N + 5 mL ACN, 2x USE, shaking, + MN 7 (Lechner et al., 2010) shaking, transfer to vial	38	24	yellowish brown
	X	5 g peat, ASE extraction with ACN, concentration to 5 mL,+ H2O+ Mix MN1[a], shaking, centrifuge, ACN phase +MN4[b], shaking, centrifuge, transfer to vial, N2	n.d.	n.d.	greenish yellow, fine precipitation
	X	5 g peat, ASE extraction with ACN, concentration to 5 mL,+ H2O+ Mix MN1[a], shaking, centrifuge, ACN phase +MN5[c], shaking, centrifuge, transfer to vial, N2	8	4	greenish yellow, clear; *suited best*
	X	5 g peat, ASE extraction with ACN, concentration to 5 mL,+ H2O+ Mix MN1[a], shaking, centrifuge, ACN phase +MN6[d], shaking, centrifuge, transfer to vial, N2	6	3	yellow, clear
X		5 mL ACN + 5 mL H2O, Mix 1[a] only, shaking, centrifuge, 1x ACN phase,	56	68	

X	transfer to vial, N2 5 mL ACN + 5 mL H2O, shaking, Mix MN1[a], shaking, ACN phase + MN5[c], shaking, transfer to vial	21	23	
X	5 mL ACN + 5 mL H2O, shaking, Mix MN1[a], shaking, centrifuge, ACN phase +MN5[c] +400 µL HAc (pH3-4) shaking, centrifuge, transfer to vial, N2	63	45	*suited best (final method; for details, refer to the main text)*
X	5 mL ACN + 5 mL H2O, shaking, Mix MN1[a], shaking, centrifuge, ACN phase + MN5[c] +150 µL 1N HCl (pH1-2) shaking, centrifuge, transfer to vial, N2	50	50	

[a] Macherey & Nagel, QuEChERS Mix I [b] Macherey & Nagel, QuEChERS Mix IV
[c] Macherey & Nagel, QuEChERS Mix V [d] Macherey & Nagel, QuEChERS Mix VI
[e] Supelco, QuEChERS Mix 2 [f] Supelco, QuEChERS Mix 4
[g] Supelco, QuEChERS Mix 1 [h] Supelco, QuEChERS Mix 5

Conclusions
- The clean-up described by Rubart et al. (2011) for biota samples is not suited because it did not result in measurable extracts
- Of those dispersive SPE (QuEChERS) clean-ups investigated, MN1 + MN5 + 400 µL HAc was suited best with absolute recovery rates up to 63 %. Future studies should improve this clean up that higher recovery rates are achieved.
  → Finally chose clean up, may be improved in future

3. Final analytical procedure
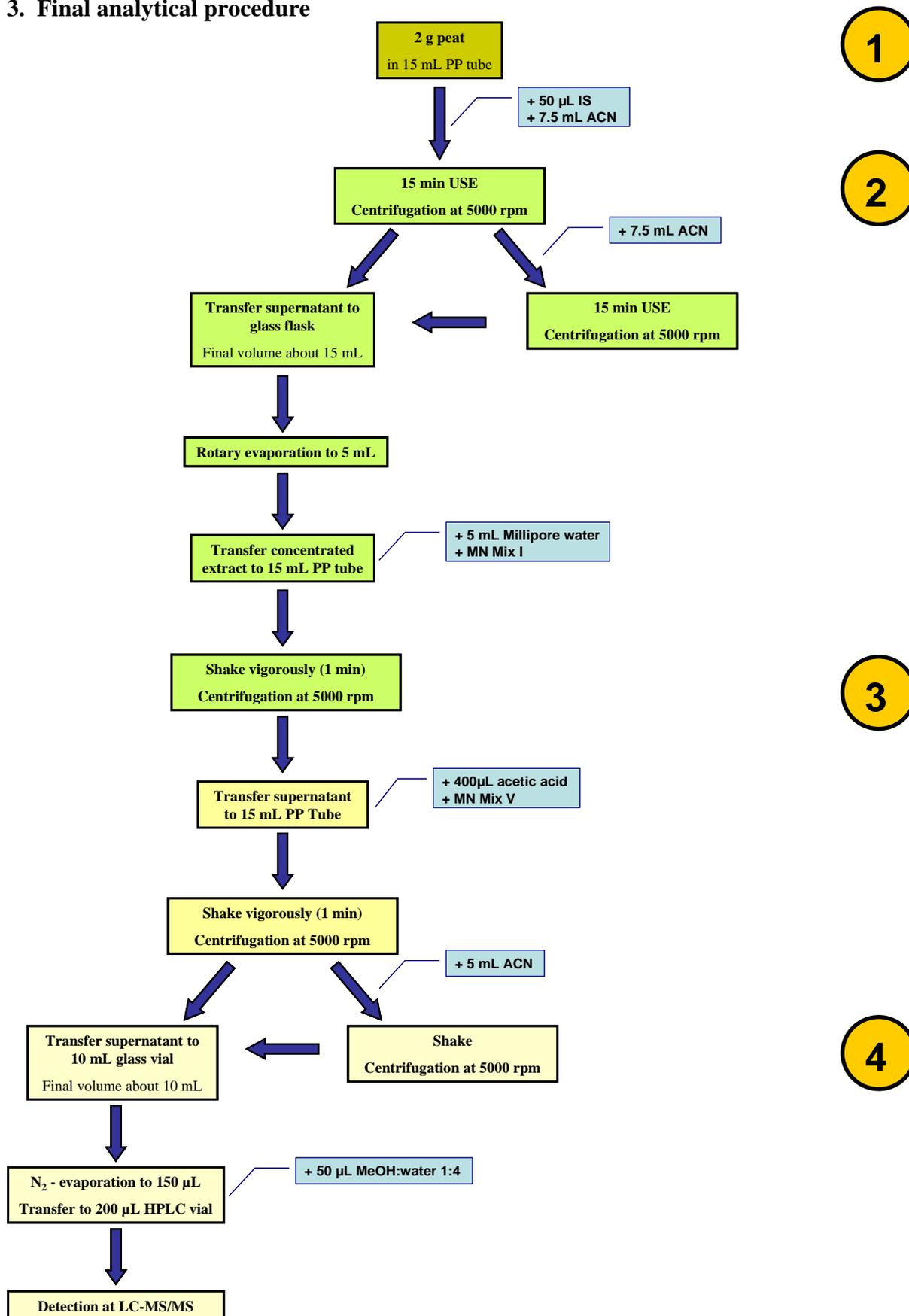
Figure S 1: Overview about the analytical procedure. USE: ultra sonic extraction. ACN: acetonitrile.
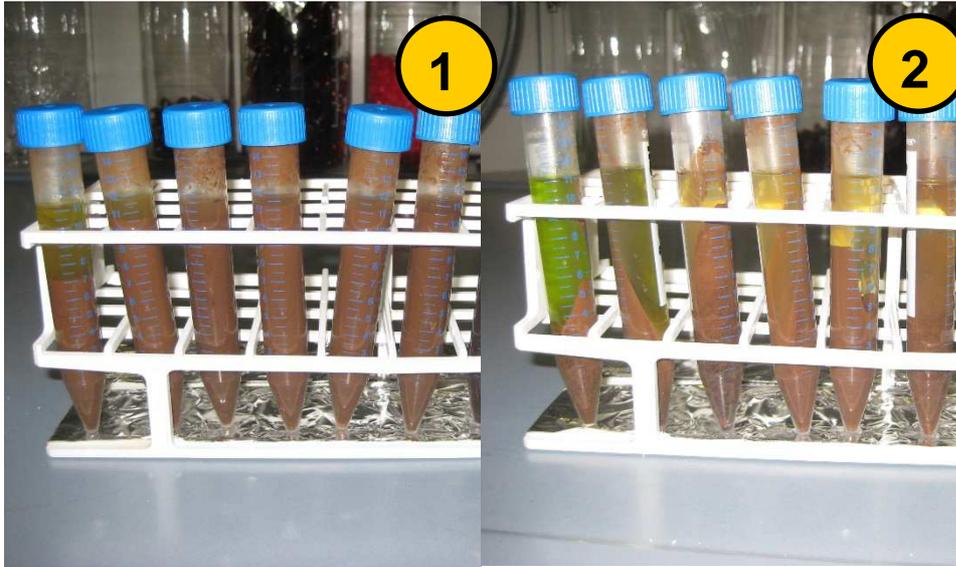
after the extraction

after the centrifugation
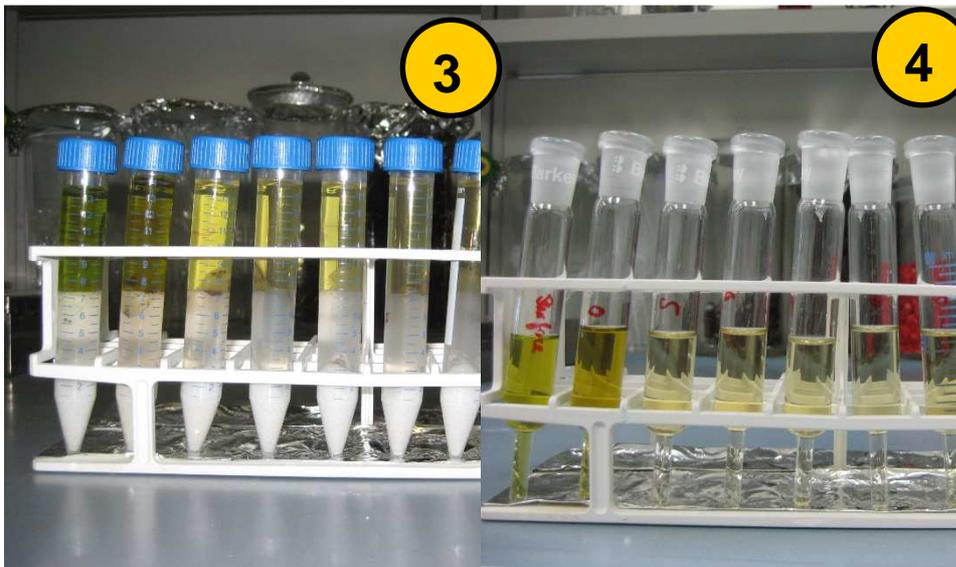
after clean-up 1 with MN Mix I

after clean-up 2 with MN Mix V

4. Validation of the analytical method

4.1 Detection & Quantification limits

Table S 8: Instrumental detection limits (IDL), method detection limits (MDL) and method quantification limits (MQL).

	IDL[a]	MDL[b]	MQL[c]
	(ng kg^{-1})	(ng kg^{-1})	(ng kg^{-1})
PFBS	1.9	24	62
PFHxS	2.2	-	-
PFHpS	2.0	67	186
PFOS	2.6	25	64
PFDS	1.6	16	44
PFBA	15.5	141	282
PFPA	4.2	54	140
PFHxA	2.7	6	17
PFHpA	2.6	25	70
PFOA	2.8	46	74
PFNA	3.0	19	48
PFDA	4.4	9	23
PFUnDA	6.4	8	20
PFDoDA	3.8	15	41
PFTrDA	5.1	4	11
PFTeDA	7.5	-	-
PFHxDA	15.6	61	160
PFOcDA	11.6	95	247
MeFOSA	12.4	-	-
EtFOSA	12.1	-	-
MeFOSE	8.0	-	-
EtFOSE	6.5	-	-
MeFBSA	32.6	-	-
MeFBSE	6.0	-	-
FOSA	9.4	-	-

a   calculated on the basis of signal to noise ratios of standards (IDL at S/N<3)

b   calculated as average of substance's method blank + 3.3 * standard deviation

c   calculated as average of substance's method blank + 10 * standard deviation

4.2   Analyte losses stepwise

The investigation of analyte losses for major analytical steps occurred as illustrated in figure S2. Figure S2 also summarizes losses for PFOS, PFOA and for all analytes on average. Overall, major losses occur during the clean-up and the evaporation to 150 µL and transfer to the vial. Thus, if overall performance of the analytical method is to be improved in future, efforts should focus on these steps.

	LOSSES	
average -54 %	PFOS -57 %	PFOA -53%
Spike step 1		
PEAT EXTRACTION (+ 5%)	(+ 1%)	(+1%)
Spike step 2		
ROTARY EVAPORATION 0 %	0 %	(+2 %)
Spike step 3		
CLEAN-UP -34 %	-37 %	-39 %
Spike step 4		
N₂ EVAPORATION DETECTION -20 %	-20 %	-14 %
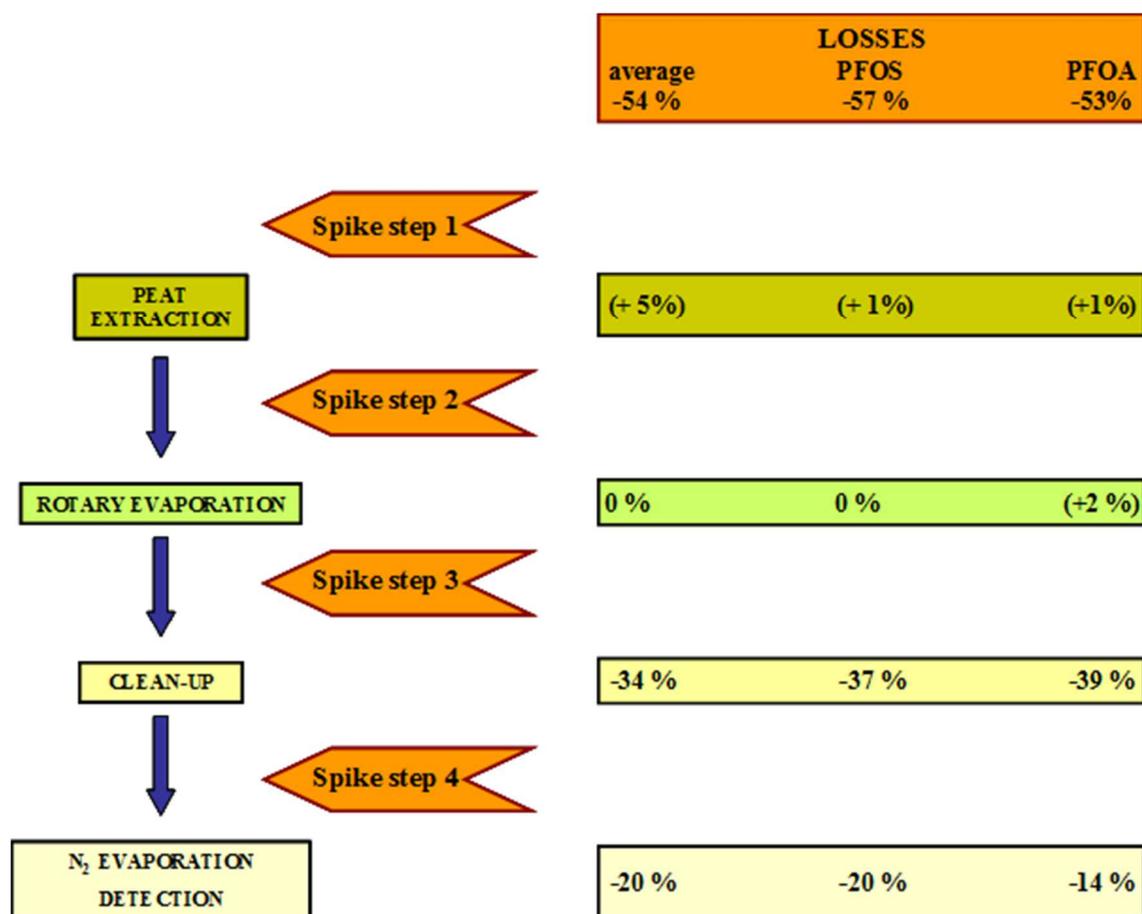
Figure S 2: Overview about losses during major extraction steps. Positive values are given in brackets since this would mean a gain of analytes from one step to the other.
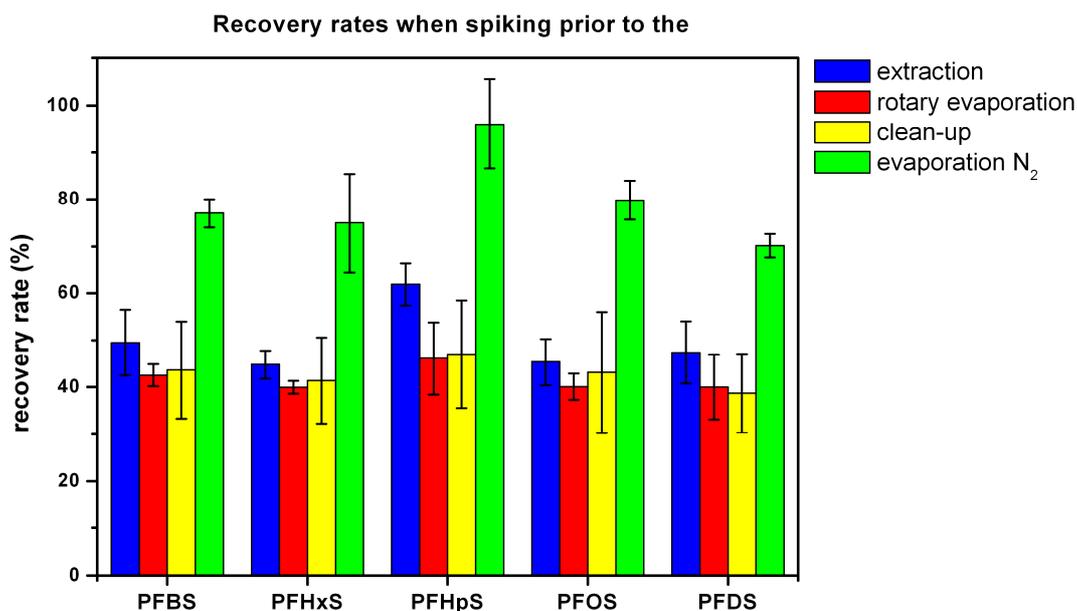
Figure S 3: Recovery rates +/- standard deviations (%) illustrating losses of per-fluoroalkane sulfonates during major analytical steps. Substances were spiked prior to the extraction, rotary evaporation, clean-up and final evaporation using N2.
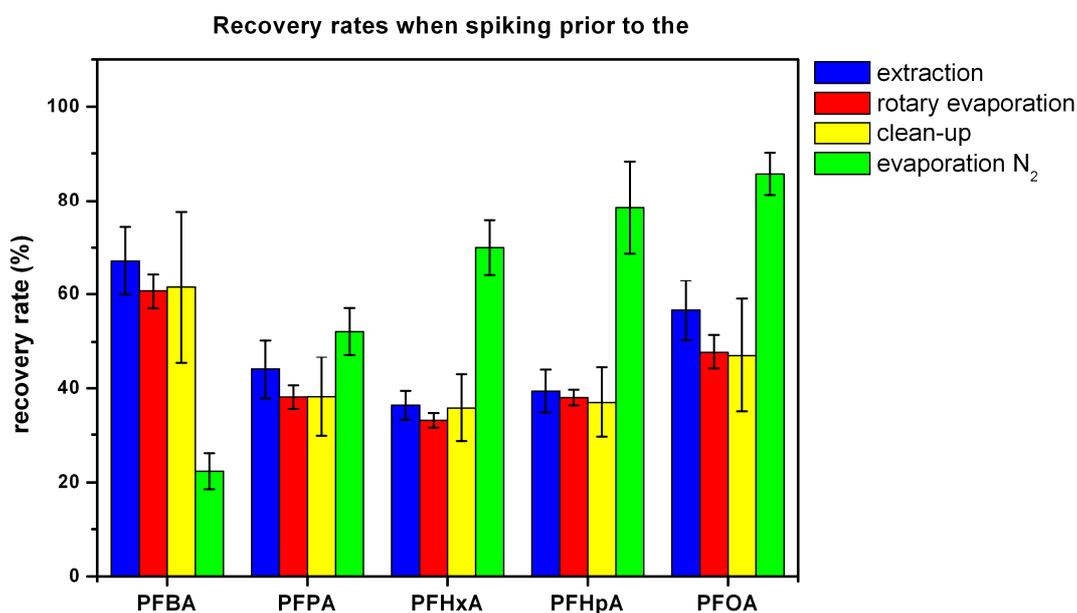
Figure S 4: Recovery rates +/- standard deviations (%) illustrating losses of C4 - C8 perfluoroalkyl carboxylates during major analytical steps. Substances were spiked prior to the extraction, rotary evaporation, clean-up and final evaporation using N2.
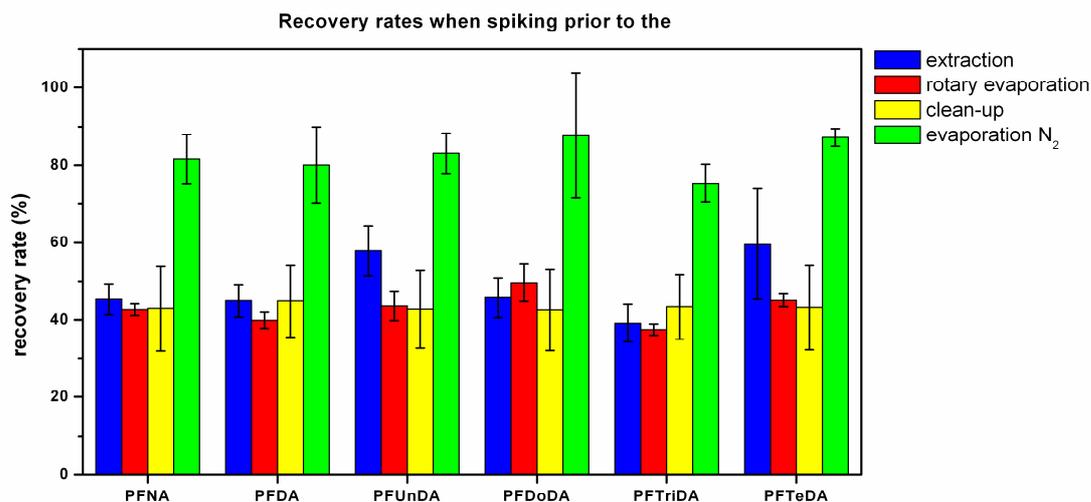
Figure S 5: Recovery rates +/- standard deviations (%) illustrating losses of C9-C14 perfluoroalkyl carboxylates during major analytical steps. Substances were spiked prior to the extraction, rotary evaporation, clean-up and final evaporation using N2.
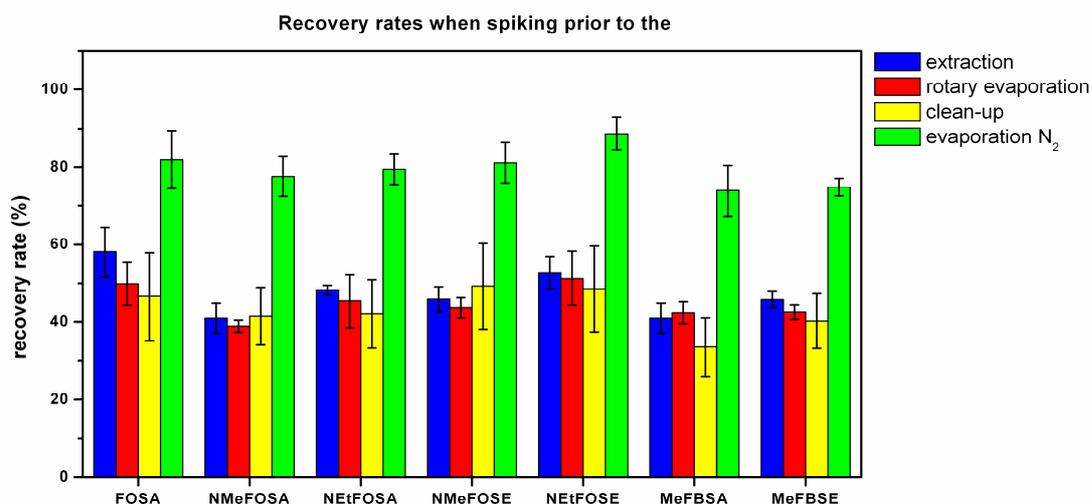
Figure S 6: Recovery rates +/- standard deviations (%) illustrating losses of perfluoroalkana sulfonamide substances. Substances were spiked prior to the extraction, rotary evaporation, clean-up and final evaporation using N2.
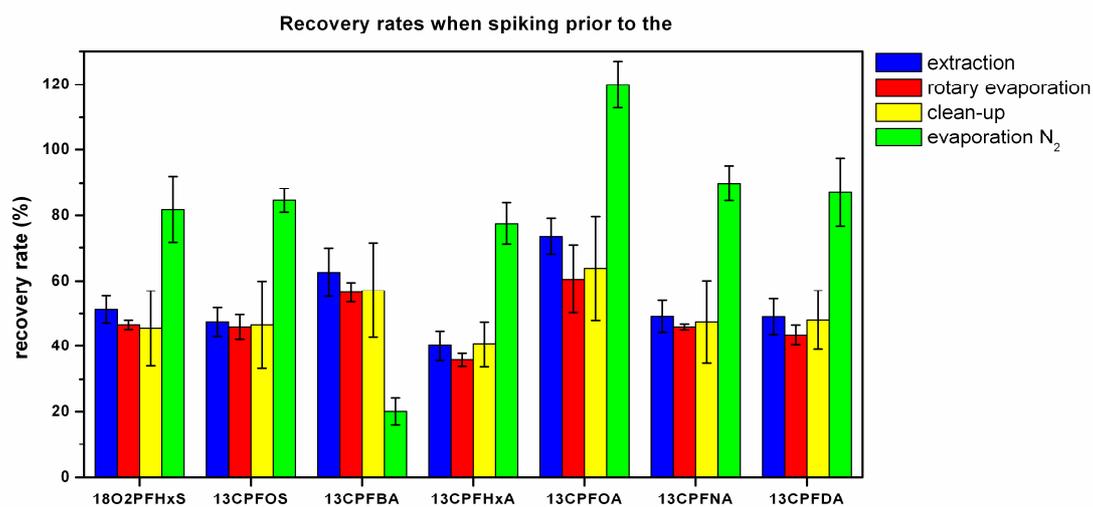
Figure S 7: Recovery rates +/- standard deviations (%) illustrating losses of several mass-labelled PFASs. Substances were spiked prior to the extraction, rotary evaporation, clean-up and final evaporation using N2.
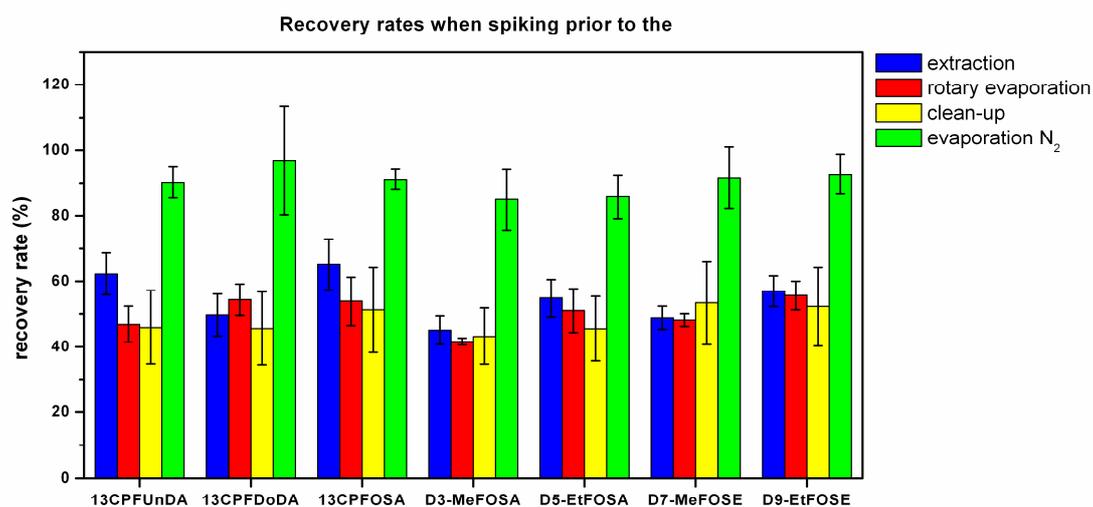
Figure S 8: Recovery rates +/- standard deviations (%) illustrating losses of several mass-labelled PFASs. Substances were spiked prior to the extraction, rotary evaporation, clean-up and final evaporation using N2.

4.3 Matrix effect

The matrix effect of mass-labelled PFASs was evaluated in an extracted and cleaned peat sample. The matrix effect was calculated as:

Matrix effect = 100 % - ($C_{sample + IS}$ − C_{sample}) / $C_{solvent+IS}$. (Kromidas, 2003)

with $C_{sample + IS}$: substance concentration in a spiked sample (2 g peat sample, extracted and cleaned up, concentrated to 100 µL, + 50 µL of a solution containing mass-labelled
PFASs (5 ng abs.), + 50 µL water:MeOH 4:1

C_{sample}: substance concentration in a 'normal' sample (same as above without spiking mass-labelled PFASs)

$C_{solvent+IS}$: substance concentration in spiked solvent (100 µL acetonitrile + 50 µL of a solution containing mass-labelled PFAS (5 ng abs.), + 50 µL water:methanol 4:1)

Despite the clean- up which reduced lots of visible matrix components, matrix still reduced recovery rates by roughly 30 to 60 %. Thus, future studies should improve the clean up procedure or apply matrix-matched calibrations or standard addition for quantification. In the present study, this was not possible, since a similar PFASs-free matrix was not available and the available amount of peat was not enough to apply standard addition as described by Rubarth et al. (2011).

Table S 9: Matrix effect for mass-labelled PFASs.

	matrix effect (%)
$^{18}O_2$-PFHxS	46
^{13}C-PFOS	51
^{13}C-PFBA	66
^{13}C-PFHxA	30
^{13}C-PFOA	55
^{13}C-PFNA	47
^{13}C-PFDA	51
^{13}C-PFUnDA	52
^{13}C-PFDoDA	45
^{13}C-PFOSA	54
D_3-MeFOSA	51
D_5-EtFOSA	63
D_7-MeFOSE	52
D_9-EtFOSE	48

4.4   Relative recovery rates of native PFASs

Relative recovery rates (i.e. recovery rate of native PFASs corrected by recovery rate of the corresponding mass-labelled PFASs) were calculated as quality measure for the correction of native PFASs by mass-labelled PFASs. Ideally, relative recovery rates are 100 %, i.e. the correcting mass -labelled compound behaves exactly the same as the native substance. Usually, relative recovery rates are classified as acceptable if they are between 80 and 120 %. Table S10 presents relative recovery rates calculated for the entire method including peat extraction, clean-up and detection. For most analytes, correction by their corresponding mass-labelled standards was acceptable (within 80-120 %). Compounds with relative recovery rates outside of this range were usually those for which substance-specific mass-labelled internal standards were not available. This also demonstrated the importance of substance-specific mass-labelled internal standards in PFAS analyses.

Table S 10: Relative recovery rates of native PFASs (i.e. recovery rate of native PFAS corrected by recovery rate of the corresponding mass-labelled PFASs).

compound	corrected by	relative recovery rate (%)	error (abs., %)	recovery rate within 80-120 % ?
PFBS	$^{18}O_2$ -PFHxS	90	10	Yes
PFHxS	$^{18}O_2$ -PFHxS	83	17	Yes
PFHpS	^{13}C -PFOS	149	-49	No
PFOS	^{13}C -PFOS	102	-2	Yes
PFDS	^{13}C -PFOS	106	-6	Yes
PFBA	^{13}C -PFBA	111	-11	Yes
PFPA	^{13}C -PFHxA	96	4	Yes
PFHxA	^{13}C -PFHxA	92	8	Yes
PFHpA	^{13}C -PFOA	65	35	No
PFOA	^{13}C -PFOA	95	5	Yes
PFNA	^{13}C -PFNA	97	3	Yes
PFDA	^{13}C -PFDA	89	11	Yes
PFUnDA	^{13}C -PFUnA	88	12	Yes
PFDoDA	^{13}C -PFDoA	93	7	Yes
PFTrDA	^{13}C -PFDoA	109	-9	Yes
PFTeDA	^{13}C -PFDoA	140	-40	No
PFOcDA	^{13}C -PFDoA	85	15	Yes
FOSA	^{13}C PFOSA	108	-8	Yes
MeFOSA	D_3-MeFOSA	94	6	Yes
EtFOSA	D_5-EtFOSA	89	11	Yes
MeFOSE	D_7-MeFOSE	93	7	Yes
EtFOSE	D_9-EtFOSE	97	3	yes
MeFBSA	D_3-MeFOSA	91	9	yes
MeFBSE	D_7-MeFOSE	94	6	yes

4.5   Absolute recovery rates of mass-labelled PFASs

Absolute recovery rates of mass-labelled internal standards (IS) were determined for each sample. Whereas concentrations of native compounds were calculated using a 6-point response factor calibration, concentrations of mass-labelled PFASs were calculated with a separate 4-point calibration containing IS at different 'concentration levels' as well.

Absolute recovery rates of mass-labelled IS in blank samples were similar to those observed in preliminary experiments (figures S3-S8). Absolute recovery rates of samples were lower which is probably due to the matrix effect (table S10). Thus, future studies should further improve the method performance.

Table S 11: Average absolute recovery rates and standard deviations (SD) of blanks (n=4) and samples (n=38).

	blanks		samples	
	recovery (%)	SD (%)	recovery (%)	SD (%)
$^{18}O_2$-PFHxS	47.0	3.9	18.1	9.6
^{13}C-PFOS	54.1	9.0	23.0	12.6
^{13}C-PFBA	49.9	9.3	7.6	7.1
^{13}C-PFHxA	35.7	8.5	5.5	5.8
^{13}C-PFOA	36.6	8.2	9.2	6.1
^{13}C-PFNA	40.3	8.9	11.3	6.6
^{13}C-PFDA	40.7	3.9	8.9	3.9
^{13}C-PFUnDA	43.2	3.3	13.7	6.4
^{13}C-PFDoDA	39.6	2.1	14.2	8.0
^{13}C-FOSA	44.7	2.2	17.5	8.1
D_3-MeFOSA	41.4	3.4	17.3	8.3
D_5-EtFOSA	38.9	1.2	15.9	7.1
D_7-MeFOSE	40.5	6.2	17.5	8.3
D_9-EtFOSE	44.2	4.2	17.2	11.0

4.6 Accuracy & precision of the analytical method

In order to determine accuracy and precision of the method, three peat samples were spiked with 50 µL (about 5 ng abs.) of a solution containing mass-labelled and native PFASs. Peat samples were analysed with the final method described in the main text and in figure S1. Concentrations of native PFASs were calculated by the response factor method. For accuracy, the measured amount of PFASs was compared to the spiked amount. Precision of the method was determined using standard deviations of the triplicates.

Accuracy and precision of the method to determine PFASs in peat are given in table S12. Except for few exceptions, relative standard deviations as measure of precision were below 5 % and differences between spiked and measured amounts as measure for accuracy were below 20 %. Compounds with higher deviations were usually those for which substance-specific mass-labelled internal standards were not available.

Table S 12: Accuracy (ng, %) and precision (ng, %) of the method. SD: standard deviation. RSD: relative standard deviation.

	PFAS amount		accuracy		precision	
	m_{spiked} (ng)	$m_{measured}$ (ng)	m_{spiked}-$m_{measured}$ (abs.) (ng)	m_{spiked}-$m_{measured}$ (rel.) (%)	SD (ng)	RSD (%)
PFBS	4.4	4.0	0.5	10	0.35	8.9
PFHxS	4.6	3.8	0.8	17	0.17	4.4
PFHpS	4.8	7.1	-2.3	-49	0.42	6.0
PFOS	4.8	4.9	-0.1	-2	0.21	4.4
PFDS	4.8	5.1	-0.3	-6	0.46	9.0
PFBA	5	5.6	-0.6	-11	0.14	2.6
PFPA	5	4.8	0.2	4	0.17	3.4
PFHxA	5	4.6	0.4	8	0.20	4.2
PFHpA	5	3.2	1.8	35	0.28	8.7
PFOA	5	4.7	0.3	5	0.22	4.6
PFNA	5	4.8	0.2	3	0.10	2.1
PFDA	5	4.5	0.5	11	0.12	2.7
PFUnDA	5	4.4	0.6	12	0.06	1.4
PFDoDA	5	4.7	0.3	7	0.06	1.3
PFTrDA	5	5.4	-0.4	-9	0.10	1.9
PFTeDA	5	7.0	-2.0	-40	0.87	12.4
PFOcDA	5	5.4	-0.4	-8	0.73	13.6
FOSA	5	4.2	0.8	15	0.07	1.7
MeFOSA	5	4.7	0.3	6	0.03	0.7
EtFOSA	5	4.5	0.5	11	0.49	10.9
MeFOSE	5	4.7	0.3	7	0.17	3.6
EtFOSE	5	4.9	0.1	3	0.10	2.1
MeFBSA	5	4.6	0.5	9	0.19	3.8
MeFBSE	5	4.7	0.3	6	0.16	3.2

4.7 Method uncertainties (EURACHEM / CITAC Guide & ISO 20988)

The uncertainties of the entire method were calculated according to EURACHEM/CITAC guidelines (EURACHEM / CITAC, 2000) and on the basis of paired measurements according to ISO 20988 (ISO-20988, 2007). Uncertainty calculation according to EURACHEM was performed on the basis of standard uncertainties estimated for each parameter (e.g. standard purities, peat weighing, slope and intercept of calibration curve, precision of instrumental detection) that was involved in the calculation of PFAS concentrations in peat. Combined and expanded uncertainties related to average PFAS peat concentrations are presented in Table S13. In contrast, uncertainty calculations according to ISO 20988 (Tables S14, S15) involved results of parallel measurements. In this study, two types of parallel samples were separated: 1st intra-core parallels and 2nd inter-core parallels. Uncertainty calculations on intra-core parallels (i.e. paired measurements of samples from the same core) depict the analytical uncertainty. Uncertainty calculations on inter-core parallels (i.e. paired measurements of samples from two different cores) additionally account for the sampling process.

Table S 13: Combined and expanded uncertainties (%) calculated for detected PFASs in peat according to EURACHEM guidelines. Uncertainties were related to the average PFAS concentrations in peat.

	combined uncertainty (%)	expanded uncertainty (%)
PFHxS	45	91
PFOS	8	16
PFBA	2	4
PFPA	150	300
PFHxA	30	60
PFHpA	203	406
PFOA	6	13
PFNA	30	60
PFDA	25	50
PFUnDA	12	23
PFDoDA	39	79
PFTrDA	122	245
PFTeDA	142	284

Table S 14: Combined and expanded uncertainties (%) calculated for detected PFASs in peat according to ISO 20988 on the basis of paired intra-core measurements. Uncertainties were related to the average PFAS concentrations in peat.

	combined standard uncertainty (%)	expanded uncertainty (%)
PFHxS	144	302
PFOS	24	51
PFBA	43	90
PFPA	164	345
PFHxA	48	100
PFHpA	53	111
PFOA	10	21
PFNA	15	30
PFDA	24	51
PFUnDA	17	37
PFDoDA	26	55
PFTrDA	24	50
PFTeDA	28	59

Table S 15: Combined and expanded uncertainties (%) calculated for detected PFASs in peat according to ISO 20988 on the basis of paired inter-core measurements. Uncertainties were related to the average PFAS concentrations in peat.

	combined standard uncertainty (%)	expanded uncertainty (%)
PFHxS	142	299
PFOS	46	97
PFBA	63	132
PFPA	279	586
PFHxA	62	129
PFHpA	101	211
PFOA	45	94
PFNA	38	80
PFDA	47	98
PFUnDA	61	127
PFDoDA	74	156
PFTrDA	81	170
PFTeDA	81	171

As observed in previous validation experiments, uncertainties were usually highest for those analytes which were rarely detected or for which compound-specific mass-labelled internal standards were not available. For the other compounds, combined uncertainties according to Eurachem guidelines and ISO 20988 (intra-core approach) were roughly between 5 and 50 %. Precision of the measurements and errors of the calibration curves' intercepts usually contributed the most. Inter-core uncertainties were higher than intra-core uncertainties, demonstrating that the sampling (different compaction of peat during sampling, different peat microstructure, choice of site) is an important factor influencing concentrations.

4.8 Analytical blanks

Table S 16: Concentrations (ng kg^{-1}) of those analytes detected in analytical blanks.

	MBI-BW1	MBI-BW2	MBII-BW1	MBII-BW2	average	SD
PFBS	12	7	<MDL	<MDL	4.6	5.8
PFHpS	35	<MDL	<MDL	<MDL	8.9	17.7
PFOS	10	10	<MDL	<MDL	5.1	5.9
PFDS	<MDL	8	<MDL	<MDL	2.1	4.2
PFBA	74	77	93	43	71.7	21.0
PFPA	<MDL	22	23	<MDL	11.1	12.9
PFHxA	<MDL	3	3	<MDL	1.3	1.5
PFHpA	<MDL	13	<MDL	<MDL	3.3	6.7
PFOA	33	37	30	28	32.1	4.2
PFNA	<MDL	9	7	2	4.4	4.4
PFDA	5	1	<MDL	<MDL	1.5	2.2
PFUnDA	3	2	4	<MDL	2.2	1.7
PFDoDA	8	<MDL	<MDL	<MDL	2.0	3.9
PFTrDA	<MDL	<MDL	2	<MDL	0.5	1.0
PFHxDA	31	15	<MDL	<MDL	11.6	14.8
PFOcDA	44	33	<MDL	<MDL	19.4	22.8

5. Sampling
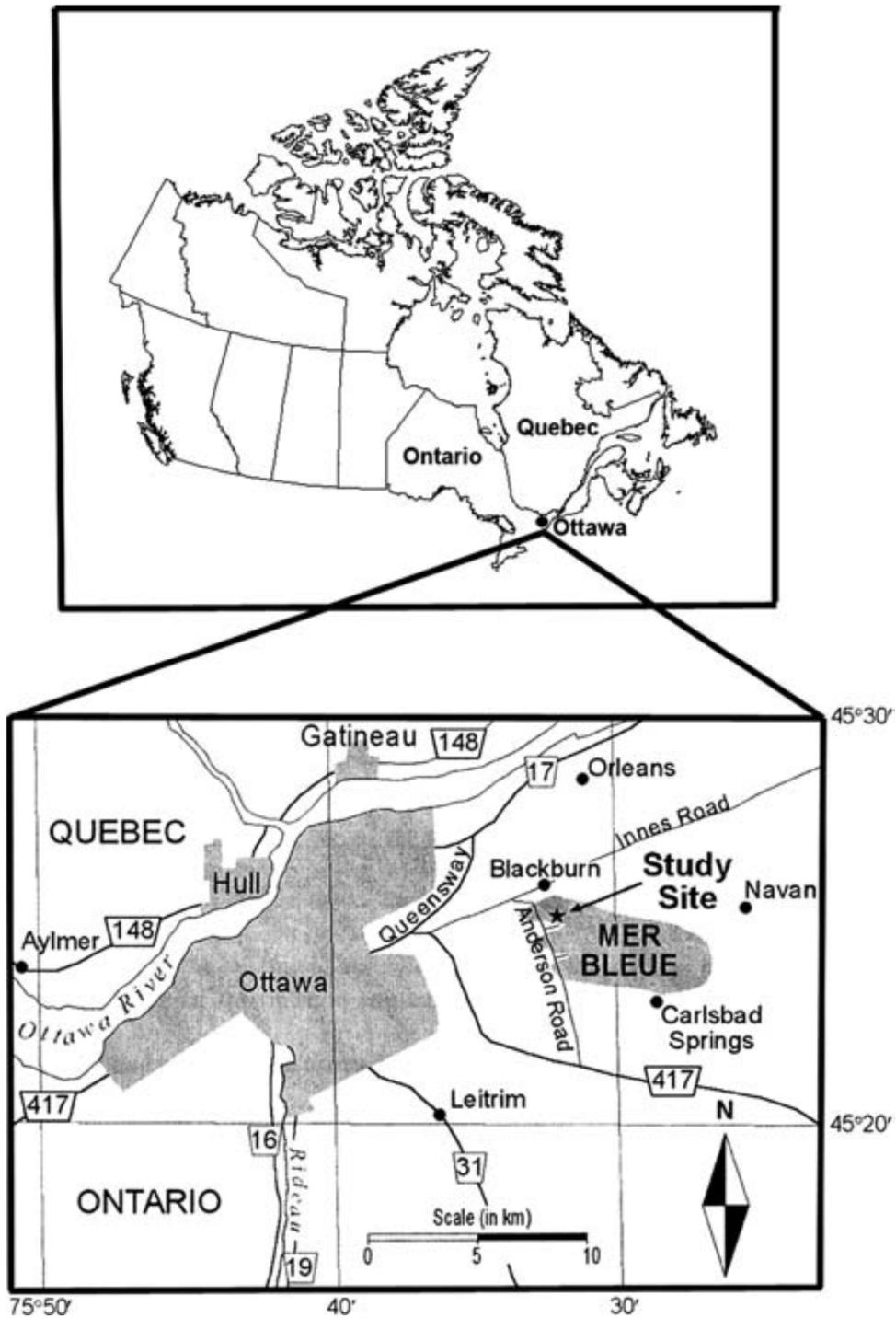
Figure S 9: Location of Mer Bleue Bog, Canada. Figure adapted from Lai (2009).

Figure S 10: Mer Bleue Bog, Canada.

Figure S 11: Peat core taken at Mer Bleue Bog.

6. Dating approach, used in this study

In this study, two peat cores were taken at Mer Bleue in 2009 and cut into 5 cm segments after the sampling. In order to obtain the age of each segment, dating was applied from another study (Thuens 2012, personal communication) analysing peat cores taken at Mer Bleue in the same year to investigate the contamination history on other organic pollutants. This appeared to be a cost-effective and suited approach for studying additional organic pollutants beforehand because of the following reasons.

1st The age of the 5 cm sections of three ^{210}Pb dated peat cores taken in that study (Thuens 2012, personal communication) correlated strongly with the accumulated dry weight of the cores ($R^2 = 0.98$) and three cores differed not substantially. Therefore, a uniform growth rate can be assumed, indicating that dating of one core may be applied to another core without adding too much uncertainty. Of course, this implies that the peat layers are parallel and evenly distributed over the peat bog. Although this can certainly not be completely applied for an entire bog of the size of Mer Bleue, uniform growth may be presumed when the same microstructures (i.e. hollows in this case) are sampled within a small defined area.
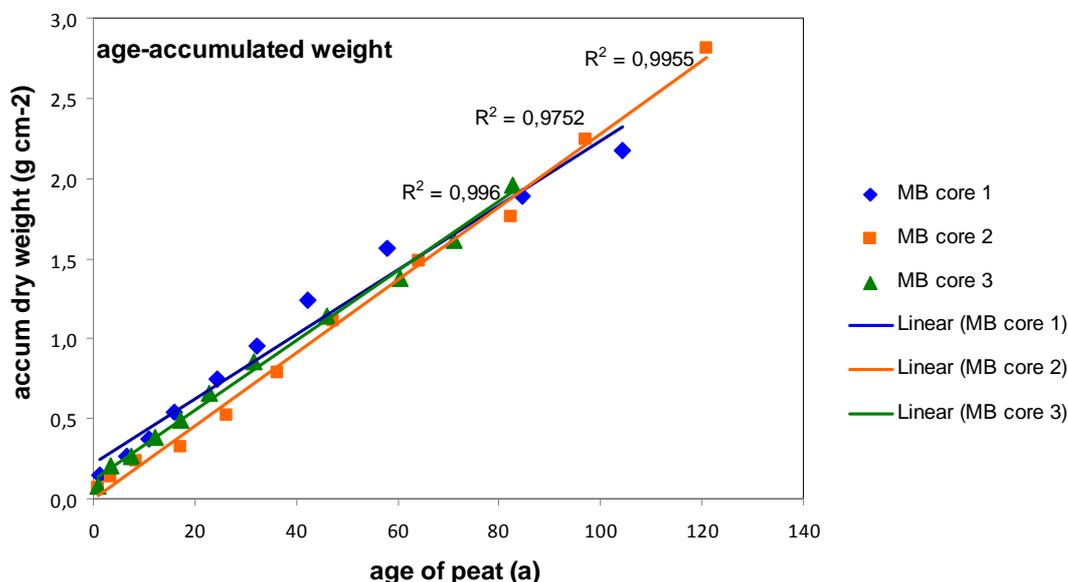
Figure S 1: Age-accumulated weight using 3 Mer Bleue peat cores (Thüns 2012, personal communication).

2nd In a previous study on PAHs in ombrotrophic bogs in Canada (Dreyer et al. 2005), peat cores were taken at Mer Bleue bog at two different times, extracted, and analysed for their PAH content. A significant difference ($p<0.05$) between both cores was not ob-

served indicating replicate cores taken at Mer Bleue provide reproducible information on historic atmospheric deposition of organic contaminants.

Differences in PAH concentrations taken at Mer Bleue

Differences in PAH concentrations taken at Mer Bleue
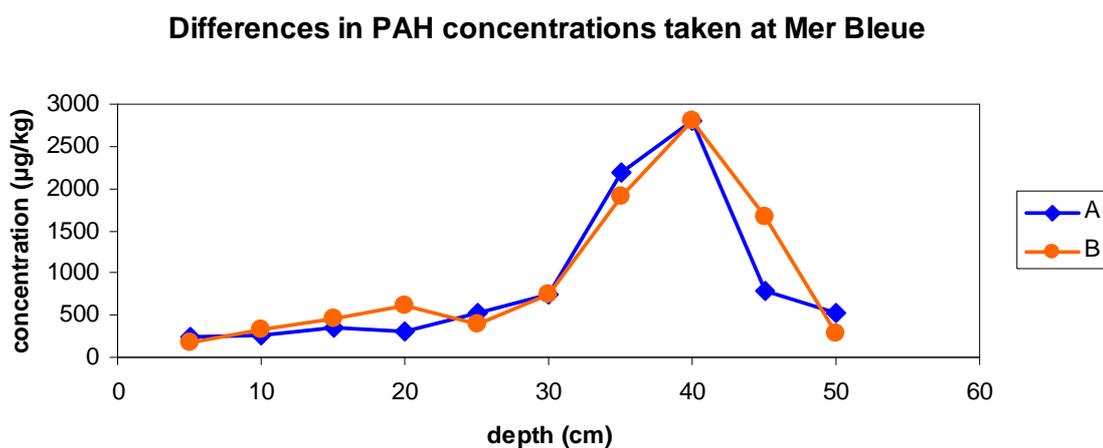
Figure S 13:Depth-dependent PAH concentrations in 2 Mer Bleue peat cores taken at two different times.

However, as we now know, significant differences were observed in the present study regarding the depth distribution of several PFASs in 2 different peat cores from Mer Bleue. Among other reasons, this may also be due to the use of an external peat core for their dating. Thus, with the knowledge we have now after having analyzed these cores for their historical PFAS contamination, it is advisable to use an internal dating of each core instead of applying external data.

Although the dating by using another peat core of the same bog may appear to be a limiting factor, major conclusions and findings of this manuscript are not depending largely on the accuracy of the dating. Consequently, dating uncertainties will not reduce the legitimacy of these other findings substantially

7. PFAS concentrations determined in peat samples

Table S 17: Blank-corrected PFAS concentrations (ng kg^{-1}) of the first parallel in the first core taken at Mer Bleue Bog (MB-I). < MDL: below the method detection limit. < MQL: below the method quantification limit. < IDL: below the instrumental detection limit. n.d.: not detected.

	MB -I Surface -1	MB -I 0-5-1	MB -I 5-10-1	MB 1 -I 0-15-1	MB 1 -I 5-20-1	MB 2 -I 0-25-1	MB 2 -I 5-30-1	MB 3 -I 0-35-1	MB 3 -I 5-40-1	MB 4 -I 0-45-1
age	0	3	8	17	26	36	47	64	82	97
year	2009	2006	2001	1992	1983	1973	1962	1945	1927	1912
PFBS	< MDL	< MDL	< IDL	< MDL	< MDL	71	< MDL	< MDL	< MDL	< MDL
PFHxS	131	28	17	6	10	14	25	14	19	19
PFHpS	n.d.	n.d.	n.d.	< MDL	< MDL	< MQL	n.d.	n.d.	n.d.	< MDL
PFOS	76	130	296	469	461	711	726	532	303	114
PFDS	n.d.	n.d.	< MDL	< MDL	< MDL	n.d.	n.d.	n.d.	n.d.	n.d.
PFBA	(654)	(1572)	(1572)	(1171)	(2084)	(1408)	(3141)	(2043)	(848)	(2131)
PFPA	n.d.	n.d.	n.d.	n.d.	n.d.	n.d.	n.d.	n.d.	n.d.	n.d.
PFHxA	88	42	38	93	53	72	108	69	120	107
PFHpA	< IDL	< MDL	35	49	54	31	60	39	< MDL	n.d.
PFOA	< MDL	66	118	192	229	352	416	364	249	232
PFNA	41	143	229	259	241	203	263	148	69	44
PFDA	12	36	65	87	49	36	32	19	13	< IDL
PFUnDA	34	144	282	291	134	78	28	10	< IDL	n.d.
PFDoDA	< MDL	32	76	110	44	41	< MDL	< MDL	< MDL	< MDL
PFTriDA	9	27	76	138	50	14	n.d.	n.d.	n.d.	n.d.
PFTeDA	13	17	21	61	40	28	n.d.	n.d.	n.d.	n.d.
PFHxDA	< IDL	< IDL	< IDL	< MDL	< MDL	< MDL	< MDL	n.d.	n.d.	n.d.
PFOcDA	< MDL	n.d.	< IDL	< IDL	< IDL	n.d.	n.d.	n.d.	n.d.	n.d.
NMeFOSA	n.d.	n.d.	n.d.	n.d.	n.d.	n.d.	n.d.	n.d.	n.d.	n.d.
NEtFOSA	n.d.	n.d.	n.d.	n.d.	n.d.	n.d.	n.d.	n.d.	n.d.	n.d.
NMeFOSE	n.d.	n.d.	n.d.	n.d.	n.d.	n.d.	n.d.	n.d.	n.d.	n.d.
NEtFOSE	n.d.	n.d.	n.d.	n.d.	n.d.	n.d.	n.d.	n.d.	n.d.	n.d.
MeFBSA	n.d.	n.d.	n.d.	n.d.	n.d.	n.d.	n.d.	n.d.	n.d.	n.d.
MeFBSE	n.d.	n.d.	n.d.	n.d.	n.d.	n.d.	n.d.	n.d.	n.d.	n.d.
FOSA	n.d.	n.d.	n.d.	n.d.	n.d.	n.d.	n.d.	n.d.	n.d.	n.d.

Table S 18: Blank-corrected PFAS concentrations (ng kg^{-1}) of the second parallel in the first core taken at Mer Bleue Bog (MB-I). < MDL: below the method detection limit. < MQL: below the method quantification limit. < IDL: below the instrumental detection limit. n.d.: not detected. PFBA values are in brackets because of insufficient peak shape in the chromatogram.

	MB-I Surface-2	MB-I 0-5-2	MB-I 5-10-2	MB-1 0-15-2	MB-1 5-20-2	MB-2 0-25-2	MB-2 5-30-2	MB-3 0-35-2	MB-3 5-40-2	MB-4 0-45-2
age	0	3	8	17	26	36	47	64	82	97
year	2009	2006	2001	1992	1983	1973	1962	1945	1927	1912
PFBS	n.d.	n.d.	< MDL	< MDL	< MDL	< MDL	< MDL	< MDL	n.d.	n.d.
PFHxS	40	33	5	10	12	29	21	22	15	17
PFHpS	n.d.	n.d.	n.d.	n.d.	n.d.	n.d.	n.d.	n.d.	n.d.	n.d.
PFOS	101	217	316	637	472	758	720	532	355	93
PFDS	< IDL	n.d.	n.d.	n.d.	< MDL	n.d.	n.d.	n.d.	n.d.	n.d.
PFBA	(574)	(1574)	(1335)	(188)	(1473)	(2814)	(317)	(453)	< MDL	(818)
PFPA	n.d.	< MDL	< MDL	< MDL	< MDL	< MDL	n.d.	n.d.	n.d.	n.d.
PFHxA	95	44	13	56	37	52	23	38	n.d.	45
PFHpA	< MDL	< MDL	< MDL	63	49	81	99	54	< MDL	n.d.
PFOA	< MDL	131	101	189	257	404	514	367	229	202
PFNA	33	192	223	271	234	322	297	156	89	44
PFDA	< MDL	73	89	81	52	53	34	23	16	n.d.
PFUnDA	43	222	273	314	129	95	37	12	n.d.	n.d.
PFDoDA	< MDL	48	75	104	36	29	< IDL	n.d.	n.d.	n.d.
PFTrDA	8	53	76	122	42	18	< IDL	n.d.	n.d.	n.d.
PFTeDA	n.d.	10	12	42	27	13	n.d.	n.d.	n.d.	n.d.
PFHxDA	n.d.	< IDL	< IDL	< MDL	< MDL	< MDL	< MDL	n.d.	n.d.	n.d.
PFOcDA	< IDL	n.d.	n.d.	< IDL	< IDL	< MDL	n.d.	n.d.	n.d.	n.d.
MeFOSA	n.d.	n.d.	n.d.	n.d.	n.d.	n.d.	n.d.	n.d.	n.d.	n.d.
EtFOSA	n.d.	n.d.	n.d.	n.d.	n.d.	n.d.	n.d.	n.d.	n.d.	n.d.
MeFOSE	n.d.	n.d.	n.d.	n.d.	n.d.	n.d.	n.d.	n.d.	n.d.	n.d.
EtFOSE	n.d.	n.d.	n.d.	n.d.	n.d.	n.d.	n.d.	n.d.	n.d.	n.d.
MeFBSA	n.d.	n.d.	n.d.	n.d.	n.d.	n.d.	n.d.	n.d.	n.d.	n.d.
MeFBSE	n.d.	n.d.	n.d.	n.d.	n.d.	n.d.	n.d.	n.d.	n.d.	n.d.
FOSA	< IDL	< IDL	n.d.	n.d.	n.d.	n.d.	n.d.	n.d.	n.d.	n.d.

Table S 19: Blank-corrected PFAS concentrations (ng kg $^{-1}$) of the first parallel in the second core taken at Mer Bleue Bog (MB-II). < MDL: below the method detection limit. < MQL: below the method quantification limit. < IDL: below the instrumental detection limit. n.d.: not detected.

	MB-II Surface-1	1-0-5-1	1-5-10-1	1-II0-15-1	1-II5-20-1	2-II0-25-1	2-II5-30-1	3-II0-35-1	3-II5-40-1
age	0	3	8	17	26	36	47	64	82
year	2009	2006	2001	1992	1983	1973	1962	1945	1927
PFBS	n.d.	n.d.	n.d.	n.d.	n.d.	n.d.	n.d.	n.d.	n.d.
PFHxS	n.d.	46	6	n.d.	10	11	17	12	n.d.
PFHpS	n.d.	n.d.	n.d.	n.d.	n.d.	n.d.	n.d.	n.d.	n.d.
PFOS	74	376	573	894	950	539	294	570	n.d.
PFDS	n.d.	n.d.	n.d.	n.d.	n.d.	n.d.	n.d.	n.d.	n.d.
PFBA	(2780)	(4865)	(1123)	(2005)	(2438)	(1357)	(1273)	(1131)	(1253)
PFPA	154	171	82	< MDL	n.d.	< IDL	< IDL	n.d.	n.d.
PFHxA	148	115	86	131	101	32	32	40	n.d.
PFHpA	< MDL	86	54	29	56	34	< MDL	< MDL	n.d.
PFOA	136	211	241	436	509	346	243	278	194
PFNA	52	193	162	320	396	206	82	160	< MQL
PFDA	21	36	47	57	60	27	n.d.	< MQL	n.d.
PFUnDA	122	123	116	160	122	37	< MQL	< MQL	n.d.
PFDoDA	47	56	42	72	65	< MDL	n.d.	n.d.	n.d.
PFTrDA	46	28	39	42	37	< MQL	< MDL	n.d.	n.d.
PFTeDA	18	63	40	88	65	n.d.	n.d.	< IDL	n.d.
PFHxDA	n.d.	n.d.	n.d.	n.d.	n.d.	n.d.	n.d.	n.d.	n.d.
PFOcDA	n.d.	n.d.	n.d.	< MDL	< MDL	n.d.	n.d.	n.d.	n.d.
MeFOSA	n.d.	n.d.	n.d.	n.d.	n.d.	n.d.	n.d.	n.d.	n.d.
EtFOSA	n.d.	n.d.	n.d.	n.d.	n.d.	n.d.	n.d.	n.d.	n.d.
MeFOSE	n.d.	n.d.	n.d.	n.d.	n.d.	n.d.	n.d.	n.d.	n.d.
EtFOSE	n.d.	n.d.	n.d.	n.d.	n.d.	n.d.	n.d.	n.d.	n.d.
MeFBSA	n.d.	n.d.	n.d.	n.d.	n.d.	n.d.	n.d.	n.d.	n.d.
MeFBSE	n.d.	n.d.	n.d.	n.d.	n.d.	n.d.	n.d.	n.d.	n.d.
FOSA	n.d.	n.d.	n.d.	n.d.	n.d.	n.d.	n.d.	n.d.	n.d.

Table S 20: Blank-corrected PFAS concentrations (ng kg^{-1}) of the second parallel in the second core taken at Mer Bleue Bog (MB-II). < MDL: below the method detection limit. < MQL: below the method quantification limit. < IDL: below the instrumental detection limit. n.d.: not detected.

	MB-II Surface-2	MB-II 0-5-2	MB-II 5-10-2	MB-II 10-15-2	MB-II 15-20-2	MB-II 20-25-2	MB-II 25-30-2	MB-II 30-35-2	MB-II 35-40-2
age	0	3	8	17	26	36	47	64	82
year	2009	2006	2001	1992	1983	1973	1962	1945	1927
PFBS	n.d.	n.d.	n.d.	< MDL	< MDL	< MDL	n.d.	n.d.	n.d.
PFHxS	157	n.d.	n.d.	14	18	7	15	8	n.d.
PFHpS	n.d.	n.d.	n.d.	n.d.	n.d.	n.d.	n.d.	n.d.	n.d.
PFOS	88	296	319	469	732	546	242	432	n.d.
PFDS	n.d.	n.d.	n.d.	n.d.	n.d.	n.d.	n.d.	n.d.	n.d.
PFBA	(2265)	(3901)	(1380)	(1771)	(3028)	(1536)	(1152)	(1281)	(875)
PFPA	< MDL	117	87	n.d.	< MDL	< MDL	n.d.	n.d.	n.d.
PFHxA	162	140	100	61	48	49	37	51	n.d.
PFHpA	< MDL	72	95	86	56	45	< MDL	< MDL	n.d.
PFOA	160	225	237	394	568	351	268	296	167
PFNA	62	166	234	319	412	206	81	149	< MDL
PFDA	12	35	49	62	66	18	n.d.	< MDL	n.d.
PFUnDA	108	138	147	130	116	27	n.d.	< MDL	n.d.
PFDoDA	52	45	25	38	54	< MDL	n.d.	n.d.	n.d.
PFTrDA	37	44	43	49	49	n.d.	n.d.	n.d.	n.d.
PFTeDA	20	70	59	85	66	n.d.	n.d.	n.d.	n.d.
PFHxDA	n.d.	n.d.	n.d.	n.d.	n.d.	n.d.	n.d.	n.d.	n.d.
PFOcDA	< IDL	< IDL	< IDL	< MDL	< MDL	n.d.	n.d.	n.d.	n.d.
MeFOSA	n.d.	n.d.	n.d.	n.d.	n.d.	n.d.	n.d.	n.d.	n.d.
EtFOSA	n.d.	n.d.	n.d.	n.d.	n.d.	n.d.	n.d.	n.d.	n.d.
MeFOSE	n.d.	n.d.	n.d.	n.d.	n.d.	n.d.	n.d.	n.d.	n.d.
EtFOSE	n.d.	n.d.	n.d.	n.d.	n.d.	n.d.	n.d.	n.d.	n.d.
MeFBSA	n.d.	n.d.	n.d.	n.d.	n.d.	n.d.	n.d.	n.d.	n.d.
MeFBSE	n.d.	n.d.	n.d.	n.d.	n.d.	n.d.	n.d.	n.d.	n.d.
FOSA	n.d.	n.d.	n.d.	n.d.	n.d.	n.d.	n.d.	n.d.	n.d.

8. PFAS deposition rates determined in peat samples

Table S 21: PFAS deposition rates (ng m^{-2} a^{-1}) of the first parallel in the first core taken at Mer Bleue Bog (MB- I). < MDL: below the method detection limit. < MQL: below the method quantification limit. < IDL: below the instrumental detection limit. n.d.: not detected.

	MB -I Surface -1	MB -I 0-5- 1	MB -I 5-10- 1	MB 1 -I 0 - 15 -1	MB 1 -I 5 - 20 -1	MB 2 -I 0 - 25 -1	MB 2 -I 5 - 30 -1	MB 3 -I 0 - 35 -1	MB 3 -I 5 - 40 -1	MB 4 -I 0 - 45 -1
age	0	3	8	17	26	36	47	64	82	97
year	2009	2006	2001	1992	1983	1973	1962	1945	1927	1912
PFBS	< MDL	< MDL	< IDL	< MDL	< MDL	35	< MDL	< MDL	< MDL	< MDL
PFHxS	59	12	4	1	2	7	9	3	5	6
PFHpS	n.d.	n.d.	n.d.	< MDL	< MDL	< MQL	n.d.	n.d.	n.d.	< MDL
PFOS	34	55	61	74	101	351	245	107	73	38
PFDS	n.d.	n.d.	< MDL	< MDL	< MDL	n.d.	n.d.	n.d.	n.d.	n.d.
PFBA	(295)	(666)	(323)	(185)	(458)	(696)	(1061)	(412)	(204)	(705)
PFPA	n.d.	n.d.	n.d.	n.d.	n.d.	n.d.	n.d.	n.d.	n.d.	n.d.
PFHxA	40	18	8	15	12	35	36	14	29	36
PFHpA	< IDL	< MDL	7	8	12	15	20	8	< MDL	n.d.
PFOA	< MDL	28	24	30	50	174	140	73	60	77
PFNA	19	61	47	41	53	100	89	30	17	14
PFDA	5	15	13	14	11	18	11	4	3	< IDL
PFUnDA	15	61	58	46	29	38	9	2	< IDL	n.d.
PFDoDA	< MDL	14	16	17	10	20	< MDL	< MDL	< MDL	< MDL
PFTrDA	4	11	16	22	11	7	n.d.	n.d.	n.d.	n.d.
PFTeDA	6	7	4	10	9	14	n.d.	n.d.	n.d.	n.d.
PFHxDA	< IDL	< IDL	< IDL	< MDL	< MDL	< MDL	< MDL	n.d.	n.d.	n.d.
PFOcDA	< MDL	n.d.	< IDL	< IDL	< IDL	n.d.	n.d.	n.d.	n.d.	n.d.
MeFOSA	n.d.	n.d.	n.d.	n.d.	n.d.	n.d.	n.d.	n.d.	n.d.	n.d.
EtFOSA	n.d.	n.d.	n.d.	n.d.	n.d.	n.d.	n.d.	n.d.	n.d.	n.d.
MeFOSE	n.d.	n.d.	n.d.	n.d.	n.d.	n.d.	n.d.	n.d.	n.d.	n.d.
EtFOSE	n.d.	n.d.	n.d.	n.d.	n.d.	n.d.	n.d.	n.d.	n.d.	n.d.
MeFBSA	n.d.	n.d.	n.d.	n.d.	n.d.	n.d.	n.d.	n.d.	n.d.	n.d.
MeFBSE	n.d.	n.d.	n.d.	n.d.	n.d.	n.d.	n.d.	n.d.	n.d.	n.d.
FOSA	n.d.	n.d.	n.d.	n.d.	n.d.	n.d.	n.d.	n.d.	n.d.	n.d.

Table S 22: PFAS deposition rates (ng m^{-2} a^{-1}) of the second parallel in the first core taken at Mer Bleue Bog (MB-I). < MDL: below the method detection limit. < MQL: below the method quantification limit. < IDL: below the instrumental detection limit. n.d.: not detected.

	MB-I Surface -2	MB-I 0-5- 2	MB-I 5-10- 2	MB-I 10- 15 -2	MB-I 15- 20 -2	MB-I 20- 25 -2	MB-I 25- 30 -2	MB-I 30- 35 -2	MB-I 35- 40 -2	MB-I- 40- 45 -2
age	0	3	8	17	26	36	47	64	82	97
year	2009	2006	2001	1992	1983	1973	1962	1945	1927	1912
PFBS	n.d.	n.d.	< MDL	< MDL	< MDL	< MDL	< MDL	< MDL	n.d.	n.d.
PFHxS	18	14	1	2	3	14	7	4	4	6
PFHpS	n.d.	n.d.	n.d.	n.d.	n.d.	n.d.	n.d.	n.d.	n.d.	n.d.
PFOS	45	92	65	101	104	375	243	107	86	31
PFDS	< IDL	n.d.	n.d.	n.d.	< MDL	n.d.	n.d.	n.d.	n.d.	n.d.
PFBA	(259)	(667)	(274)	(30)	(324)	(1391)	(107)	(91)	< MDL	(271)
PFPA	n.d.	< MDL	< MDL	< MDL	< MDL	< MDL	n.d.	n.d.	n.d.	n.d.
PFHxA	43	19	3	9	8	26	8	8	n.d.	15
PFHpA	< MDL	< MDL	< MDL	10	11	40	34	11	< MDL	n.d.
PFOA	< MDL	55	21	30	56	200	173	74	55	67
PFNA	15	81	46	43	52	159	100	31	22	15
PFDA	< MDL	31	18	13	11	26	11	5	4	n.d.
PFUnDA	20	94	56	50	28	47	12	2	n.d.	n.d.
PFDoDA	< MDL	20	15	16	8	14	< IDL	n.d.	n.d.	n.d.
PFTrDA	4	22	16	19	9	9	< IDL	n.d.	n.d.	n.d.
PFTeDA	n.d.	4	2	7	6	6	n.d.	n.d.	n.d.	n.d.
PFHxDA	n.d.	< IDL	< IDL	< MDL	< MDL	< MDL	< MDL	n.d.	n.d.	n.d.
PFOcDA	< IDL	n.d.	n.d.	< IDL	< IDL	< MDL	n.d.	n.d.	n.d.	n.d.
MeFOSA	n.d.	n.d.	n.d.	n.d.	n.d.	n.d.	n.d.	n.d.	n.d.	n.d.
EtFOSA	n.d.	n.d.	n.d.	n.d.	n.d.	n.d.	n.d.	n.d.	n.d.	n.d.
MeFOSE	n.d.	n.d.	n.d.	n.d.	n.d.	n.d.	n.d.	n.d.	n.d.	n.d.
EtFOSE	n.d.	n.d.	n.d.	n.d.	n.d.	n.d.	n.d.	n.d.	n.d.	n.d.
MeFBSA	n.d.	n.d.	n.d.	n.d.	n.d.	n.d.	n.d.	n.d.	n.d.	n.d.
MeFBSE	n.d.	n.d.	n.d.	n.d.	n.d.	n.d.	n.d.	n.d.	n.d.	n.d.
FOSA	< IDL	< IDL	n.d.	n.d.	n.d.	n.d.	n.d.	n.d.	n.d.	n.d.

Table S 23: PFAS deposition rates (ng m^{-2} a^{-1}) of the first parallel in the second core taken at Mer Bleue Bog (MB-II). < MDL: below the method detection limit. < MQL: below the method quantification limit. < IDL: below the instrumental detection limit. n.d.: not detected.

	MB -II Surface -1	I- 0-5- 1	I- 5-10- 1	MB -II 0 -15 -1	MB -II 5 -20 -1	MB -II 0 -25 -1	MB -II 5 -30 -1	MB -II 0 -35 -1	MB -II 5 -40 -1
age	0	3	8	17	26	36	47	64	82
year	2009	2006	2001	1992	1983	1973	1962	1945	1927
PFBS	n.d.	n.d.	n.d.	n.d.	n.d.	n.d.	n.d.	n.d.	n.d.
PFHxS	n.d.	17	2	n.d.	2	3	5	3	n.d.
PFHpS	n.d.	n.d.	n.d.	n.d.	n.d.	n.d.	n.d.	n.d.	n.d.
PFOS	26	142	223	188	199	141	86	128	n.d.
PFDS	n.d.	n.d.	n.d.	n.d.	n.d.	n.d.	n.d.	n.d.	n.d.
PFBA	(991)	(1841)	(437)	(421)	(510)	(356)	(373)	(254)	(512)
PFPA	55	65	32	< MDL	n.d.	< IDL	< IDL	n.d.	n.d.
PFHxA	53	43	34	27	21	8	9	9	n.d.
PFHpA	< MDL	32	21	6	12	9	< MDL	< MDL	n.d.
PFOA	49	80	94	92	107	91	71	62	79
PFNA	18	73	63	67	83	54	24	36	< MQL
PFDA	7	14	18	12	13	7	n.d.	< MQL	n.d.
PFUnDA	44	47	45	34	26	10	< MQL	< MQL	n.d.
PFDoDA	17	21	16	15	14	< MDL	n.d.	n.d.	n.d.
PFTrDA	17	11	15	9	8	< MQL	< MDL	n.d.	n.d.
PFTeDA	6	24	16	18	14	n.d.	n.d.	< IDL	n.d.
PFHxDA	n.d.	n.d.	n.d.	n.d.	n.d.	n.d.	n.d.	n.d.	n.d.
PFOcDA	n.d.	n.d.	n.d.	< MDL	< MDL	n.d.	n.d.	n.d.	n.d.
MeFOSA	n.d.	n.d.	n.d.	n.d.	n.d.	n.d.	n.d.	n.d.	n.d.
EtFOSA	n.d.	n.d.	n.d.	n.d.	n.d.	n.d.	n.d.	n.d.	n.d.
MeFOSE	n.d.	n.d.	n.d.	n.d.	n.d.	n.d.	n.d.	n.d.	n.d.
EtFOSE	n.d.	n.d.	n.d.	n.d.	n.d.	n.d.	n.d.	n.d.	n.d.
MeFBSA	n.d.	n.d.	n.d.	n.d.	n.d.	n.d.	n.d.	n.d.	n.d.
MeFBSE	n.d.	n.d.	n.d.	n.d.	n.d.	n.d.	n.d.	n.d.	n.d.
FOSA	n.d.	n.d.	n.d.	n.d.	n.d.	n.d.	n.d.	n.d.	n.d.

Table S 24: PFAS deposition rates (ng m^{-2} a^{-1}) of the second parallel in the second core taken at Mer Bleue Bog (MB-II). < MDL: below the method detection limit. < MQL: below the method quantification limit. < IDL: below the instrumental detection limit. n.d.: not detected.

	MB-II Surface -2	MB-II 0-5- 2	MB-II 5-10- 2	MB-II 10- 15 - 2	MB-II 15- 20 -2	MB-II 20- 25 -2	MB-II 25- 30 -2	MB-II 30- 35 -2	MB-II 35- 40 -2
age	0	3	8	17	26	36	47	64	82
year	2009	2006	2001	1992	1983	1973	1962	1945	1927
PFBS	n.d.	n.d.	n.d.	< MDL	< MDL	< MDL	n.d.	n.d.	n.d.
PFHxS	56	n.d.	n.d.	3	4	2	5	2	n.d.
PFHpS	n.d.	n.d.	n.d.	n.d.	n.d.	n.d.	n.d.	n.d.	n.d.
PFOS	31	112	124	98	153	143	71	97	n.d.
PFDS	n.d.	n.d.	n.d.	n.d.	n.d.	n.d.	n.d.	n.d.	n.d.
PFBA	(807)	(1476)	(537)	(371)	(634)	(402)	(337)	(287)	(357)
PFPA	< MDL	44	34	n.d.	< MDL	< MDL	n.d.	n.d.	n.d.
PFHxA	58	53	39	13	10	13	11	11	n.d.
PFHpA	< MDL	27	37	18	12	12	< MDL	< MDL	n.d.
PFOA	57	85	92	83	119	92	78	66	68
PFNA	22	63	91	67	86	54	24	33	< MDL
PFDA	4	13	19	13	14	5	n.d.	< MDL	n.d.
PFUnDA	39	52	57	27	24	7	n.d.	< MDL	n.d.
PFDoDA	18	17	10	8	11	< MDL	n.d.	n.d.	n.d.
PFTrDA	13	17	17	10	10	n.d.	n.d.	n.d.	n.d.
PFTeDA	7	27	23	18	14	n.d.	n.d.	n.d.	n.d.
PFHxDA	n.d.	n.d.	n.d.	n.d.	n.d.	n.d.	n.d.	n.d.	n.d.
PFOcDA	< IDL	< IDL	< IDL	< MDL	< MDL	n.d.	n.d.	n.d.	n.d.
MeFOSA	n.d.	n.d.	n.d.	n.d.	n.d.	n.d.	n.d.	n.d.	n.d.
EtFOSA	n.d.	n.d.	n.d.	n.d.	n.d.	n.d.	n.d.	n.d.	n.d.
MeFOSE	n.d.	n.d.	n.d.	n.d.	n.d.	n.d.	n.d.	n.d.	n.d.
EtFOSE	n.d.	n.d.	n.d.	n.d.	n.d.	n.d.	n.d.	n.d.	n.d.
MeFBSA	n.d.	n.d.	n.d.	n.d.	n.d.	n.d.	n.d.	n.d.	n.d.
MeFBSE	n.d.	n.d.	n.d.	n.d.	n.d.	n.d.	n.d.	n.d.	n.d.
FOSA	n.d.	n.d.	n.d.	n.d.	n.d.	n.d.	n.d.	n.d.	n.d.

9. PFAS in Bog Water

Table S 25: Concentrations of quantified PFASs (ng L^{-1}) in a peat water sample from Mer Bleue

	concentration
PFBS	(1.64)
PFHxS	0.10
PFOS	0.77
PFBA	0.33
PFHxA	0.25
PFHpA	0.07
PFOA	0.73
PFNA	0.78
PFDA	0.16
PFUnDA	0.08
PFDoDA	0.06

10. Information on Peatlands and Ombrotrophic Bogs

Classification of peatlands is quite diverse and generally involves peatland-specific characteristics such as vegetation, geomorphology, hydrology, or chemistry. In North America, four main types of peatlands (> 40 cm peat) are distinguished: ombrotropic bogs, minerotrophic fens, intermediate or poor fens, and calcerous fens (Blodau 2002). Whereas bogs receive their water (and thus nutrients and contaminants) from atmospheric sources, only, fens are connected to the ground water or surface water system.

Peatlands are distributed in those areas where peat formation is enabled by hydrological and climatic conditions (Göttlich 1990). With more than $4 * 10^6$ km^2 they comprise about 3 % of the global land surface and are widely spread around the globe (Figure S14) (Succow and Joosten 2001). About ¾ are located in northern latitudes (Canada, USA, North Europe, Siberia). The remaining ¼ are located in humid tropical areas (Gorham 1990).
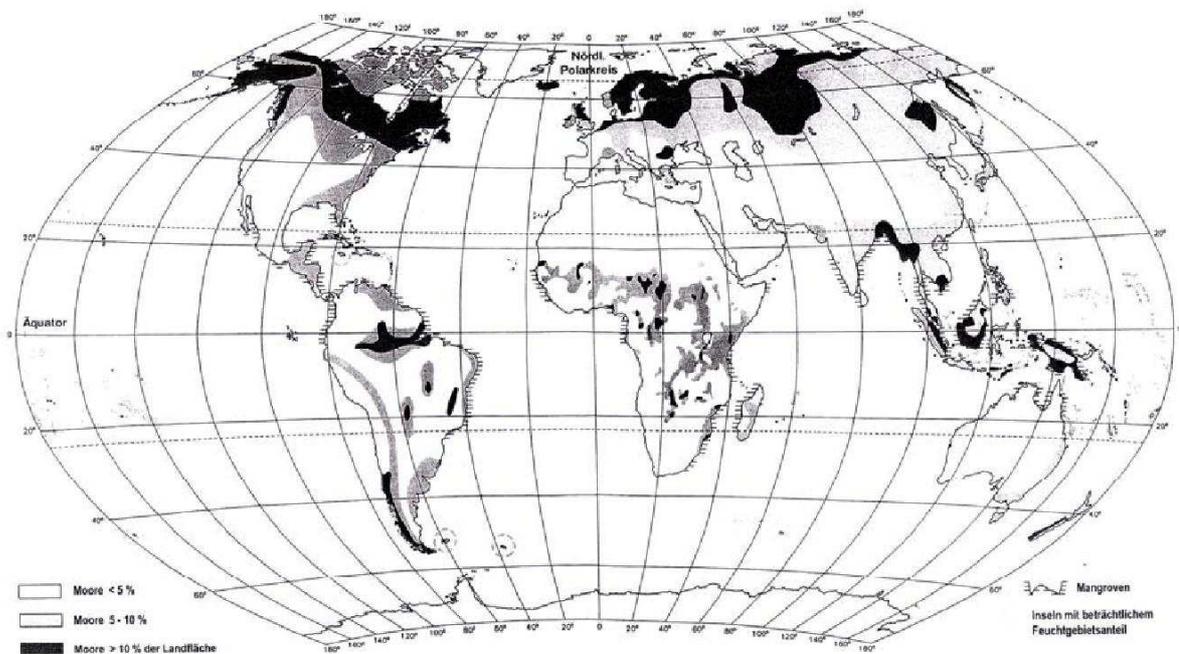

Figure S 14: Global distribution of peatlands (Succow and Joosten 2001).

Peatlands are ecosystems with a positive carbon budget, i.e. the production of organic material exceeds its degradation. As peat is the prevailing matrix formed, peatlands develop by peat accumulation (Succow and Joosten 2001). The main reason for the incomplete degradation of organic material is a lack of oxygen caused by water saturation which limits the activity of (micro)organisms (Succow and Joosten 2001). Other limiting parameters are the type of vegetation, low temperatures, low pH values, and/or large C/N (> 50 in bogs) ratios.

Undisturbed ombrotrophic peat bogs form an ideal medium for studies investigating temporal trends of contaminants for various reasons. Ombrotrophic peatlands have an autonomous water regime, they are isolated from surface and groundwater flow. Thus chemical input occurs only by atmospheric deposition (Berset et al. 2001; Rapaport and Eisenreich 1988;

Sanders et al. 1995). Up to 90 % of peat consists of organic material (Berset et al. 2001; Gorham 1990). Hydrophobic contaminants have a high affinity to organic substances and surfaces to which they tend to adsorb. Thus, the high content of organic matter of peat may enhance the adsorbed proportion of a contaminant and minimizes their post-depositional mobility. For PAHs for example, post depositional mobility is thought to be negligible (Berset et al. 2001; Rapaport and Eisenreich 1988; Sanders et al. 1995). However, the high content of organic matter may reduce the extractability of organic contaminants. Due to the prevailing anaerobic and acidic conditions in ombrotrophic bogs microbiological degradation and transformation of hydrophobic organic compounds are minimized (Aamot et al. 1996; Berset et al. 2001; Rapaport and Eisenreich 1988). Also, in contrast to soils or sediments there is no strong turnover by fauna (Berset et al. 2001). In conclusion, organic contaminants such PAHs or PCBs are conserved in the peat matrix (Berset et al. 2001; Rapaport and Eisenreich 1988; Sanders et al. 1995). Because bogs accumulated peat since the last ice age they form an excellent archive for the determination of depositional changes of environmental contaminants.

11. References

Aamot, E., E. Steinnes, and R. Schmid. 1996. Polycyclic aromatic hydrocarbons in Norwegian forest soils: Impact of long range atmospheric transport. Environmental Pollution 92: 275-280.

Berset, J. D., P. Kuehne, and W. Shotyk. 2001. Concentrations and distribution of some polychlorinated biphenyls (PCBs) and polycyclic aromatic hydrocarbons (PAHs) in an ombrotrophic peat bog profile of Switzerland. Science of the Total Environment 267: 67-85.

Blodau, C. 2002. Carbon cycling in peatlands - A review of processes and controls. Environmental Reviews 10: 111-134.

EURACHEM / CITAC, 2000. Quantifying Uncertainty in Analytical Measurement. EURACHEM / CITAC guide CG 04, http://www.measurementuncertainty.org /mu/QUAM2000-1.pdf.

Gorham, E. 1990. Biotic impoverishment in northern peatlands, p. 65-98. In G. M. Woodwell [ed.], The earth in transition: patterns and processes of biotic impoverishment. Cambridge University Press Cambridge.

Göttlich, K. 1990. Moor- und Torfkunde, 3 ed.

Higgins, C. P.; Field, J. A.; Criddle, C. S.; Luthy, R. G., 2005. Quantitative determination of perfluorochemicals in sediments and domestic sludge. Environmental Science & Technology, 39, 3946-3956.

ISO-20988, 2007. Air quality - Guidelines for estimating measurement uncertainty.

Kromidas, S., 2003. Validierung in der Analytik. Wiley-Vch.

Lai, D. Y. F., 2009. Modelling the effects of climate change on methane emission from a

northern ombrotrophic bog in Canada. Environmental Geology, 58, 1197-1206.

Lechner, M.; Knapp, H.; Pischetsrieder, M., 2010. Analysis of perfluorinated acids in biological and environmental matrices using a modified QuEChERS-method. 2nd IN-TERNATIONAL WORKSHOP Fluorinated Surfactants:New Developments, http://pft.hs-fresenius.de, June 17-19, 2010, Idstein, Germany.

Rapaport, R. A., and S. J. Eisenreich. 1988. Historical atmospheric inputs of high molec-ular-weight chlorinated hydrocarbons to eastern north America. Environmental Science & Technology 22: 931-941.

Rubarth, J.; Dreyer, A.; Guse, N.; Einax, J. W.; Ebinghaus, R., 2011. Perfluorinated compounds in red-throated divers from the German Baltic Sea. Environmental Chemis-try, in press.

Sanders, G., K. C. Jones, J. Hamilton-Taylor, and H. Dorr. 1995. PCB and PAH Fluxes to a dated UK peat core. Environmental Pollution 89: 17-25.
Succow, M., and H. Joosten. 2001. Landschaftsökologische Moorkunde, 2 ed.

Study 5

Comparison of atmospheric travel distances of several PAHs calculated by two fate and transport models (The Tool and ELPOS) with experimental values derived from a peat bog transect

Sabine Thuens, Christian Blodau, Frank Wania and Michael Radke

Comparison of atmospheric travel distances of several PAHs calculated by two fate and transport models (The Tool and ELPOS) with experimental values derived from a peat bog transect

Sabine Thuens[1], Christian Blodau[1, 2], Frank Wania[3] and Michael Radke[1, 4, *]

[1] Department of Hydrology, BayCEER, University of Bayreuth, Bayreuth, Germany

[2] Hydrology Group, Institute of Landscape Ecology, University of Münster, Münster, Germany

[3] Department of Physical and Environmental Sciences, University of Toronto Scarborough, Toronto, Canada

[4] Department of Applied Environmental Science (ITM), Stockholm University, Sweden

[*] Author to whom correspondence should be addressed; E-Mail: michael.radke@itm.su.se; Tel. : +46-8674-7136.

Abstract: Multimedia fate and transport models are used to evaluate the long range transport potential (LRTP) of organic pollutants, often by calculating their characteristic travel distance (CTD). We calculated the CTD of several polycyclic aromatic hydrocarbons (PAHs) and metals using two models: the OECD P_{OV}& LRTP Screening Tool (The Tool), and ELPOS. The absolute CTDs of PAHs estimated with the two models agree reasonably well for predominantly particle-bound congeners, while discrepancies are observed for more volatile congeners. We test the performance of the models by comparing the relative ranking of CTDs with the one of experimentally determined travel distances (ETDs). ETDs were estimated from historical deposition rates of pollutants to peat bogs in Eastern Canada. CTDs and ETDs of PAHs indicate a low LRTP. To eliminate the high influence of the wind speed and to emphasize the difference between the travel distances of single PAHs, ETDs and CTDs were analyzed relative to the travel distances of particle-bound compounds. The ETDs determined for PAHs, Cu, and Zn ranged from 173 to 321 km with relative uncertainties between 26 and 46 %. The ETDs of two metals were shorter than those of the PAHs. For particle-bound PAHs the relative ETDs and CTDs were similar while they differed for Chrysene.

Graphical Abstract
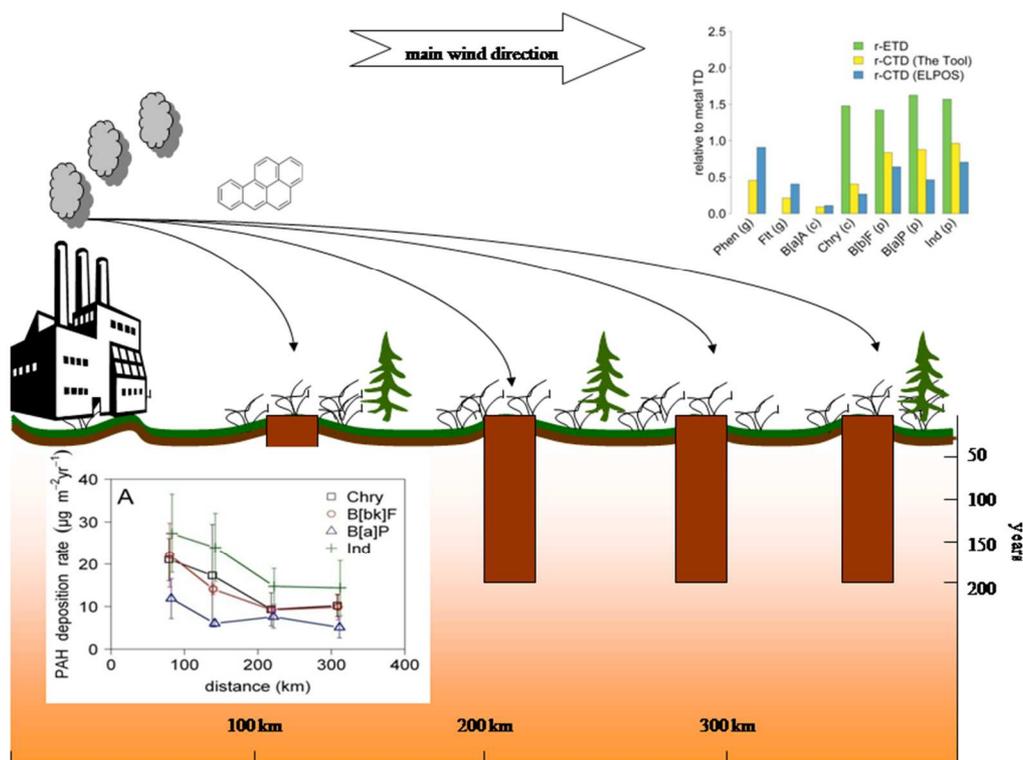
Keywords: long-range transport potential; PAHs; characteristic travel distance; transport modeling

1. Introduction

In the atmosphere, some semi-volatile organic chemicals (SVOCs) are transported long distances before being deposited [1]. To evaluate whether the environmental release of a man-made chemical may need to be curtailed through international agreements like the Stockholm Convention on Persistent Organic Pollutants, a number of compound-specific hazard indicators is often determined and compared with threshold criteria [2]. One of these indicators is a contaminant's spatial range or long-range transport potential (LRTP) [3], which can be characterized by the characteristic travel distance (CTD) [4]. The CTD is defined as the distance from a source where the concentration of a chemical is reduced by 63 %. A fraction of the chemical can travel a multiple of the CTD.

Several models such as the "Environmental Long-range Transport and Persistence of Organic Substances Model" (ELPOS) [5] and the P_{OV} & LRTP Screening Tool ("The Tool") [6] have been developed and applied to estimate the CTD of various chemicals. Both are steady-state fugacity models that estimate the CTD based on a compound's

equilibrium partitioning properties, transformation rates in environmental media, and environmental properties such as wind speed. The Tool has been designed to be as basic as possible while including all essential information [7], whereas ELPOS is more complex and includes more compartments and additional options. Both models can be used to assess a chemical's LRTP by comparing and ranking its CTD against that of identified persistent organic pollutants [8]. By comparing the results of various models the influence of different model assumptions and design features can become apparent [9]. Both models are not intended to simulate real world conditions. However, to increase confidence in the results and to identify possible model failure, their estimates should qualitatively agree with empirically derived data. To date, experimental data that facilitate the evaluation of these models with respect to the estimated CTDs are sparse [10,11].

Polycyclic aromatic hydrocarbons (PAHs) are emitted by natural combustion processes, such as forest fires, but anthropogenic emissions dominate, specifically through the incomplete combustion of carbon-based fuels. They undergo atmospheric long-range transport [12]. Their saturation vapor pressures and, therefore, their gas/particle partitioning characteristics span a wide range [13]. Based on their gas/particle partitioning behavior in the rural atmosphere of Eastern Canada, PAHs can be divided in 3 groups [14]: g-PAHs that are almost exclusively present in the gas phase (e.g.,phenanthrene (Phen) and fluoranthene (Flt)), c-PAHs (c for changing partitioning behavior) that are present in the gas phase in summer and particle-bound in winter (e.g.,benzo[a]anthracene (B[a]A) and chrysene (Chry), and p-PAHs that are almost exclusively particle-bound all year long (e.g.,benzo[b+k]fluoranthene (B[b+k]F), benzo[a]pyrene (B[a]P) and indeno[1,2,3-cd]pyrene(Ind)). To empirically determine LRTP, measurements at variable distance from a distinct contaminant source generating measurable concentrations have to be done [5]. The rates of decline of log-transformed concentrations over large latitudinal gradients in North America have been used to determine empirical travel distance (ETDs) of pesticide chemicals [10,11]. A general problem with such an approach is that additional sources along a long transect may affect the results. Moreover, substantial changes in temperature and precipitation along latitudinal gradients might complicate data interpretation due to the temperature dependence of gas/particle partitioning and atmospheric reaction rates and the dependence of deposition rates on the magnitude and temporal variability of precipitation. This study aimed at using a shorter, regional transect downwind of a dominant point source to determine ETDs of a range of PAHs, which were then used to evaluate the CTDs derived with The Tool and ELPOS.

CTDs not only scale linearly with wind speed, but also rely on several simplifying and generalizing assumptions and are based on a simplistic representation of the environment. Therefore absolute values given by the models are not directly comparable to ETDs.

To facilitate a comparison, both ETDs and CTDs were normalized to those of inert aerosol particles and Ind. Therefore, we compare relative rather than absolute values. Because most metals, including zinc (Zn) and copper (Cu), undergo atmospheric transport exclu-

sively bound to particles [15] and are not degraded in the atmosphere, they can be used to estimate the atmospheric transport distance of particles. As Ind is also mainly bound to particles we used it as a second proxy for particle-bound substances when normalizing travel distances.

We selected four ombrotrophic bogs along a ~400 km transect downwind of a large mining and smelting operation in Eastern Canada (Greater Sudbury area, Ontario; Fig. 1) to derive the temporal trend of atmospheric deposition of PAHs, Zn and Cu. The smelters in the Greater Sudbury area have been a known source of air pollution, especially for copper and sulphur-based acid precipitation, to the surrounding area for the last century [16]. Smelters emit PAHs and metals to the atmosphere as a consequence of wood or coal firing and roasting processes [15,17,18]. Ombrotrophic peat bogs have previously been used as archives of the atmospheric deposition of several classes of organic and inorganic contaminants [19-22]. The combination of continuous growth and limited bio-turbation with atmospheric wet and dry deposition as the only source of contaminants makes them well suited to derive the historical atmospheric deposition trend of non-polar contaminants. Historical depositions were used here as they represent a long term average. More importantly, the Greater Sudbury area was the dominant regional source in the past, whereas today there are many potential sources of PAHs. As deposition rates of pollutants correlate to their air concentrations [23], the decline of deposition rates over distance can be used to derive the ETD.

Fig.1: Locations of sampled peat bogs in Ontario, Canada.
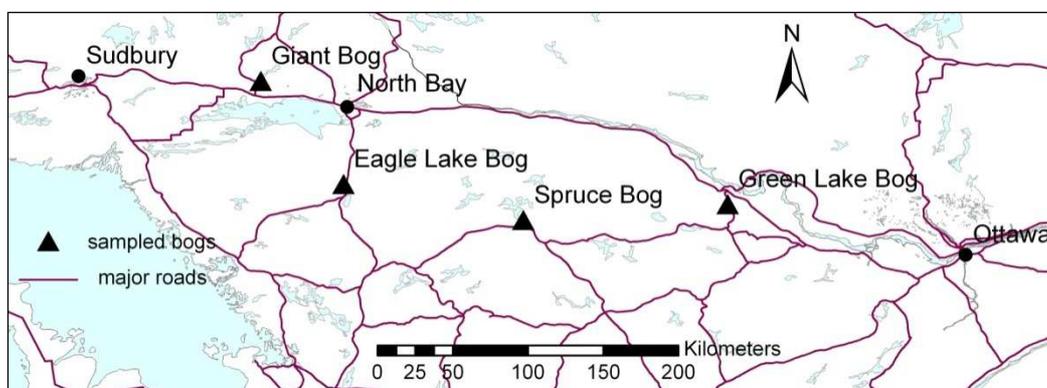
2. Methods

2.1. Sampling and Analysis

Peat cores were sampled at four bogs located downwind of the Greater Sudbury area (Canada; Fig. 1) in summer 2008. Coordinates of the sampling locations are given in Table S1 in the Supplementary Material. At each site, three peat cores were sampled in hollows with a box corer and cut into 5 cm segments in the field. Samples were transported to the laboratory, frozen, freeze dried, and milled to a fine powder. For determination of PAHs, recovery standards (mixture of 7 deuterium-substituted PAHs) were added

to 5 g (dry weight) of sample before extraction by accelerated solvent extraction with hexane. Extracts were purified by column chromatography (5 g silica, 3g alox 15 % deactivated) followed by size exclusion chromatography. The concentrations of 12 PAHs (10 EPA-PAHs: phenanthrene, fluoranthene, pyrene (Pyr), benzo[*a*]anthracene, chrysene, benzo[*b*]fluoranthene, benzo[*k*]fluoranthene, benzo[*a*]pyrene, indeno[1,2,3-*cd*]pyrene, and benzo[*ghi*]perylene (B[ghi]P), and additionally benzo[*e*]pyrene (B[e]P), and benzo[*j*]fluoranthene (B[j]F)) were determined as described in [22]. Due to the incomplete chromatographic separation of B[b]F and B[k]F, the sum of the compounds is reported as B[b+k]F. Because these isomers have similar physico-chemical properties (less than 10 % difference) [24], the ETD of B[b+k]F was compared to the CTD of B[b]F. A mass of 200 mg of the milled peat samples was digested by a microwave assisted acid dissolution technique [25] and Cu and Zn analyzed by ICP-MS. The peat cores were dated using ^{210}Pb ($t_{1/2}$ =22.26 years) by applying the constant rate of supply model [26].

2.2. Calculation of ETDs

The temporal resolution that can be achieved with peat cores is relatively low [22]. Individual segments of 5 cm span periods of 20 to 30 years. In contrast to previous work [20] we did not calculate 10 year-averaged deposition rates, as this procedure might reduce the absolute magnitude of reconstructed deposition rates. Instead, we based our analyses on the segments showing the maximum PAH deposition rate. Such maxima have previously been suggested as chrono-stratigraphic markers in peat profiles by Turetsky et al. [27]. In all peat cores PAH deposition rates peaked around 1880 – 1930, coinciding with the onset of intensive smelter operations in Sudbury. At that time the smelters were one of the main sources of PAHs in the study region as the population was small and other sources, such as traffic, were not that relevant yet.

For each compound, the maximum deposition rates from each of the three replicate cores per bog were ln-transformed and linearly regressed against the distance of the sampling site from the Inco Superstack in Sudbury. In cases where the decline of the deposition rates was significant (p < 0.1) the negative reciprocal of the slope m (km^{-1}) of the regression line corresponds to the ETD for the respective compound, and the ETD consequently corresponds to the distance where the air concentration of a compound declined by 63 % (1/e). The error of the slope of the regression was used to estimate the uncertainty of the ETDs. The software package R [28] was used for these calculations.

Wind speed is an important parameter constraining atmospheric transport of contaminants, but reliable data on average wind speed are difficult to obtain for large areas and longer periods. To facilitate the comparison of measured and calculated transport distances, we eliminated this source of uncertainty by normalizing the PAH transport distances to those of aerosol particles. As a proxy for the transport distance of particles, we used the average transport distance of the metals Cu and Zn or the PAH Ind. Subsequently, we refer to these normalized distance as r_{metal}-ETD and r_{Ind}-ETD.

2.3. Model description

The Tool and ELPOS have both been designed to distinguish between chemicals with low and high LRTP [29]. They are steady state fugacity models (level III, no equilibrium, inter-compartment transport [30]) that assess the environmental hazard of organic chemicals using the metrics of CTD and overall persistence (P_{OV}) under different emission scenarios [7]. With only three generic compartments (air, soil and water), The Tool requires five input parameters for each compound: the air-water (K_{AW}) and octanol-water (K_{OW}) partition coefficients as well as degradation half-lives ($t_{1/2}$) in air, water, and soil. A Monte Carlo (MC) analysis routine estimates the 95 % confidence interval of P_{OV} and CTD. In this study we used dispersion factors of 5 and 10 for partition coefficients and half-lives, respectively, comparable to the factors of 3 and 10 used previously [8]. ELPOS (version 2.2) has eight compartments: air, water, sediment, four soil compartments (natural, agricultural, industrial, urban), and plants [5], necessitating seven chemical input parameters: K_{AW}, K_{OW} and the organic carbon partition coefficient (K_{OC}); as well as $t_{1/2}$ in air, water, soil and sediment. Instead of estimating the K_{OC} from K_{OW}, we used the option to supply it directly as well as the K_{OA}-approach to estimate the particle-bound fraction in air.

Besides the CTD, both models also provide the fraction of a compound bound to particles in air as output information. As degradation rates for pollutants bound to particles are generally slow compared to the gas phase [31] and reliable estimates are difficult to obtain, both models assume that compounds associated with particles do not degrade [29].

Some of the default environmental input parameters of both models were adjusted to reflect the characteristics of Southern Ontario (fraction of model region covered by water = 10 %, average water depth = 10 m, yearly average precipitation = 1008 mm, average wind speed = 13.1 km h^{-1} taken from Canadian Climate Normals for North Bay-A, WMO ID: 71731, period 1971-2000 [32]). More detailed information on the model input parameters is provided as Supporting Material (Tables S2 and S3). Three temperature scenarios reflect the annual average (4°C), summer (13 °C), and winter (limited to 0 °C as partition behavior to frozen compartments might differ and is not taken into account by the model calculations) conditions in Southern Ontario [32].

Partition coefficients (K_{OW} and K_{AW}) at 25 °C for the PAHs were taken from Ma et al. [24]. The K_{OC} values at 25 °C were estimated using a poly-parameter linear free energy relationship (pp-LFER) [33] and solute descriptors from Absolv online[34]. While ELPOS has a built-in routine to adjust these coefficients to a user-supplied temperature, The Tool requires the user to supply temperature-adjusted input information. The K_{AW} values were adjusted using the temperature dependent pp-LFERs from Goss et al. [35]; K_{OA} values from Ma et al. [24]were adjusted using enthalpies of vaporization, derived as described in Goss and Schwarzenbach[36]. Finally, temperature-adjusted K_{OW} were obtained as the product of K_{AW} and K_{OA}. We preferred predicted values since consistency

between the properties of different PAHs is more important than accuracy of single properties. Degradation half-lives in air reflecting the reaction of PAHs in the gas phase with hydroxyl radicals were estimated with the Atmospheric Oxidation Program (AOPWIN v1.92) using default settings for a 12h-day[10,11]. However, AOPWIN does not estimate activation energies, which are necessary to calculate degradation rate constants at different temperatures [29]. Temperature dependent rate constants for the reaction with hydroxyl radicals are only available for Phen and Flt [37]. The temperature dependence is so small that in case of The Tool degradation of all PAHs in air can be assumed to not depend on temperature [29]. However, the variability in daytime length and OH radical concentration with season was taken into account. Therefore we used the averaged OH concentrations calculated for the atmospheric boundary layer (1000 and 900 hPa) by Spivakovsky et al. [38]. Average daylight hours were taken from [39].Degradation half-lives in water, soil and sediment were estimated with EPISuite v4.0 [40] and retrieved through the Level III Fugacity Model implemented in this software. In ELPOS degradation rates are temperature adjusted by an implemented routine. By setting the temperature to 25°C and using the manually adjusted values calculated for the Tool the implemented temperature adjustment was bypassed.

Whereas the two models were not designed to estimate CTDs of metals, it is possible to use them to calculate the CTD of exclusively particle-bound substances. As the metals for which we were able to determine ETDs (Cu, Zn) do not partition into the gas phase, they can be considered surrogates for particle-bound organic contaminants. The CTDs for such particle-bound contaminants was estimated by assigning partition coefficients that ensured almost exclusive partitioning to particles (log K_{OW} = 10, log K_{AW} = -9, yielding log K_{OA} of 19). In addition, we assigned a very long environmental half-life ($t_{1/2} = 10^{10}$ h). Additional information on this choice of parameters is available as Supporting Material (Figure S1). All model input parameters are listed in Tables S4 and S5. Table S6 summarizes the temperature-adjusted chemical properties. As for the ETDs, relative CTDs were calculated by normalizing the CTDs of the PAHs to the CTD of Ind (r_{Ind}-CTD) and of exclusively particle-bound compounds ($r_{particle}$-CTD).

The sensitivity of the CTD to changes in input values was tested by a sensitivity analysis as described in Wania and Dugani[41]. A sensitivity of 1 indicates proportional changes of input values and CTDs. A sensitivity < 1 indicates that the CTD does not respond linearly to changes of the input value. We analyzed the sensitivity of temperature (ELPOS only), wind speed, height of the air compartment, aerosol deposition velocity, precipitation rate, rain scavenging ratio, half-life times in all compartments, and partition coefficients for the 4 °C scenario by varying the values by 10 %.

3. Results and Discussion

3.1. Empirically determined travel distances

The maximum deposition of PAHs and the two metals was measured in peat segments dated to the period 1880-1930 (Fig. S2 in Supporting Material, data given in Table S7). The increase in deposition around 1880 coincides with the onset of intense smelting operations in Sudbury. In most peat profiles, we observed declining deposition rates from 1920 onwards, when blast furnaces and roast yards were replaced by multi-hearth roasters and reverberatory furnaces for smelting [42]. More detailed data and interpretation is available in Thuens et al. [22].

The maximum deposition rates of Chry, B[b+k]F, B[a]P and Ind, as well as of Cu and Zn declined exponentially ($p < 0.1$) with distance from Sudbury (Fig.2). Together with the prevailing westerly winds, this finding is a powerful indication that the dominant source of atmospheric contamination to the studied bogs during the time of peak deposition was located in the Greater Sudbury area. For Phen, Flt, Pyr, and B[a]A, this decline was not significant (see Fig. S3 in Supporting Material); for B[ghi]P, B[e]P, and B[j]P no ETD could be calculated, as concentrations were below the level of quantification in several samples. Therefore, these compounds are not considered in the following discussion.

The ETDs of PAHs, Cu, and Zn are shown in Table 1. They range from 173 to 321 km with relative uncertainties between 26 and 46 %. The ETDs of the two metals were shorter than those of the PAHs. The discrepancy between the two metal ETDs reflects the overall uncertainty of our approach. Their average ETD (198 ± 45 km) was used to calculate the r_{metal}-ETD of PAHs.

Table 1: Empirical travel distances with standard error (SE), significance level (p), coefficient of determination (R^2), and relative ETDs (r_{metal}-ETD and r_{Ind}-ETD) with SE.

	ETD (km)	SE (km)	p	R^2	r_{metal}-ETD (-)	SE (-)	r_{Ind}-ETD (-)	SE (-)
Phen	n/a[*]		0.222	0.14	n/a[*]			
Flt	n/a		0.195	0.16	n/a			
Pyr	n/a		0.402	0.07	n/a			
B[a]A	n/a		0.119	0.23	n/a			
Chry	292	119	0.034	0.37	1.47	0.54	0.94	0.56
B[b+k]F	281	74	0.003	0.59	1.42	0.44	0.91	0.46
B[a]P	321	148	0.055	0.32	1.62	0.58	1.04	0.60
Ind	310	119	0.026	0.41	1.57	0.52		
Cu	173	31	0.0002	0.76	-			
Zn	222	56	0.003	0.61	-			

[*]**n/a: value not available as correlation of deposition rate with distance was not significant**

Fig.2: Average maximum deposition rates of (A) PAHs and (B) metals as a function of distance from the Greater Sudbury source area. The error bars represent the standard deviation of the three replicate peat cores.
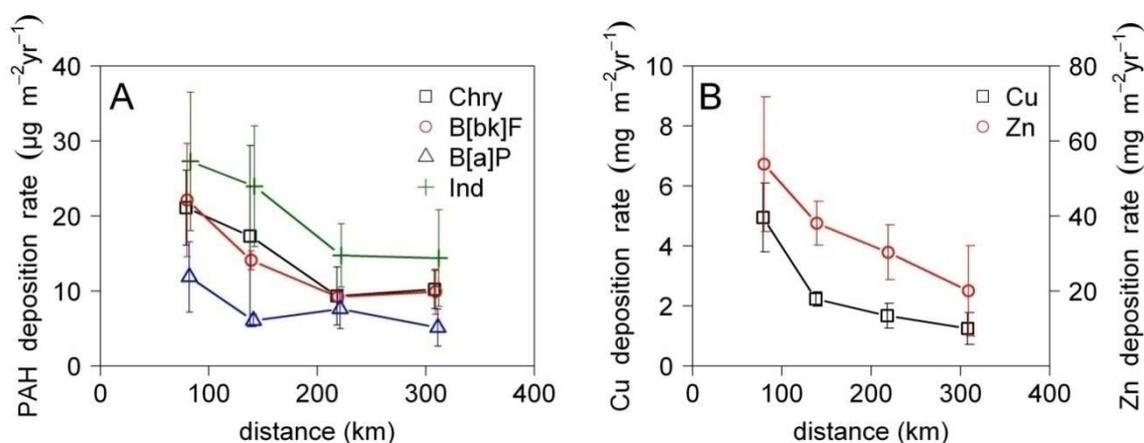
Using data from several studies reporting metal deposition rates at variable distance from smelters [43-45], we calculated ETDs for Cu, Zn, Pb and Ni between 21 and 67 km. Average uncertainty was 17 % (Table S8 in Supporting Material). These ETDs are con-

siderably lower than those we have obtained here. In these previous studies, samples were taken within a distance of up to 125 km from the smelters. It is known that metals such as Ni, Zn, and Cu are associated with both smaller and larger aerosol particles in the atmosphere [46]. As larger particles are deposited more rapidly than smaller ones [47], large particles will dominate the deposition close to the emission source, while fine particles will be deposited at longer distances. This might cause divergent ETDs depending on the spatial scale and resolution of a particular study: the apparent ETD may be short in the immediate vicinity of the smelter, where deposition of coarse particles dominates, and long at larger distances, where mainly fine particles are deposited. This interpretation would explain the longer metal ETDs observed in our study, as the distances of the sites we analyzed are outside the range influenced by larger particles. As coarse particles are not subject to atmospheric long-range transport, we conclude that the metal ETDs determined in this study are more representative of the travel distances of the particles relevant for long-range transport.

3.2.Characteristic Travel Distance

3.2.1 The Tool

With the default settings of The Tool, CTDs up to 2860 km were calculated for particles at 4°C. After adjusting the settings and input parameters to the specific conditions in the study region the estimated CTDs were lower by a factor of 7.5. This reduction is mainly caused by changes in the partition coefficients and changes in size of the individual compartments, while wind speed contributed to a minor extent. The 95 % confidence intervals of the absolute CTDs were larger for g-PAHs than p-PAHs (e.g., factor of 46for B[a]A, 40 for Phen, 9for Chry and 2 to 3 for the p-PAHs) indicating a higher uncertainty of the CTD for B[a]A and the g-PAHs. Details are summarized in Table S9 (Supporting Material). The confidence intervals cover ranges from almost 10 to 5500 km, indicating the high uncertainty of the model results.

Using The Tool, the CTD of particles was longer than the CTDs of the PAHs except for the CTD of Phen and Flt in winter. Consequently, most $r_{particle}$-CTDs are <1 (Fig. 3A). The CTD for Phen in winter was greater than all other CTDs by a factor of 4. The p-PAHs had almost the same CTD as the particles, while those of g- and c-PAHs were substantially shorter. B[a]A had the shortest CTD. As the CTD of Ind was almost the same as the one of particles, r_{Ind}-CTDs were equal to the $r_{particle}$-CTDs.

The CTD of particles was identical for the three temperature scenarios. The CTDs of all PAHs decreased with increasing temperature, which can be attributed to a higher proportion of these compounds being in the gas phase at higher temperatures and the gas phase degradation half-lives in air being shorter because of longer days and higher OH concentrations in summer, when temperatures are higher. Conversely, the high CTD of Phen and Flt for the 0 °C scenario is caused by the long half-lives in air, which are a result of short days and low OH concentrations in winter. The Tool predicted the c-PAHs

to be mainly particle-bound in winter and equally distributed between gas and particle phase in summer (13 °C), whereas the p-PAHs were almost exclusively particle-bound at all temperatures. This is in good agreement with measured gas-particle distributions [14].

The CTDs of all studied compounds were directly proportional to wind speed (sensitivity of 1, Fig. 3B). For the g-PAHs, half-life in air was the only other parameter with high sensitivity. The CTDs of the less volatile PAHs were sensitive to the particle deposition velocity, the precipitation rate, and the height of the air compartment while the sensitivity to the half-life in air was lower (Fig. 3B). This finding reflects the importance of the removal of c- and p-PAHs from the atmosphere by dry or wet deposition.

Fig.3: Characteristic Travel Distance (CTD) of selected PAHs normalized to the CTD of particles estimated with (A) The Tool and (C) ELPOS for the three temperature scenarios and sensitivity of the CTD at 4 °C to different model input parameters estimated with (B) The Tool and (D) ELPOS (note: data not presented here available in Supporting Material, tables S11 and S12; the lines in sub-figures B and D are shown for visual support in identifying the individual parameters). The assignment of PAHs to groups according to their atmospheric partition behavior is indicated in brackets. depovelo = dry particle deposition velocity.
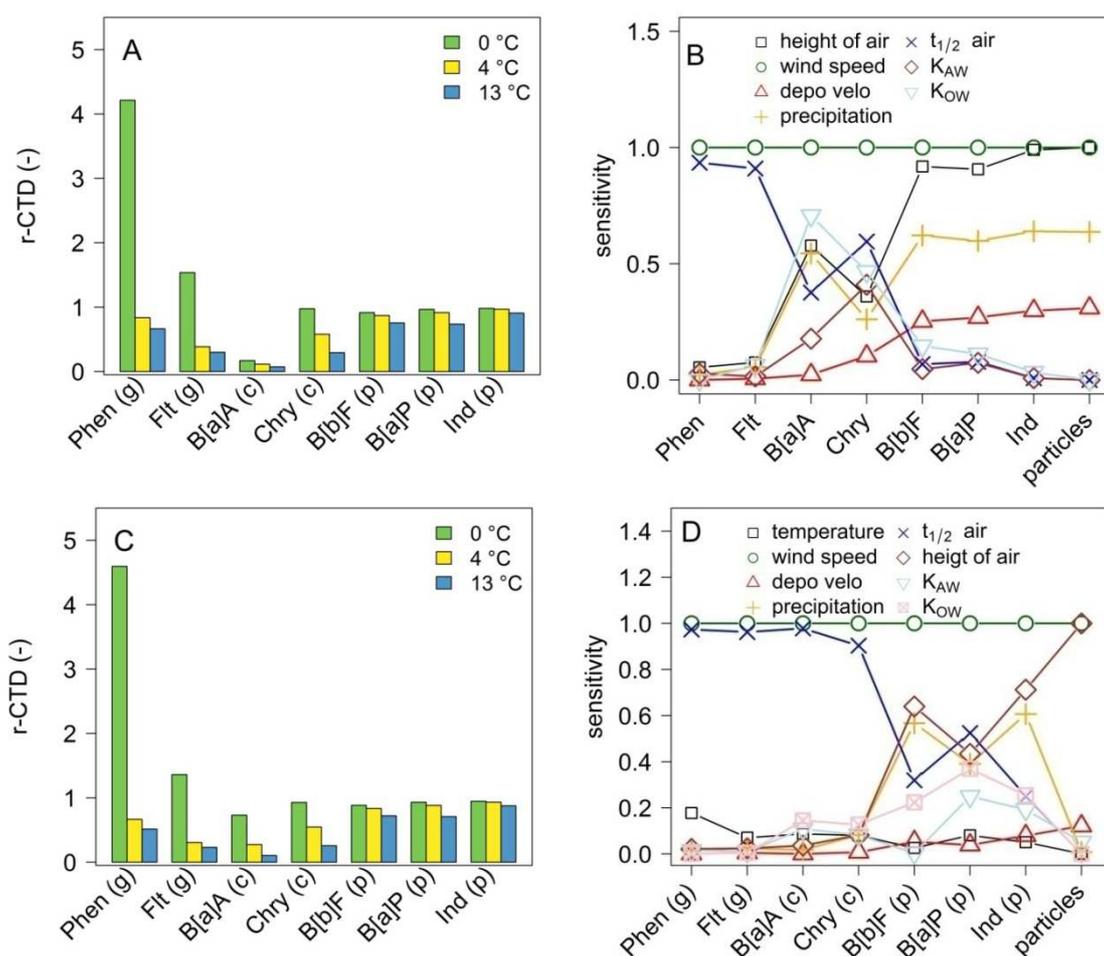
3.2.2 ELPOS

With default settings, CTDs from 295 km (Flt) to 700 km were calculated with ELPOS (particles, 4 °C). With region-specific settings, CTDs between 142 km (B[a]A) and 517 km (particles) were estimated for the annual average temperature of 4 °C (Table S10 in Supporting Material). This reduction was caused by a lower height of the air compartment and a higher precipitation in the study area. The $r_{particle}$-CTDs for all PAHs covered the range from 0.10 to 4.6 under the three temperature scenarios (Fig. 3C). B[a]A

had the shortest $r_{particle}$-CTD due to its high degradation rate in air in summer, Phen had the longest in winter.

The temperature dependence of the chemical properties was substantial, e.g. K_{AW} were up to 90 % lower and half-lives 200 % longer in the winter scenario compared to summer (Table S6). This effect had a high impact on the calculated CTDs. With rising temperature, the CTDs of all PAHs diminished due to increased reactive loss from air. The relation between temperature and CTD was almost linear, with coefficients of determination for the regression of CTD against temperature > 0.98 (Fig. 3). The effect of temperature was largest for B[a]A and B[a]P and the CTD in winter double that in summer.

The particle-bound fraction of B[a]P and Ind estimated by ELPOS was less than 100 % (given in Table S10 in Supporting Material) for all temperature scenarios and decreased with increasing temperature. This contrasted with measurements in Southern Ontario [14] where these PAH could not be detected in the gas phase. The overestimation of the gaseous fraction by ELPOS might cause an overestimation of B[a]P and Ind removal by degradation.

The estimated CTD of all compounds was directly proportional to wind speed (Fig. 3D). The half-life of the volatile compounds in air was another highly sensitive parameter, whereas the particle-bound substances were more sensitive to precipitation and the height of the air compartment. The dry particle deposition velocity only substantially influenced the p-PAHs and particles. The sensitivity of the CTD against changes in temperature was ≤ 0.21 and similar regarding all compounds other than B[b]F and particles.

3.2.3 Model comparison

When the same degradation half-lives and temperature-adjusted partition coefficients were used in both models, i.e., the internal temperature correction of ELPOS was not used, the CTDs calculated by both models agreed reasonably well (Fig. 4A) and were significantly correlated ($R^2 = 0.92$, $p < 0.00015$).

However, most ELPOS-CTDs were above the 1:1-line, i.e., ELPOS systematically estimated longer CTDs than The Tool. CTDs normalized to that of the particles agreed very well between both models, with all compounds falling close to the 1:1-line (Fig. 4B). Clearly, normalization eliminates systematic difference between the models. The agreement for p- and c-PAHs was even better after normalizing the CTDs to that of Ind (Fig. 4C).

Fig.4: Comparison of characteristic transport distances predicted by The Tool and ELPOS for the average temperature scenario (4 °C). Results from ELPOS were obtained both with the built-in temperature correction of partition coefficients and reaction rates (ELPOS auto T-adj) and with the parameters that were temperature-adjusted manually as in The Tool (ELPOS man. T-adj). A: Absolute CTDs; B: CTDs relative to the particle-CTD; C: CTDs relative to Ind. The 1:1-line is shown as dotted line.
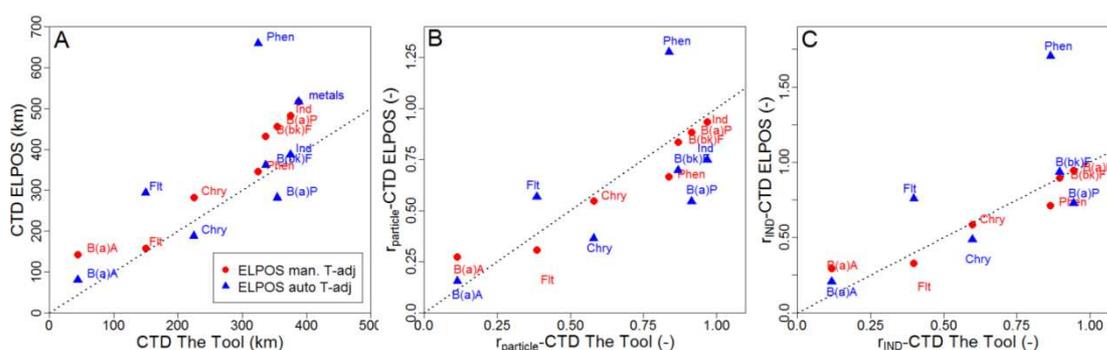
When the in-built temperature-adjustment of ELPOS was used, the agreement between the models diminished. On the one hand, a substantial increase of CTDs calculated using ELPOS was observed for Phen and Flt (Fig. 4A) with the temperature adjustment. This finding was not surprising as the temperature-adjustment of the atmospheric half-lives in ELPOS substantially increased the half-lives with decreasing temperatures (for 0 °C the increase was 200 %, see table S6), while the half-lives were not adjusted in The Tool. Moreover, the sensitivity of the two gas-phase PAHs Phen and Flt against changes in half-lives was high in both models (Fig. 3B and D). For this reason these two PAHs should indeed be most affected by the discrepancy of the degradation rates in the gas phase. ELPOS applies a default activation energy of 30 kJ mol^{-1} for the temperature adjustment of the atmospheric degradation rate for all compounds. Using 10 kJmol^{-1} instead, the increase of $t_{1/2}$ of Phen in air at lower temperatures was reduced by 46 %. The experimentally determined activation energy of Phen and Flt is less than 10 kJmol^{-1} [37]. Therefore, the temperature adjustment in ELPOS might underestimate atmospheric degradation of PAHs at low temperature. On the other hand, the CTDs of the less volatile PAHs generally decreased when the implemented temperature adjustment was used. This is because the default temperature dependence of the partitioning coefficients implemented in ELPOS was larger than the dependence obtained manually, i.e. the PAHs partitioned more into the particulate phase in ELPOS than this was the case for the adjusted input values we used in The Tool.

When comparing the r$_{particle}$-CTDs, the pattern was basically the same (Fig. 4B). With the built-in adjustment, however, the r$_{particle}$-CTDs of the less volatile PAHs calculated by ELPOS were now consistently smaller than those with the manual temperature adjustment. Overall, the major discrepancies between the two models can be seen for the more

volatile compounds, while the $r_{particle}$-CTDs for the less volatile PAHs were comparatively consistent. This finding is important for the comparison with measured ETDs, as these are only available for the less volatile compounds and thus for compounds with a lower overall deviation between the two models.

The sensitivity of both models against changes in the individual input parameters was similar for the g-PAHs, and only wind speed and $t_{1/2}$ in air had a strong influence. However, while this half-life still strongly influenced the CTD of the c-PAHs in ELPOS, i.e. sensitivity was close to 1, the influence was substantially lower in The Tool (Fig. 3B and D). This result can be attributed to a substantially lower fraction of B[a]A and Chry in the atmospheric gas phase in The Tool (20%) than in ELPOS (84%) (see Supporting Material for details). As Su et al. [14] found them to be 80 % in the gas phase in summer and 40 % in winter, The Tool obviously under-predicts the gaseous fraction. The sensitivity of these compounds against K_{AW} in The Tool was higher than that of the other PAHs and than found in ELPOS. This observation is most likely due to its sensitivity to $K_{OA,}$ which was governing the gas/particle partitioning. Sensitivity to K_{OA}, which was calculated from the $K_{AW,}$ thus indicates which compounds primarily partition from gas to particle phase and are crucially affected by the partitioning coefficient. In the Tool the c-PAHs, whereas in ELPOS the p-PAHs were affected. For the predominantly particle-bound PAHs, processes determining the fate of atmospheric particles, such as precipitation and dry particle deposition velocity, became more influential in both models, although the dry deposition velocity was more influential in The Tool.

3.2.4 Comparison of CTDs and ETDs

The absolute ETDs of PAHs derived from the peat transect were between 281 and 321 km, whereas the absolute CTDs with regional settings were between 44 and 480 km (average temperature scenario, 4 °C). The latter are comparable to the CTD calculated for aldrin (~200 km (The Tool) and 95 km (ELPOS), using the input values implemented in both models), a pesticide banned by the Stockholm Convention on Persistent Organic Pollutants [48], and which has – compared to most banned substances –a relatively low LRTP [49].

The direct comparison between measured ETDs and calculated CTDs was impeded by the fact that the Greater Sudbury area is a point source on the regional scale. Even without any degradation and deposition, the PAH concentrations would thus decline with distance from the source because of radial dilution. Such a dilution is not implemented into either model, and instead a line source and wind that is blowing in a constant direction are assumed. However, by normalizing the measured and calculated transport distances to a common reference, i.e. non-reactive particles, the comparison between measurements and model becomes feasible as the effects of radial dilution, wind speed, and a changing wind direction are eliminated. Moreover, when using a particle-bound substance as a reference, differences in parameters that affect the deposition of atmospheric particles between the real environment and the model settings are eliminated as well, and

the relative comparison of a given set of compounds in terms of atmospheric transport distance is possible.

Fig.5: Comparison of relative ETDs and CTDs of PAHs at 4° C (left: relative to metals (ETD) and particles (CTD); right: relative to Ind).
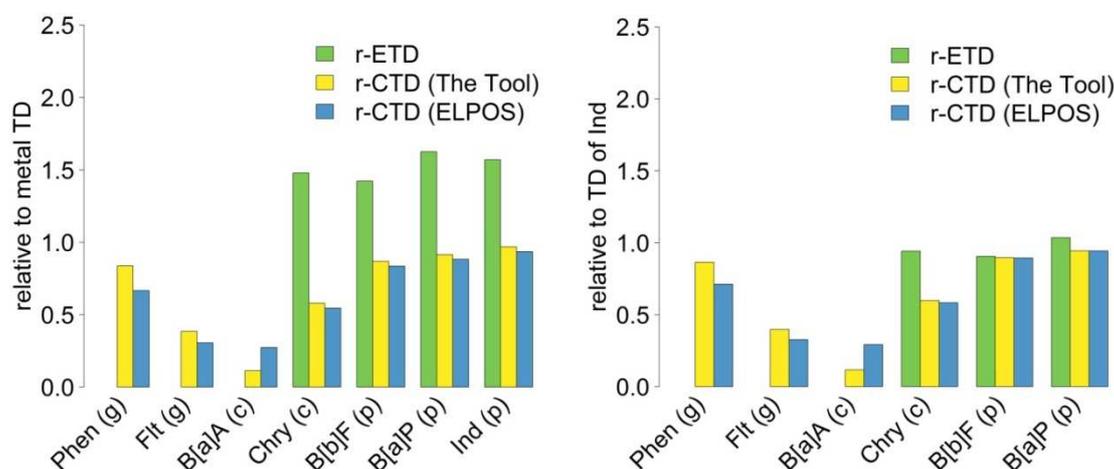
As both models are intended to calculate the transport potential and to compare compounds relative to each other, rather than to reproduce real transport distances in the environment, it is more meaningful to compare relative CTDs with relative ETDs instead of absolute values. This comparison is illustrated in Fig. 5. When normalized to particles, the $r_{particle}$-CTDs of both models agreed very well, and the $r_{particle}$-CTDs of the three p-PAHs were close to 1, whereas the $r_{particle}$-CTD of Chry was substantially lower. However, the measured r_{metal}-ETD for all four compounds was much higher and around 1.5 for all compounds. Thus, the agreement between measured and modeled relative transport distances was not very good. This outcome might be attributed to a different atmospheric behavior of the particles that metals and PAHs are associated with, or to some inaccuracy of the estimated particle-CTDs. Although it is very likely that PAHs and metals in historic samples shared the same dominant source in the Greater Sudbury area, they might be associated with different aerosol size classes. The particles contained differ in their atmospheric transport behavior and metals associated with somewhat larger particles than PAHs may consequently be removed from the atmosphere faster. Alternatively, PAHs might not be as reactive as the models assume. The importance of these factors for the discrepancy between r_{metal}-ETDs and $r_{particle}$-CTDs of PAHs cannot be decided based on the currently available knowledge.

To further reduce uncertainty, the CTD of PAHs can be normalized to the travel distance of Ind (or any other of the p-PAHs) instead of metals (Fig. 4C and 5B), thereby referencing the transport distance to a compound with identical emission behavior and that is association with particle of similar size. This procedure yielded a very good agreement between measurement and model for B[b]F and B[a]P, while the estimated

r_{Ind}-CTDs for Chrysene (ELPOS: 0.38; The Tool: 0.42) were much lower than the actually measured r_{Ind}-ETD (0.94).

The finding that the measured r-ETD of Chry was almost identical to the r-ETDs of the other three PAHs was unexpected, as Chry is substantially more volatile (see Supporting Material, Table S4 for partition coefficients). Both Chry and Ind have similar atmospheric half-lives but Chry is the compound with the higher volatility and it should thus be removed faster if the assumption is correct that particle-bound PAHs are degraded much slower than gas phase PAHs [29]. The discrepancy between r-ETD and r-CTD can have two reasons: i) The volatility of Chry might be overestimated in the models which assume an ideal partitioning behavior of PAHs. For 0 °C ELPOS assumed 24 % of Chry to be bound to particles, while Su et al. [14] found about 60 % of Chry bound to particles in winter. Harner and Bidleman[50] supposed that PAHs might be bound within particles during their formation in combustion processes and thus might be non-exchangeable with the atmosphere. Moreover, PAHs initially present on the surface of particles may become less accessible for reactions, partitioning and volatilization due to a coating of the particles by secondary aerosol components [17,31]. ii) The actual atmospheric half-life of Chry might be much longer than that used for estimating its CTD. However, in order to reach a r_{Ind}-CTD equal to the r_{Ind}-ETD, in ELPOS a nearly 10-fold increase in $t_{1/2}$ would be necessary, while it is even impossible to reach such a CTD in The Tool by increasing the atmospheric half-life.

Two previous studies aimed at comparing measured and calculated transport distances of organic pollutants. Shen et al. [10] found a good agreement between ETDs of pesticides with high LRTP determined from latitudinal gradients of air concentrations and CTDs calculated by ELPOS and two other models. In contrast, ETDs for pesticides derived from water concentrations in North American lakes were tenfold higher than the CTDs calculated by four models. This difference could be reduced by lowering the hydroxyl radical concentration and introducing dry weather conditions [11]. Unfortunately both studies did not measure metals or other predominantly particle-bound reference substances to allow for the calculation of relative travel distances.

4. Conclusions

In this study the comparison between modeled and measured transport distances was limited to only a few compounds, as the peat profiles did not reveal statistically significant ETDs for more PAH congeners. Keeping this in mind, several general conclusions can be drawn:

- The absolute CTDs of PAHs estimated with the two models agreed reasonably well for predominantly particle-bound congeners, while discrepancies were observed for the more volatile congeners (Fig. 4). This could be attributed to the temperature-adjustment of input parameters (in particular, K_{AW} and half-life in air) in ELPOS, which relies on generic assumptions, most importantly with re-

spect to the temperature dependence of the atmospheric degradation half-life. Since the CTDs of rather volatile compounds in both models are highly sensitive to the half-life in air (Fig. 3), the quality of the predictions would improve with better data on the temperature dependence of the atmospheric degradation half-lives of PAHs and the implementation of this dependence in both models.

- Peat archives sampled from bogs at variable distance from a single dominant point source can be used to experimentally determine travel distances of pollutants.

- Particles deposit onto peat and, therefore, peat archives can provide information about the relative transport distances of particle-bound compounds. Most other passive samplers collect only compounds in the gas phase.

- Data from peat archives are suitable to experimentally evaluate predicted CTDs of PAHs if data are normalized to a reference compound with similar behavior, even if the source characteristics (point vs. linear source) differ between model and reality. However, in the present study, the results from the peat archive limited the number of compounds available for such an evaluation. This conclusion might also apply to other non-polar atmospheric contaminants measured in peat archives.

- The underestimation of the $r_{particle}$-CTD of Chry might be due to a "non-ideal" partitioning behavior, i.e. Chry associated to aerosol particles might not freely partition to the gas phase. More information on such processes is needed to verify this hypothesis experimentally. Such a process could also apply to other contaminants that are already particle-bound during their emission. Compounds predominantly emitted as gaseous compounds would be less affected.

Acknowledgments

Conflicts of Interest

The authors declare no conflict of interest

Supplementary Information

A file with Supplementary Information is available on the journal website.

References

1. van Pul, W.A.J.; de Leeuw, F.A.A.M.; van Jaarsveld, J.A.; van der Gaag, M.A.; Sliggers, C.J., The potential for long-range transboundary atmospheric transport. *Chemosphere* **1998**, *37*, 113-141.

2. Scheringer, M., Persistence and spatial range as endpoints of an exposure-based assessment of organic chemicals. *Environ. Sci. Technol.* **1996**, *30*, 1652-1659.

3. Rodan, B.D.; Pennington, D.W.; Eckley, N.; Boethling, R.S., Screening for persistent organic pollutants: Techniques to provide a scientific basis for pops criteria in international negotiations. *Environ. Sci. Technol.* **1999**, *33*, 3482-3488.

4. Bennett, D.H.; McKone, T.E.; Matthies, M.; Kastenberg, W.E., General formulation of characteristic travel distance for semivolatile organic chemicals in a multimedia environment. *Environ. Sci. Technol.* **1998**, *32*, 4023-4030.

5. Beyer, A.; Matthies, M., Criteria for atmospheric long-range transport potential and persistence of pesticides and industrial chemicals. *German Federal Environmental Agency, Berlin, Germany.* **2001**, Technical Report FKZ 299 265 402.

6. Scheringer, M.; MacLeod, M.; Wegmann, F., The OECD P_{OV} and LRTP screening tool, version 2.0. *http://www.sust-chem.ethz.ch/docs/Tool2_0_Manual.pdf* **2006**.

7. Wegmann, F.; Cavin, L.; MacLeod, M.; Scheringer, M.; Hungerbuehler, K., The OECD software tool for screening chemicals for persistence and long-range transport potential. *Environ. Modell. Softw.* **2009**, *24*, 228-237.

8. Klasmeier, J.; Matthies, M.; Macleod, M.; Fenner, K.; Scheringer, M.; Stroebe, M.; Le Gall, A.C.; McKone, T.; Van De Meent, D.; Wania, F., Application of multimedia models for screening assessment of long-range transport potential and overall persistence. *Environ. Sci. Technol.* **2005**, *40*, 53-60.

9. Fenner, K.; Scheringer, M.; Hungerbuhler, K., Prediction of overall persistence and long-range transport potential with multimedia fate models: Robustness and sensitivity of results. *Environ. Pollut.* **2004**, *128*, 189-204.

10. Shen, L.; Wania, F.; Lei, Y.D.; Teixeira, C.; Muir, D.C.G.; Bidleman, T.F., Atmospheric distribution and long-range transport behavior of organochlorine pesticides in North America. *Environ. Sci. Technol.* **2004**, *39*, 409-420.

11. Muir, D.C.G.; Teixeira, C.; Wania, F., Empirical and modeling evidence of regional atmospheric transport of current-use pesticides. *Environ. Toxicol. Chem.* **2004**, *23*, 2421-2432.

12. Björseth, A.; Lunde, G.; Lindskog, A., Long-range transport of polycyclic aromatic hydrocarbons. *Atmospheric Environment (1967)* **1979**, *13*, 45-53.

13. Yamasaki, H.; Kuwata, K.; Miyamoto, H., Effects of ambient temperature on aspects of airborne polycyclic aromatic hydrocarbons. *Environ. Sci. Technol.* **1982**, *16*, 189-194.

14. Su, Y.; Lei, Y.D.; Wania, F.; Shoeib, M.; Harner, T., Regressing gas/particle partitioning data for polycyclic aromatic hydrocarbons. *Environmental Science & Technology* **2006**, *40*, 3558-3564.

15. Steinnes, E.; Allen, R.O.; Petersen, H.M.; Rambæk, J.P.; Varskog, P., Evidence of large scale heavy-metal contamination of natural surface soils in Norway from long-range atmospheric transport. *Sci. Total Environ.* **1997**, *205*, 255-266.

16. Chan, W.H.; Vet, R.J.; Ro, C.-U.; Tang, A.J.S.; Lusis, M.A., Impact of INCO smelter emissions on wet and dry deposition in the Sudbury area. *Atmospheric Environment (1967)* **1984**, *18*, 1001-1008.

17. Ravindra, K.; Sokhi, R.; Van Grieken, R., Atmospheric polycyclic aromatic hydrocarbons: Source attribution, emission factors and regulation. *Atmospheric Environment* **2008**, *42*, 2895-2921.

18. Venkataraman, C.; Friedlander, S.K., Size distributions of polycyclic aromatic hydrocarbons and elemental carbon. 2. Ambient measurements and effects of atmospheric processes. *Environ. Sci. Technol.* **1994**, *28*, 563-572.

19. Biester, H.; Bindler, R.; Martinez-Cortizas, A.; Engstrom, D.R., Modeling the past atmospheric deposition of mercury using natural archives. *Environ. Sci. Technol.* **2007**, *41*, 4851-4860.

20. Dreyer, A.; Radke, M.; Turunen, J.; Blodau, C., Long-term change of polycyclic aromatic hydrocarbon deposition to peatlands of eastern Canada. *Environ. Sci. Technol.* **2005**, *39*, 3918-3924.

21. Shotyk, W., Peat bog archives of atmospheric metal deposition: Geochemical evaluation of peat profiles, natural variations in metal concentrations, and metal enrichment factors. *Environ. Rev.* **1996**, *4*, 149-183.

22. Thuens, S.; Blodau, C.; Radke, M., How suitable are peat cores to study historical deposition of PAHs? The Science of the Total Environment: 2013; Vol. **accepted/in press**.

23. Sehmel, G.A., Particle and gas dry deposition: A review. *Atmospheric Environment (1967)* **1980**, *14*, 983-1011.

24. Ma, Y.-G.; Lei, Y.D.; Xiao, H.; Wania, F.; Wang, W.-H., Critical review and recommended values for the physical-chemical property data of 15 polycyclic aromatic hydrocarbons at 25 °c. *Journal of Chemical & Engineering Data* **2009**, *55*, 819-825.

25. Bauer, M.; Fulda, B.; Blodau, C., Groundwater derived arsenic in high carbonate wetland soils: Sources, sinks, and mobility. *Sci. Total Environ.* **2008**, *401*, 109-120.

26. Appleby, P.G.; Oldfield, F., The calculation of lead-210 dates assuming a constant rate of supply of unsupported ^{210}Pb to the sediment. *CATENA* **1978**, *5*, 1-8.

27. Turetsky, M.R.; Manning, S.W.; Wieder, R.K., Dating recent peat deposits. *Wetlands* **2004**, *24*, 324-356.

28. Institute for Statistics and Mathematics of the WU Wien, R version 2.13.1. *http://www.r-project.org/***2011**.

29. Beyer, A.; Wania, F.; Gouin, T.; Mackay, D.; Matthies, M., Temperature dependence of the characteristic travel distance. *Environmental Science & Technology* **2003**, *37*, 766-771.

30. Mackay, D., Multimedia environmental models - the fugacity approach. *Lewis Publishers* **2001**, *Second Edition*.

31. Zhou, S.; Lee, A.K.Y.; McWhinney, R.D.; Abbatt, J.P.D., Burial effects of organic coatings on the heterogeneous reactivity of particle-borne benzo[a]pyrene (BaP) toward ozone. *The Journal of Physical Chemistry A* **2012**, *116*, 7050-7056.

32. Environment Canada, Canadian climate normals for North Bay -A, WMO ID: 71731, period 1971-2000. *www.climate.weatheroffice.gc.ca***2011**.

33. Bronner, G.; Goss, K.-U., Predicting sorption of pesticides and other multifunctional organic chemicals to soil organic carbon. *Environ. Sci. Technol.* **2010**, *45*, 1313-1319.

34. Absolv Online http://www.acdlabs.com/products/percepta/predictors/absolv/

35. Goss, K.U., Prediction of the temperature dependency of Henry's law constant using poly-parameter linear free energy relationships. *Chemosphere* **2006**, *64*, 1369-1374.

36. Goss, K.-U.; Schwarzenbach, R.P., Empirical prediction of heats of vaporization and heats of adsorption of organic compounds. *Environ. Sci. Technol.* **1999**, *33*, 3390-3393.

37. Brubaker, W.W.; Hites, R.A., OH reaction kinetics of polycyclic aromatic hydrocarbons and polychlorinated dibenzo-p-dioxins and dibenzofurans. *Journal of Physical Chemistry A* **1998**, *102*, 915-921.

38. Spivakovsky, C.M.; Logan, J.A.; Montzka, S.A.; Balkanski, Y.J.; Foreman-Fowler, M.; Jones, D.B.A.; Horowitz, L.W.; Fusco, A.C.; Brenninkmeijer, C.A.M.; Prather, M.J.*, et al.*, Three-dimensional climatological distribution of tropospheric OH: Update and evaluation. *Journal of Geophysical Research: Atmospheres* **2000**, *105*, 8931-8980.

39. USNO http://aa.usno.navy.mil/data/docs/Dur_OneYear.php (2014-03-27),

40. EPA Estimation program interface (EPI) suite. http://www.epa.gov/opptintr/exposure/pubs/episuite.htm

41. Wania, F.; Dugani, C.B., Assessing the long-range transport potential of polybrominated diphenyl ethers: A comparison of four multimedia models. *Environ. Toxicol. Chem.* **2003**, *22*, 1252-1261.

42. SARA, Volume I - chapter 3 : Historical review of air emissions from the smelting operations. *http://www.sudburysoilsstudy.com/EN/media/volume_I.asp* **2008**.

43. Freedman, B.; Hutchinson, T.C., Pollutant inputs from the atmosphere and accumulations in soils and vegetation near a nickel-copper smelter at Sudbury, Ontario, Canada. *Canadian Journal of Botany-Revue Canadienne De Botanique* **1980**, *58*, 108-132.

44.   Nieboer, E.; Ahmed, H.M.; Puckett, K.J.; Richardson, D.H.S., Heavy metal content of lichens in relation to distance from a nickel smelter in Sudbury, Ontario. *The Lichenologist* **1972**, *5*, 292-304.

45.   Kettles, I.M.; Bonham-Carter, G.F., Modelling dispersal of metals from a copper smelter at Rouyn-Noranda (Quebec, Canada) using peatland data. *Geochemistry: Exploration, Environment, Analysis* **2002**, *2*, 99-110.

46.   Allen, A.G.; Nemitz, E.; Shi, J.P.; Harrison, R.M.; Greenwood, J.C., Size distributions of trace metals in atmospheric aerosols in the United Kingdom. *Atmospheric Environment* **2001**, *35*, 4581-4591.

47.   Caffrey, P.F.; Ondov, J.M.; Zufall, M.J.; Davidson, C.I., Determination of size-dependent dry particle deposition velocities with multiple intrinsic elemental tracers. *Environ. Sci. Technol.* **1998**, *32*, 1615-1622.

48.   UNEP, Final act of the conference of plenipotentaries on the Stockholm Convention on persistent organic pollutants. *United Nations Environment Program: Stockholm, Sweden* **2001**.

49.   Beyer, A.; Mackay, D.; Matthies, M.; Wania, F.; Webster, E., Assessing long-range transport potential of persistent organic pollutants. *Environ. Sci. Technol.* **2000**, *34*, 699-703.

50.   Harner, T.; Bidleman, T.F., Octanol-air partition coefficient for describing particle/gas partitioning of aromatic compounds in urban air. *Environ. Sci. Technol.* **1998**, *32*, 1494-1502.

Supporting Material

Comparison of atmospheric travel distances of several PAHs calculated by two fate and transport models (The Tool and ELPOS) with experimental values derived from a peat bog transect

Sabine Thuens[1], Christian Blodau[1, 2], Frank Wania[3] and Michael Radke[1, 4, *]

[1] Department of Hydrology, BayCEER, University of Bayreuth, Bayreuth, Germany

[2] Institute of Landscape Ecology, University of Münster, Münster, Germany

[3] Department of Physical and Environmental Sciences, University of Toronto Scarborough, Toronto, Canada

[4] Department of Applied Environmental Science (ITM), Stockholm University, Sweden

[*] Correspondence: michael.radke@itm.su.se

Table S2: Coordinates of Greater Sudbury and sampling locations

site name	latitude	longitude	distance from Superstack (km)
Sudbury (Superstack)	N 46.48011	W 81.056506	-
Giant Bog †	N 46.42422	W 79.937056	81
Eagle Lake Bog	N 45.80572	W 79.444830	140
Spruce Bog	N 45.59050	W 78.373055	220
Green Lake Bog	N 45.68517	W 77.151194	310

† while the names of the other sampling sites have previously been reported, the name Giant Bog was assigned to this site as no previous description and thus no established name was available

Table S3: Original and adjusted settings in The Tool

	temperature (K)	area of water (%)	depth of water (m)	wind speed (km h^{-1})	height of air (m)	precipitation rate (mm a^{-1})
original	298.15	71	100	14.4	6000	850
adjusted	276.95	10	10	13.1	1000	1008

Table S4: Original and adjusted settings in ELPOS

	length of study region (m)	wind speed (km h⁻¹)	precipitation rate (mm a⁻¹)	area of water (%)	depth of water (m)	area of industry (%)
original	200 000	14.4	760	3	3	10
adjusted	450 000	13.1	1008	10	10	3

Table S5: Input values for The Tool at 4 °C, partition coefficients taken from Ma et al. (2009) and temperature adjusted as described in the manuscript, half-life times taken from AOPWIN[1]; partition coefficients and degradation rates for particlesare hypothetical values.

	molar mass (g/mol)	log K_{AW}			log K_{OW}			half-life air (h)	half-life water (h)	half-life soil (h)
		0 °C	**4 °C**	**13 °C**	**0 °C**	**4 °C**	**13 °C**			
Phen	178.23	-4.27	-4.14	-3.86	4.68	4.58	4.39	14.44	1440	2880
Flt	202.26	-4.95	-4.82	-4.53	5.31	5.19	4.95	6.42	1440	2880
B[a]A	228.30	-7.06	-6.89	-6.53	4.86	4.74	4.50	1.49	1440	2880
Chry	228.29	-5.38	-5.24	-4.91	6.61	6.46	6.17	3.76	1440	2880
B[b]F	252.31	-6.27	-6.11	-5.76	6.58	6.47	6.25	10.12	1440	2880
B[a]P	252.31	-6.27	-6.11	-5.76	7.03	6.87	6.55	3.76	1440	2880
Ind	276.33	-7.15	-6.99	-6.62	7.33	7.14	6.76	2.91	1440	2880
particles	63.55	-9.00	-9.00	-9.00	10.00	10.00	10.00	10×10^9	10×10^9	10×10^9

Table S6: Input values for ELPOS.Partition coefficients (25 °C) taken from Ma et al. (2009).Half-life timesestimated with AOPWIN, and melting point taken from EPISuite[1]. The partition coefficients and degradation rates for particlesare hypothetical values.

	mol. mass(g/mol)	melt. point (°C)	log K_{AW}	log K_{ow}	log K_{OC}	half-life (h) air	half-life (h) water	half-life (h) soil	half-life (h) sediment
Phen	178.23	372	-2.76	4.47	3.65	14.44	1440	2880	13000
Flt	202.26	382.00	-3.27	4.97	4.52	6.42	1440	2880	13000
B[a]A	228.30	431.80	-3.59	5.83	4.61	1.49	1440	2880	13000
Chry	228.29	530.00	-3.82	5.67	5.06	3.76	1440	2880	13000
B[b]F	252.31	441.20	-4.58	5.86	5.73	10.12	1440	2880	13000
B[a]P	252.31	452.00	-4.51	6.05	5.73	3.76	1440	2880	13000
Ind	276.33	436.00	-4.70	6.57	6.40	2.91	1440	2880	13000
particles	63.55	1084.62	-9.00	10.00	-0.5	10×10^9	10×10^9	10×10^9	10×10^9

Table S7: Input values for ELPOS calculated by the implemented temperature adjustment; not presented as not changed are log K_{OW} and K_{OC}

|	log K_{AW}			half-life (h) air			half-life (h) water			half-life (h) sediment			half-life (h) soil		
	0 °C	4 °C	13 °C	0 °C	4 °C	13 °C	0 °C	4 °C	13 °C	0 °C	4 °C	13 °C	0 °C	4 °C	13 °C
Phen	-3.72	-3.56	-3.20	1.82	1.50	1.00	4359.06	3602.44	2392.04	39352.67	32522.02	21594.76	8718.13	7204.88	4784.07
Flt	-4.23	-4.07	-3.71	0.81	0.67	0.44	4359.06	3602.44	2392.04	39352.67	32522.02	21594.76	8718.13	7204.88	4784.07
B[a]A	-4.55	-4.39	-4.03	0.19	1.06	0.10	4359.06	3602.44	2392.04	39352.67	32522.02	21594.76	8718.13	7204.88	4784.07
Chry	-4.78	-4.62	-4.26	0.47	0.39	0.26	4359.06	3602.44	2392.04	39352.67	32522.02	21594.76	8718.13	7204.88	4784.07
B[b]F	-5.54	-5.38	-5.02	1.28	1.06	0.70	4359.06	3602.44	2392.04	39352.67	32522.02	21594.76	8718.13	7204.88	4784.07
B[a]P	-5.47	-5.31	-4.95	0.47	0.39	0.26	4359.06	3602.44	2392.04	39352.67	32522.02	21594.76	8718.13	7204.88	4784.07
Ind	-5.66	-5.50	-5.14	0.37	0.30	0.20	4359.06	3602.44	2392.04	39352.67	32522.02	21594.76	8718.13	7204.88	4784.07
particles	-9.96	-9.80	-9.44	3×10^{10}	2.5×10^{10}	1.6×10^{10}	3×10^{10}	2.5×10^{10}	1.6×10^{10}	3×10^{10}	2.5×10^{10}	1.6×10^{10}	3×10^{10}	2.5×10^{10}	1.6×10^{10}

A

B
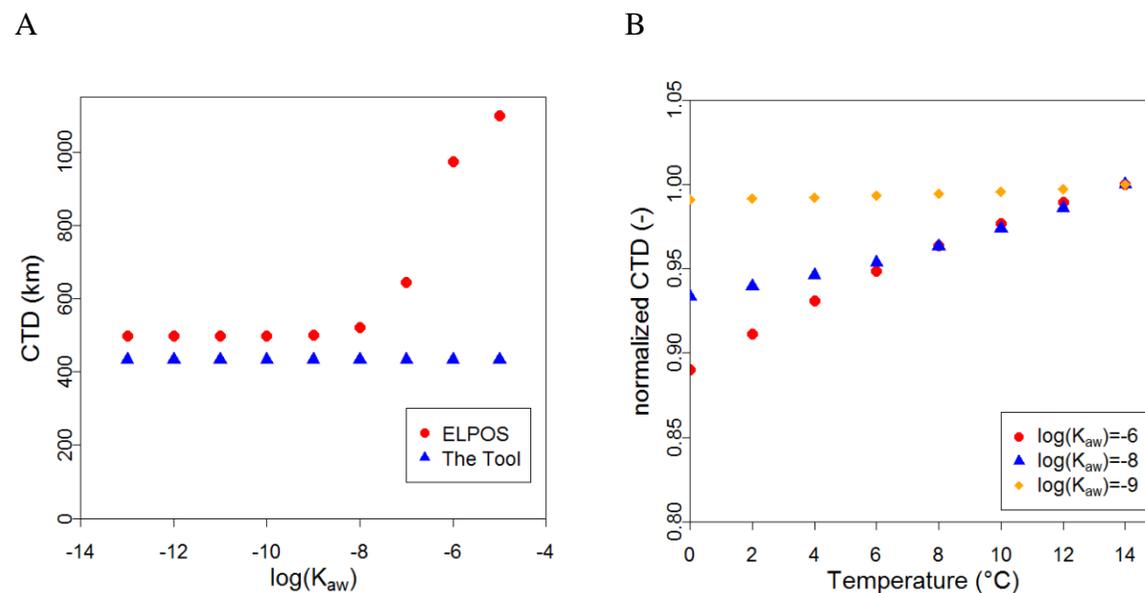
Fig. S6: (A) Particle-CTD calculated by both models as a function of the air-water partition coefficient (K_{aw}), and **(B)** Particle-CTD (normalized to the CTD at 14 °C) calculated with ELPOS as a function of temperature for three air-water partition coefficients. The CTD of a completely particle bound substance should not depend on the air-water partition coefficient and also not on the temperature (as in both models, wet and dry deposition are not implemented as temperature-dependent processes). For The Tool, no dependence of CTD on K_{aw} was observed, whereas the CTD calculated by ELPOS was increasing with temperature for $\log(K_{aw})>-9$. Therefore, we chose a K_{aw} of -9 to simulate the particle behavior. Moreover, the temperature dependence of CTD in ELPOS was negligible for this $\log(K_{aw})$, whereas a clear dependence on temperature (caused by apparent partitioning into the gas phase) was observed for $\log(K_{aw})>-9$. Therefore, we chose $\log(K_{aw})=-9$ for simulating the metal CTD in ELPOS.
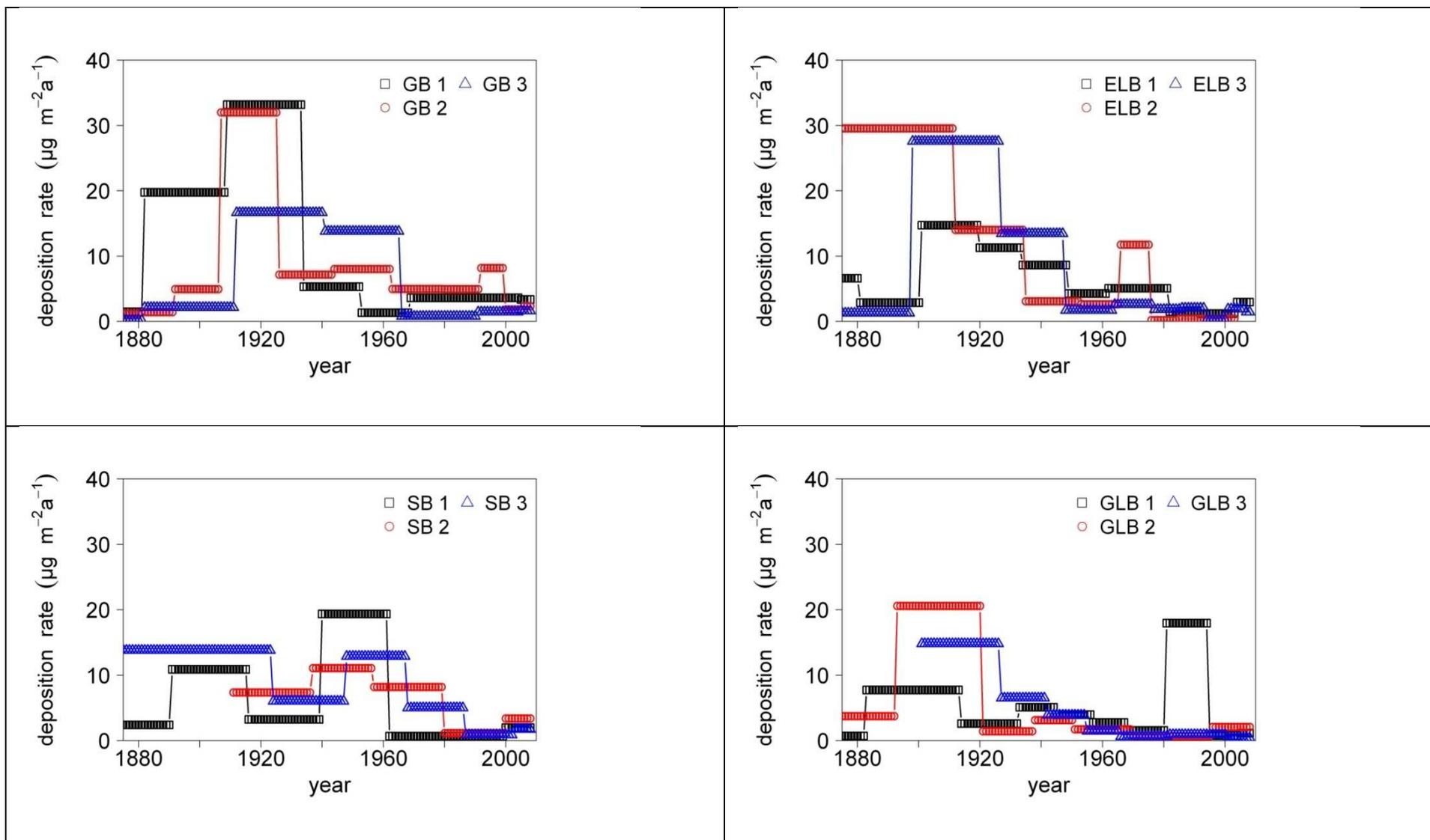
Fig. S7: Time trends of reconstructed deposition rates of Ind in the sampled bogs (Giant Bog (GB). Eagle Lake Bog (ELB). Spruce Bog (SB) and Green Lake Bog (GLB). The three data series per bog represent the three replicate cores per site.

Table S8: Maximum deposition rates of PAHs (µg m^{-2}a^{-1}) and metals (mg m^{-2}a^{-1}) in each of the sampled peat cores and calculated ETD (km).

	Chry	B[b+k]F	B[a]P	Ind	Cu	Zn
GB 1	15	30	15	33	6	55
GB 2	24	15	14	32	5	35
GB 3	24	22	6	17	4	71
ELB 1	31	13	7	15	2	42
ELB 2	10	14	5	30	2	40
ELB 3	10	15	6	28	2	31
SB 1	7	9	10	19	2	23
SB 2	14	10	7	11	2	37
SB 3	7	9	5	14	1	31
GLB 1	7	6	2	8	2	34
GLB 2	12	12	7	21	1	16
GLB 3	11	11	6	15	1	10
ETD (km)	292	281	321	310	173	222
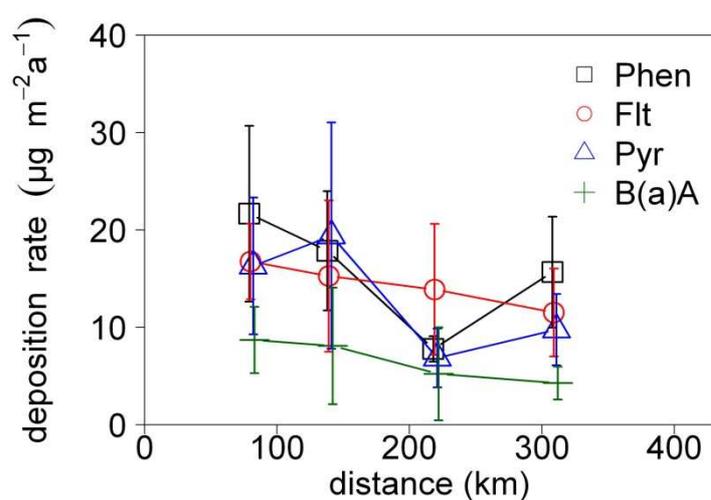
Fig. S8: Average maximum PAH deposition rates along the transect; error bars indicate standard deviation of the three peat profiles per bog.

Table S9: Empirically determined travel distances of several metals derived from other studies with standard error (SE), significance level (p), and coefficient of determination (R^2).

Study	metal	ETD (km)	SE (km)	p (-)	R^2 (-)
Freedman et al.[2]	Ni	23.53	1.25	0.000	0.92
	Cu	22.36	1.12	0.000	0.91
Nieboer et al.[3]	Cu	30.74	5.75	0.001	0.78
	Ni	21.31	4.74	0.002	0.72
	Zn	67.15	24.64	0.026	0.48
Kettles and Bonham-Carter [4]	Cu	32.56	4.14	0.000	0.64
	Pb	21.32	2.69	0.000	0.64
	Zn	66.47	12.71	0.000	0.44

Table S10: Characteristic travel distances of PAHs and particles, 95 % confidence intervals (CI) and fraction bound to particles calculated by The Tool for different temperature scenarios and with regionalized settings.

	0 °C			4°C			13 °C		
	CTD (km)	95 % CI	particle fraction (%)	CTD (km)	95 % CI	particle fraction (%)	CTD (km)	95 % CI	particle fraction (%)
Phen	1633	483 - 5514	0.7	325	51 - 2066	0.4	258	50 - 1329	0.2
Flt	596	212 - 1673	13.4	149	33 - 675	8.0	116	29 - 458	2.5
B[a]A	66	13 - 329	87.4	44	6 - 298	78.4	28	4 - 205	47.4
Chry	378	295 - 483	89.2	225	75 - 672	80.9	113	31 - 409	50.0
B[b]F	355	305 - 405	98.4	336	231 - 489	97.0	293	153 - 559	89.6
B[a]P	375	346 - 405	99.4	355	220 - 571	98.8	285	142 - 572	94.5
Ind	380	364 - 398	100	375	343 - 410	99.9	352	257 - 487	99.5
particles	388	388 - 388	100	388	388 - 388	100	388	388 - 388	100

Table S11: Characteristic travel distances of PAHs and metals and fraction bound to particles calculated by ELPOS for different temperature scenarios and with re-gionalized settings.

	0 °C		4 °C		13 °C	
	CTD (km)	particle fraction (%)	CTD (km)	particle fraction (%)	CTD (km)	particle fraction (%)
Phen	2376	0.2	345	0.1	266	0.1
Flt	704	1.7	158	1.2	120	0.5
B[a]A	378	21.1	142	15.4	54	7.4
Chry	480	23.9	282	17.6	133	8.6
B[b]F	457	73.6	432	65.6	373	45.7
B[a]P	482	78.6	456	71.6	366	52.6
Ind	490	95.0	483	92.8	454	85.0
particles	517	100.0	517	100.0	517	100.0

Table S12: Sensitivity of the CTD to different model input parameters estimated with The Tool.

	windspeed	height of air	aerosol deposition velocity	rain rate	$t_{1/2}$ in air	$t_{1/2}$ in water	$t_{1/2}$ in soil	K_{AW}	K_{OW}
Phen	1.00	0.05	0.00	0.02	0.93	0.01	0.00	0.03	0.00
Flt	1.00	0.08	0.01	0.06	0.91	0.00	0.00	0.02	0.06
B[a]A	1.00	0.58	0.02	0.54	0.38	0.00	0.00	0.18	0.71
Chry	1.00	0.36	0.10	0.26	0.60	0.00	0.00	0.41	0.47
B[b]F	1.00	0.92	0.25	0.62	0.07	0.00	0.00	0.05	0.15
B[a]P	1.00	0.91	0.27	0.60	0.08	0.00	0.00	0.07	0.11
Ind	1.00	0.99	0.30	0.64	0.01	0.00	0.00	0.01	0.03
particles	1.00	1.00	0.31	0.64	0.00	0.00	0.00	0.00	0.00

Table S13: Sensitivity of the CTD to different model input parameters estimated with ELPOS.

	temperature	windspeed	height of air	aerosol deposition velocity	rain rate	vapor pressure	$t_{1/2}$ in air	$t_{1/2}$ in water	$t_{1/2}$ in soil	$t_{1/2}$ in sed	K_{AW}	K_{OW}	K_{OC}
Phen	0.18	1.00	0.02	0.00	0.02	0.00	0.97	0.00	0.00	0.00	0.02	0.00	0.00
Flt	0.07	1.00	0.02	0.00	0.02	0.00	0.96	0.00	0.00	0.00	0.01	0.00	0.00
B[a]A	0.09	1.01	0.04	0.00	0.02	0.00	0.98	0.00	0.00	0.00	0.11	0.14	0.00
Chry	0.08	1.00	0.08	0.01	0.08	0.00	0.90	0.00	0.00	0.00	0.08	0.13	0.00
B[b]F	0.03	1.00	0.64	0.05	0.57	0.00	0.32	0.00	0.00	0.00	0.00	0.22	0.00
B[a]P	0.08	1.00	0.43	0.04	0.39	0.00	0.52	0.00	0.00	0.00	0.25	0.37	0.00
Ind	0.05	1.00	0.71	0.08	0.61	0.00	0.25	0.00	0.00	0.00	0.19	0.25	0.00
particles	0.00	1.00	1.00	0.12	0.01	0.00	0.00	0.00	0.00	0.00	0.05	0.00	0.00

Literature

1. **EPA Estimation program interface (EPI) suite.** http://www.epa.gov/opptintr/exposure/pubs/episuite.htm

2. **Freedman, B.; Hutchinson, T.C., Pollutant inputs from the atmosphere and accumulations in soils and vegetation near a nickel-copper smelter at Sudbury, Ontario, Canada.** *Canadian Journal of Botany-Revue Canadienne De Botanique* **1980,** *58***, 108-132.**

3. **Nieboer, E.; Ahmed, H.M.; Puckett, K.J.; Richardson, D.H.S., Heavy metal content of lichens in relation to distance from a nickel smelter in Sudbury, Ontario.** *The Lichenologist* **1972,** *5***, 292-304.**

4. **Kettles, I.M.; Bonham-Carter, G.F., Modelling dispersal of metals from a copper smelter at Rouyn-Noranda (Quebec, Canada) using peatland data.** *Geochemistry: Exploration, Environment, Analysis* **2002,** *2***, 99-110.**

Acknowledgements

(Eidesstattliche) Versicherungen und Erklärungen

(§ 5 Nr. 4 PromO)

Hiermit erkläre ich, dass keine Tatsachen vorliegen, die mich nach den gesetzlichen Bestim-
mungen über die Führung akademischer Grade zur Führung eines Doktorgrades unwürdig
erscheinen lassen.

(§ 8 S. 2 Nr. 5 PromO)

Hiermit erkläre ich mich damit einverstanden, dass die elektronische Fassung meiner Disser-
tation unter Wahrung meiner Urheberrechte und des Datenschutzes einer gesonderten
Überprüfung hinsichtlich der eigenständigen Anfertigung der Dissertation unterzogen werden
kann.

(§ 8 S. 2 Nr. 7 PromO)

Hiermit erkläre ich eidesstattlich, dass ich die Dissertation selbständig verfasst und keine an-
deren als die von mir angegebenen Quellen und Hilfsmittel benutzt habe.

Ich habe die Dissertation nicht bereits zur Erlangung eines akademischen Grades anderweitig
eingereicht und habe auch nicht bereits diese oder eine gleichartige Doktorprüfung endgültig
nicht bestanden.

(§ 8 S. 2 Nr. 9 PromO)

Hiermit erkläre ich, dass ich keine Hilfe von gewerbliche Promotionsberatern bzw. -vermittlern in Anspruch genommen habe und auch künftig nicht nehmen werde.

…………………………………………………………………………………..

Ort, Datum, Unterschrift